The Bed Nucleus of the Stria Terminalis: Connections, Genetics, & Trait Associations

by

Samuel Berry

A thesis submitted in partial fulfilment of the
requirements of Cardiff University,
for the award of Doctor of Philosophy

March 2022

Summary

This thesis examines the functional and structural connections of the Bed Nucleus of the Stria Terminalis (BNST). The principal motivation in doing so stems from the documented gap in our knowledge between the prolific pre-clinical animal BNST research, and that of human BNST research (Lebow & Chen, 2016). Understanding the human BNST may prove to be clinically important, as animal models often implicate this structure as being key in processes underlying the stress-response, disorders of negative affect, and in substance misuse- particularly related to alcohol (Herman et al., 2020; Maita et al., 2021). Therefore I further set out to test BNST connectivity relationships with related psychological phenotypes and examine any genetic associations.

Chapter 1 provides an overview of the relevant BNST literature and a brief summary of the methods used in this thesis. In Chapter 2 I use the Human Connectome Project young human adults sample (n = ~1000) to map the intrinsic connectivity network of the BNST. In addition, I compare this network to that of the central nucleus of the amygdala, an area anatomically and functionally associated with the BNST (Alheid, 2009). Next, I test for associations across this network with self-report traits relating to dispositional negativity and alcohol use. Finally, I examine the heritability of specific BNST- amygdala sub-region functional connectivity, and co-heritability with the self-report traits. In Chapter 3 I use the large UK biobank sample (n = ~ 19,000) to run a genome-wide association analysis, aiming to uncover specific common genetic variants that may be linked with BNST – amygdala sub-region functional connectivity. In Chapter 4, I focus on structural connectivity and use a mixture of macaque tract-tracing analysis, and human and macaque diffusion MRI probabilistic tractography to examine the evidence for a connection between the subiculum and the BNST. As well, I test for associations between measures of white-matter microstructure and self-report dispositional negativity and alcohol-use phenotypes. Finally, in the Discussion, I bring together the findings of the research, noting their implications within the wider BNST literature and making several suggestions for improving similar analysis in future.

Publications associated with this research

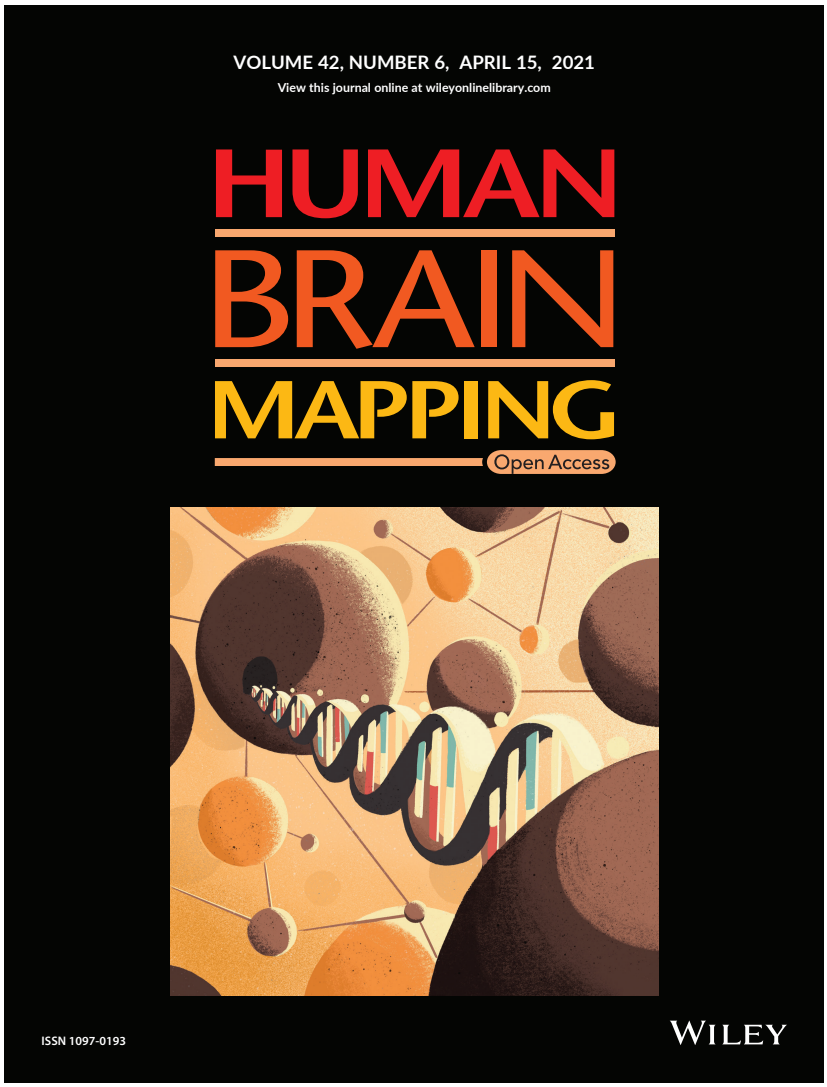

Berry, S. C., Wise, R. G., Lawrence, A. D., & Lancaster, T. M. (2021). Extended-amygdala intrinsic functional connectivity networks: A population study. Human brain mapping, 42(6), 1594–1616. https://doi.org/10.1002/hbm.25314

Berry, S. C., Lawrence, A. D., Lancaster, T. M., Casella, C., Aggleton, J. P., & Postans, M. (2022). Subiculum—BNST Structural Connectivity in Humans and Macaques. NeuroImage, 119096. https://doi.org/10.1016/j.neuroimage.2022.119096

Acknowledgements

I would first of all like to thank my supervisors. Thank you Tom, for taking me on as your first PhD student and for being so generous with your time. You have been incredibly supportive and have always sought to praise my work, whilst simultaneously providing me with insightful feedback that has helped me to grow as a scientist. Thank you Andrew, for your support and for taking to time to engage with my ideas. Your meticulous feedback and push for me to expand my knowledge of the literature has undoubtably improved my work and I am looking forward to continue working with you in future.

Thank you to my colleagues at CUBRIC. In particular to Mark Postans, who unquestioningly agreed to support me when pivoting projects during the pandemic and who continued to give me generous amounts of his time, knowledge, and support. As well, thank you to Tom Chambers, who was kind enough to provide me with advice and ideas even after he had left CUBRIC. Thank you also to John Aggleton, for your excellent contributions to Chapter 4 of this thesis.

Thank you to my Cardiff friends, it is you who have made these years special. Thank you to my friends from home, who have great admiration for what I do despite not quite knowing what it is. In particular I would like to thank Jasper and Mike for letting me work in their office when working from home was getting old. Thank you as well to Matt for your constant support as a friend and for listening to me moan on our walks.

Thank you to my family, who provide me with love and support. In particular my two mums, who are always there for me. Thank you also to my Italian family, grazie di tutto, vi amo! Finally, thank you to my amazing partner, Chiara. Following you to Cardiff in the vain hope that I would also get onto a PhD course somehow worked. It was the right choice. You are an inspiration to me, and these years we have spent together we will remember forever as the ones that shaped our lives.

Common Abbreviations

TERM	DEFINITION
BNST	Bed Nucleus of the Stria Terminalis
BOLD	Blood-oxygenation Level Dependant
CeA	Central Nucleus of the Amygdala
DN	Dispositional Negativity
dMRI	Diffusion Magnetic Resonance Imaging
ExTA	Central Extended Amygdala
fMRI	Functional Magnetic Resonance Imaging
ICN	Intrinsic Connectivity Network
IFC	Intrinsic Functional Connectivity
tf-FMRI	Task-free Functional Magnetic Resonance Imaging
GWAS	Genome-wide Association Study
HCP	Human Connectome Project
MRI	Magnetic resonance imaging
UKBB	UK Biobank

Thesis Outline

Table of Contents

List of figures

List of tables

Chapter 1: Introduction

This thesis is focused on the structural and functional connections of bed nucleus of the stria terminalis (BNST) grey matter region and their potential associations with psychological phenotypes. In this section I will outline the background relevant for understanding the aims and implications of this research. Firstly I will outline what we currently know about BNST anatomy. In the second section I summarise research regarding the BNSTs association with numerous phenotypes that are important to human health research, with a focus on anxiety, stress, and addiction. Finally, I describe some common genetic analysis approaches and how they can be used along with neuroimaging to uncover novel insights regarding neural mechanisms related to the BNST. Finally, I provide an outline of the thesis research aims and detail what each chapter will be addressing.

1.1 The Bed Nucleus of the Stria Terminalis

1.1.1 BNST Anatomy

The bed nucleus of the stria terminalis (BNST, or BST), surrounded on all sides by the hypothalamus, thalamus, striatum, septum, and lateral ventricles, is a grey matter region within the basal forebrain (Alheid, 2009; Giardino et al., 2018; Johnston, 1923). At approximately 190mm^3 in humans, this small structure is deceivingly complex, with a diverse range of cell types expressing a plethora of different neuropeptides and neurotransmitters (Giardino & Pomrenze, 2021; Lebow & Chen, 2016). First described by Johnston in 1923, the BNST, along with the central nucleus of the amygdala (CeA) medial amygdala (MeA) and the shell of the nucleus accumbens (NAc), is considered a key part of the 'extended amygdala' (Alheid, 2009; Johnston, 1923). In particular, the 'central extended amygdala' (ExtA), consisting solely of the BNST and the CeA, are often grouped together because of their dense interconnections and shared cellular populations (Figure 1) (Ahrens et al., 2018; Alheid, 2009; Fox & Shackman, 2019). The degree to which these two ExtA structures can be considered a single functional unit is a key research question addressed in Chapter 2.

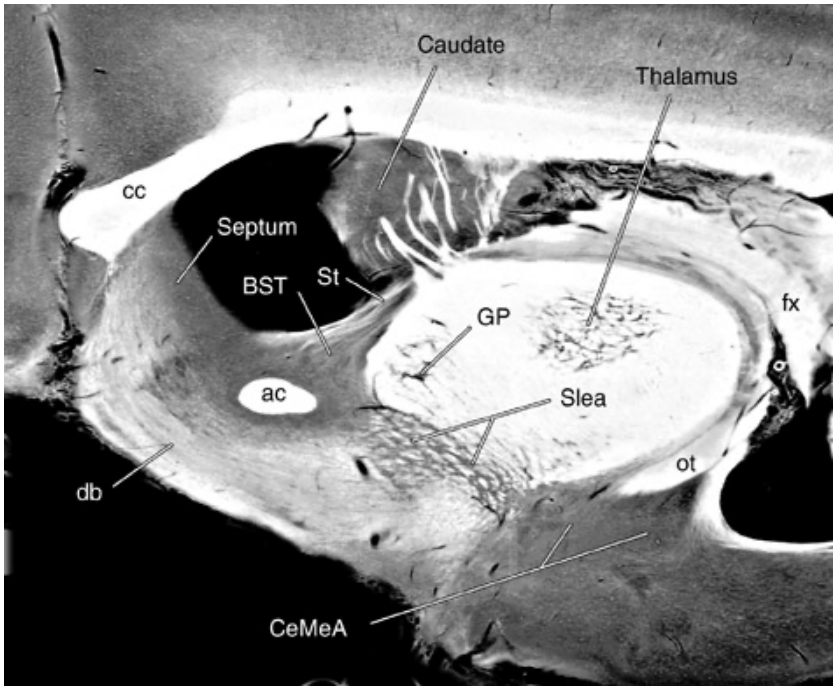

Figure 1 Anatomical Image of the BNST (adapted from Alheid 2009)

Anatomical photographic print of an unstained section of a rat brain showing the BNST. Note how the BNST wraps around either side of the anterior commissure and is at the ventral/ anterior end of the stria terminalis white matter bundle. This image also demonstrates anatomical connections to the central nucleus of the amygdala via the sub-lenticular extended amygdala. BST = BNST, Slea = Sublenticular extended amygdala, fx = fornix, ac = anterior commissure, GP = globus pallidus, cc = corpus collosum.

The BNST itself is a heterogenous region and has traditionally been subdivided into various sub-nuclei (e.g., De Olmos & Ingram, 1972; Dong et al., 2001; Giardino & Pomrenze, 2021; Walter et al., 1991). The BNST has been parcellated principally along two topographical directions, the medial-lateral axes and anterior-posterior axes (Bota et al., 2012). The medial-lateral parcellation is based on chemo/ cytoarchitecture and amygdala-BNST structural termination sites (Bota et al., 2012). The anterior-posterior parcellation is also based upon cytoarchitecture and amygdala connectivity, but as well includes studies on gene expression and BNST outputs to numerous other brain regions (for a review, see Bota et al., 2012). A synthesis of BNST rat research, which looked at studies reporting BNST neural populations and mRNA transcription, found evidence supporting a division primarily along the anterior-posterior axis, with 16-18 different BNST subregions described (Bota et al., 2012). The most accepted of these

subregions includes eight anterior areas, including the anteromedial, oval, fusiform, juxtacapsular, rhomboid, dorsomedial, ventral nucleus, and magnocellular nuclei, and three posterior areas, including the principal, the interfascicular, and the transverse nuclei (Bota et al., 2012; Lebow & Chen, 2016). These two BNST parcellations are not, however, mutually exclusive and in fact share a number of common nuclei (Bota et al., 2012; Giardino & Pomrenze, 2021).

Around 90% of the neurons within the BNST are thought to be GABAergic, however these neurons respond to a diverse range of neuromodulators and neurotransmitters, including corticotrophin release factor (CRF), noradrenaline, dopamine, and serotonin (Glangetas & Georges, 2016; Hammack et al., 2021; Maita et al., 2021). In terms of delineating regions based on cell-types, researchers using single cell RNA transcriptional profiling of BNST neurons reported as many as forty-one different transcriptional clusters (Welch et al., 2019), whilst a more recent study, using similar methods, reported evidence for eleven (Ortiz-Juza et al., 2021). These grouping differences are likely due to variations in clustering criterion (Maita et al., 2021), however these studies serve to highlight that the BNST, despite its small size, is a complex neural region containing a diverse array of cell types.

Although the BNST has been studied extensively in the rat, much less is known about BNST topology in humans (Fox & Shackman, 2019; Lebow & Chen, 2016). This is largely due to the difficulties of obtaining human brain tissue and preferential focus on other regions, such as the amygdala (Lebow & Chen, 2016). Nonetheless, a handful of human BNST tissue studies do exist (Allen & Gorski, 1990; Gaspar et al., 1985, 1987; Lesur et al., 1989; Walter et al., 1991). Of particular note, Walter et. al., (1991) used six adult human brain samples to investigate the spatial distribution of thirteen immunohistochemical markers. This work identified, with reference to previous human chemoarchitectonic descriptions (Lesur et al., 1989), evidence for three distinct human BNST areas: the lateral, central, and medial subdivisions (Walter et al., 1991).

Other studies of the human BNST have taken place using magnetic resonance imaging (MRI). Until the last decade, the resolution of MRI did not permit accurate study of the BNST even as a single structure, with researchers only able to refer to "an area consistent with the BNST" (Avery et al., 2016). More recent advances in ultra-high field 7T MRI imaging has allowed for the development of standardised BNST masks and manual segmentation protocols (Avery et al., 2014; Theiss et al., 2017; Tillman et al., 2018; Torrisi et al., 2015). The problem of low resolution in MRI is further compounded by MRI images of the BNST not showing clear tissue contrasts between its subregions, making visual delineation of subnuclei extremely challenging (Fox & Shackman, 2019). Straddling either side of the anterior commissure, one way to divide the structure has been to simply consider the section above the commissure as the dorsal BNST and the section below as the ventral BNST (Giardino & Pomrenze, 2021). In practice, however, the ventral BNST is often excluded all together due to difficulties differentiating it visually from neighbouring structures (Theiss et al., 2017).

Our understanding of BNST internal anatomy remains a work in progress and although MRI techniques continue to be improved, *in vivo* MRI parcellation of the human BNST remains an ambitious target (Maita et al., 2021). Even more precise tissue level examination may not provide much clarity, as researchers have reported that the distribution of cell types in the BNST are frequently overlapping, with unclear spatial distinctions resulting in conflicting numbers of subnuclei being identified (Maita et al., 2021). It has been have noted, however, that precisely mapping the anatomy of the BNST subregions may not be necessary for understanding the contributions of the structure to neural processes, in particular with regards to understanding how the BNST is involved in human pathological traits and behaviours (Giardino & Pomrenze, 2021). It may be that other techniques, such as mapping long-range connections to other brain regions and/or using experimental paradigms to understand the BNSTs functions, will be prove to be sufficient for improving our knowledge of the BNST to a level that is clinically useful (Giardino & Pomrenze, 2021).

1.1.2 The BNST Within the Neural Network

Like all brain regions, the BNST does not function alone but exists within a complex network of interconnected structures. Therefore, to properly understand the role of the BNST, it is necessary to consider its position within the wider network. The BNST in particular is connected to a diverse group of neural structures, leading to a popular hypotheses that the BNST is key hub that integrates bottom-up sensory information and top-down cognitive processes, before outputting signals to areas linked to regulation of the neuroendocrine system (Avery et al., 2016; Fox & Shackman, 2019; Herman et al., 2020; Lebow & Chen, 2016). This section outlines the research regarding the structural and functional connectivity networks of the BNST.

1.1.2.1 Structural Connectivity

Structural connectivity research aims to understand the physical connections between brain regions, primarily mediated by bundles of myelinated axons known as white matter pathways (Lebel & Deoni, 2018). When testing neural tissue directly, this is typically achieved by using tract-tracing methods in which a molecular marker, or virus, is injected into a target cell group (Saleeba et al., 2019). These markers then travel along the pathway of a neuron's axon, revealing its connections. These experiments can be anterograde, where the molecular marker propagates to the neurons target, retrograde, where the marker propagates back to the cell body, both anterograde and retrograde, and some pass transsynaptically (for a review of these techniques see Saleeba et al., 2019).

Structural connectivity can also be measured indirectly at a macro level using diffusion magnetic resonance imaging (dMRI) (Le Bihan et al., 1986; Le Bihan & Breton, 1985; Soares et al., 2013). This technique uses the magnetic and diffusion properties of water molecules to model the restriction of water in the brain (Soares et al., 2013). Because water is generally more restricted within white matter tracts, this method permits estimations of the presence, direction, and structural properties of the brain's white matter pathways (Soares et al., 2013) (see also Chapter 4). Although the resolution of the dMRI method is much lower than tract-tracing methods (typically

1.25mm in dMRI vs the microscopic or 'synapse level' of tract tracing imaging techniques), dMRI has the benefit of being non-invasive and thus is able to be used *in-vivo*.

A review by Lebow and Chen summarised years of work in BNST rodent tract-tracing research, detailing in some detail the different efferent and afferent connectivity profiles of the BNST and its subnuclei (Figure 2) (Dong et al., 2000, 2001; Dong & Swanson, 2003, 2004, 2006; Lebow & Chen, 2016). In sum, the BNST has been shown to have dense reciprocal projections to the amygdala and hypothalamus, but also demonstrates connectivity with several other limbic regions including the hippocampus (via the ventral subiculum), lateral septum, ventral tegmental area (VTA), and nucleus accumbens (NAc) (Lebow & Chen, 2016). As well, there is tract-tracing evidence for structural connectivity to the striatum, thalamus, anterior insular, olfactory bulb, basal ganglia, frontal cortex, and brain stem regions including the locus coeruleus and nucleus of the solitary tract (for reviews see Lebow & Chen, 2016; Maita et al., 2021).

Though comparatively fewer studies exist, human and non-human primate (NHP) dMRI work has so far provided complementary evidence for a general conservation of these BNST connections across species; though without the anatomical specificity afforded to tract-tracing experiments (Avery et al., 2014; Oler et al., 2017a). Additional connections reported from dMRI in humans include connectivity to the orbital frontal cortex (OFC), temporal pole, and paracingulate gyrus (Avery et al., 2014).

One of the principal structural pathways connecting the BNST is the stria terminalis (ST) white matter bundle (Alheid, 2009; De Olmos & Ingram, 1972; Dong et al., 2001; Koller et al., 2019). The ST is one of the major efferent pathways of the amygdala (Pardo-Bellver et al., 2012). Arching dorsally over the thalamus and along the medial border of the caudate nucleus, the ST carriers fibres from the CeA towards the anterior commissure (Klingler & Gloor, 1960; Oler et al., 2017b). The majority of these ST fibres terminate in the BNST, with others joining the anterior commissure or continuing onto the hypothalamus (Dong et al., 2001). These amygdala-BNST projections terminate

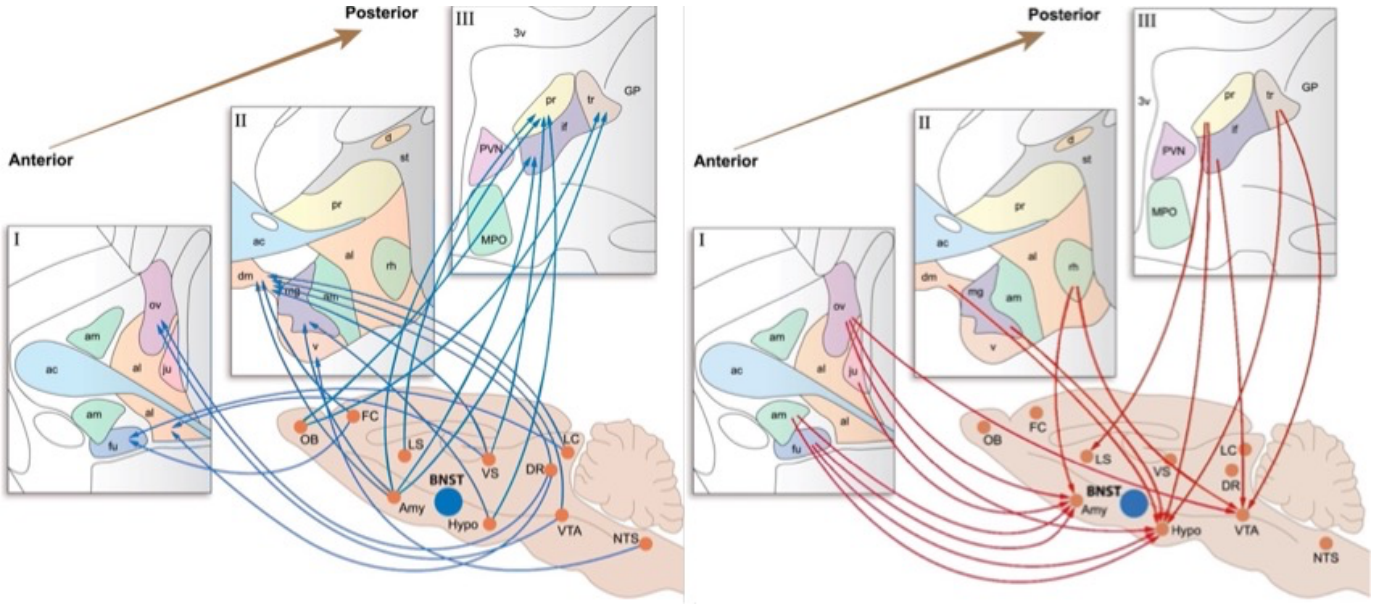

Figure 2: BNST Subdivisions with Efferent and Afferent Projections in the Rat (adapted from Lebow & Chen, 2016).

BNST subdivisions with efferent (left) and afferent (right) projections within the rat BNST. (I) represents projections of the anterolateral (al), anteromedial (al) and ventral (fu) areas of the BNST at the level of the anterior commissure (ac). (II) represents projections relating to the anterolateral and medial BNST areas posterior to the anterior commissure (ac). (III) represents projections relating to the posterior BNST comprising of three nuclei: the principle (pr), the interfascicular (if) and the transverse (tr). 3v, third ventricle; ac, anterior commissure; al, anterolateral BNST; am, anteromedial BNST; Amy, amygdala; BNST, bed nucleus stria terminalis; d, dorsal nucleus; dm, dorsomedial nucleus; DR, dorsal raphe; FC, frontal cortex; fu, fusiform nucleus; GP, globus pallidus; hypo, hypothalamus; if, interfascicular nucleus; ju, juxtacapsular nucleus; LC, locus coeruleus; LS, lateral septum; mg, magnocellular nucleus; MPO, medial preoptic area; NTS, nucleus solitary tract; OB, olfactory bulb; ov, oval nucleus; pr, principle nucleus; PVN, paraventricular nucleus; rh, rhomboid nucleus; st, striatum; tr, transverse nucleus; VS, ventral subiculum; VTA, ventral tegmental area.

within the lateral BNST in the rat, but additionally innervate the medial and precommissural areas in the monkey (Dong et al., 2001). As well as amygdala to BNST $projections, the ST is bidirectional, with anterograde tract-tracing experiments demonstrating projections from the BNST back to the CeA in rats (Dong & Swanson, 2004).

An additional fibre bundle linking the BNST to the amygdala is the ventral amygdalofugal pathway (Dong et al., 2001; Kamali et al., 2016). This pathway, sometimes known as or considered a part of the *ansa peduncularis*, is much shorter and denser than the ST, traversing from the CeA and MeA to the BNST through a region known as the sublenticular extended amygdala (SLEA) (Figure 1) (Dong et al., 2001; Kamali et al., 2016). In addition, there is evidence for basolateral amygdala (BLA)

fibres passing to the BNST, some crossing directly through the CeA region (Stamatakis et al., 2014). Tract tracing data has demonstrated the ventral amygdalofugal connection to be partly bi-directional, with efferent fibres passing from the BNST to the CeA (Hammack et al., 2021).

Hippocampal inputs to the BNST, via the ventral subiculum complex (anterior in primates), have been described in a large number of rodent studies, with some reports in the tree shrew and squirrel monkey (Cullinan et al., 1993; Herman et al., 2020; Ni et al., 2016; Poletti & Sujatanond, 1980; Radley & Sawchenko, 2011). This projection has been shown to occur via the fornix and a route involving the amygdala; likely via the stria terminalis and/or ventral amygdalofugal pathway (for a review see Herman et al., 2020). Researchers have demonstrated that outputs from this pathway converge on the anterior BNST alongside outputs from the mPFC (Radley & Sawchenko, 2011). This area of the BNST then projects to the paraventricular nucleus of the hypothalamus (PVN), an area directly involved in initiating the HPA axis response to stressful stimuli (Radley & Sawchenko, 2011). Subsequently, the BNSTs potential role as a key relay of information relevant to stress-responding has meant that this pathway has received a lot of attention in rodent stress literature (Cullinan et al., 1993; Herman et al., 2020; Radley & Sawchenko, 2011). Despite this, research into this supposedly important stress-regulatory pathway in humans and NHPs is lacking. Addressing this translational gap forms a key part of Chapter 4, where this research is discussed in more detail.

1.1.2.2 Functional Connectivity

As well as mapping structural pathways that connect regions in the brain, either by directly testing neural tissue or by using macroscale diffusion MRI estimates, another way to assess connectivity is to examine how brain regions are functionally connected (Soares et al., 2016). Functional connectivity (FC) is typically inferred by using functional magnetic resonance imaging (fMRI) to test the temporal relationship of neural activation between different brain areas. Neural activation is measured via the blood-oxygen-level-dependent (BOLD) signal, which reflects changes in

Figure 3: Timeseries of BOLD activation within two different brain regions

This figure illustrates how functional connectivity analysis is performed. In this example, BNST BOLD activations (blue) are plotted against BOLD activation of a different random region (orange). The correlation between the two areas activation over time is used to infer functional connectivity.

deoxyhaemoglobin, driven (mostly) by changes in brain blood flow and oxygenation in response to neural activity (Hall et al., 2016). Though FC is not a direct measure of connectivity *per se*, with the correspondence between structural and functional connectivity being no more than 50% (Suárez et al., 2020), the temporal coherence of BOLD activity between brain regions is used as a proxy for communication between areas that may only be sparsely connected via direct (monosynaptic) or indirect (polysynaptic) structural connections (Soares et al., 2016).

FC is assessed either by eliciting BOLD activation during a task, or by testing how brain regions activate together at 'rest' whilst a participant simply lays down quietly within an MRI scanner; this is known as task-free (tf-MRI) or resting-state MRI (Smith, Vidaurre, et al., 2013). Typically, researchers compute a series of pair-wise correlations between brain areas which reflects the temporal coherence of brain activation over time (Figure 3), though other more complex temporally dynamic models are available (Hutchison et al., 2013; Soares et al., 2016). The correlations between brain regions BOLD activity during tf-MRI are used to compute intrinsic connectivity networks (ICN), which serve as a map of FC in the brain (Battistella et al., 2020; Seeley et al., 2007). As well as providing clues as to a brain regions function via its associations with other regions, individual or group ICNs can be used to test relationships with traits,

behaviours, genetics, or investigate developmental trajectories (Battistella et al., 2020; Elliott et al., 2018; Laird et al., 2011; Luna et al., 2010; Park et al., 2021). ICNs have been shown to be highly organised, reproduceable, and in some cases have been linked to human psychological phenotypes (Battistella et al., 2020; Thomas Yeo et al., 2011). Thus, understanding the ICN of the BNST may prove useful for furthering our understanding of its role within the brain .

Since the availability of BNST anatomical masks and better manual delineation procedures, several fMRI studies attempting to map the BNST ICN have taken place (see Table 1, Chapter 2). These studies, using both 3T and 7T imaging, have reported a fairly consistent ICN, with FC described primarily to proximal basal ganglia areas, VTA, paracingulate, thalamic, amygdala, anterior insular, hippocampal, and medial prefrontal regions. These results are largely in agreement with structural connectivity studies, although some differences, such as paracingulate connections, do exist. ICN BNST studies are discussed in more detail in Chapter 2, where computing the BNST ICN using a large human fMRI sample forms a central part of the analysis.

As well as investigating brain-wide connectivity networks, another approach is to focus on FC to between specific brain regions, often selected based upon anatomical evidence that suggests a connection *a-priori*. For the BNST, given the significant structural connectivity, a lot of focus has been on examining FC to the amygdala and its

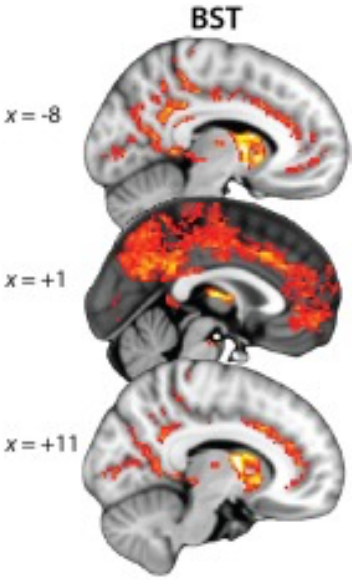

Figure 4 Intrinsic Functional Connectivity of the BNST (adapted from Tillman et. al., 2018)

This image demonstrates the intrinsic connectivity network of the BNST (BST), created via seed-based correlation analysis in a sample of 185 adults (Tillman et. al., 2018).

various sub nuclei (e.g., Fox et al., 2018; Hofmann & Straube, 2019; Oler et al., 2017b; Pedersen et al., 2020; Torrisi et al., 2019). For example, an fMRI study using macaques and human adolescents reported strong CeA – BNST functional coupling using 3T MRI (Oler et al., 2017b). More recently, Hofmann and Straube compared BNST FC to three amygdala subregions – the laterobasal (LB), Centromedial (CM), and superficial (SF) nucleus, finding evidence for connectivity between all of these regions, but demonstrating strongest BNST connectivity to the LB region, followed by the SF, and the CM (Hofmann & Straube, 2019). These FC studies can be used to compute individual differences in FC between brain regions, subsequently testing for associations of these connectivity differences with traits, states, or clinical diagnoses. This research, with regards the BNST, is discussed in section 1.2 and is an approach used in chapters 2 and 3.

In sum, the BNST demonstrates a fairly consistent pattern of structural and functional connectivity to both limbic and frontal regions, with significant outputs to hypothalamic and brain stem areas. This suggests that the BNST plays a role in the integration of physiological and cognitive responses, connecting structures including the amygdala, hippocampus and mPFC, to those hypothalamic and brainstem regions that are associated with autonomic and neuroendocrine functions (Crestani et al., 2013; Herman et al., 2020; Maita et al., 2021). Although initial indications suggest that the connectivity profile of the BNST is relatively stable across species, the vast majority of our BNST connectivity knowledge is thus far derived from anatomical tract-tracing studies in rodents, with BNST human MRI research (in particular structural MRI) still in its infancy.

1.2 BNST Associated Functions

The BNST has been linked to a diverse range of functions, including anxiety, fear, depression, stress-responding, addiction, sleep, mating behaviours, and hunger (Lebow & Chen, 2016). The present body of work has a specific focus on BNST associations with stress-related traits, in particular anxiety, fear, depression, and addiction. Thus, whilst acknowledging that the BNST is linked with a variety of

functions, this section focuses on the evidence for the BNST's involvement in the aforementioned processes.

1.2.1 The BNSTs' Role in Anxiety & Fear Processing

As outlined in section 1.1, the BNST's position within the brain means that it is well placed to consolidate and relay activity from cortical (e.g. mPFC), subcortical/ allocortical (e.g, anterior hippocampus, amygdala), and brain stem regions (e.g., ventral tegmental area), before outputting signals to the hypothalamus and influencing stress responding via the HPA axis. A large body of research regards the BNST, and the larger ExtA region more generally, as key for assembling states of fear and anxiety through these extensive connections with autonomic and mood regulatory regions.

In the psychology literature, fear can be conceptualised as being an immediate response generated to a discrete, proximal, or certain threat, whereas anxiety is a generalised and longer-term response to an unknown, distant, or uncertain threat (Steimer, 2002). These differences are largely based upon Predatory Imminence Theory (PIT), which differentiates species-specific defensive responses according to the proximity of a predator (or threat in general) (Fanselow, 1994; Perusini & Fanselow, 2015). In this evolutionarily informed model, there is a distinction between three phases, each of which involves specific defensive behaviours. There phases are: pre-encounter , for when the proximity of the threat is low and/ or undetected (anxiety), post-encounter, for when a threat has been detected (fear), and circa-strike, for when a threat has been engaged (panic) (Perusini & Fanselow, 2015). Although mostly built upon rodent research, these stages are thought to be conserved in humans and there is some evidence to suggest that the neural mechanisms underpinning them may be specifically relevant for particular clinical disorders. For example, allowing for some overlap, it has been suggested that fear processing may be more implicated for phobias, anxiety processing for generalised or social anxiety disorders, and panic processing for panic disorders and PTSD (Perusini & Fanselow, 2015).

One popular theory posits that the ExtA's two key components, the BNST and CeA, are separately involved in generating states of anxiety and fear. In this hypothesis, the BNST is responsible for long-duration responding to diffuse threats (anxiety) and the CeA is responsible for immediate responses to proximal threats (fear). Although the original theories proponents, following further evidence from rodent lesion studies, abandoned this strict functional dissociation hypothesis for a more nuanced view that includes both structures in both processes, the double dissociation theory continues to shape fear and anxiety research today (Davis et al., 2010; Fox & Shackman, 2019; Hulsman et al., 2021). Of particular note, the influential funding body the National Institute of Mental Health (NIMH) continues to set out a clear distinction within its Research Domain Criteria (RDoC) programme, differentiating between a fear circuit (acute threat) involving the CeA, and an anxiety circuit (potential threat) involving the BNST (Wegener, 2016). It is within this context that much of the work on the BNSTs contribution to fear and anxiety states has taken place over the last two decades.

Several human neuroimaging studies lend support to the double dissociation hypothesis (Alvarez et al., 2011; Brinkmann, Buff, Feldker, et al., 2017; Buff et al., 2017; Grupe et al., 2013; Herrmann et al., 2016; Klumpers et al., 2017; McMenamin et al., 2014; Somerville et al., 2013). In one highly cited example, researchers used electric shocks during an fMRI scan to demonstrate that BNST activity was greater during shock anticipation, whereas amygdala activity was greater during shock confrontation (Klumpers et al., 2017). Another study reported that the amygdala responds transiently to the appearance of negative images, whereas the BNST demonstrates sustained activity during a block of negative vs neutral images and for uncertain vs certain blocks (Somerville et al., 2013). Despite this, a number of critical commentaries have emerged regarding these studies, suggesting that they are often underpowered, that they fail to control for confounding variables, or that they fail to statistically test the region X condition interactions (Fox & Shackman, 2019; Goode et al., 2020; Hulsman et al., 2021). Further, these results are not in agreement with other human fMRI studies which describe evidence against a double dissociation. For example, researchers have reported both that the amygdala provides sustained activation in

anticipation to uncertain threat (Andreatta et al., 2015; Lieberman et al., 2017; Williams et al., 2015) and that the BNST responds transiently to the presence of immediate threat cues (J. M. Choi et al., 2012; Klumpers et al., 2015; Mobbs et al., 2010; Pedersen, 2017). Another study reported no statistical differences between the CeA and BNST when viewing briefly presented (800ms) aversive images (Brinkmann et al., 2018a), and research with children reported that it was the amygdala, instead of the BNST, which showed greater activation in response to unpredictable threat cues (Feola et al., 2021). The findings of BNST and amygdala involvement in processes seemingly ascribed to the other region have also been detailed in several loss of function rodent studies (for a review, see Gungor & Paré, 2016).

These conflicting results have led to much confusion in the literature (Fox, Oler, Tromp, et al., 2015; Fox & Shackman, 2019; Gungor & Paré, 2016; Hulsman et al., 2021). Some of this may be explained by researchers using a variety of paradigms (often a new paradigm for every experiment) to test different aspects of threat processing. For example, in any one experiment researchers may assess an amalgam of threat probability, visual proximity to threat, temporal proximity to threat, threat duration, or threat contextual learning. Further, the use of unstandardised paradigms and imaging methods mean that there are many researcher degrees of freedom involved, including variations in the MRI acquisition parameters, image processing, data analysis, experimental design, and type of aversive stimuli used (Wicherts et al., 2016).

Another reason for the inconsistent results is that the BNST, rather than being generally selective to long-duration threats (such as contexts), may have a more prescribed role in the expression of defensive behaviours to threats which are temporally unpredictable. A series of rat experiments attempted to test whether this may be the case (Goode et al., 2019, 2020; Hammack et al., 2015). In one example (Goode et al., 2020), this was achieved by placing rats into contexts that would condition them to either an imminent shock (1 minute after placement) or a delayed shock (9 minutes after placement). Pharmacological inactivation of the BNST was

shown to disrupt the expression of freezing behaviours when conditioning was with the delayed shock, but not the imminent shock. This demonstrated that it was not the context *per se* (a long duration threat stimulus) that was BNST reliant, but rather that it was the temporal unpredictability of the aversive stimulus (Goode et al., 2020). Unfortunately, in the contextual condition purporting to measure 'temporal unpredictability', the shock was always delivered at 9 minutes following introduction, raising questions as to whether this was really measuring threat unpredictability or simply delayed threat. Nonetheless, this temporal unpredictability hypothesis is supported by other rodent work (Goode et al., 2019; Hammack et al., 2015) and some recent human fMRI research (Clauss et al., 2019; Figel et al., 2019; Naaz et al., 2019).

Though the precise conditions under which the BNST responds is still a matter of debate, researchers have largely converged on the idea that, whilst not completely interchangeable, the BNST and CeA likely share responsibility for orchestrating both fear and anxiety processes (Fox & Shackman, 2019; Gungor & Paré, 2016; Hulsman et al., 2021). As noted in a critical review (Fox & Shackman, 2019), such highly interconnected regions as the BNST and CeA are unlikely to be strictly functionally dissociable, with most researchers now ascribing functional *preferences* to each region (Hulsman et al., 2021). As discussed in section 1.1, despite its small size the BNST is a complex anatomical region which has a number of subcomponents, some of which may even be involved in opposing functions (Choi, Evanson, et al., 2008). In general though, animal work and human fMRI studies have clearly implicated the BNST in fear and anxiety processing, with the evidence pointing towards a *preferential* role in responding to long-duration and/or uncertain threats; processes that are likely associated with the experience of anxiety (Hulsman et al., 2021).

1.2.2 The BNST and Dispositional Negativity

1.2.2.1 What is Dispositional Negativity?

Dispositional negativity (DN) is a term used to describe individual differences in the propensity to experience and express more frequent, intense, or enduring negative affect (Hur et al., 2019; Shackman, Tromp, et al., 2016). It is a broad, trait-like phenotype subsuming several more narrowly focused traits including neuroticism, trait anxiety, self-criticism, behavioural inhibition, and low self-esteem (Shackman et al., 2018). This concept is viewed as a fundamental aspect of childhood temperament and adult personality, which researchers have demonstrated is relatively stable across cultures, languages, and the lifespan (at least from the early teens) (reviewed in Hur et al., 2019a; Shackman et al., 2016, 2018). Individual differences in DN show extensive agreement across instruments taken via self-report or through informants (Shackman, Stockbridge, et al., 2016). An individual's DN scores predict psychophysiological measures of stress and anxiety in the laboratory, as well as life outcomes including physical health, happiness, loneliness, education, wealth, and relationship satisfaction (Hur et al., 2019; Shackman, Stockbridge, et al., 2016). DN has also been strongly linked to the development of psychiatric disorders related to anxiety, depression, stress, and addiction (Hur et al., 2019a; Shackman et al., 2016, 2018). For example, using a large cohort study (n=591) researchers demonstrated that a one standard-deviation increase in DN at the time of baseline assessment increased the odds of developing a major depressive episode by 41% and an anxiety disorder by 32% within the next twenty years (Hengartner et al., 2016). Given the numerous significant effects of this trait on public health, researchers have been interested in understanding the associated biological and psychological mechanisms behind it (Hur et al., 2019; Shackman et al., 2016).

Self-report data suggest that most of the heightened negative affect associated with DN can be explained via three key pathways – increased stressor reactivity, tonic increases in negative affect, and increased stressor exposure (Figure 5) (Shackman, Tromp, et al., 2016). DN, like other psychological traits, reflects the combination of environmental and genetic effects on brain structure and function. Given the evidence outlined in section 1.2.1 regarding the BNST's involvement in aversive stimuli responding and the generation of anxiety-like states, the BNST has been suggested to play a key role in mediating several aspects of DN (Shackman, Tromp, et al., 2016). In

particular, a network of regions that includes the BNST, CeA, and orbitofrontal cortex (OFC), is hypothesised to orchestrate the maintenance of tonic increases in negative affect (Shackman, Tromp, et al., 2016). Studies directly testing for BNST associations with DN and DN-associated traits are outlined in the section below.

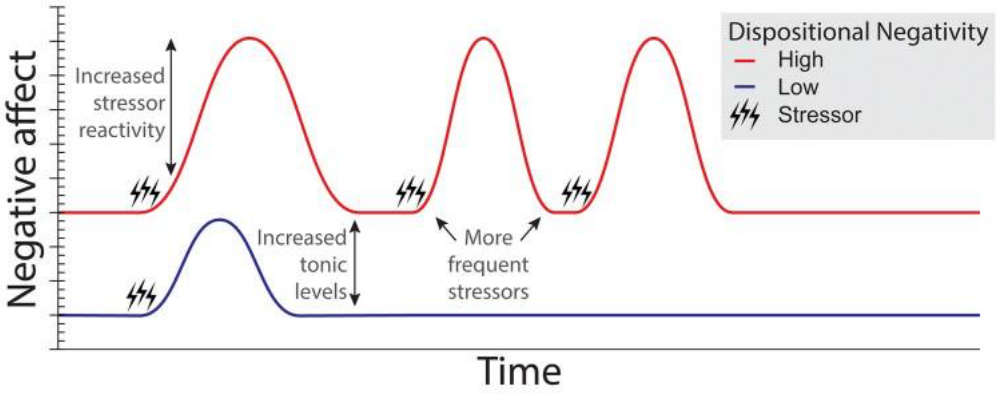

Figure 5 Dispositional Negativity Key Mechanisms (adapted from Shackman, Tromp, et al., 2016)

Graphic demonstrating the hypothesised three key pathways underlying dispositional negativity (DN) – increased stressor reactivity, increased tonic levels of stress, and more frequent stressors. The lines represent hypothetical momentary negative affect in a person with high DN (red) low DN (blue).

1.2.2.2 BNST associations with dispositional negativity traits

1.2.2.2.1 Dispositional Negativity in Rodents

Some behavioural elements of DN, such as heightened vigilance and increased behavioural inhibition, are expressed similarly across mammalian species (Hur et al., 2019). This has led researchers to use mechanistic studies of these DN-associated behaviours in rodents to infer which brain regions may be important in human DN expression. In rodents, heightened vigilance is typically measured by testing for increases in the startle response to aversive stimuli (Davis et al., 2010). Increases in startle responses following conditioning to aversive stimuli (also known as potentiated startle) are also seen in humans, with increased startle being associated with higher levels of trait anxiety (Poli & Angrilli, 2015). Behavioural inhibition, another

behavioural marker of DN, is typically assessed by recording decreases in exploratory behaviours in environments that are intrinsically aversive (such as an open bright environment) or that have been previously associated with an aversive stimuli (Lezak et al., 2017). As discussed in section 1.2.1, numerous studies strongly implicate the BNST in various mechanisms underlying anxiety and fear processing, with selective lesioning of the BNST in rodents (as well as the amygdala proper) demonstrating an important role in these DN-associated behaviours (Fox & Shackman, 2019; Gungor & Paré, 2016).

As well as anxiety and fear processing, the BNST has been implicated in rodent measures of depression. A commonly used test of depression-like behaviour in rodents is the forced swim test (Miles & Maren, 2019). In this experiment, rats are required to swim in deep water for fifteen minutes. Typically, rodents will present with escape behaviours (i.e. thrashing about in the water trying to get out), but when escape fails will adopt an immobile posture. Because this immobility is seen as 'giving up', which mimics some signs of depression in humans, this paradigm has been used to assess treatments and mechanisms related to depression (Lezak et al., 2017; Miles & Maren, 2019). Permanent and temporary BNST lesions in rodents have been shown to increase immobility in the forced swim task (suggesting an increase in depression-like behaviours) (Crestani et al., 2010; Pezuk et al., 2008). Other evidence for BNST involvement includes CRF antagonist intraperitoneal injections and subcutaneous administration of opioid agonists resulting in decreases in immobility, both of which act upon stress-associated brain regions including the BNST. More evidence comes from lentivirus overexpression of CRF directly within the BNST, which caused increased immobility during the forced swim test (Regev et al., 2011). Although the forced swim test has faced criticism with regards to its validity (does this task really measure depression, can a rat be depressed?), it is the case that commonly prescribed antidepressants do result in rodents swimming for longer – thus seeming to provide some predictive validity in humans (Lezak et al., 2017).

In general, an issue with these mechanistic studies in rodents is that it is not always clear how the behavioural measures of anxiety/fear/depression are translatable to

human traits. In particular, most of these paradigms are testing immediate responses to an aversive stimuli, and therefore are always testing a *state* response to an event. Although we know that state responses and traits are related (Schmitt & Blum, 2020), with state responses at least sometimes predicting traits (e.g., potentiated startle) (Grillon et al., 1993), when it comes to understanding the neural mechanisms underlying traits it is not clear that the mechanisms underlying an, even enhanced, state response should necessarily be the same (Saviola et al., 2020). In addition, although behavioural parallels can be drawn between rodent and human responses, there remain significant differences both neurally and behaviourally between rodents and humans (Gururajan et al., 2019). For example, some key mechanisms associated with DN in humans include rumination and the employment of maladaptive cognitive coping strategies. Presumably this is not something that rats do, or at least is something that would be hard to assess. Crucially, these aspects of DN have also been shown to involve pre-frontal areas which do not have obvious homologues in rodents (Fox & Kalin, 2014; Picó-Pérez et al., 2017; Shiba et al., 2017).

In addition to inferring human DN mechanisms from rodent responses to aversive stimuli, researchers have begun taking advantage of improvements in genetic engineering technologies to breed mice with particular genetic mutations that confer elevated baseline anxiety levels. These models may therefore be more indicative of the trait-like nature of DN in humans, although of course still do not permit the understanding of the more primate frontal-lobe mediated (or top-down) aspects of DN. In one study, researchers bred mice with an Erbb4 gene deficiency in somatostatin-expressing neurons (Ahrens et al., 2018). These mice demonstrated greater levels of anxiety, as measured via an elevated plus maze and open field test (Ahrens et al., 2018; Lezak et al., 2017) . By using a combination of electrophysiological, genetic, molecular, and pharmacological techniques the authors showed that the increased anxiety was mediated via increased excitatory inputs into the CeA, which in turn reduced inhibition of downstream BNST neurons. Thus, in agreement with studies that induce potentiated state anxiety, this study provides important additional evidence that the BNST is implicated in genetic mouse models of trait anxiety that are likely more similar to human DN. However, it should be noted

that the 'trait anxiety' in this case was still assessed by using the same 'response to an aversive stimulus' method as the studies mentioned above. Research assessing the presence of rodent anxiety behaviours in the absence of aversive stimuli, i.e at rest, could help to alleviate some of these methodological issues.

1.2.2.2.2 Dispositional Negativity In Non-Human Primates

Studies of non-human primates (NHP), typically rhesus macaques (*macaca mulatta)*, can perhaps provide more human-relevant insights. This is because macaques are evolutionarily closer to humans (with divergence occurring 25 million years ago, as opposed to 70 million for rodents) and have brains which are more similar than that of rodents (Murray et al., 2017). In addition, humans and macaques share comparable complex social environments, which are crucial for species survival and serve as key factors in the development and expression of DN behaviours (Fox & Kalin, 2014). In addition, work with macaques permits unique methodological opportunities to obtain metabolic measures from brain tissue samples, enabling exploration of brain activity following more naturalistic defensive behaviours in response to ethologically relevant threats than would be possible through experiments using motion-sensitive and highly controlled fMRI methods (Hur et al., 2019). Subsequently, neuroscientists have been developing NHP models of dispositional negativity and are using a variety of techniques including lesion methods, metabolic analysis, and neuroimaging to understand which brain regions may contribute to this trait.

In a series of studies, researchers used a large multi-generational cohort of macaques (n = 592) to model childhood anxious temperament (AT) and make inferences regarding the associated brain regions and networks. AT is a term almost synonymous with DN, but it is used to refer specifically to human childhood expression of DN (Fox, Oler, Shackman, et al., 2015). AT is studied in macaques by measuring anxiety markers following an ethnologically relevant threat paradigm. Specifically, monkeys undergo a no eye-contact (NEC) task, whereby a human intruder comes into a standard testing cage and presents their profile whilst avoiding direct eye-contact (Fox, Oler, Shackman,

et al., 2015). This procedure is known to induce anxiety in monkeys, with the level of anxiety being measured via mean increases in freezing, reductions in vocalisations, and increases in cortisol following a subsequent blood test. The procedure is similar those used to measure anxiety in human children (although humans are conversely aversive *to* eye-contact) with behavioural and endocrine responses also paralleling those assessed in human children (Birn et al., 2014).

This body of work has specifically implicated the BNST in levels of AT via various methodologies. For example, researchers used fluorodeoxyglucose positron emission tomography (FDG-PET) to assess metabolic neural activity following the NEC task (Fox, Oler, Shackman, et al., 2015). The findings revealed a significant association between AT and metabolic activity in a network of regions that includes the BNST, CeA, anterior hippocampus, orbital frontal cortex, anterior insular, and midbrain regions including the periaqueductal gray (PAG). Interestingly, these regions are very similar to the networks revealed in anxiety/fear state induction studies in rodents and in human fMRI work (see section 1.2.1). In another example, researchers used fMRI in a large subset of these macaques (n=378) to test for functional connectivity associations with AT, with results demonstrating that functional connectivity between the CeA and BNST was predictive of AT (Fox et al., 2018).

Importantly, two earlier studies using the FDG-PET method also identified similar brain regions/networks as being active following the NEC task, but crucially also reported that higher AT individuals demonstrated metabolic increases in these regions even in safe environments (Fox et al., 2008; Kalin et al., 2005). Therefore, this suggests that the neural network (and this model of AT/DN), reflects well the trait-like nature of DN which is characterised in part by increases in negative affect even in the absence of aversive stimuli (Fox et al., 2008; Hur et al., 2019; Kalin et al., 2005). This study also moves beyond an important limitation previously discussed whereby DN is typically assessed only using state-dependent threat-imminent responses.

In sum, NHP models of DN implicate the BNST as being a key part of neural network underlying the trait, a network which is highly similar to those seen in studies probing state anxiety and fear processing.

1.2.2.2.3 The BNST and Non-Clinical Dispositional Negativity in Humans

Given the limitations of animal models for studying human traits, human neuroimaging research provides an opportunity to non-invasively study brain mechanisms directly in human subjects. Non-clinical human neuroimaging studies of DN are important as they allow inferences regarding variation in DN free from the confounders, comorbidities, and effects of psychiatric disease and treatment (Shackman & Fox, 2021). As previously discussed, DN is highly predictive of internalising psychiatric disorders, particularly those related to depression and anxiety; BNST associations with these clinical disorders are discussed specifically in section 1.2.3.

There have been many human neuroimaging studies of DN and DN-associated trait variation (e.g., trait neuroticism, anxiety, and depression). Although recent reviews point to the BNST as being an important structure underlying DN (e.g. Hur et al., 2019), its involvement is primarily based upon inferences from animal work and state inductions of anxiety/fear, with surprisingly little human research implicating the BNST directly in non-clinical trait variation (Clauss, 2019). Part of this may be explained by the fact that many studies simply do not include the BNST in their analysis, with many methods relying on pre-defined brain maps which rarely include the BNST (Avery et al., 2016; Lebow & Chen, 2016). Nonetheless, other candidate subcortical brain regions that typically form part of the BNSTs identified functional network (e.g., the amygdala, anterior hippocampus, PAG) have been examined.

Early neurophysiological research suggested that hyperarousal of limbic structures, in particular the amygdala, was associated with DN. Recently, however, this view has been challenged as fMRI studies have not found convincing evidence for this limbic

hyperactivation hypothesis (reviewed in Silverman et al., 2019). Though increased activation itself may not be reliably associated with DN trait variation, fMRI research has implicated the amygdala via functional connectivity associations with the anterior cingulate cortex (ACC) and mPFC (Cremers et al., 2010; Silverman et al., 2019; Xu et al., 2019; Yang et al., 2020); findings supported by diffusion MRI research (Xu & Potenza, 2012).

A recent meta-analysis examining grey matter volume relationships with neuroticism reported consistent associations only with the mPFC and dorsal anterior cingulate cortex (dACC) (Liu et al., 2021). Other findings demonstrate cognitive evaluation of threatening stimuli results in reductions of amygdala activity with concomitant increases in mPFC and ACC structures (Kim et al., 2011). Together this evidence has led some researchers to suggest that DN variation in humans may have more to do with top-down regulation of emotion rather than increases in limbic-system baseline responding (LeDoux & Hofmann, 2018; Silverman et al., 2019). Given that many of these studies do not include the BNST however, and given the prominent role of the structure demonstrated in pre-clinical and human anxiety/fear processing (Avery et al., 2016), the BNST's role in non-pathological trait variation of DN should not be ruled out, despite the lack of direct evidence currently.

1.2.3 The BNST and Pathological Dispositional Negativity and Stress

Anxiety, fear, and stress are normal adaptive processes that can help to inform about, and prepare the body for, dangerous or difficult situations. For example, feeling anxious about walking down a dark alleyway at night will keep you more alert to danger, if you then encounter a hooded figure running towards you the fear/ stress response will kick-in and prepare a set of defensive behaviours that can keep you safe (i.e., fight, flight, or freeze). When these processes become overactive, or operational in inappropriate situations, they can become maladaptive and result in disordered behaviours (e.g., never leaving the house due to overwhelming anxiety). As well as the BNST being been closely linked to everyday anxiety, fear, and stress-processing, the

BNST has also been implicated in clinical disorders associated with pathological forms of these processes (Hur et al., 2019; Lebow & Chen, 2016).

1.2.3.1.1 Evidence for BNST Involvement in Anxiety Disorders

The BNST has become an area of interest for understanding anxiety disorders, largely due to the aforementioned mechanistic work linking the BNST to anxiety processing (Clauss, 2019). Until recently, however, many neuroimaging studies of anxiety disorders did not include the BNST in their analysis, either due to its relative obscurity (e.g., compared to the amygdala) or because of its small size (Lebow & Chen, 2016; Torrisi et al., 2019). Despite this, a growing number of studies have begun to observe BNST differences directly in anxiety disorder patients (Goossen et al., 2019). For example, Yassa and colleagues compared generalised anxiety disorder (GAD) patients to controls using a gambling task designed to illicit sustained stress, reporting that GAD patients showed decreased activity in the amygdala and increased activity in the BNST (Yassa et al., 2012). Similarly, in an experiment using unpredictable aversive screaming noises during an MRI scan, researchers reported heightened amygdala responses and an increased latent BNST response in GAD patients compared to controls (Buff et al., 2017). Increased activation of the BNST has additionally been reported in studies of social anxiety disorder (SAD) patients. For example, Figel and colleagues demonstrated an increase in phasic activation of both the CeA and BNST in response to unpredictable threat cues in SAD patients compared to controls (Figel et al., 2019). Using a cohort of SAD and GAD patients, another group of researchers reported that patients had stronger functional connectivity between the BNST and CeA at rest when compared to a control group (Torrisi et al., 2019). Interestingly, this study also reported that the task-free BNST functional connectivity patterns in SAD and GAD patients did not recapitulate those seen in the induced state anxiety responses of healthy participants. This may have implications for the commonly held hypothesis that the neural mechanisms underlying clinical anxiety disorders are simply extreme versions of those seen in studies of induced anxiety in healthy people (Torrisi et al., 2019).

Other anxiety disorders in which the BNST has been implicated include specific phobia (SP) where, for example, greater BNST activation has been reported for arachnophobes when shown pictures of spiders (Münsterkötter et al., 2015; Straube et al., 2007). In addition, female PTSD patients have been demonstrated to have higher sustained BNST activation in anticipation of the aversive stimuli when compared to controls (Brinkmann, Buff, Neumeister, et al., 2017). This finding of PTSD association is supported by rodent studies, which have largely focused on the BNSTs connections to mnemonic systems (e.g., hippocampus, amygdala) and its role in mediating stress-responding via its HPA axis projections (Choi, Evanson, et al., 2008; Choi, Furay, et al., 2008; Lebow & Chen, 2016; Miles & Maren, 2019). Finally, researchers demonstrated that panic disorder patients had greater phasic and sustained BNST responses during the anticipation of aversive verses neutral stimuli (Brinkmann, Buff, Feldker, et al., 2017).

Despite these results, it should be noted that other studies have reported no such anxiety disorder associations with the BNST. For example, a meta-analysis of fMRI differences in DN-linked disorders found evidence only for greater activation within the amygdala (not including the BNST) (Ashworth et al., 2021). In a task-free fMRI study of GAD patients, researchers reported no differences in BNST connectivity from controls and no association between CeA and BNST FC with trait anxiety (Wang et al., 2021). A recent large-scale analysis from the ENIGMA consortium tested over 1020 people with GAD and 2999 healthy controls (Harrewijn et al., 2021). Though only focused on grey matter volume, the authors reported no significant associations of GAD with any region in the brain (Harrewijn et al., 2021), with the authors suggesting that the clinical heterogeneity of this condition may be reflected by diverse neurological correlates that are hard to detect when studying GAD patients all together.

1.2.3.1.2 BNST Involvement in Clinical Depression

Anxiety and depression disorders are highly comorbid, and this may be partly explained by a similar underlying neural circuitry (Hur et al., 2019). Whilst there is much research linking wider amygdala functioning to depression (e.g. Castanheira et al., 2019), the evidence for BNST involvement in depression is limited to a few studies. For example, Abler and colleagues found that depression scores in major depressive disorder (MDD) patients correlated with activity in the bilateral SLEAc region that connects the CeA to the BNST (Abler et al., 2007). Although still in the early stages, several patients have undergone surgery to install deep-brain stimulation (DBS) electrodes into the BNST as an experimental treatment of serious and chronic treatment resistant depression. One patient, with comorbid anorexia nervosa, showed a remarkable recovery following implantation and was able to return home after spending years in a psychiatric ward and having experienced several suicide attempts (Blomstedt et al., 2017). A larger study of five patients with highly treatment resistant depression reported complete remission of two patients, substantial clinical improvement in a further two, and no effect in one patient (Fitzgerald et al., 2018).

Although these are preliminary case-studies with a small number of participants, the reports suggest that stimulation of the BNST may have remarkable effects on people with severe depressive symptoms. Of course, until further clinical studies are conducted strong conclusions should not be drawn from this, particularly in the absence of converging evidence from other imaging studies (e.g. Ashworth et al., 2021).

1.2.4 The BNST's Role in Addiction and Substance Use Disorders

Drug addiction can be defined as a chronically relapsing disorder that is characterised by compulsion to seek out and take the drug, loss of control in limiting intake, and the emergence of a negative emotional state when drug access is prevented (Koob & Volkow, 2016). Early research into the neurobiology of addictions focused on the hedonic pleasure that drugs can provide (Koob & Volkow, 2016). Whilst hedonic pleasure is a key facet, especially for understanding the initial motivations for drug-

taking, researchers later began to emphasise the equally important role of negative reinforcement on perpetuating use and increasing the likelihood of addiction (Koob & Volkow, 2016). Negative reinforcement refers to the process of drug consumption as a means to end to the stress, anxiety, and general dysphoria associated with drug withdrawal. As detailed throughout this chapter, the BNST forms a key part of the stress-system via extensive inputs to the HPA-axis and is associated with negative affect, in particular in relation to feelings of anxiety. Therefore the BNST has become a prime candidate for mediating the processes associated with negative reinforcement following drug withdrawal, with an increasing body of research demonstrating that drugs of abuse directly affect BNST cellular processes (Avery et al., 2016; Koob & Volkow, 2016; Maita et al., 2021).

1.2.4.1.1 Neurochemical Changes in the BNST Associated with Substance Misuse

Corticotropin release factor (CRF) is a key hormone related to addiction and drug-use, with CRF signalling in the BNST having been demonstrated to play an important role in rodent models of addiction (Stamatakis et al., 2014; Vranjkovic et al., 2017). For example, studies in mice report that promotion of CRF in the BNST directly result in increased drug seeking behaviour (Dong & Swanson, 2006; Erb & Stewart, 1999). CeA projections of CRF into the BNST were recently demonstrated to be activated by withdrawal from chronic alcohol exposure, with optogenetic inactivation of these projections resulting in the reversal of addiction associated anxiety behaviours in mice (de Guglielmo et al., 2019). CRF in the BNST is thought to effect drug-use via downstream outputs to the VTA (reviewed in Vranjkovic et al., 2017), an area heavily implicated in addictions via its central role in the dopamine reward/ motivation system (Bouarab et al., 2019). Evidence linking this pathway to addiction comes from chemical deactivation studies in mice, where BNST to VTA projections have been shown to be both necessary and sufficient for the promotion of drug seeking behaviours; particularly following stress (Erb & Stewart, 1999; Maita et al., 2021; McFarland et al., 2004; Vranjkovic et al., 2014).

Many commonly abused drugs have been shown to alter BNST CRF levels (Maita et al., 2021; Vranjkovic et al., 2017). In terms of alcohol, both binging and withdrawal have been shown to induce neuroplasticity in BNST CRF signalling (Pleil et al., 2015; Silberman et al., 2013). Additionally, there is evidence for alcohol-related changes to BNST glutamatergic signalling, something dependent on the NDMA receptor GluN2B (reviwed in Kash et al., 2015). Further implicating this mechanism, a study using post-mortem human brains of alcohol and cocaine addicts reported an upregulation of the GRIN2B gene, which encodes for the GluN2B receptor (Enoch et al., 2014). Dysregulation of the stress system can be long-lasting and can result in a cyclical process of increased negative affect followed by (temporary) substance-mediated relief (Centanni et al., 2019). This in turn causes more alterations to the BNST stress system, thus resulting in a downward spiral of addiction (Centanni et al., 2019; Koob & Volkow, 2016).

Another neurotransmitter implicated in the BNST addiction processes is noradrenaline (NE) (also known as norepinephrine) (Ch'ng et al., 2018; Maita et al., 2021). The BNST receives a strong projection NE from the nucleus of the solitary tract (NTS), with other regions including the locus coeruleus (LC) also contributing (Stamatakis et al., 2014). NE is thought to have a generalised effect on stress-induced anxiety behaviour, potentially linking it to the aforementioned negative reinforcement mechanisms (Ch'ng et al., 2018; Koob & Volkow, 2016). Researchers have shown increases in BNST NE levels following nicotine, cocaine, amphetamine, morphine, and ethanol consumption in rats (Jadzic et al., 2021). Rat research also suggests that NE signalling drives the affective symptoms of cocaine intoxication, with receptor antagonism in the ventral BNST decreasing stress-induced drug reinstatement and the anxiogenic effects of cocaine (Brown et al., 2009). Further evidence for NE involvement comes directly from a series of human studies, where treatment of cocaine addicts with NE agonists resulted in decreased stress-related drug-cravings and improvements in relapse outcomes (Fox et al., 2012; Jobes et al., 2011).

Evidence suggests that BNST involvement is not limited to stress induced drug re-uptake. In a study of cocaine-addicted male rats, researchers measured the return of drug-seeking behaviour in the presence of a stressor or drug-associated cues, whilst pharmacologically silencing BNST activity (Buffalari & See, 2011). The authors reported reductions in reinstatement during both conditions, suggesting that the BNST is sensitive to cue-based reinstatement, as well as reinstatement in response to stressors. Researchers typically emphasise a central role for the dopamine reward circuit in drug-cue responding, in particular via the VTA and the PFC, however amygdala associations have also been noted via the BLA (Feltenstein & See, 2008). It has been suggested that as the BLA does not directly project to the VTA it may then rely on indirect projections to the VTA via the CeA and BNST (Buffalari & See, 2011).

Several studies have reported that dopamine transmission is increased within the BNST itself following exposure to drugs including cocaine, alcohol, opioids, and nicotine (Carboni et al., 2000; Ch'ng et al., 2018). Although the role of dopamine in the BNST is not yet fully understood (Maita et al., 2021), a study of cocaine-addicted rats reported that dopamine inhibited activity within the dorsal BNST (dBNST) (Krawczyk et al., 2011). Along with previous work demonstrating the anxiolytic effects of reducing dBNST activity , this suggests that BNST dopamine projections (mostly from the VTA and PAG) may work to decrease stress responding and increase reward following drug administration (Krawczyk et al., 2011; Maita et al., 2021).

In sum, numerous neurochemical mechanisms that are targeted by drugs of abuse and/or are implicated in addiction behaviours have been linked to the BNST (Ch'ng et al., 2018; Koob & Volkow, 2016; Maita et al., 2021; Vranjkovic et al., 2017). In addition to those mentioned here, researchers have also identified changes to dynorphin, kappa-opioid, and mu opioid signalling (Maita et al., 2021). Whilst most research has focused on the BNST's role in the 'dark side' of addiction (i.e. feelings of negative affect) (Koob & Volkow, 2016), the BNST's role is likely complex and multifaceted, reflecting its diverse cellular make-up and complex pattern of afferent and efferent connections.

1.2.4.1.2 BNST Neuroimaging Associations with Substance Misuse

Despite the central role given to the BNST in human models of addiction, there is very little direct evidence from human neuroimaging studies demonstrating BNST involvement. Nonetheless, a handful of studies have tested for BNST associations with substance misuse (Dagher et al., 2009; Flook et al., 2021; Hur et al., 2018; O'Daly et al., 2012). For example, a recent study reported differences in BNST probabilistic structural connectivity to mPFC and insular regions in abstinent alcoholics verses light social drinkers (Flook et al., 2021). Interestingly, these differences were only significant for women; although interpretation of this study is somewhat hampered by small within-sex sample sizes (Flook et al., 2021). In another fMRI experiment researchers gave alcohol to people before a scan, demonstrating that alcohol acutely dampened BNST reactivity to emotional faces (Hur et al., 2018). Though not implicating the BNST in alcohol addiction *per se* the study at least demonstrates that alcohol has an effect on the BNST related to the processing of emotional stimuli, something consistent with theories of stress-related changes in the BNST underlying addiction processes. This research supported an earlier fMRI study that demonstrated that alcohol use disorder patients had increased FC between the BNST and amygdala when viewing fearful faces (O'Daly et al., 2012). The relative paucity of human research regarding BNST involvement in addiction/ substance use behaviours is striking given the substantial pre-clinical work. I attempt to address this question by testing BNST associations with alcohol-use measures in chapters 2,3, & 4.

1.2.5 Is the BNST Sexually Dimorphic?

It is frequently mentioned by researchers that the BNST is a sexually dimorphic brain region (Chung et al., 2002; Flook et al., 2020; Hulsman et al., 2021; Lebow & Chen, 2016; Maita et al., 2021; Zhou et al., 1995). This assertion is largely based upon evidence from rodent research, which appear to show differences in size, connectivity, and in the expression of sex-related hormones that act directly on the BNST or project

from the BNST to the HPA-axis (reviewed in Maita et al., 2021). As well, research in rats appear to show differences in sexual behaviours related to BNST function (Claro et al., 1995; Maejima et al., 2015). It should be noted that strong sex differences detectable in rodent brains are not necessarily translatable to humans (Eliot et al., 2021). For example the, appropriately named, 'sexually-dimorphic nucleus' (SDN) in rodents is 5-fold larger in male rats and is implicated in sexual behaviour, however its human homologue is only 1.6-fold larger with no replicable evidence thus far for a link to sexual behaviour (Eliot et al., 2021).

In humans, there is some evidence for sex differences in BNST anatomy and function (Allen & Gorski, 1990; Avery et al., 2014; Chung et al., 2002; Flook et al., 2020, 2020; Zhou et al., 1995). In terms of anatomy, a study of twenty-six age-matched male and female post-mortem human brains reported that the BNST was 2.47 times greater in males than in females (Allen & Gorski, 1990). A couple of different post-mortem studies have also found evidence for size differences between males and females in the same direction (Chung et al., 2002; Zhou et al., 1995). These studies are frequently cited as evidence of sexual dimorphism, however they are relatively few in number, contain small sample sizes, and have not been backed up by further in-vivo MRI evidence. In addition, the researchers do not appear to control for overall brain size which is known to be around 11% bigger in males (Eliot et al., 2021; Ritchie et al., 2018). If confirmed, however, that the male BNST is indeed close to 2.5 times larger on average then this difference would far exceed the average 11% difference in overall brain volume.

In terms of functional and structural connectivity of the BNST, a handful of studies have noted sex differences in humans (Avery et al., 2014; Feola et al., 2021; Flook et al., 2020, 2021). For example, Avery et al reported that 76% of the brain regions tested had greater diffusion MRI inferered structural connectivity with the BNST, although found relatively little evidence for differences in functional connectivity (Avery et al., 2014) and did not compare with structural connectivity of other brain regions.

In general, there is some evidence for differences in BNST structure and function between males and females and these are hypothesised to be linked to differences in behaviours and traits, particularly those related to anxiety (Flook et al., 2020, 2021; Lebow & Chen, 2016; Maita et al., 2021). However, large-scale studies in humans have demonstrated that sex differences between human brains are not especially robust and when present are largely overlapping and cannot be accurately described as dimorphic (Eliot et al., 2021). In addition, neuroimaging sex differences research has come in for criticisms because of failures to replicate and concerns regarding publication bias. One reason proposed for failures to replicate is the binary definition of sex often used in research, which may not reflect the underlying biology and complexities of, perhaps more dimensional, sex-related effects on the brain (Wiersch & Weis, 2021).

The BNST might be an interesting exception to this due to the presence of sex-linked hormone receptors and its potential role in mediating behaviours in the few traits and/or disorders that do reliably differ between males and females (i.e. higher anxiety levels in females and higher alcohol use disorder in males) (Bangasser & Wiersielis, 2018; Eliot et al., 2021; Lebow & Chen, 2016; Maita et al., 2021). Thus far, however, research on this topic in humans is mostly reliant upon small sample sizes and this, given the failures to replicate sex differences in other brain regions, means that further research, with large samples, is required to back up this frequently made claim of sexual dimorphism. The work in this thesis includes sex as a covariate in all analysis, however due to the nature of the data it was not possible to include a more dimensional scale, account for hormonal levels, or model the effects of the menstrual cycle (Hidalgo-Lopez et al., 2020).

1.3 The Genetics of the BNST

1.3.1 What can genetics tell us about the BNST?

Genetics research on BNST connectivity metrics could be useful for learning more about the biological mechanisms that underpin differences in connectivity. For example, techniques such as genetic correlation analyses allow for comparison of genetics information implicated in multiple phenotypes. Therefore, if it could be shown that some of the genetics underlying anxiety disorders are also implicated in BNST connectivity metrics, this may prove useful for developing medications to target these connections. In this section I will outline several genetic analyses techniques and their applicability to BNST research.

1.3.2 Twin-Based Heritability Analysis

Nearly all of human biology, traits, and behaviours are now understood to be influenced by a complex mix of environmental and genetic factors (Turkheimer, 2016). Heritability is the estimate of how much variation in a given characteristic, in a studied population, is attributable to genetics. Put more formally, heritability (H^2) is defined as the proportion of phenotypic variation (V_P) that is due to variation in genetic factors (V_G). As this estimate is a ratio ($H^2 = V_P / V_G$), H^2 is always a value between 0 and 1, with a higher number indicating that more of the population variance is explained by genetic factors (Jansen et al., 2015; Schwabe et al., 2017). An example of some heritability estimates include height, which ranges from H^2= 0.7- 0.9, and personality traits, which range from H^2 = 0.2 – 0.5 (Polderman et al., 2015).

Just because a trait aggregates within a family does not necessarily mean that genes influence the phenotype (Smoller et al., 2008). Non-genetic reasons, such as a shared (or common) environment (e.g., socioeconomic status, parenting style) may produce the same phenotype in multiple family members (Smoller et al., 2008). To separate these shared-environmental factors from genetic effects, researchers have made extensive use of twin designs. This method also permits researchers to estimate the heritability of a trait without access to the underlying molecular information or knowledge about all the possible environmental influences.

Heritability in twin-based analysis is conducted by comparing the concordance between monozygotic (MZ) twins (who are genetically identical) and dizygotic (DZ) twins (who share 50% of their alleles). If a trait is fully influenced by genetic factors, then you would expect the phenotypic correlation between MZ twins to be r=1, and for DZ twins to be r=0.5. For quantitative traits, H^2 is calculated as $2(r_{MZ} – r_{DZ})$, with r_{MZ} representing the phenotypic correlation of MZ twins and r_{DZ} the phenotypic correlation between DZ twins (Smoller et al., 2008, p. 63). Whilst twin-studies provide a unique way to understand the contribution of genetics to a phenotype, they rely upon the assumption that the shared environment across MZ and DZ twins is the same, an assumption that if invalidated may lead to inflated estimates of heritability. Researchers have used studies of 'perceived zygosity' to examine whether parents wrongly perceiving their children to identical or non-identical had an influence on the phenotype, with evidence suggesting that it does not (Conley et al., 2013).

Bivariate heritability analysis uses a similar approach, however in this model two traits are decomposed into genetic and environmental components. The covariance of the decomposition then tells you how much of the phenotypic correlation is explained by genetic or environmental factors. It is also then possible to compute the correlation between the genetic and environmental factors underlying each trait. The genetic correlation here then reflects the extent to which the genetic factors underlying one trait overlap with the genetic factors that influence the other (de Vries et al., 2021). For example, bivariate heritability analysis was conducted on a measure of well-being and depression (Baselmans et al., 2018). The model found that genetic factors explained 46% of the covariance between the traits. In addition, the model demonstrated that of this genetic covariance, the genetic factors influencing wellbeing and depression were correlated by -0.60, with the negative value indicating that the genetic factors which increased wellbeing had the opposite effect on depression (Baselmans et al., 2018; de Vries et al., 2021).

An important caveat to heritability estimates is that they are always specific to a particular time, place, and population. This means that it is not the case that

heritability represents a fixed unchangeable value; complex interactions with the environment are always present. For example, the heritability estimate of height may be lower in a population where some are malnourished (Bozzoli et al., 2009). This is because the environmental variable (access to food) will explain a higher proportion of that variance. On the other hand, in an equitable nutrient and calorie-rich environment, everyone has access to the same food to assist growth and thus genetic factors will play a bigger role in determining height. Heritability can also change over the course of development, with height, for example, having a H^2 of 0.2-0.5 in infancy and 0.7-0.9 in adulthood (Jelenkovic et al., 2016). With these important considerations acknowledged, knowing the relative amount of genetic variation that influences a trait can be the first step in assisting researchers to understand more about a given characteristics aetiology.

1.3.2.1 The Heritability of the BNST

The heritability of specific brain regions is a topic that is usually addressed by examining genetic contributions to their size (e.g., volume, thickness) and structural and/or functional connections to other brain regions. The heritability of brain regions varies, with not all areas demonstrating a significant genetic component. For those regions that do demonstrate heritability, recent estimates suggest volumetric measures and structural connectivity are typically between 20 – 60 % heritable (Elliott et al., 2018; Roshchupkin et al., 2016), with task-free fMRI ranging from 20-40% and task-based fMRI demonstrated showing little significant heritability (Adhikari et al., 2018; Elliott et al., 2018). An example of these results from a large heritability analysis in the UK biobank sample is presented in Figure 6.

Unfortunately, given the relatively new interest in the BNST by neuroimagers, the structure is almost always excluded from these large scale analyses and so estimates of heritability for any BNST metric in humans is absent. In macaques, however, researchers have used a familial multi-generational sample to assess the heritability of BNST metabolism and BNST FC to the CeA (Fox et al., 2018). Interestingly, they further employed bivariate heritability analysis to assess the phenotypic and genetic

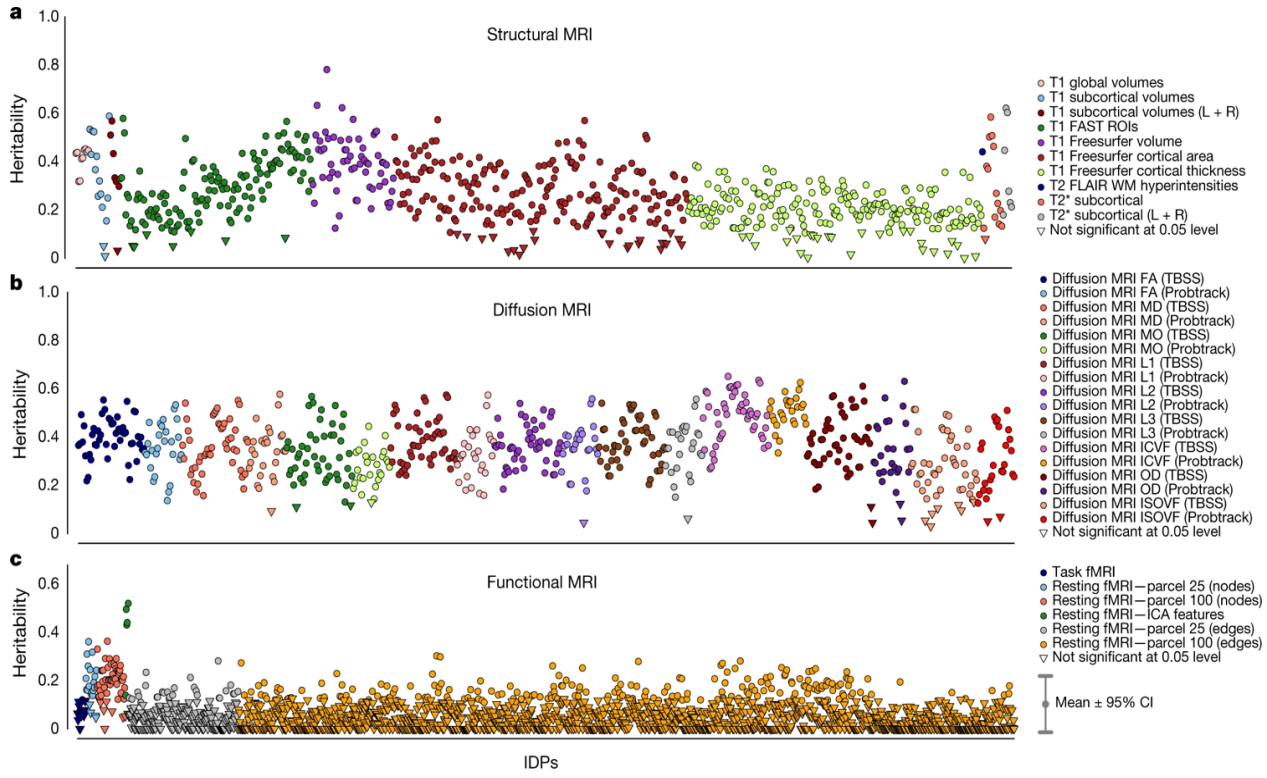

Figure 6 The Heritability of Brain Imaging Measures (adapted Elliot et al., 2018)

This figure demonstrates the heritability estimates of various neuroimaging derived phenotypes from the large UK Biobank sample (n= 8,428). The highest heritability estimates were for structural (e.g. volumetric) and diffusion MRI phenotypes. By contrast, functional MRI measures had fewer significantly heritible measures, and where significant had lower on average heritability estimates (~0.2). Note that these estimates are for SNP-based heritability, and so are typically lower than twin-based heritability estimates (see section 1.3.3).

correlations between these BNST measures and a model of DN (Fox et al., 2018). This work is discussed in more detail in Chapter 2 where a similar analysis is conducted in a large human sample.

1.3.3 Genome-Wide Association Studies

Research in the last few decades has comprehensively shown that most human traits are determined at least partly by genetic factors, meaning that demonstrating something is heritable alone is not especially interesting (Turkheimer, 2016). However, advances in genetic sequencing technologies have enabled scientists to directly analyse DNA, permitting tests of association between individual genetic variations (single nucleotide polymorphisms or SNPs) and traits or conditions (Uffelmann et al.,

2021; Visscher et al., 2017). These studies are typically conducted in large populations of unrelated individuals and are known as Genome-Wide Association Studies (GWAS).

GWAS is used to test which common genetic variants are associated with a given phenotype. GWAS can be used either for a case-control analysis (e.g. GAD vs healthy controls) or for the study of trait variation (e.g. level of day-to-day anxiety). Most complex phenotypes are polygenic, meaning that they are influenced by many individual SNPs of small effect, meaning that large samples ($n > 10,000$) are required in order to detect them (Uffelmann et al., 2021). Each individual's genetic information is recorded via a process known as genotyping. This is typically done by using specialist arrays that detects common SNP variants, followed by comparison of this information to a refence database for further imputation. Following careful quality control (see Chapter 3 for a description), a series of univariate regression analyses are run to test which variants are related to the phenotype. This results in millions of tests being conducted, meaning that strict multiple testing thresholds ($p< 5 \times 10^{-8}$) are needed in order to control for false positives. If a SNP passes this threshold, it is said to be 'genome-wide significant' (for reviews on the GWAS method see Tam et al., 2019; Uffelmann et al., 2021).

SNPs close to each other are often inherited together in blocks, a process known as linkage disequilibrium (Ramakrishnan, 2013). This is important because it means that SNPs are not fully independent and so it is not clear which of any significantly associated SNPs in a given block may be causally relevant to the phenotype. Typically a 'lead SNP' is identified based on the strength of association, with an understanding that follow-up functional/ mechanistic investigations will be required to identify the actual casual variant. In other words, GWAS provides flags along the genome identifying regions of interest, but does not alone signify the precise casual variants (Speakman et al., 2018).

Due to the large sample sizes needed and relatively recent decreases in cost relating to large-scale genetic sequencing, GWAS has only been available to most researchers in

the last decade, with the first ever GWAS being published in 2005 (Klein et al., 2005). In this relatively short time, GWAS has led to the discovery of more than 50,000 associations of genome-wide significant SNPs with diseases and traits (Tam et al., 2019). These discoveries have led to several novel insights regarding biological mechanisms underlying many phenotypes, for example, by revealing previously unknown neural processes involved in BMI variation in the general population (Speakman et al., 2018).

As well as following up on individual GWAS-significant SNPs to infer their function, additional tools are available in order to make use of the of the variants analysed in within the GWAS. This includes estimating the SNP-based heritability of a trait (h^2_{SNP}), correlating the genetic associations of one phenotype with another, and computing polygenic scores (PGS).

1.3.3.1 SNP-based Heritability

SNP-based heritability refers to the proportion of phenotypic variance explained by all SNP's on a given genotyping array (Yang et al., 2010). This method has the advantage of using the actual genetic information of (unrelated) individuals to understand how genetics contributes to a trait, thus circumventing some of the confounding environmental influences present in twin-based estimates (see section 1.3.3). Although methods exist to calculate h^2_{SNP} using each individual's genetic information, these methods are computationally expensive (Yang et al., 2017). A faster and more efficient way to calculate h^2_{SNP} is to use GWAS summary statistics (i.e. the statistics representing each SNP's relationship to a given phenotype) (Yang et al., 2017). This works by using the deviation of each SNP's observed $\chi 2$ test statistic from is expected value under the null hypothesis of no association (Shi et al., 2016). Although faster and widely used, this method has the disadvantage of not being able to model the effects of rare variants (typically excluded in GWAS), which may have large effects on the phenotype (Yang et al., 2017). SNP-based heritability estimates in general are typically

lower than those observed using twin-based analyses, an issue briefly discussed in section 1.3.3.3 and in Chapter 3.

1.3.3.2 Polygenic Scores

PGS are a particularly interesting use of GWAS data and refer to the assigning of a 'score' to an individual based upon how their own genetic variants align with results of a GWAS for any given trait (Choi et al., 2020; Yang et al., 2010). Put simply, if person A has more genetic variants associated with a disorder than person B, person A will have a higher PGS for that disorder and will be considered at greater relative risk for that disorder. PGS has the additional advantage of not being limited to SNPs that pass the genome-wide significance threshold, as many studies have shown that a PGS is more predictive when a higher number of SNPs are included; likely reflecting the highly polygenic nature of many traits and disorders (Yang et al., 2010). PGS may prove to be clinically useful if indeed they can meaningfully predict which individuals are more likely to have a disorder or certain trait. For example, people with a high PGS for certain types of cancer or serious mental health disorder could be targeted for earlier screening and interventions (Hyman, 2018).

1.3.3.3 GWAS criticisms and limitations

Despite these successes, GWAS has received criticism, in particular regarding the relatively low amount of variation that is explained by the results (e.g., 3-4% of BMI's variation vs an expected 65% based on twin-based heritability estimates) (Müller et al., 2018). The discrepancy between the amount of variance explained by GWAS and that predicted by familial designs is known as the 'missing heritability' problem (Yang et al., 2010; Young, 2019). This may be caused by several factors including: over-estimation of heritability in twin-studies, the effects of rare variants being not detectable by (typical) GWAS, too small sample sizes, strict multiple comparison corrections, not effectively controlling for ancestry effects, a narrow focus on European ancestry populations, and not accounting for gene-gene and gene-environment interactions

(reviewed in Tam et al., 2019). Many of these factors are likely to be addressed by increasing sample sizes, conducting further analysis using non-European samples, adopting whole-genome sequencing approaches, and improving methodologies such as finding more precise ways to account for ancestry effects (Tam et al., 2019). Other issues, such as the questionable usefulness of implicating more and more loci of small effects and the lack of clinical utility gleaned from GWAS analyses, may prove more difficult to address (Boyle et al., 2017; Müller et al., 2018) (for in-depth recent discussions of GWAS see Müller et al., 2019; Tam et al., 2019; Visscher et al., 2017).

1.3.3.4 Neuroimaging Genetics

GWAS of neuroimaging phenotypes, including measures of brain-region size, thickness, functional networks, structural connectivity, and white matter microstructure (collectively known as image-derived phenotypes or IDPs), has been made possible by the large-scale collaborative efforts of researchers to collect both genetic information and MRI images of thousands of participants. Because brain structure and function varies between individuals and differences detectable by MRI are known to underly various disorders (e.g., Alzheimer's or schizophrenia), researchers have been interested in using MRI to provide intermediate 'endophenotypes' that can be used to assess the genetic architecture of disorders and traits (Elliott et al., 2018). GWAS analysis of the large UK biobank (UKBB) neuroimaging dataset (n = 20,000) tested for genetic associations related to various IDPs. This analysis reported 148 clusters of associations between SNPs and all IDPs, except for those related to task fMRI measures. The SNPs identified were mostly related to genes involved in brain development and plasticity, many of which had in turn been previously associated with mental health disorders such as MDD and schizophrenia (Elliott et al., 2018).

Another large-scale initiative is the Enhancing Neuroimaging Genetics through Meta-Analysis (ENIGMA) consortium, who, as well as recruiting broadly from the general population to answer basic neuroscience questions, also focus on imaging individuals with specific disorder (Thompson et al., 2020). So far ENIGMA has published, or are

working on, the largest clinical neuroimaging studies to date, including those relevant to BNST-associated phenotypes such as GAD (n = 1112), MDD (n = 10,105), PTSD (n = 1968), and substance-use disorders (n = 3240) (Thompson et al., 2020). These large-scale studies are important because, as well as improving the reliability of IDP associations, they enable researchers to test for potentially informative associations between 1) disorder-linked brain differences 2) genetics associated with brain differences 3) genetics associated with disorders. For example, researchers used this technique to find evidence for a significant concordance between increased anxiety risk variants and variants associated with smaller amygdala volumes; an area of the brain implicated in anxiety disorders (van der Merwe et al., 2019).

1.3.3.5 GWAS of BNST associated variables

Despite GWAS now being possible with neuroimaging data due to large-scale data collection efforts, there have been no studies, to my knowledge, which have run a GWAS on any BNST-associated IDP. This is because, as mentioned previously, most of the commonly used brain atlases used in neuroimaging analysis do not include the BNST and so this region is simply omitted from these studies. Given the perceived importance, outlined in section 1.2, of the BNST and amygdala in mechanisms related to stress-associated psychopathology, a GWAS of BNST functional connectivity to various amygdala subregions forms the key research question of Chapter 3.

1.4 Thesis Research Summary and Aims

As stated in various places throughout the introduction, our knowledge of the human BNST is lacking in comparison to other brain regions and this relative lack of knowledge is at odds with the importance placed on this region by preclinical animal work. This thesis aims to increase our knowledge of the human BNST by employing a number of different neuroimaging and genetic analysis techniques.

Chapter 2: Functional Connectivity Networks of the Extended Amygdala – A Population Study

This chapter uses the large human-connectome project (HCP) sample (n=1200) to investigate the functional connectivity network of the BNST and contrast it with that of the closely linked CeA area of the amygdala. This work was performed in order to estimate how closely the BNST and CeA are related functionally under task-free conditions, a topic of much contention in the literature. Additionally, I tested the associations of these functional networks with measures of DN and alcohol use. Finally, based on previous work in macaques, I used twin-based heritability analysis to obtain a measure of how heritable functional connections between the BNST and various amygdala sub-regions are in humans.

Chapter 3: A Genome-Wide Association Study of BNST-Amygdala Functional Connectivity in the UK Biobank.

Here I use the very large UK biobank neuroimaging sample (n=20,000) to follow up on the analysis in Chapter 2 by 1) repeating the analysis of functional connectivity between the BNST and various amygdala sub-regions, 2) running a GWAS on these functional connectivity measures in an attempt to reveal the specific genetic associations underlying BNST-amygdala sub-region functional connectivity. In addition, I test for associations between BNST-amygdala sub region connectivity to traits putatively linked to the BNST including anxiety, depression, and substance-use measures.

Chapter 4: Subiculum – BNST Structural Connectivity in Humans and Macaques

In this chapter I investigate whether a structural connection between the BNST and subiculum is present in humans. This follows a large body of preclinical work that strongly implicates this connection as being important to stress-responding, thus potentially implicating it in processes relevant for several stress-related disorders. This

is approached in three separate ways. Firstly, macaque anterograde tract-tracing results are described following a collaborative study with Prof John Aggleton at Cardiff University (Berry et al., 2022), secondly, probabilistic diffusion tractography MRI analysis is run in a separate sample of macaques, and thirdly, probabilistic tractography analysis is repeated in the human adult HCP sample. Additionally, in the HCP sample measures of white-matter integrity are assessed within the tracts and are tested for association, heritability, and co-heritability with DN traits.

Chapter 2: Functional Connectivity Networks of the Extended Amygdala – A Population Study

2.1 Chapter Summary

Pre-clinical and human neuroimaging research implicates the extended-amygdala (ExtA) (including the bed nucleus of the stria terminalis (BNST) and central nucleus of the amygdala (CeA)) in networks mediating negative emotional states associated with stress and substance-use behaviours. The extent to which individual ExtA structures form a functionally integrated unit is controversial. In this chapter I use a large sample (n > 1,000 healthy young adult humans) to compare the intrinsic functional connectivity networks (ICNs) of the BNST and CeA using task-free functional magnetic resonance imaging (fMRI) data from the Human Connectome Project. I assess whether inter-individual differences within these ICNs are related to two principal components representing negative disposition and alcohol use. Building on recent primate evidence, I test whether within BNST-CeA intrinsic functional connectivity (iFC) is heritable and further examine co-heritability with the principal components. I demonstrate the BNST and CeA to have discrete, but largely overlapping ICNs similar to previous findings. I report no evidence that within BNST—CeA iFC is heritable; however, post hoc analyses reveals significant BNST iFC heritability with the broader superficial and centromedial amygdala regions. There were no significant correlations or co-heritability associations with the principal components either across the ICNs or for specific BNST-Amygdala iFC. Possible differences in phenotype associations across task-free, task-based, and clinical fMRI are discussed, along with suggestions for more causal investigative paradigms that make use of the now well-established ExtA ICNs.

2.2 Introduction

As described in the General Introduction (section 1.1), the ExtA is a basal forebrain macrosystem that describes a set of small, complex and heterogenous subcortical nuclei between the amygdala and ventral striatum (Alheid et al., 1998; Alheid & Heimer, 1988; Alheid, 2009; Cassell et al., 1999; Fudge et al., 2017; Johnston, 1923). Its principal structures include the bed nucleus of the stria terminalis (BNST) and the central nucleus of the amygdala (CeA), as well as portions of the shell of the nucleus accumbens and the sublenticular extended amygdala (SLEA) (an extension of amygdala neurons that connect the CeA and BNST) (Alheid, 2009; Cassell et al., 1999; Fox et al., 2015; Fox & Shackman, 2019; Lebow & Chen, 2016; Martin et al., 1991; Stamatakis et al., 2014). This macrostructure, or neuronal continuum, has emerged as key area of interest in the investigation of anxiety, fear, and substance use (see section 1.2) (Ahrens et al., 2018; Avery et al., 2016; Fox & Shackman, 2019; Gilpin et al., 2015; Goode et al., 2019; Goode & Maren, 2017; Lebow & Chen, 2016; Roberto et al., 2020; Stamatakis et al., 2014; Volkow et al., 2016).

Advances in neuroimaging techniques and the recent availability of high-quality ExtA anatomical masks (Theiss et al., 2017; Tillman et al., 2018; Torrisi et al., 2015; Tyszka & Pauli, 2016), have enabled several studies to use task-free fMRI (tf-fMRI) data to map the intrinsic connectivity networks (ICNs) of the BNST and/ or CeA regions (Table 1) (Avery et al., 2014; Gorka et al., 2018; Hofmann & Straube, 2019; Motzkin et al., 2015; Oler et al., 2012; Tillman et al., 2018; Torrisi et al., 2015, 2019; Weis et al., 2019). (See General Introduction section 1.1.2 for a brief discussion of ICNs)

CITATION	SAMPLE	N	COVERAGE	NATIVE EPI RESOLUTION	SMOOTHING	SCANNER(S)	CEA SEED	BNST SEED	TECHNIQUE
OLER ET AL, 2012	Combination of three independent samples of adolescents and children (aged between 7.8 - 18 years old)	105	Whole brain	3 x 3 x 3mm	6mm	3T Siemans Allegra, 3T Siemens Magnetom Trio Tim, 3T Discovery MR750	Manually prescribed in right amygdala on a standard 152-brain MRI template using ROI drawing tool in AFNI and Mai brain atlas.	N/A	Voxel-wise seed-based correlation analysis
AVERY ET AL, 2014	Adults from ages 17-57 (M = 30.6, SD +- 11.3) years old	99	Whole brain	3 x 3 x 4mm	3mm	3T Tesla Phillips Achieva	N/A	Manually prescribed on 7T anatomical GRASE image from a 42 year old Caucasian male.	Voxel-wise and targeted region seed-based correlation analysis
MOTZKIN ET AL, 2015	4 adult vmPFC lesion patients and 19 healthy adults.	23	Whole brain	3.5 x 3.5 x 3mm	4mm	3T Discovery MR750	N/A	Manually prescribed on MNI template brain using Mai brain atlas.	Cerebral blood flow case/ control seed-based correlation analysis
TORRISI ET AL, 2015	Healthy adult volunteers (M 27.3, SD = 6, years old)	27	Partial	1.3 x 1.3 x 1.3mm	2.6mm	7T Siemens Magnetom	N/A	Manually prescribed by 3 raters on subjects structural images.	Voxel-wise seed-based correlation analysis
GORKA ET AL, 2017	Same as Torrisi et al, 2015 sample	27	Partial	1.3 x 1.3 x 1.3mm	2.6mm	7T Siemens Magnetom	Mask from Tyszka & Pauili (2016) amygdala sub-regions atlas. 20% thresholded	As prescribed in Torrisi et al, 2015	Voxel-wise seed-based correlation analysis
TILLMAN ET AL, 2017	Healthy adults from the NKI dataset (M=25.3, SD=6.1 years old)	130	Whole brain	2 x 2 x 2mm	None	3T Siemens Magnetom Trio Tim	Mask from Tyszka & Pauli (2016) amygdala sub-regions atlas. Specially adapted (see supplementary methods in paper) and 25% thresholded.	Probabilistic mask developed by Theiss et al (2017). Thresholded at 25%	Voxel-wise seed-based correlation analysis
HOFMANN & STRAUBE, 2019	Healthy unrelated young adults from the Human Connectome Project (m=28, SD = 3.6, years old)	391	Whole brain	2 x 2 x 2mm	None	3T Skyra Siemans	N/A	Probabilistic mask from Torrisi et al, 2015. Thresholded at 20%	Dynamic causal modelling
TORRISI ET AL, 2019	Healthy adult volunteers (n= 30, 19 of whom from previous Torrisi et al 2015 sample) and 30 demographically matched patients with GAD and/or SAD.	60	Partial	1.3 x 1.3 x 1.3mm	2.6mm	7T Siemens Magnetom	Mask from Tyszka & Pauili (2016) amygdala sub-regions atlas	As proscribed in Torrisi et al, 2015	Case/ Control seed-based correlation analysis
WEIS ET AL, 2019	Healthy young adults (M=22.2, sD=3.62, years old)	57	Partial	0.859 X 0.859 X 1.80mm	3.6mm	7T MR950 General Electric	Mask from Tyszka & Pauili (2016) amygdala sub-regions atlas.	Probabilistic mask developed by Theiss et al (2017).	Voxel-wise seed-based correlation analysis
THIS STUDY	Healthy young adults, mostly made up of family groups, from the human connectome project (M=28.8, SD=3.7, years old).	1071	Whole brain	2 x 2 x 2mm	None	3T Skyra Siemans	Mask from Tyszka & Pauili (2016) amygdala sub-regions atlas. Same version as Tillman et al, 2017	Probabilistic mask developed by Theiss et al (2017). Thresholded at 25%	Voxel-wise and targeted region seed-based correlation analysis.

Table 1: Summary of Previous Resaerch on Human ExtA Intrinsic Functional Connectivity Networks

Despite some agreement regarding the ExtA ICNs (overlapping connections to medial prefrontal, hippocampal, wider amygdala, and thalamic regions), because of data acquisition, processing differences (such as brain coverage and choice of mask), and repeated use of the same samples, the convergence between studies can be hard to assess (Table 1). Thus, the first aim was to establish the ICNs of the BNST and CeA in a large (n=>1000) independent dataset - the Young Adults Human Connectome Project (HCP). A major strength of this approach is the use of the HCP data. The HCP contains high-quality imaging data, with most participants having undergone an hour of tf-fMRI (Glasser et al., 2013, 2016). Scan lengths longer than ten minutes are important as studies have highlighted the negative effects of short scan times on the stability of brain function estimates (Birn et al., 2013; Elliott et al., 2020). As mentioned in General Introduction section 1.2, there is some debate as to whether the ExtA acts mostly as a unified structure, or whether its components represent separate systems underlying different processes, in particular with regards to fear vs. anxiety processing or in the tracking of threat imminence (Fox & Shackman, 2019; Goode et al., 2019, 2020; Hur et al., 2020; Tillman et al., 2018; Walker et al., 2009). Therefore, I utilised this sample to examine the degree of overlap between the ICNs of the CeA and BNST; giving an indirect indication as to the similarity of their functions (Gorka et al., 2018; Oler et al., 2012; Tillman et al., 2018; Torrisi et al., 2015, 2019; Weis et al., 2019).

Whilst phenotypes such as anxiety, fear, depression, and substance use are often studied as if they were separate constructs, they are frequently highly comorbid and demonstrate an overlap of symptoms (Hur et al., 2019; Plana-Ripoll et al., 2019). Recent work has suggested that these phenotypes can be represented by broader overarching constructs, conceptualised as ‘dispositional negativity’ or simply ‘negative affect’ (see General Introduction section 1.2, Hur et al., 2019; Krueger et al., 2018; Shackman et al., 2018; Shackman, Stockbridge, et al., 2016; Shackman, Tromp, et al., 2016; Waszczuk et al., 2020). Genetic correlation studies have lent credence to this hypothesis, demonstrating that many phenotypically similar traits such as anxiety and depression also share a large proportion of underlying genetic risk factors (Allegrini et

al., 2020; Hur et al., 2019; Waszczuk et al., 2020). Human and non-human primate neuroimaging work suggests that dispositional negativity traits are associated with networks that include the ExtA, with a particular focus on the central amygdala (Hur et al., 2019). Consequently, to expand on this previous work, I conducted principal component analysis (PCA) on several self-report questionnaire items examining phenotypes of interest (anxiety, depression, fear, and alcohol use). I then used these principal components to test for associations with the ExtA ICNs. Human studies examining self-report trait associations with ExtA ICNs have so far been limited by small sample sizes, which hinder the power to detect an effect. Here, I addressed this issue by using a large population-level sample containing multiple measures of relevant phenotypes.

Psychological traits and aspects of brain function, such as iFC, can be partly attributed to genetics (Adhikari et al., 2018; Colclough et al., 2017; Elliott et al., 2018; Elliott et al., 2019; Yang et al., 2016). Because psychological traits are underpinned by the brain, understanding whether psychological traits and brain function share underlying genetic influences can be useful for identifying where research may be able to detect biological mechanisms contributing to both. Despite its apparent importance in a range of psychopathology-linked behaviours, to my knowledge only one study to date has examined genetic co-variance of psychopathology-associated traits with ExtA iFC. This study used a pedigree of rhesus monkeys to demonstrate that iFC between the CeA and an area consistent with the BNST was co-heritable with anxious temperament (pgr = 0.87) (Fox et al., 2018). Whilst heritability estimates do not alone provide information about the nature of shared genetic mechanisms (Turkheimer, 2016), this result suggests that ExtA iFC and anxiety-related traits may be influenced by common genetic factors.

Therefore, I used the kinship structure of the HCP data to estimate within BNST – CeA iFC heritability and co-heritability with the principal components. Thus, I aimed to extend the non-human primate finding of Fox et al. to humans by demonstrating that

within BNST-CeA iFC is both heritable and co-heritable with anxiety-related traits (A. S. Fox et al., 2018). Previous evidence has also reported significant BNST iFC to other amygdala sub nuclei in humans (Hofmann & Straube, 2019). Hence, I ran an additional post-hoc analysis to assess the heritability and co-heritability (with the principle components) of BNST iFC to the centromedial, laterobasal, and superficial amygdala regions.

2.3 Methods

2.3.1 Sample descriptions

2.3.1.1 The Human Connectome Project

Participants were drawn from the April 2018 release of the Young Adults Human Connectome Project (HCP) study (n=1206) (Van Essen et al., 2012). Participants were between the ages of 25-37 and primarily made up of family groups, with an average size of 3-4 members and most containing a MZ (273) or DZ (166) twin pair. Participants were excluded during initial recruitment for psychiatric, neurological, or other long-term illnesses, although participants who were overweight, smoked, or had a history of recreational drug use and/or heavy drinking were included (Van Essen et al., 2012). For the imaging analysis, the samples included participants who had at least one tf-fMRI scan (n=1096). Of these, there were 596 females and 500 males. For detailed recruitment information and for a full-list of procedures see:

https://www.humanconnectome.org/study/hcp-young-adult. See the supplementary material for a breakdown of participant's demographic information.

2.3.2 Principal Component Analysis

In this study, phenotypes of interest were those related to anxiety, depression, fear, and substance use. There are multiple instruments in this dataset measuring each of these constructs and these phenotypes are frequently highly correlated. Therefore, I performed PCA and reduced data dimensionality by extracting the minimum number of latent components that summarise the maximum amount of information contained in the original measures. The questionnaire measures outlined in the next section were joined into a single dataset and were tested for sampling adequacy using a Kaiser-Meyer-Olkin test (KMO; Dziuban and Shirkey, 1974), followed by the Barlett's test of sphericity. The measures were standardised automatically during analysis and missing values were imputed by the mean of the variable (a maximum of 25/1206 datapoints, see Table 2). Following the PCA, components were selected if they had an eigenvalue

ITEM	QUESTIONNAIRE	DESCRIPTION	N (/1206)	MEAN	SD
DSM_ANXI_RAW	Achenbach Self Report	SUB-scale reflecting DSM oriented anxiety traits	1198	3.94	2.70
DSM_DEPR_RAW	Achenbach Self Report	SUB-scale reflecting DSM oriented depression traits	1198	4.24	3.45
ASR_ANXD_RAW	Achenbach Self Report	Sub-scale reflecting 'anxious-depression' (traits empirically derived)	1198	5.93	5.40
FEARSOMAT_UNADJ	NIH Fear Affect Survey	Somatic symptoms related to arousal	1205	52.03	8.31
FEAR_AFFECT_UNADJ	NIH Fear Affect Survey	Self-reported fear and anxious misery	1205	50.28	8.08
PERCSTRESS_UNADJ	Stress and Efficacy Self Report	A scale representing how unpredictable, uncontrollable and overloading respondents find their lives	1205	48.48	9.17
TOTAL DRINKS 7 DAYS	Alcohol use survey	Self-reported alcoholic drinks over the last seven days	1179	4.75	7.04
SSAGA_ALC_D4_DP_SX	Alcohol use survey	DSM4 Alcohol dependence criteria count	1204	0.55	0.84
SSAGA_ALC_D4_AB_SX	Alcohol use survey	DSM4 Alcohol abuse symptoms count	1204	0.27	0.58

Table 2: A description of questionnaire measures

N = to the number of participants who had data for that particular questionnaire, SD = standard deviation, PCA = principal component analysis

greater than 1 (Bourbon-Teles et al., 2019). The PCA was conducted in R Studio using the software package FactoMineR (Lê et al., 2008).

2.3.3 Questionnaire Selection

The questionnaires used were administered to each participant by the HCP team via a computerised adaptive testing method (Pilkonis et al., 2013), with all measures being selected from the NIH toolbox, a well validated set of metrics for quick assessment of cognitive, emotional, sensory and motor functions (Pilkonis et al., 2013; Weintraub et al., 2013). Questionnaires were selected if they measured anxiety, stress, fear, or substance use. Where individual items were not provided, I used the relevant questionnaire subscales (Table 2). For the substance use metrics, I only included measures of alcohol use, as self-reported smoking and 'harder' drug use rates were low (< 20% for tobacco use, < 8% ever used cocaine). In total nine measures were selected (Table 2).

2.3.4 Image Acquisition and Pre-Processing

2.3.4.1 HCP Image Acquisition

All images were acquired on a 3 Tesla Skyra Siemens system using a 32-channel head coil, a customised SC72 gradient insert (100 mT/m) and a customised body transmit coil. Tf-fMRI scans took place over four 15-minute runs, split between two sessions (two runs in each session). Participants were instructed to keep their eyes open with a fixation cross being projected onto a screen with a dark background in front of them. Within each session oblique axial acquisition alternated between phase encoding in a left-to-right or right-to-left direction. Functional images were acquired using a $2mm^3$ multiband gradient echo EPI sequence (TR 720ms, TE 33.1ms, 72 oblique axial slices, FOV 208 X $108mm^2$ flip angle 52^o matrix 104 x 90, echo spacing 0.58 ms, 1200 images per run). High resolution anatomical images were also acquired using a 0.7mm isotropic T1-weighted 3D magnetisation-prepared rapid gradient echo sequence (TR

2400ms, TE 2.14ms, FOV 224 x 224 mm^2, flip angle 8^o) (Glasser et al., 2013; Smith, Andersson, et al., 2013).

2.3.4.2 HCP Pre-processing

I used the minimally processed tf-fMRI 3T dataset, described elsewhere (Glasser et al., 2013). Scripts to run the pipeline are freely available online at https://github.com/Washington-University/HCPpipelines. Briefly, the pipeline applies gradient distortion correction to account for spatial distortions, followed by volume realignment to compensate for subject motion, co-registration of the fMRI data to the structural image, non-linear registration to MNI space, intensity normalisation to a mean of 10,000, bias field removal, and masking of data with a brain mask. Structured noise was cleaned from the data by combining independent component analysis (ICA) with the automated component classifier tool FIX ICA (Griffanti et al., 2014; Salimi-Khorshidi et al., 2014). Finally, head motion time series were regressed out using a 24 confound time series containing the 6 rigid body parameter time series, their temporal derivatives as well as the resulting 12 regressors squared (Glasser et al., 2013, summarised by Hofmann & Straube, 2019). This pipeline was optimised for the HCP dataset and had the aim of maximising the reduction of structured noise components, such as those caused by subject motion, whilst retaining spatially specific bold signal components (i.e. ICNs) (Glasser et al., 2016). This was reportedly achieved with better than 99% accuracy (Glasser et al., 2016; Griffanti et al., 2014). To reduce the effects of signal drop-out (Schwaferts, 2017), for each participant a single 4D image was created by taking a mean of their scans using the FSLMaths (Jenkinson et al., 2012) mean function. To further mitigate against spurious and systematic iFC correlations resulting from subject motion, I included mean frame-wise displacement (MeanFD) as a covariate in the phenotype and (co)heritability analyses. Participants with a MeanFD of > 0.2mm were excluded from these analyses (n = 9) (Power et al., 2012). As a final precautionary check, I ran a correlation between MeanFD and the phenotypes of interest (the principal components and functional connections), which revealed no

significant correlations (supplementary material).

2.3.5 Seed-based Correlation Analysis

2.3.5.1 ExtA Seed Regions

I used two anatomically-derived bilateral seed regions for the ExtA, one for the BNST and one for the CeA (Figures 7, 8). The masks were downloaded on the 25th of March 2019 from a repository on the NeuroVault website (https://neurovault.org/collections/3245) (Tillman et al., 2018). All analyses were run separately for each seed region. Both seeds were thresholded at 25% before use (Tillman et al., 2018) (Figures 7, 8).

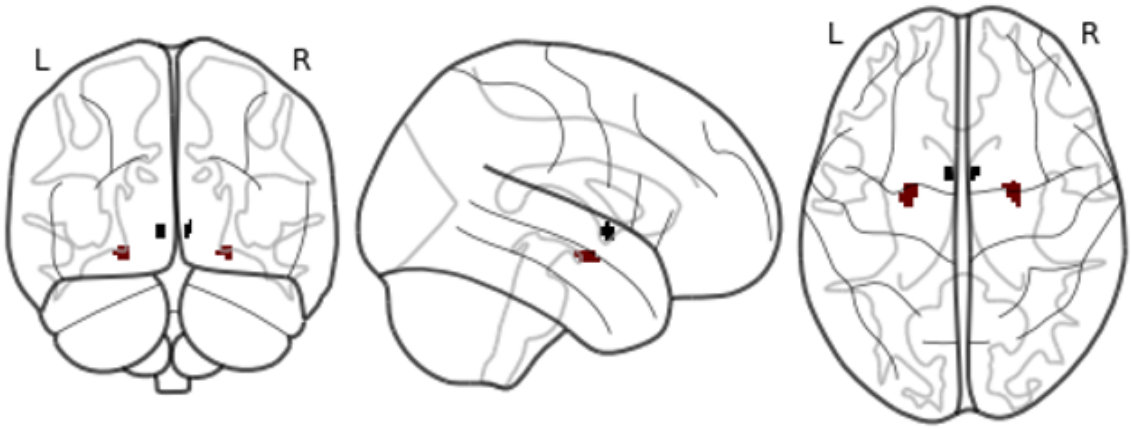

Figure 7: The bed nuclues of the stria terminalis (BNST) (blue) and the central nucleus of the amygdala (CeA) (red).

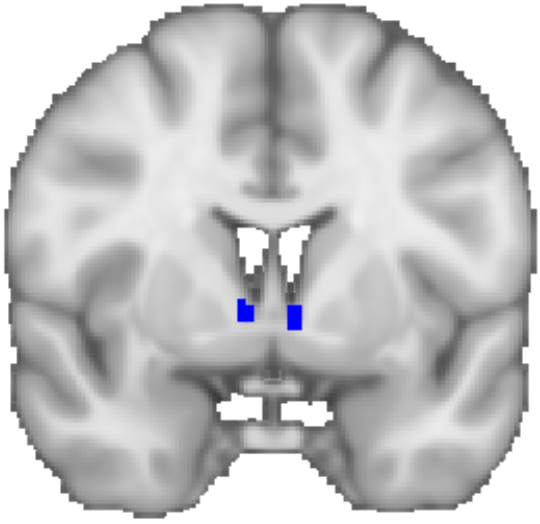

Figure 8: The bed nucleus of the stria terminalis (BNST) seed (blue), coronal section.

The 3T 2mm BNST mask was generated by a manual segmentation process undertaken on 10 healthy individuals using a scanning sequence that provided high grey matter/ white matter/ CSF contrast (Theiss et al., 2017) (Figures 7, 8). The protocol was found to have high reliability amongst raters (Dice similarity coefficient ≥ 0.85).

The CeA mask was generated by an experienced neuroanatomist, building on a process developed through a series of studies (Birn et al., 2014; Najafi et al., 2017; Oler et al., 2012, 2017b; Tillman et al., 2018). Briefly, this was achieved using a specially processed version of the CITI168 high-resolution (0.7 mm), multimodal (T1/T2) probabilistic template (Tyszka & Pauli, 2016), and was guided by the Mai human brain atlas (Mai et al., 2015).

2.3.5.2 Whole-brain Seed-based Correlation Analysis

Seed-based correlation iFC analysis provides a measure of temporal coherence between a seed-region's blood-oxygenation-level-dependent (BOLD) activation over time and that of the target regions. Temporal coherence in tf-fMRI data is used to infer iFC (Battistella et al., 2020; Suárez et al., 2020; Thomas Yeo et al., 2011). To run the analysis I used the *ciftify_seed_corr* tool downloaded from

https://edickie.github.io/ciftify/#/ (Dickie et al., 2019), which was in turn adapted from the HCP minimal processing pipeline (Glasser et al., 2013). This works by first extracting a mean time-series of the seed-region. This time-series is then correlated with the mean time-series of the target regions, producing a Fisher's r correlation map. These correlation coefficients are then converted to normally distributed z-scores using a Fisher r-z transform (Fisher, 1915). This produces a z-map for each participant that represents the strength of the correlation of BOLD activity for each target region and the seed-region. I used a whole-brain voxel-wise approach, meaning that the target regions were every 2mm voxel in the brain.

2.3.6 fMRI statistical analysis

2.3.6.1 Permutation-based One-sample T-tests

Following the creation of a single z-map for each participant, all of these images were visually inspected. 23 participants had images removed from further analysis due to having either sections of the signal missing or for having z-score distributions containing too many values within the outer or inner tail distributions (assessed via fslstats -r -R and histogram plots). The remaining 1071 participants had their images merged across all participants to create a 4d image using the fslmerge tool (Jenkinson et al., 2012). Permutation-based one-sample t-tests were then run to see which voxels had BOLD activity that was significantly correlated with the seed-regions across all participants. This was done using FSL's PALM command line tool (Winkler et al., 2016).

For the quantification of the whole brain ICNs, I wanted the results to be generalisable to the wider population, thus I was not interested in the influence of family-effects across the whole network. Therefore, because the sample was made up of siblings, it was important to account for relatedness such that model estimations were not inflated. PALM permits a kinship matrix that details the family structures within the population. PALM shuffles the data within and between blocks according to this family

structure, avoiding relatedness confounding the results. The kinship file was generated with the HCP2Blocks MATLAB script provided online at https://brainder.org/2016/08/01/three-hcp-utilities (Winkler et al., 2015).

PALM has several optional commands. I used Threshold-free Cluster-Enhancement (TFCE) and Gamma approximation. Briefly, TFCE enhances cluster-like structures in the data without having to define somewhat arbitrary cluster thresholds beforehand (S. M. Smith & Nichols, 2009). Gamma approximation is an option used to speed up the analysis by running a smaller number of permutations, computing empirically the moments of the permutation distribution and then fitting a gamma distribution (Winkler et al., 2016). The number of permutations used was 1000.

2.3.6.2 Post-hoc Thresholding of PALM Output Images

Given the large sample size, the vast majority of voxels in the brain were statistically significantly correlated to the seed-regions after family-wise error rate (FWER) correction. To reveal meaningful connections and to reduce noise, I further thresholded the images post-hoc using the t-statistic. This was done by visually inspecting the output images and choosing a t-score that met the criteria of delineating meaningful anatomical structures in the brain, whilst keeping the maximum amount of signal (Tillman et al., 2018). The t-threshold I used for both seed-images was 9. Using the -saveglm option from PALM, This equated to a minimum Cohen's d value of 0.275 (Winkler et al., 2016). Whilst I was confident this was an appropriate threshold, given the somewhat arbitrary nature of this method, thresholded and un-thresholded output images have been uploaded to NeuroVault for inspection at https://identifiers.org/neurovault.collection:8076.

2.3.6.3 Analysing Shared and Unique BNST and CeA Networks

To assess the shared ICNs between the BNST and CeA, I used a minimum conjunction (Boolean 'AND') to combine the t-thresholded PALM output images of each seed (Nichols et al., 2005; Tillman et al., 2018). This created a new image displaying the areas of ICNs that overlapped between the two ExtA regions.

To assess the unique BNST and CeA networks, I performed a single group paired difference t-test using the method outlined on the FSL GLM website (https://fsl.fmrib.ox.ac.uk/fsl/fslwiki/GLM#Single-Group_Paired_Difference_.28Paired_T-Test.29). Briefly, to get the unique BNST ICN, I subtracted each participants BNST z-score image from their CeA z-score image and then ran a one-sample permutation t-test on this difference map. This was repeated for the CeA network (CeA – BNST z maps, followed by a one-sample t-test). A mask was used to restrict analysis to the regions that were found to be connected to one or both seeds in the original one-sample t-tests, thus avoiding the need to interpret differences in regions not significantly connected to the seeds (Tillman et al., 2018).

2.3.6.4 Region identification

Connected regions were identified using a mixture of the Oxford Cortical/ Sub-cortical atlas and the Juliech Histological atlas (Figure 9), both provided with FSL (Jenkinson et al., 2012). For iFC to basal ganglia structures and the hypothalamus I used a collection of masks provided online at Neurovault (https://identifiers.org/neurovault.collection:3145) (Pauli et al., 2018).

2.3.7 Intrinsic Connectivity Networks and Principal Component Association Tests

Following the one-sample t-tests for each seed region, I then created a mask of the t-thresholded significantly connected regions. This mask was then applied to the 4d image of participants connectivity z-maps to select only the thresholded connected

voxels for association testing with the PC's and for gender effects. I used the PALM command-line tool, with TFCE, Gamma-approximation, and event blocks to control for family relatedness (see section 2.5.1). As well as the standard correction for multiple comparisons within each image, PALM further allows for correction across different contrasts with the -corr-con option (Winkler et al., 2016). This option was used along with the -demean function, which mean-centres the variables, and the -cmcx function, which allows for synchronised permutations accounting for repeated elements in the design matrix. Three tests were run in total on each seed-image, one each for the two principal components and one for gender (male, female). Age, age^2, gender, and mean framewise displacement were used as covariates for all tests, except that gender was of course not included as a covariate for the direct test of gender effects. The number of permutations was 2000 for each test.

2.3.8 Within BNST – Amygdala Heritability, Co-heritability, and Phenotype Association Analysis.

I used the SOLARIUS package for R (Ziyatdinov et al., 2016) to assess the following 1) the heritability of within BNST-CeA iFC 2) the co-heritability of the within BNST-CeA iFC with each of the two principal components 3) the phenotypic (rho), genetic (rhog), and environmental (rhoe) correlations between BNST-CeA iFC and each of the two principal components. I further ran a post-hoc analysis, conducting the same tests but examining BNST iFC with the superficial, centromedial, and basolateral amygdala regions. These regions were defined using the Juelich Histological Atlas, thresholding the probabilistic masks at 50% (Eickhoff et al., 2005) (Figure 9).

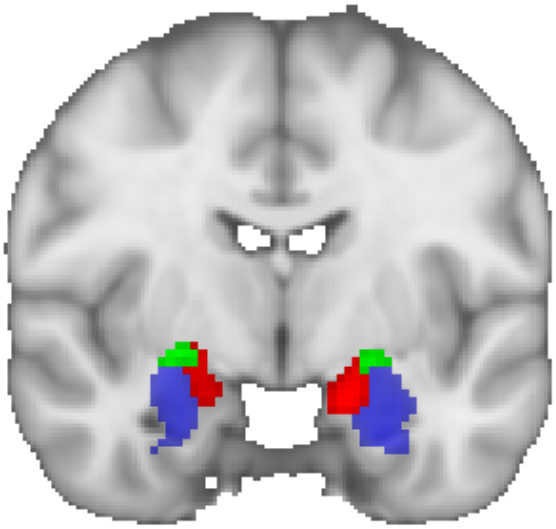

Figure 9: The Juelich Histological Atlas (Eickhoff et al., 2005) amygdala subregions.

Blue = basolateral, green = centromedial, red = superficial. Masks shown were thresholded at 50%

SOLARIUS is the R version of the widely used SOLAR-eclipse software for genetic analysis (Almasy & Blangero, 2010). SOLAR uses a kinship matrix to estimate the proportion of variance in a phenotype attributable to additive genetics, the environment, or to residual error. In this case, I was only permitted to calculate the additive genetic component, as to partition environmental and error effects you require household information that is not provided by the HCP. In this model, monozygotic twins are given a score of 1 and dizygotic twins / siblings of 0.5 to indicate the estimated proportion of shared genetic variation. Half-siblings were excluded from the analysis (n = 88). The pedigree file was created using the HCP2Solar MATLAB function, a tool specifically designed for the HCP participants (https://brainder.org/2016/08/01/three-hcp-utilities) (Winkler et al., 2015). Because the model is sensitive to kurtosis, the phenotype values were inverse normally transformed. SOLARIUS allows analysis of co-heritability by computing bi-variate genetic correlations (Kochunov et al., 2019). During the analysis SOLARIUS computes an estimate of phenotypic, genetic, and environmental correlation between the variables, which I used to assess the relationships between the clusters iFC and component scores. Participants were excluded if they had a MeanFD > 0.2mm (N = 9). The covariates for all analyses were MeanFD, sex, age, age^2, sex * age, and sex * age^2.

The final number of participants in these analyses was n = 933. For discussion on using SOLAR for genetic neuroimaging see (Kochunov et al., 2019).

2.4 Results

2.4.1 BNST and CeA Intrinsic Functional Connectivity Networks

All connected regions described below are the regions visible after the thresholding at t => 9. Negative correlations were observed only within small regions surrounding the ventricles or white matter, and are not reported here. See tables 3 & 4 for significantly connected clusters with more than 10 voxels. Interactive 3D images of the results have been uploaded to NeuroVault at https://identifiers.org/neurovault.collection:8076.

CLUSTER INDEX	VOXELS	MAX T	X	Y	Z	HEMI	REGION(S) IN CLUSTER
271*	6135	16.6	45.8	30	46.2	B	Precuneus cortex, lateral occipital cortex, occipital pole, posterior cingulate gyrus, intracalcarine cortex, middle/superior temporal gyrus, angular gyrus, left hippocampus dentate gyrus, left hippocampus subiculum, left hippocampus cornu ammonis, lingual gyrus, ventral posterior thalamus
270	3419	15.3	47.5	53.6	61.5	B	Post-central gyrus, pre-central gyrus, primary somatosensory cortex, pre-motor cortex, primary motor cortex, inferior-frontal gyrus, Brocas area, anterior cingulate gyrus
269	665	14.8	70.9	53.4	41.5	L	Central opercular cortex, primary auditory cortex, insular cortex
268	565	15.2	18.5	54.7	41.9	R	Central opercular cortex, primary auditory cortex, insular cortex
267	279	13.1	45.2	91.8	39.3	B	Frontal pole, paracingulate gyrus, frontal medial cortex
266	138	11.9	33.3	24.9	28.2	R	Occipital fusiform, lingual gyrus
265	136	13	56.5	77.2	59.7	L	Middle frontal gyrus, superior frontal gyrus
264	86	12.1	64.6	62.7	65.2	L	Pre-central gyrus, middle frontal gyrus, pre-motor cortex BA6L
263	50	10.7	20.1	74	49.8	R	Middle frontal gyrus, Brocas area BA45, inferior frontal gyrus
262	43	12.2	32.5	77.2	59.9	R	Superior frontal gyrus, middle frontal gyrus
261	36	15.4	32.5	54.2	27.9	R	Hippocampus cornu ammonis, hippocampus dentate gyrus, hippocampus subiculum, posterior amygdala
260	32	11.2	27.7	80.7	30.3	R	Frontal pole, frontal orbital cortex
259	24	10.6	24.5	36.8	25.2	R	Temporal occipital fusiform cortex
258	22	11.5	70.2	29.4	30.1	L	Lateral occipital cortex inferior division
257	21	11.4	63	79.6	29.9	L	Frontal orbital cortex
256	21	12	35.9	62.9	29.3	R	Amygdala superficial group
255	19	10.2	62.8	17.8	38	L	Visual cortex V3VL, visual cortex V4
254	19	11.9	53.8	62.2	29	L	Amygdala superficial group
253	16	12.4	62.3	65.6	27.3	L	Insular cortex (anterior, ventral regions)
252	14	11.5	28.2	66.7	27.2	R	Insular cortex (anterior, ventral regions)
251	14	10	29.6	35.2	66.4	R	Superior parietal lobule 7AR
250	14	10.9	32.1	72.6	58	R	Middle frontal gyrus
249	13	10.5	57.2	16	44.6	L	Occipital pole, visual cortex V2 BA18L, visual cortex V3VL
248	13	10.1	52.3	26.1	63.9	L	Superior parietal lobule 7P
247	12	11.3	40.7	88	31.3	R	Frontal medial cortex, frontal pole
246	12	47.9	41.1	63.1	35.8	R	Thalamus (anterior)
245	12	10	24.9	20.1	42.9	R	Lateral occipital cortex superior division
244	12	10.6	68.4	22.7	38.8	L	Lateral occipital cortex inferior division
243	11	16.8	41.6	66.9	37.4	R	Caudate (posterior)
242	10	10.7	61.9	33.7	65.2	L	Lateral occipital cortex superior division, superior-parietal lobule 7AL
241	10	10.7	61.2	35	26.4	L	Temporal occipital fusiform cortex

Table 3: Significantly connected clusters to the BNST

Significantly connected clusters to the BNST following the one-sample permutation test. Images were thresholded at t=>9 before clusters were identified. Brain regions were listed if they had > 50% chance of being within a cluster. Max t is the maximum t-stat located within a cluster. X, Y, and Z columns represent the location of the centre of gravity for the cluster. Hemi indicates the hemisphere in which the cluster resides where B = bilateral, R = right and L = Left. For ease of interpretation clusters shown are those with a minimum of 10 connected voxels.

* The large 271 cluster may better be reflected as two clusters, one within the occipital/ parietal cortex and the other covering the left hippocampal regions seen in cluster 261.

CLUSTER INDEX	VOXELS	MAX T	X	Y	Z	HEMI	REGION(S) IN CLUSTER
101	1303	20.3	71	55.9	52.3	L	Somatosensory cortex BA1/ BA3b, primary motor cortex BA4a, premotor cortex BA6, planum temporale, central opercular cortex, precentral gyrus, temporal pole, primary auditory cortex, dorsal posterior insular
100	1141	19.9	18.9	56.6	54.1	R	Somatosensory cortex OP4/ BA3b/ BA1, primary motor cortex BA4p, planum temporale, central opercular cortex, precentral gyrus, primary auditory cortex
99	831	18	72.8	44.4	38.8	L	Superior temporal gyrus anterior and posterior division, temporal pole, lateral occipital cortex superior division, supramarginal gyrus posterior division, angular gyrus, inferior parietal lobule
98	803	17.7	16.8	48.7	36.5	R	Superior temporal gyrus anterior and posterior division, temporal pole, middle temporal gyrus posterior division, supramarginal gyrus posterior division, angular gyrus, lateral occipital cortex superior and inferior division
97	318	14.9	45.8	91.7	49.2	B	Frontal pole (dorsal), superior frontal gyrus (anterior)
96	263	46.5	32.8	60	28.5	R	Insular cortex, superficial amygdala, temporal pole, laterobasal amygdala, hippocampus cornu ammonis, hippocampus dentate gyrus, sublenticular extended amygdala
95	221	47.4	56.4	59.5	28.3	L	Insular cortex, superficial amygdala, temporal pole, laterobasal amygdala, hippocampus cornu ammonis, hippocampus dentate gyrus, sublenticular extended amygdala
94	174	17.1	44.9	91	31.7	B	Frontal medial cortex, frontal pole
93	145	15.5	44.9	33.8	51.7	B	Precuneus cortex, posterior cingulate gyrus
92	57	15.6	64.8	76.9	29	L	Frontal orbital cortex, dorsal temporal pole
91	41	13.7	24.5	48.2	45.9	R	Parietal operculum cortex, inferior parietal lobule PFcm
90	35	17.6	45	65.5	29.5	B	Posterior subcallosal cortex
89	33	15	26	58.9	43.9	R	Insular cortex (dorsal, posterior), central opercular (posterior)
88	32	12.9	66.1	45	45.1	L	Parietal operculum cortex, planum temporale, primary auditory cortex
87	31	14.8	26.5	80.2	30	R	Frontal pole (ventral), frontal orbital cortex (anterior)
86	16	12.2	46	50.1	64.4	L	Primary motor cortex BA4a
85	14	12.5	29.6	22.6	18.6	R	Cerebellum horizontal fissure

Table 4: Significantly connected clusters to the CeA

Significantly connected clusters with the CeA following the one-sample permutation test. Images were thresholded at t=>9 before clusters were identified. Brain regions were listed if they had => 50% chance of being within a cluster. Max t is the maximum t-stat located within a cluster. X, Y, and Z columns represent the location of the centre of gravity for the cluster. Hemi indicates the hemisphere in which the cluster resides where B = bilateral, R = right and L = Left. For ease of interpretation clusters shown are those with a minimum of 10 connected voxels.

2.4.1.1 Shared BNST and CeA Intrinsic Functional Connectivity

Both the BNST and CeA showed significant connectivity with areas including the bilateral hippocampus, superficial amygdala, anterior and posterior-dorsal insula, frontal orbital cortex, medial prefrontal cortex, frontal pole, anterior paracingulate gyrus, superior temporal gyrus, central opercular cortex, precuneus cortex, and the hypothalamus (Figures 10 & 11, right). There was further shared iFC with pre- and post-central gyri, extending bilaterally to primary motor and sensory regions, and shared connectivity with the angular gyrus/ superior lateral occipital cortex. There were no significant voxels directly within either the BNST or CeA masks, suggesting that the two regions were not coactivated at rest. There was however a bilaterally BNST-connected amygdala cluster directly adjacent (within a single voxel) to the CeA mask (Figure 12). The bilateral SLEA region connecting the BNST and CeA also demonstrated overlapping connectivity (Figure 11).

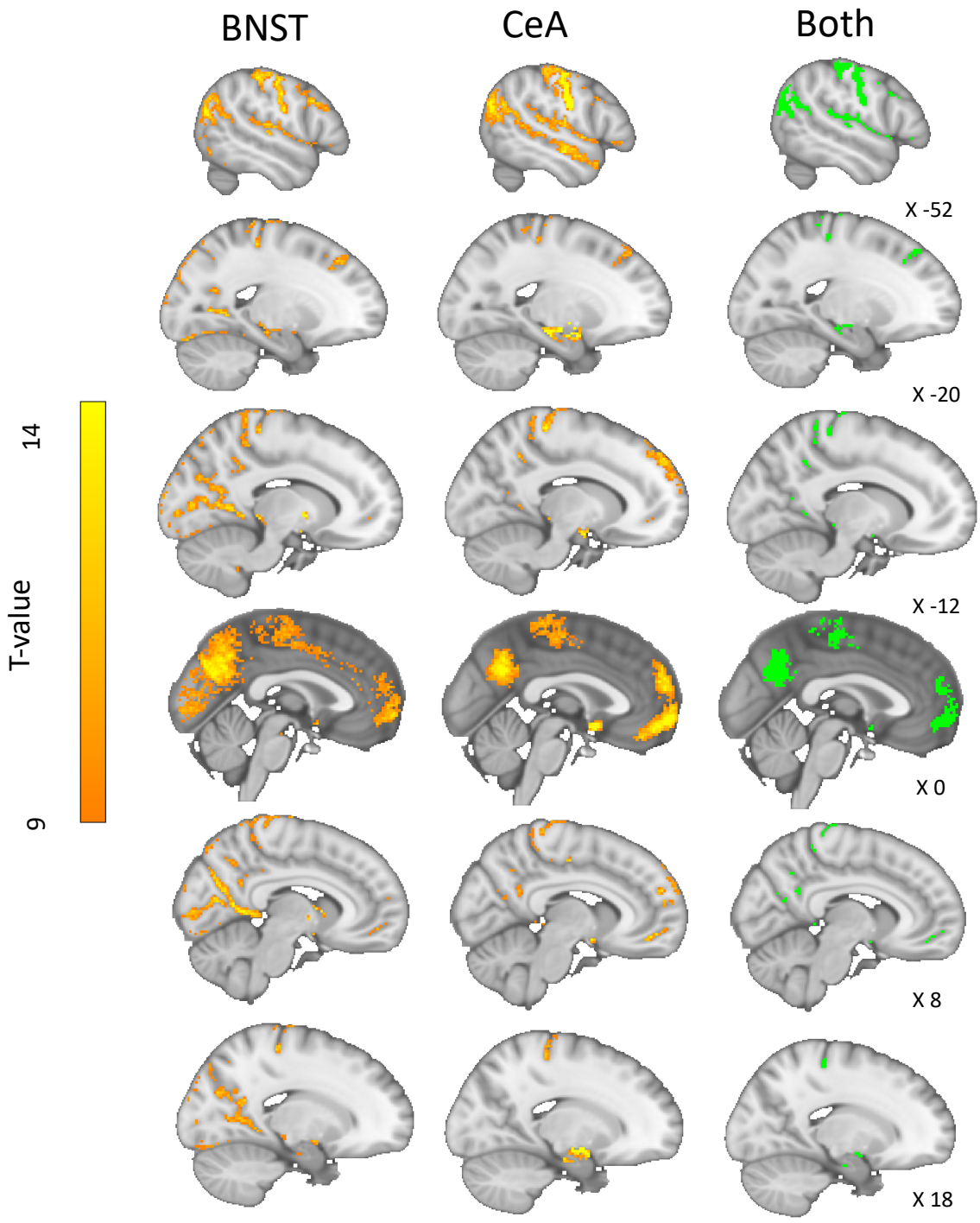

Figure 10: Saggital view of the Extended Amygdala's Intrinsic Connectivity Networks

The bed nucleus of the stria terminalis (BNST) and central nucleus of the amygdala (CeA) share a common intrinsic functional connectivity pattern, in particular with pre-frontal cortex, amygdala, hippocampus, superior temporal sulcal, insula, and precuneus. They also share connectivity with areas of the motor and sensory cortex.

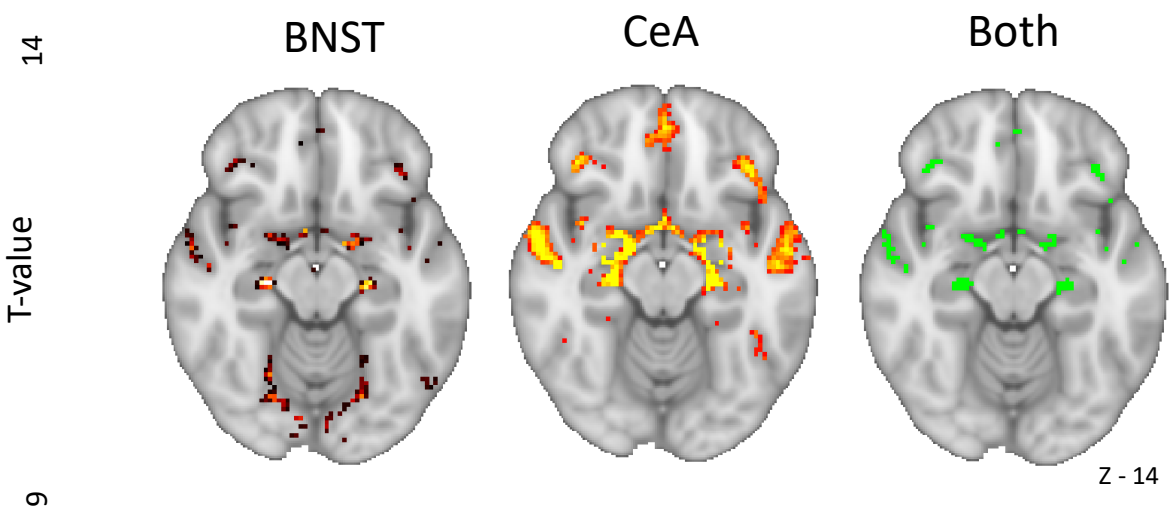

Figure 11: Axial view of the Extended Amygdala's Intrinsic Functional Connectivity Networks

Axis section demonstrating shared connectivity of bed nucleus of the stria terminalis (BNST) and central nucleus of the amygdala (CeA) with the hippocampus, insular, temporal gyri, frontal orbital, and medial prefrontal cortex. The CeA has more extensive connectivity generally with each of these regions and of note displays unique connectivity along amygdalo-hippocampal regions.

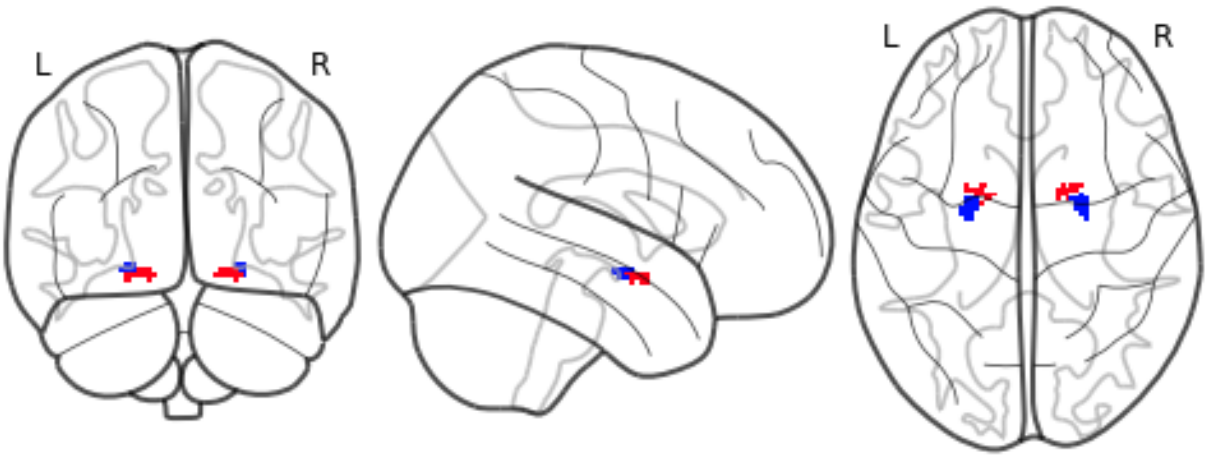

Figure 12: Bed nuclues of the stria terminalis functional correlation with the amygdala

This figure demonstrates the area of significant BNST – amygdala functional correlation (red) and it's close proximity to the central nucleus of the amygdala (blue).

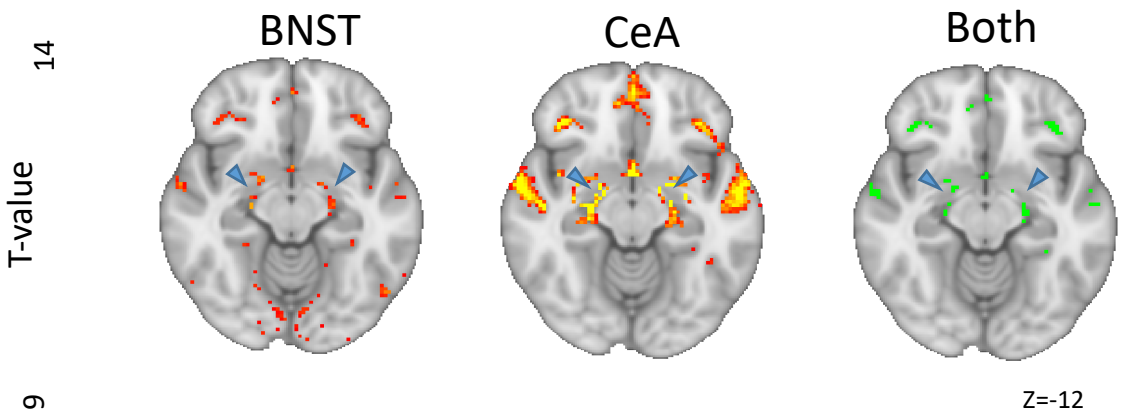

Figure 13: ExtA functional connectivity within the sublenticular extended amygdala

Clusters of connectivity in the region of the sublenticular extended amygdala (SLEA) (blue arrows). This pattern of activity is similar to that reported by Tillman et al, (2018) (Figure 3).

2.4.1.2 BNST > CeA Connectivity

The BNST had more extensive iFC with the occipital lobe, in particular within the superior occipital cortex, the intracalcarine cortex, and at the occipital pole (Figures 10 & 11, left). There was also greater BNST iFC with the posterior and anterior cingulate gyrus, posterior thalamus, precuneus cortex, left and right caudate, globus pallidus, lateral superior frontal gyrus, paracingulate gyrus, and ventral tegmental area (Figures 10 & 11, left).

2.4.1.3 CeA > BNST Connectivity

The CeA had greater iFC with the dorsal medial pre-frontal cortex (dmPFC), frontal pole, temporal pole, central insular, anterior and superior temporal gyrus, supramarginal gyrus, mid-line superior frontal gyrus, subcallosal cortex, and lateral globus pallidus (Figure 10, middle; Figure 14 right). There was also greater iFC around the surrounding amygdaloid areas (Figure 10, middle) and more extensive connectivity within the SLEA and amygdo-hippocampal regions (Figure 10, middle).

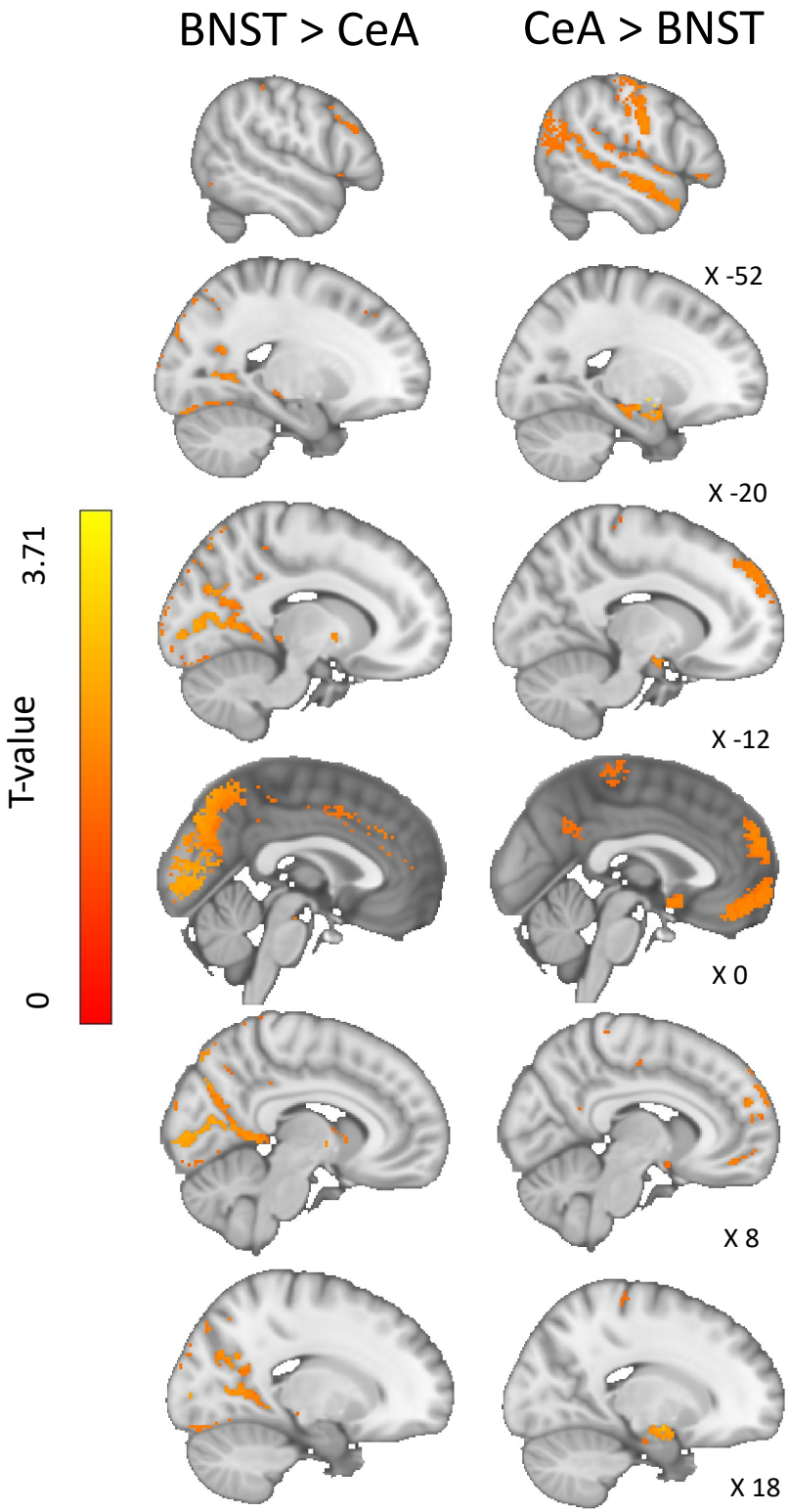

Figure 14:Unique intrinsic connectivity of the BNST and CeA

Results of the single group paired-difference t test, showing the unique intrinsic functional connectivity of the BNST or CeA seeds. The BNST had greater connectivity with lateral occipital regions and paracingulate gyrus, whereas the CeA has stronger connectivity with the surrounding amygdala, temporal poles, and the anterior and superior temporal gyri.

2.4.2 PCA results

The selected questionnaire items (Table 2) passed the KMO test (overall MSA = 0.8) and Bartlett's test of sphericity (Chisq(36) = 5103.77, p < .001) indicating that the data was appropriate for PCA. PCA revealed two components with eigenvalues greater than 1 (3.84 and 1.75). These components together explained 62.12% of variability in the data (Figure 16, right). The first component loaded positively on measures capturing negative disposition, such as anxiety, depression and perceived stress, and was therefore named the "negative disposition" component (Figure 15). The second component had significant loadings from alcohol measures and was therefore labelled the "alcohol use" component. See Table 5 and Figures 15,16 for a breakdown of the PCA results.

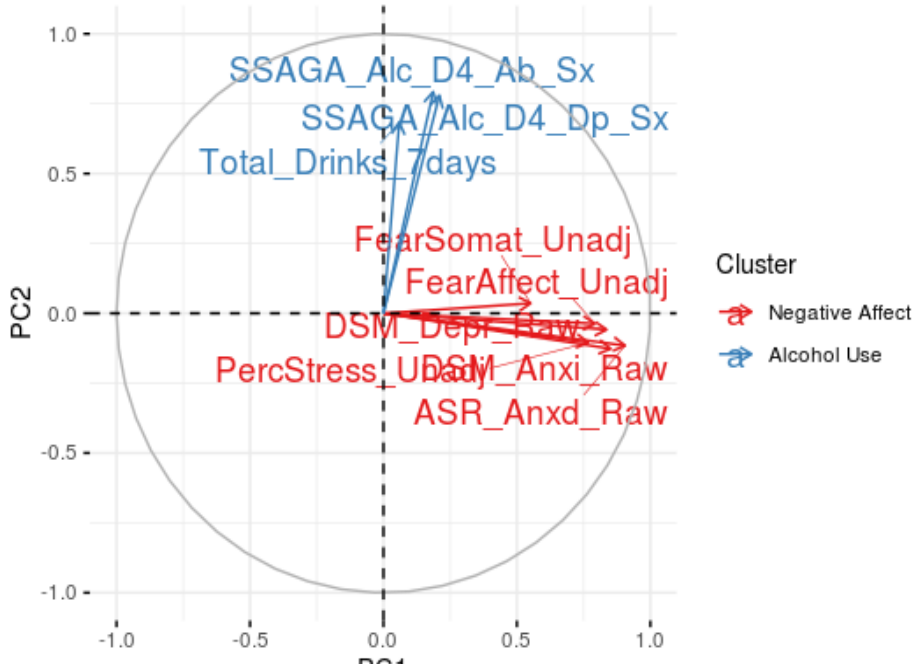

Figure 15: Principal component analysis correlation circle

The correlation circle shows positively correlated variables as being grouped together. Negatively correlated variables are positioned on opposite sides of the plot. Variables that are away from the centre are well represented by that component. Here, it is shown that I can neatly cluster two separate components, representing dispositional negativity (PC1) and alcohol use (PC2).

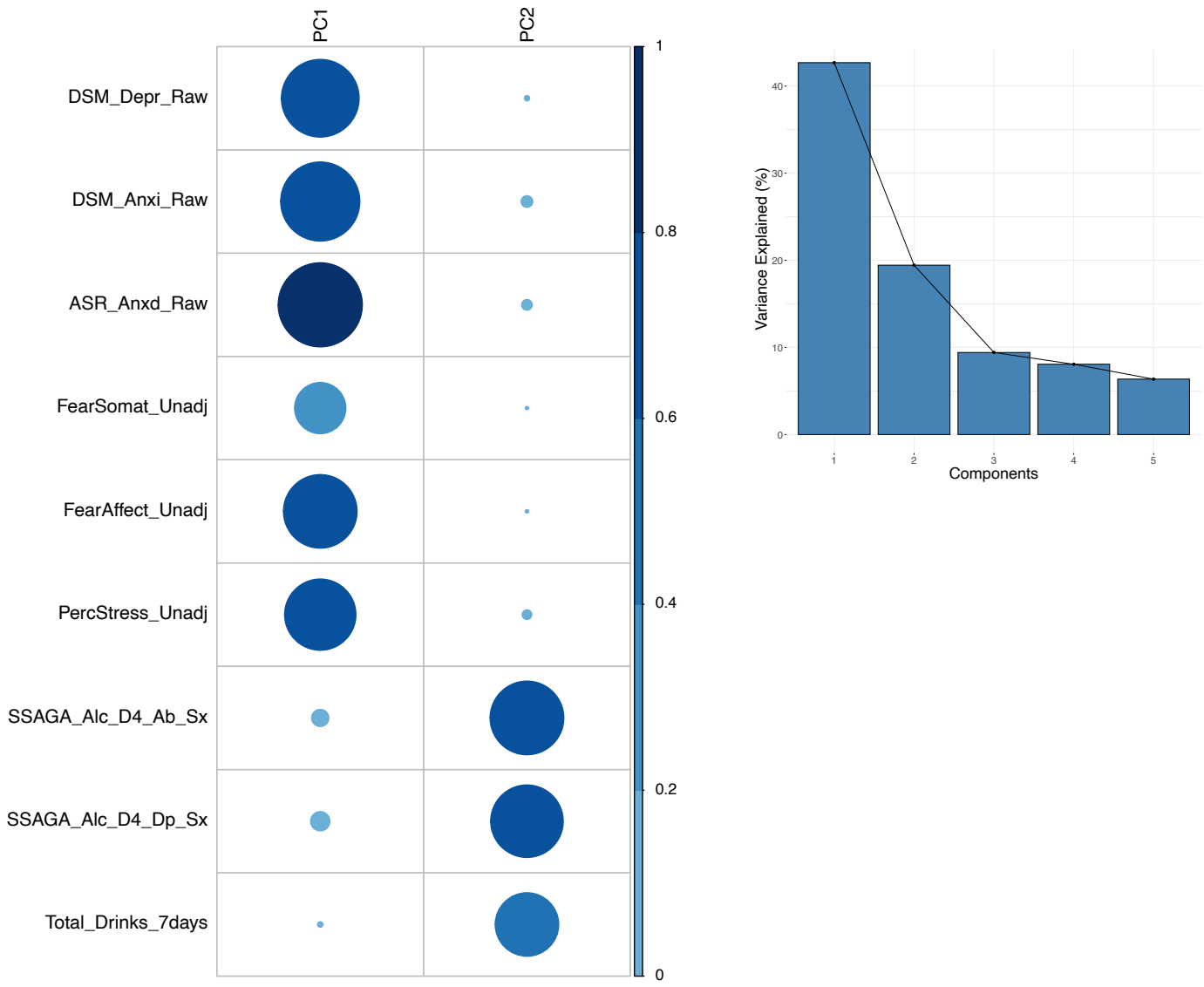

Figure 16: Principal component analysis results

Left: The circles represent the strength of contribution (cos2) of each questionnaire measure to the principal component. Most measures are represented well by the two principal components (cos2 > 5), with FearSomat and Total Drinks 7Days being the least well represented. Right: The scree plot displays the amount of variance explained by each component. The first two components capture 62% of the total variance of the original questionnaire measures. See table 2 for a description of the questionnaire measures.

ITEM	DIM.1 (COS2)	DIM.2 (COS2)
DSM_DEPR_RAW	**0.700**	0.003
DSM_ANXI_RAW	**0.724**	0.016
ASR_ANXD_RAW	**0.819**	0.013
FEARSOMAT_UNADJ	0.304	0.001
FEARAFFECT_UNADJ	**0.626**	0.001
PERCSTRESS_UNADJ	**0.587**	0.011
SSAGA_ALC_D4_AB_SX	0.035	**0.628**
SSAGA_ALC_D4_DP_SX	0.044	**0.608**
TOTAL_DRINKS_7DAYS	0.003	0.467

Table 5: Variable contributions to principal components.

This table shows the contribution of each variable to the two principal components (cos2). Highlighted values are the items that have a cos2 of .5 and above.

2.4.3 ExtA Intrinsic Connectivity Networks and Principal Component Associations

2.4.3.1 Intrinsic Functional Connectivity Networks and Principal Components

The PALM corr-con analysis provided no evidence that the negative disposition or alcohol use components were significantly associated with increased or decreased iFC across the ExtA ICNs in the sample. Gender was also not associated with the BNST or CeA ICNs after correction for multiple comparisons.

2.4.4 Within BNST- Amygdala iFC Heritability Analysis

2.4.4.1 Univariate Heritability Analysis

Twin-based heritability analysis of within BNST - CeA iFC found no evidence for heritability (Table 6). Analysis of within BNST-centromedial iFC found that this connection was significantly heritable at H2r = 0.15 (Table 6). BNST-superficial iFC had a heritability estimate of H2r = 0.14, but was marginally outside the bounds of

statistical significance after FDR correction (Table 6). BNST-basolateral iFC showed no evidence of significant heritability (Table 6). PC1 (negative disposition) was significantly heritable at H2r = 0.22, and PC2 was significantly heritable at H2r = 0.23 (Table 6). Age^2 was a significant co-variate for the negative disposition PC, however it only explained a small amount of variance (0.009). Sex was a significant covariate for the alcohol use PC, with being male demonstrating a small positive influence on the score (0.01).

PHENOTYPE	H2R	H2R STD ERROR	P	FDR-CORRECTED	SIGNIFICANT COVARIATES
BNST - SUPERFICIAL AMYGDALA IFC	0.138	0.079	0.035*	**0.052**	None
BNST - LATEROBASAL AMYGDALA IFC	0.032	0.076	0.334	0.401	None
BNST - CEA AMYGDALA IFC	0^{+}	NA	0.500	0.5	None
BNST - CENTROMEDIAL AMYGDALA IFC	0.149	0.077	0.021*	**0.042***	None
PC1 (NEGATIVE DISPOSITION)	0.218	0.081	0.002**	**0.006****	Age^2 (p = 0.02*, variance explained = 0.009)
PC2 (ALCOHOL USE)	0.225	0.078	0.001**	**0.006****	Sex (p= 0.01*, variance explained = 0.016)

Table 6: Univariate heritability analysis results

SOLARIUS heritability analysis revealed BNST iFC to the centromedial amygdala region was significantly heritable, with BNST iFC to the superficial amygdala moving marginally outside the bounds of statistical significance after false-discovery-rate (FDR) correction. Principal components one and two were significantly heritable, with Age^2 and Sex explaining a small amount of variance in each, respectively. $^{+}$ BNST-CeA amygdala iFC had only a fractional difference between the sporadic and polygenic model likelihood values, therefore the heritability estimate was 0.

2.4.4.2 Bivariate Heritability Analysis

Co-heritability analysis did not reveal any significant phenotypic, environmental, or genetic correlations with either of the principal components for any of the amygdala sub-regions (see supplementary material for bivariate SOLARIUS outputs).

2.5 Chapter Conclusions

2.5.1 Summary of findings

Using a large young adult human sample, I revealed distinct, but overlapping, ExtA ICNs that are largely consistent with findings from smaller previous human neuroimaging studies (Avery et al., 2014; Gorka et al., 2018; Oler et al., 2012, 2017; Tillman et al., 2018; Torrisi et al., 2015; Weis et al., 2019). Genetic analysis of within BNST- CeA iFC provided no evidence for a heritable connection. However, post-hoc analysis of amygdala sub-regions revealed evidence for small heritability estimates for BNST-centromedial and superficial regions. Principal component analysis reduced scores on nine questionnaire measures of anxiety, fear, depression, and substance use to two components, which I interpret as 'negative disposition' and 'alcohol use'. Contrary to my hypotheses, I report no evidence for associations of these phenotypes across the ExtA ICNs. I also found no evidence that specific BNST iFC to any of the tested amygdala regions were co-heritable or otherwise correlated with either of the components.

2.5.2 Intrinsic Connectivity Networks of the Extended Amygdala

Our shared ICN results are in broad agreement with the previous literature, specifically demonstrating overlapping connections within a now widely reported ExtA ICN that

includes the mPFC, bilateral hippocampus, insular regions, wider amygdala areas, and the precuneus (Avery et al., 2014; Gorka et al., 2018; Pedersen et al., 2020; Tillman et al., 2018; Torrisi et al., 2015, 2019; Weis et al., 2019). I report shared iFC to lateral temporal regions, including the superior and middle temporal gyri and the temporal poles, again largely consistent with previous human iFC results. Whist amygdala structural connections to lateral temporal regions are well characterised (Folloni et al., 2019; Janak & Tye, 2015; Klingler & Gloor, 1960), this is not the case for the BNST and it has been suggested that BNST-temporal pole connectivity may even be unique to humans (Avery et al., 2014). I demonstrate shared iFC to areas of the sensory/ motor cortex, auditory regions, and to lateral occipital areas, something also reported by Tillman et al. (2018). This largely cortical sensory-motor connectivity is consistent with the suggestion that the ExtA serves as an integrator of sensory information, which can then prepare the motor and endocrine systems to act according to the emotional salience and threat-relevance of the stimuli (Ahrens et al., 2018; Fox & Shackman, 2019; Goode & Maren, 2017; Lebow & Chen, 2016). Our finding of iFC with frontal regions, in particular the mPFC, is consistent with non-human primate neural tracer studies and human structural imaging work demonstrating direct structural connectivity with both the amygdala and BNST (Chiba et al., 2001; Crawford et al., 2020; Folloni et al., 2019; Krüger et al., 2015); a finding coherent with theories of emotion regulation (e.g. Banks et al., 2007; Fox et al., 2010).

For the BNST, I report a unique cluster of iFC within visual areas (including V1, V2, and the occipital fusiform gyrus), the posterior thalamus, and the posterior cingulate gyrus. Although BNST-occipital connectivity is not commonly reported in human or pre-clinical research (McDonald, 1998), a similar pattern was revealed by Tillman et al (2018), who demonstrated a remarkably similar cluster of iFC in humans stretching from the posterior thalamus, through the lingual gyrus and into the visual cortices. Additionally, a recent study comparing patients with anxiety disorder to controls also reported an unexpected coupling of these two regions, suggesting that abnormal coupling of the BNST to the occipital cortex could reflect differences in anxiety-based interpretation of, or attention to, visual stimuli (Torrisi et al., 2019). Our finding of

BNST connectivity with areas of the basal ganglia and VTA has been widely reported in human imaging and pre-clinical neuronal tracer work, whereas iFC with the paracingulate gyrus is only reported in the human literature (Avery et al., 2014; Gorka et al., 2018, 2018; Tillman et al., 2018; Torrisi et al., 2015; Weis et al., 2019). Diffusion tensor imaging (DTI) by Avery et al. suggested that the human BNST and paracingulate are not structurally connected, indicating an indirect functional connection mediated through other structures (Avery et al., 2014).

The CeA exhibited a large cluster of iFC within the mPFC, commensurate with pre-clinical tracer and human neuroimaging research demonstrating widespread reciprocal structural connections between the amygdala and pre-frontal regions (Aggleton et al., 2015; Chiba et al., 2001; Folloni et al., 2019). Temporal lobe connectivity was more robust for the CeA than the BNST, reaching deeper into the brain to the mid-insular and extending further out to an area of the superior temporal regions to the end of the bilateral temporal poles. Extensive amygdala connectivity to the insular and lateral temporal regions has been demonstrated in non-human primate research as well as in human FC and diffusion MRI studies (Folloni et al., 2019; Janak & Tye, 2015; Klingler & Gloor, 1960). Of interest, a recent human tf-fMRI mapping of iFC in anxiety disorder patients found that CeA connectivity to the superior temporal gyrus was significantly stronger compared to a control group (Torrisi et al., 2019). The CeA demonstrated unique iFC to wider amygdala structures, as well as the amygdo-hippocampal regions. Amygdala – hippocampal connections are thought to be key in the processing of emotionally salient events and manipulation of memory under stress, with the CeA in particular implicated in context-dependent retrieval of cued fear memories (de Voogd et al., 2017; Sylvester et al., 2020; C. Xu et al., 2016). Because I only measure correlated BOLD activity, without taking into account more elaborate models that assess causality, I was not permitted to make inferences regarding the direction of connectivity (Rogers et al., 2007). However an extensive body of work on the amygdala suggests that many of the CeA connections are mediated through the basolateral amygdala to the CeA, which in turn serves primarily as an output to basal forebrain structures (Janak & Tye, 2015). The picture is complex however, and many studies

have also shown direct structural connections with the CeA region, for example from agranular and dysgranular regions of the insular in Macaques and from the ventral hippocampus in mice (Stefanacci & Amaral, 2002; C. Xu et al., 2016).

Given pre-clinical and human imaging results demonstrating structural and functional connectivity between the CeA and BNST (Avery et al., 2014; M. Davis et al., 2010; Fox et al., 2018; Gorka et al., 2018; Hofmann & Straube, 2019; Martin et al., 1991; Oler et al., 2017b; Torrisi et al., 2015), I expected to find evidence of strong iFC between the BNST and CeA masks, however this was not quite the case. After thresholding, I did not find evidence of CeA iFC with the BNST, although I did find a bilateral BNST-functionally connected region directly adjacent to the original CeA mask (Figure 12). Given the small size of the structures many studies refer to 'areas consistent with' the BNST and CeA (Fox & Shackman, 2019). These discrepancies can likely be explained by the difficultly of accurately delineating the amygdala sub-regions using MRI and/or the noisy nature of tf-fMRI data (Kedo et al., 2018; Sylvester et al., 2020) (discussed further in the General Discussion).

Our results revealed minimal connectivity to the thalamus. Given thalamic connectivity is widely reported in structural and functional studies in both pre-clinical and human studies (Fox, Oler, Tromp, et al., 2015; Fox & Shackman, 2019; Lebow & Chen, 2016), it seems likely that this may be due to a difference in data acquisition or pre-processing. Although speculative, the discrepancy could perhaps be explained by signal drop-out, something that has been shown to affect FC estimates of the thalamus in the HCP data (Schwaferts, 2017).

In general though, my findings are highly consistent with the smaller previous studies, and in particular are similar to those of Tillman et al. who, in a different sample, used the same BNST and CeA masks (Tillman et al., 2018). Whilst needing to be formally evaluated, this similar pattern of results across samples suggests the existence of a reliable ExtA ICN in healthy humans. If validated, this network could be used as a

standard to compare against clinical groups, a technique already used with some success for anxiety disorder patients (Pedersen et al., 2020; Torrisi et al., 2019)

2.5.3 Heritability and Co-Heritability of Within BNST-Amygdala iFC

Contrary to recent primate evidence (Fox et al., 2018), I do not report evidence of a heritable functional connection between the BNST and CeA. A post-hoc analysis did reveal evidence for a small magnitude of heritability between the BNST and the centromedial and superficial amygdala regions, however there was no evidence of iFC co-heritability with either of the principal components (negative disposition, alcohol use).

As mentioned in the General Introduction (section 1.3), although brain morphology and development are reliably heritable (Jansen et al., 2015), this is not necessarily the case for iFC where heritability estimates can frequently be zero (Elliott et al., 2018; Jansen et al., 2015) (see also Figure 6). The reasons for low iFC heritability estimates are not well understood but could reflect either comparatively noisy signal or simply the greater context-dependent variability inherent within fluctuating connections (Cabeza et al., 2018). This makes the Fox primate finding of high heritability (.45) all the more interesting, although the usefulness of comparing the strength of heritability estimates across samples is limited as they are highly influenced by their particular environment; something compounded by comparing across species (Turkheimer, 2016). The fact that I found a heritable connection with the centromedial and superficial amygdala, and not specifically the CeA as was reported in Fox et al., may again reflect difficulties in locating small anatomical regions within the amygdala. With this in mind, the finding of H2r results of ~.14, whilst smaller than the non-human primate evidence, is not zero and is broadly in line with other estimates of the heritability of iFC findings in humans (Elliott et al., 2018). Further examination in other human samples could perhaps assess whether individualized task-based, naturalistic fMRI, behaviourally defined (rather than self-reported) negative disposition

phenotypes, and/or the use of clinical groups influences the heritability estimates of ExtA iFC (Finn et al., 2017). Use of novel methods, such as those combining common features across resting-state and task-based fMRI, have been shown to improve reliability and increase heritability estimates of ICNs (Elliott et al., 2019). Larger twin-samples with 7T MRI data and rich phenotyping would also help to resolve issues around the delineation of amygdala sub-region boundaries whilst allowing for co-heritability analysis, which is after all of primary interest given the suggestion of shared genetic mechanisms.

2.5.4 Principal Components and ExtA iFC

Our first principal component grouped together questionnaire items that represented aspects of negative disposition (stress, fear, anxiety, depression), supporting previous work (Hur et al., 2019; Krueger et al., 2018; Shackman et al., 2018; Shackman, Stockbridge, et al., 2016; Shackman, Tromp, et al., 2016; Waszczuk et al., 2020). The ExtA is implicated by numerous pre-clinical and human studies in aspects of negative disposition, in particular in relation to fear and anxiety (Fox & Shackman, 2019; Hur et al., 2019). It is then perhaps surprising that I report no associations with this principal component across the ICNs. On closer inspection of the literature, however, the finding is in keeping with other iFC studies that have used non-clinical populations (Pedersen et al., 2020; Weis et al., 2019). Weis et al reported no robust associations within BNST, CeA, or BLA iFC with trait anxiety in a sample of healthy undergraduates (Weis et al., 2019). This was also the case in a study by Pederson et al who, when looking at within ExtA (i.e. BNST-CeA) iFC found no significant associations with trait anxiety or negative affect in a healthy sample (Pedersen et al., 2020).

Studies that do report ExtA associations with negative disposition phenotypes are overwhelmingly conducted either in clinical populations or during task-based fMRI where state anxiety or fear is induced (Andreatta et al., 2015; Brinkmann et al., 2018b; Choi et al., 2012; Grupe et al., 2013; Klumpers et al., 2017; Mobbs et al., 2010; Naaz et

al., 2019; Pedersen et al., 2020; Torrisi et al., 2019). There could be a number of reasons for this discrepancy. It may simply be that in a relatively healthy sample, even with a large number of participants, the variation in trait negative disposition is too small to detect any resting-state ExtA network associations. Further to this, recent research has suggested that there is a systematic sampling bias whereby more anxious individuals are reluctant to undergo MRI scanning (Charpentier et al., 2020). Second, although the ExtA is implicated in studies that induce state anxiety, the networks involved in this process may be different to those responsible for having high anxiety as a trait. Torrisi et al. have demonstrated that the ExtA ICN regions that differ between anxiety disorder patients and controls are not the same as those recruited during state anxiety induction (Torrisi et al., 2019). Further, when correlating anxiety symptoms in the patient group with iFC, they found no overlap between the specific anxiety symptoms and the regions that differentiated patients from controls. This study, along with other recent findings (Porta-Casteràs et al., 2020) suggests that clinical diagnoses, specific symptoms, and trait measures may all be underpinned by different networks. It may be the case then that at a neural level there is little continuity between otherwise healthy people with, for example, high anxiety, and clinical populations (Porta-Casteràs et al., 2020). As such, revealing the networks implicated in clinical disorders may not be as simple as looking at typical trait variation and extrapolating from these findings. As well, there is some evidence to suggest that individual differences are best observed under emotional or cognitive challenge, rather than at rest (Finn et al., 2017; Stewart et al., 2014). In any case, despite associations using task-based, clinical, and pre-clinical evidence, at present there does not seem to be good evidence that iFC of the ExtA is related to self-reported negative disposition in non-clinical human populations.

Likewise, and perhaps for similar reasons, I found no association of ExtA iFC with the second PC, which represented alcohol-use. Our sample did not consist of many heavy drinkers, with the median drinks consumed per week being just two, which likely reduced my chances of finding an effect. Despite quite a substantial body of pre-clinical work linking the ExtA to alcohol consumption (Campbell et al., 2019; Centanni

et al., 2019; de Guglielmo et al., 2019; Erikson et al., 2018; Harris & Winder, 2018; Kash, 2012; Pleil et al., 2016; Roberto et al., 2020; Volkow et al., 2016), there is very little investigation of the ExtA and alcohol use in humans; with most work tending to focus on the amygdala proper (Hur et al., 2018; Lebow & Chen, 2016). One study that did specifically examine ExtA iFC found that under the influence of alcohol, BNST and CeA reactivity to emotional faces was dampened (Hur et al., 2018). Although I did not find evidence of a self-report alcohol-use association in the sample, given the importance of understanding alcohol use behaviours and the strength of evidence from the animal literature, ExtA neuroimaging work on the effects of alcohol in humans should remain a priority. Getting participants to drink alcohol (Hur et al., 2018), utilizing heavy drinkers, or making use of task-based fMRI (Finn et al., 2017) could be a more fruitful approach for identifying ExtA-alcohol associations.

Our estimates of negative disposition and alcohol use heritability were broadly in line, if not slightly smaller, than similar human studies (Han & Adolphs, 2020; Kranzler et al., 2019; Swan et al., 1990; Zheng et al., 2016). As mentioned above however (section 4.3), direct comparison of the strength of heritability estimates across samples is of limited value, and as such should not be over-interpreted (Turkheimer, 2016). The covariates sex and age^2 were statistically significantly associated with alcohol use and negative disposition respectively. Age^2 explained only a tiny amount of variance, and so interpretation is limited in this case. The finding that being male is associated with a small increase in alcohol use scores however, is in line with recent findings of US samples (White et al., 2015)

2.5.5 Limitations

Our study has some limitations. Firstly, the analyses were conducted using 3T MRI data. Although imaging at this field strength has been found to accurately capture small regions such as the BNST (Theiss et al., 2017), higher resolution, and individualised anatomical parcellations, would enable better characterisation of ExtA

iFC networks (see the General Discussion for more on this). Additionally, it is the case that even the small BNST structure is made up of further sub-nuclei that may have distinct functions, a point that is difficult to address using human MRI (Fox & Shackman, 2019; S.-Y. Kim et al., 2013). Second, as is the case with all seed-based correlation analyses, the interpretation of the results is correlational only and mechanistic inferences including the directionality of the connections cannot be inferred (Mohanty et al., 2020; Pearlson, 2017). Thirdly, although I aimed to be consistent with similar tf-fMRI HCP studies (Hofmann & Straube, 2019), my choice to favour some pre-processing techniques over others, such as global signal regression, could have impacted my findings (Glasser et al., 2016; Murphy & Fox, 2017). This is unfortunately a limitation upon all fMRI studies until a consensus approach on pre-processing steps can be reached (Murphy & Fox, 2017). The use of tf-fMRI data acquired with the 'eyes-open' method may also have impacted findings, with researchers demonstrating that eyes-closed acquisitions increase activation in brain regions associated with introspection, a process often associated with DN (Costumero et al., 2020; Hur et al., 2019). Finally, the questionnaire measures were all self-report, which can sometimes affect the accuracy of the phenotyping (Rosenman et al., 2011). This may be a particular problem for self-reported drinking behaviour as previous studies have shown heavy-drinking to be underreported (Northcote & Livingston, 2011). Additionally, the use of PCA on sub-scales, rather than on individual questionnaire items, likely reduced the sensitivity of the principal components therefore decreasing the chances of detecting an effect (Jolliffe & Cadima, 2016).

2.5.6 Conclusions and Future Directions

I used a large sample of high quality tf-fMRI data to assess the ICNs of the two key ExtA nodes. Our ICN findings largely replicated previous tf-fMRI mapping work, implicating the nodes in mostly overlapping ICNs that includes iFC with medial pre-frontal, hippocampal, wider amygdala, lateral temporal, and precuneus regions. Although for the analysis I intended to establish the ExtA ICNs unencumbered by family relatedness, so as to enable inferences to the wider population, future work could intentionally

explore how family relatedness influences the networks. This would allow for heritability and co-heritability analysis across the entire ICNs, instead of *a priori* selected regions. I report for the first time in humans that within BNST- centromedial and superficial amygdala iFC is heritable. I did not replicate the recent non-human primate finding (Fox et al., 2018) of BNST-CeA iFC co-heritability with an anxiety-related phenotype. I found no evidence for network associations with negative disposition or alcohol use principal components. Recent work has suggested that self-report trait effects may not be associated with the same neural networks as those identified under task-based conditions and in clinical groups. Future work should explore further these differences by using a combination of self-report, task-based measures, and clinical groups (e.g. Porta-Casteràs et al., 2020)**.**

2.6 Supplementary information

FAMILY SIZE	COUNT
1	74
2	162
3	178
4	35
5	3
6	1

AGE GROUP	COUNT
22-25	227
26-30	477
31-35	377
36+	12

ETHNICITY	COUNT
WHITE	734
BLACK OR AFRICAN AMERICAN	176
HISPANIC/ LATINO	95
ASIAN/ NAT. HAWAIIAN/ OTHER PACIFIC IS.	61
MORE THAN ONE	22
UNKNOWN OR NOT REPORTED	3
AM. INDIAN/ ALASKAN NAT.	2

Table(s) 7: HCP demographic information (supplementary table)

PC2 (ALCOHOL USE) CORRELATION VARIABLE	RHOP EST	RHOP P-VAL	RHOE EST	RHOE P-VAL	RHOG EST	RHOG P-VAL
BST - SUPERFICIAL AMYGDALA IFC	-0.036	0.270	-0.278	0.699	-0.077	0.811
BST - LATEROBASAL AMYGDALA IFC	-0.012	0.702	-0.055	0.427	0.406	0.529
BST - CEA AMYGDALA IFC	-0.013	0.703	0.091	0.135	NA	NA
BST - CENTROMEDIAL AMYGDALA IFC	0.001	0.981	0.047	0.512	-0.205	0.505

Table 8: PC2 (alcohol use) bivariate SOLARIUS analysis results (supplementary table)

PC1 (NEGATIVE DISPOSITION) CORRELATION VARIABLE	RHOP EST	RHOP P-VAL	RHOE EST	RHOE P-VAL	RHOG EST	RHOG P-VAL
BST - SUPERFICIAL AMYGDALA IFC	0.012	0.700	-0.026	0.725	0.197	0.559
BST - LATEROBASAL AMYGDALA IFC	-0.002	0.943	0.027	0.702	-0.303	0.651
BST - CEA AMYGDALA IFC	0.024	0.463	-0.002	0.981	NA	NA
BST - CENTROMEDIAL AMYGDALA IFC	-0.008	0.80	0.067	0.356	-0.349	0.270

Table 9: PC1 (dispositional negativity) bivariate SOLARIUS analysis results (supplementary table)

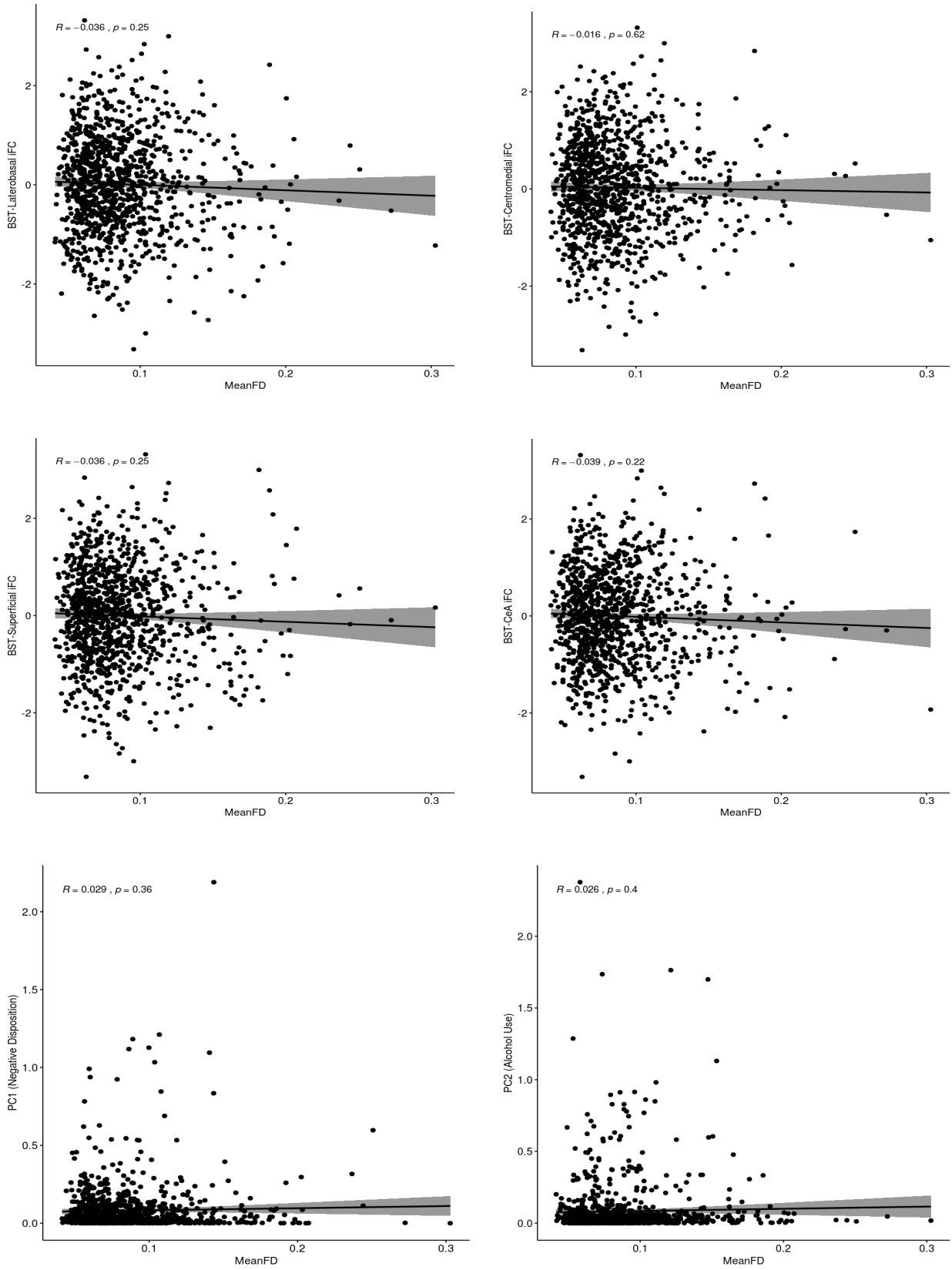

Figure 17: Mean fractional displacement correlations with analysed variables (supplementary figure)

Chapter 3: Genome-Wide Association Study of BNST – Amygdala Functional Connectivity

3.1 Chapter Summary

In this chapter I use the UK biobank (UKBB) sample (n= ~19,000) (Alfaro-Almagro et al., 2018) to run a genome-wide association study (GWAS) of BNST iFC to five amygdala sub-regions (superficial, laterobasal, centromedial, CeA, and a cluster derived from the BNST ICN analysis in Chapter 2). Results from this analysis demonstrate association of a single common genetic variant with BNST iFC to the laterobasal amygdala. This SNP (rs10786748) has been previously linked to expression of the gene *NRG3* (Neuregulin 3), which RNA expression data in human tissue demonstrates has highly specific expression within the brain; particularly in the amygdala. Using both linked medical record and self-report measures of anxiety and alcohol use disorders, I also examine associations with BNST and amygdala subregion iFC, but report no evidence for a relationship. Finally, SNP-based heritability analysis based upon the summary statistics from the GWAS found no evidence for SNP-based heritability for any BNST-amygdala iFC.

3.2 Introduction

Pre-clinical and human work implicates the Bed Nucleus of the Stria Terminalis (BNST) in stress-related processes which may be important for understanding several traits and psychiatric disorders (Herman et al., 2020; Lebow & Chen, 2016; Maita et al., 2021). In particular, the BNST is thought to work closely with amygdala sub-regions to generate states of fear and anxiety Fox et al., 2018; Fox & Shackman, 2019). Additional work has linked BNST and amygdala structural connections to processes underlying alcohol use disorder (de Guglielmo et al., 2019). In Chapter 2 I demonstrated, using a large twin-based sample, that BNST intrinsic functional

connectivity (iFC) with the centromedial and superficial amygdala subregions was modestly heritable (H^2 ~ 14). Previous work in macaques has also reported significant heritability of iFC between the BNST and the CeA amygdala subregion (Fox et al., 2018). Importantly, the authors additionally reported that this connectivity was co-heritable and correlated with a macaque measure of dispositional negativity (DN) (see section 1.3) (Fox et al., 2018).

Identifying genetic variants related to iFC may help us to understand genetic influence on brain function (Li et al., 2020). The variance of iFC attributable to genetics varies by the connection examined and the method of assessment used. When analysing intrinsic connectivity networks (ICNs), researchers have generally reported heritability estimates between h^2 = 0.1 – 0.5 (Adhikari et al., 2018; Elliott et al., 2018; Teeuw et al., 2019; Xu et al., 2017). For example, using the Genetics of Brain Structure (GOBS) cohort (n=332) and a subset of the Human Connectome Project (HCP) (n = 518), researchers investigated the stability of heritability estimates of eight ICNs across these datasets (Adhikari et al., 2018). The authors report that approximately 31% of the variance in ICNs may be explained by additive genetic variance and that these estimates were moderately consistent across the different populations (r = 0.5) (Adhikari et al., 2018). When examining task-free FC between individual brain regions, heritability estimates also range between 0.1 – 0.5, although are considerably more variable and are more likely to have non-significant heritability than estimates based upon ICNs (see Figure 6) (Colclough et al., 2017; Elliott et al., 2018). Specifically, using SNP-based heritability (h^2_{SNP}) analysis, a method which directly tests common genetic variant associations with a phenotype to estimate heritability (see General Introduction section 1.3.3.3), found that only 235 connections out of 1771 displayed statistically significant h^2_{SNP} (Elliott et al., 2018). Notably, task-based FC (i.e. variance in how a FC changes when engaged by a particular stimulus or task) demonstrate the lowest heritability estimates (Elliott et al., 2018). Authors have suggested that this may be due to high levels of noise in the data, with more recent results demonstrating that combining task-based and task-free FC measures can improve reliability and lead to higher heritability estimates (Elliott et al., 2019).

Genome-wide association analysis (GWAS) tests for association between millions of common genetic variants (minor allele frequency of > 0.01) and a given phenotype (see section 1.3). GWAS analysis of neuroimaging datasets have so far observed hundreds of associations between SNPs and MRI measures (Smith et al., 2021). Whilst functional interpretation of these SNPs is ongoing, researchers have so far related SNP - imaging associations to processes linked to extracellular matrix and epidermal growth factors, axon development, pathway signalling, and neuronal plasticity (Elliott et al., 2018). Specifically for FC measures, a recent GWAS of iFC within language-related brain regions revealed associations with three SNPs that had previously been implicated in language processing (Mekki et al., 2021). This suggests that SNPs may provide insight into the biology of functionally relevant brain processes (Cano-Gamez & Trynka, 2020).

Despite the BNST's implication in stress-processing, substance misuse, and regulation of negative affect (Maita et al., 2021), likely because of its small size and relative obscurity in comparison to other regions such as the amygdala (Lebow & Chen, 2016), a GWAS of BNST-associated imaging variables has not been undertaken. Previous evidence has demonstrated that BNST – amygdala iFC is heritable and may share genetic variance with associated behavioural phenotypes relating to anxiety (Fox et al., 2018). Therefore, a GWAS of this connection may reveal SNPs that underlie both variation in iFC between these important brain regions and those relating to variations in anxiety and other BNST-linked traits. If this is the case then follow-up analysis, for example using animal models (Meier et al., 2019), could investigate the biological role of these connectivity and trait-linked SNPs; perhaps eventually leading to treatments of BNST-linked disorders (Cano-Gamez & Trynka, 2020).

The present study uses the UK Biobank (UKBB, n = 19,829) (Sudlow et al., 2015), to test for common genetic variant associations with BNST – amygdala subregion iFC. In addition, I test for associations between BNST – amygdala iFC and measures of anxiety and alcohol use.

3.3 Methods

3.3.1 The UK Biobank Sample

The sample consisted of a sub-group (n=19,829) of participants from UK Biobank (UKBB) study who had undergone tf-fMRI and genetic testing (Sudlow et al., 2015). Participants were male and female older adults (40-69) living in the United Kingdom. Participants provided blood, urine and saliva samples, provided consent for access to medical records, and provided extensive lifestyle, demographic, behavioural and biophysical information. Ethical approval was granted by the North West Multi-Centre Ethics committee. Data were released to Cardiff University after application to the UK Biobank (project ref. 17044). For more information on recruitment and procedures see (www.ukbiobank.ac.uk).

3.3.2 Phenotype Measures

Four measures of alcohol use and anxiety were used to test for association with BNST-amygdala sub-region iFC. The first two of these were constructed from participant health records and reflected whether a participant had been diagnosed with any anxiety or alcohol-associated disorder. Diagnosis was based upon GP medical records, coded according to the International Classification of Diseases (ICD) 10. For anxiety disorder this included any diagnoses under the ICD subcategories F40 – F41, representing 'Phobic anxiety disorders' and 'Other anxiety disorders' respectively. The 'Other anxiety disorders' category includes panic disorder, generalised anxiety disorder, mixed anxiety and depressive disorder. This variable was named 'Health-record Anxiety'. Participants were said to have an alcohol-associated disorders if they had any diagnoses under the subcategory F10, representing 'Mental and behavioural disorders due to use of alcohol', and/or K70, representing 'Alcoholic liver disease. This variable was termed 'Health-record Alcohol'.

The third and fourth variables were based upon self-report data, which were coded following a verbal interview with trained staff at one of the UKBB assessment centres. The third variable, named 'Self-report Alcohol', reflected whether a participant had stated that they were alcohol dependent and/or had alcoholic liver disease. The fourth variable, termed 'Self-report Anxiety', reflected whether a participant had stated that they have an anxiety or panic disorder. The total number of subjects with these variables was n = 19,808. See Table 10 for participants demographic information.

3.3.3 Image Acquisition

UKBB participants underwent a series of MRI acquisitions in a single 31 minute scanning session, the full details of which have been described extensively elsewhere (Alfaro-Almagro et al., 2018; Miller et al., 2016). Briefly, all data was collected on the same Siemens Skyra 3T scanner type at one of two locations in the UK. For the analyses I used the T1 and tf-fMRI scans. The T1 scan lasted 4:54 mins and was acquired using 1.0mm^3 3D magnetisation-prepared rapid gradient echo sequence (T1/TR = 880/2000ms, sagittal, R=2). The tf-fMRI scan lasted 6:10 mins and was acquired using a 2.4mm^3 multiband gradient echo EPI sequence (TE/TR=39/735ms, multiband acceleration factor =8, flip angle 52^o, fat sat) (Miller et al., 2016). Participants were asked to keep their eyes open and view a fixation cross (Miller et al., 2016).

3.3.4 MRI pre-processing

Both the T1 and tf-fMRI data were run through the standardised automated UKBB MRI pre-processing pipeline, described in detail elsewhere (Alfaro-Almagro et al., 2018). Briefly, T1 data underwent gradient distortion correction, linear and non-linear transformations to standard space using FSLs FLIRT and FNIRT tools (Jenkinson et al.,

2002), brain extraction using FSLs BET function (Smith, 2002), defacing procedures, and finally segmentation into different tissues and subcortical structures using FSL FAST (Zhang et al., 2001) (Alfaro-Almagro et al., 2018). Tf-fMRI data were processed using the Melodic tool (Beckmann & Smith, 2004) and made use of various outputs from the T1 pre-processing steps. Briefly, these tf-fMRI images underwent gradient distortion correction unwarping, motion correction using MC-FLIRT (Jenkinson et al., 2002), grand-mean intensity normalisation of the entire 4D dataset by a single multiplicative factor, and high-pass temporal filtering (Alfaro-Almagro et al., 2018). In addition, structured artefacts were removed using the FIX-ICA process followed by FMRIBs ICA-based X-noiseifier (Beckmann & Smith, 2004; Griffanti et al., 2014).

3.3.5 Functional Connectivity Analysis

3.3.5.1 Region of Interest Masks

The regions of interest (ROIs) for this analysis were the BNST, and five amygdala subdivisions (Figures 6-8, 17). These included the three Juelich histological atlas (Jenkinson et al., 2012) amygdala areas; the centromedial, laterobasal, and superficial amygdala, as well as a separate central nucleus of the amygdala (CeA) ROI (Pauli et al., 2018) and the area of significant connectivity between the BNST and amygdala derived in Chapter 2 (HCP-derived). The BNST, CeA, and three Juelich amygdala ROIs are described in section 2.3 of Chapter 2. The HCP-derived mask was created using FSL maths functions and represents the voxels that were significantly functionally correlated with the BNST after thresholding at t > 9 (see Chapter 2, section 2.4).

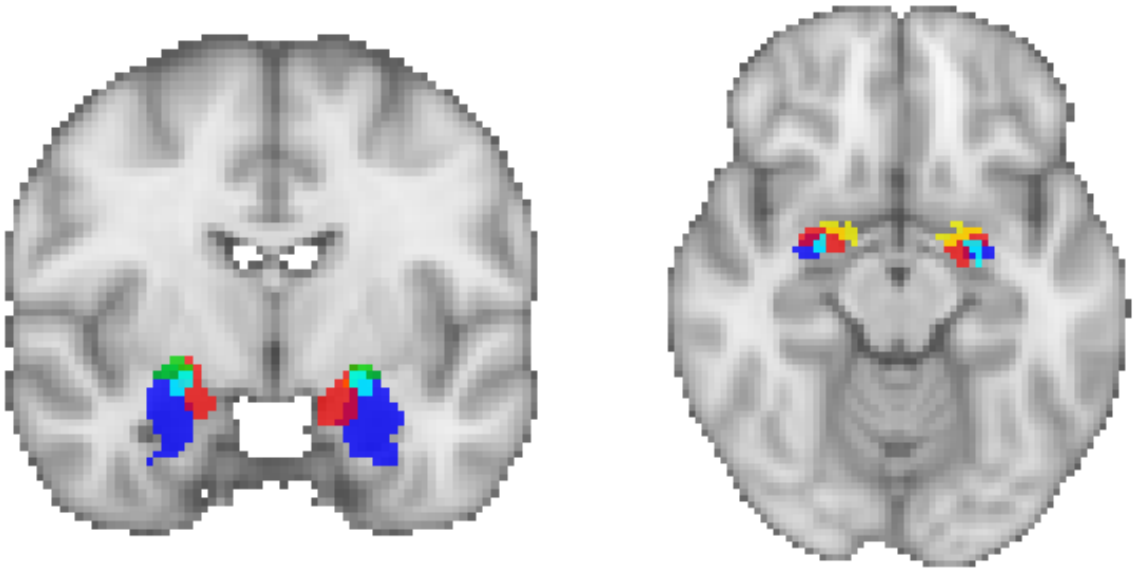

Figure 18: Amygdala ROIs for UKBB Functional Connectivity GWAS

The five amygdala subdivisions used for extracting functional connectivity between the BNST and amygdala in the UKBB sample. Green = Juelich atlas centromedial, red = Juelich atlas superficial, dark blue = Juelich atlas laterobasal, light blue = central nucleus of the amygdala (CeA), yellow = the cluster of significant BNST functional connectivity derived from previous analysis in the human connectome project (HCP-derived).

3.3.5.2 UKBB Functional Connectivity Temporal Correlation Analysis

Each of the pre-processed fMRI images (n=19,829) were analysed using a parallel processing batch system. First, using FSL's FLIRT function, each pair of masks (the BNST with each of the amygdala sub-division ROIs) were converted to each individuals subject space using the inverse of the subject space to standard space transformations provided by the UKBB, and the functional scan (in native space) as a reference (Jenkinson et al., 2012). These masks were then used to extract the mean timeseries of BOLD for the BNST and each amygdala ROI. As a check on the degree of overlap or redundancy between the ROIs, Pearson's r correlations were run on all BNST-amygdala pairwise combinations.

3.3.5.3 Post-hoc correlation analysis between amygdala ROI's

Because the amygdala ROIs were largely overlapping, we ran a Pearsons r correlation analysis to examine to degree of similarity between the BNST-amygdala subregion functional connectivity. This was performed by transforming the correlation values to z scores then correlating these Z values (Figure 18).

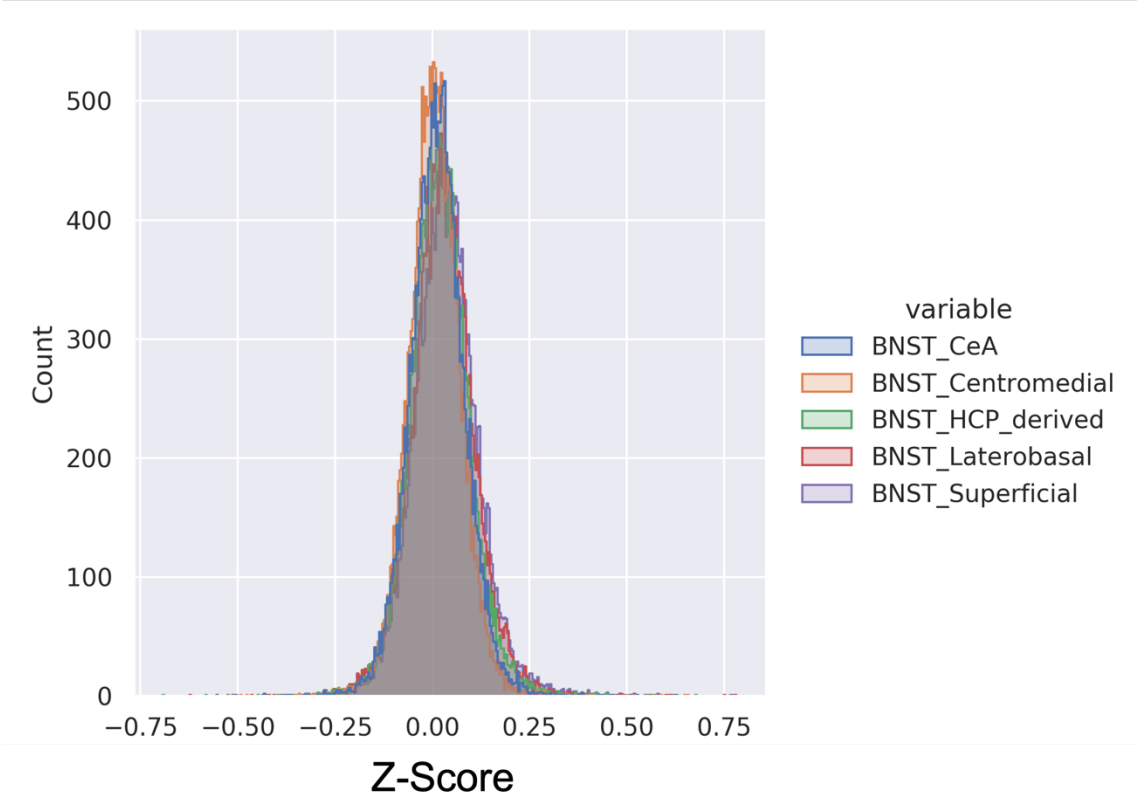

Figure 19: BNST - Amygdala Sub-Region Connectivity Distrubutions

The r-Z transformations of each BNST-amygdala subregion functional connectivity pair.

3.3.6 Anxiety and alcohol phenotype regressions on BNST-amygdala functional connectivity correlations

To test for association between BNST – amygdala sub-region FC correlations and phenotypes relating to anxiety and alcohol use a series of linear regressions were run. These were performed using lme4 (Bates et al., 2014) linear model functions in the R

programming environment. Twenty individual regressions were run in total, with the IV's being the phenotype variables the DV's as each pair of BNST-amygdala FC correlation values. For ease of interpretation, FC correlation values were scaled using the 'scale' function in R, which calculates the mean and standard deviation of the data before subtracting the mean and dividing by the standard deviation for each data point. Covariates included in the model were age, age^2, sex, age^2 * sex, date attended, centre attended, resting-state fMRI head motion (log scale), and total grey and white-matter volume (Chambers et al., 2022) (for descriptive statistics see Table 10).

3.3.7 Genetic Data Collection and Quality Control

Full descriptions of UKBB genetic data collection, initial quality control (QC) and imputation steps are reported elsewhere (http://www.ukbiobank.ac.uk/scientists-3/genetic-data/) (Bycroft et al., 2018). In brief, genetic data was obtained from blood samples of 488,377 individuals and assayed on two Axiom arrays to capture common and rare genetic variants of interest. Imputation of the remaining genotype was performed using Haplotype Reference Consortium (HRC) and UK10K haplotype resources, providing a final ~96million SNP resource per individual, harmonised to GRCh37 (hg19) genome build assembly of the human genome (Bycroft et al., 2018; S. McCarthy et al., 2016).

Further QC of the autosomal genotypes from the UK Biobank imaging sample was performed in-house using self-authored Stata functions (https://github.com/ricanney/stata summaryqc function) leveraging the PLINK command-line software developed for genetic analysis (Chang et al., 2015) (v1.90b5.4; https://www.cog-genomics.org/plink2/). Firstly, across the whole 500k UKBB sample, markers were quality controlled based on imputation quality (INFO>0.8), minor allele frequency (MAF >0.01%) and those present in HRC reference (S. McCarthy et al., 2016). Within the imaging subsample, markers were further excluded based on low minor allele count (present in <5 individuals) to exclude markers with too few

occurrences (which can lead to unstable effect sizes), excess individual marker missingness (>2% of all individuals), deviations from Hardy-Weinberg equilibrium (p<10–10) and from the expected minor allele frequency (MAF; >4 standard deviations (SD) from GBR reference MAF reported in 1000G phase 3 (McCarthy et al., 2016), all of which can indicate genotyping errors, assortative mating or residual population structure (Marees et al., 2018).

Of the initial 7,726,488 genetic markers, 7,232,075 markers remained following QC. Quality control also removed individuals with excess overall marker missingness rate (>2%), excess heterozygosity (which can indicate inbreeding or sample contamination) (>4 x SD from sample mean), those of non-British/Irish self-reported or based on similar genetic ancestry (derived from the first 3 principal components comparison 1000G GBR ancestry reference) and those with close relatives in the cohort so as to not bias SNP effect sizes and standard errors (>0.0442 i.e. 3rd degree relatives). QC was performed by Dr Richard Anney at Cardiff University (Chambers et al., 2022). For further discussion on GWAS QC parameters see Marees et al., 2018.

3.3.8 GWAS Analysis

Of the initial 20,416, the total number of individuals who passed the QC stages, had BNST-amygdala sub-region correlation values, and had entries for the covariate variables (see below) was 17,710. PLINK v1.9 (Chang et al, 2015) -assoc command was used to run GWAS analyses to test for common SNP associations with each BNST-amyg FC pair. The co-variates included were the first 10 genetic principal components (to control for population stratification), age, age^2, sex, age * sex, age^2 * sex, date attended, imaging centre attended, head and table position in the scanner, resting-state fMRI head motion (log scale), and total grey and white matter volume. Quantile-quantile (QQ) plots were also created to check for confounding effects. QQ plots show the observed SNP p-values against the p-values expected under the null hypothesis. If observed p-values are more significant than expected under the null then they will

drift away from the null hypothesis line towards the Y axis of the graph. If this separation occurs early (thus demonstrating thousands of p-values being lower than expected), this typically indicates population stratification effects. GWAS analyses were run in collaboration with Dr Tom Chambers from Cardiff University.

3.3.9 Functional Annotation and SNP-Heritability Analysis

GWAS summary statistics were entered into the online web application 'Functional Mapping and Annotation of Genome-Wide Association Studies' (FUMA) (Watanabe et al., 2017). FUMA uses information from large repositories of biological data to process GWAS summary statistics and provide a variety of (potentially) relevant functional annotations. FUMA computes the linkage disequilibrium (LD) structure, identifies lead SNPs, annotates functions to SNPs, and suggests candidate genes based on SNP location and information from expression quantitative trait loci (eQTL) and chromatin interaction studies (Watanabe et al., 2017).

Once candidate SNPs and genes were identified, this information was forwarded to databases to examine 1) the evidence for a SNP's effect on gene expression, 2) in which tissues these genes are expressed, and 3) evidence from other studies of gene or SNPs association with phenotypes. To check for the effects of a SNP on gene expression, SNP IDs were entered into the rSNPBase 3.1 website (http://rsnp3.psych.ac.cn/index.do), which pulls together information from multiple repositories to check for SNP associations with gene expression (Guo & Wang, 2018). The Human Protein Atlas (HPA) website (https://www.proteinatlas.org/) was used to identify tissues in which any associated genes were preferentially expressed. This data is based upon an integration of two mRNA expression datasets (HPA and GTEx) from 56 tissues across the body and brain derived from deep mRNA sequencing (for full details see Uhlén et al., 2015). Finally, any associated genes were entered into the National Centre for Biotechnology Information (NCBI) database (https://www.ncbi.nlm.nih.gov/), a United States national resource that provides

regularly reviewed summary information regarding genes and their currently known functions and phenotype associations (Sayers et al., 2022)

GWAS summary statistics were also used to calculate SNP-based heritability estimates (the proportion of phenotypic variance explained by SNPs) using the command-line tool 'Linkage Disequilibrium Score Regression' (LDSC) (Bulik-Sullivan et al., 2015). LDSC calculates SNP heritability by regressing the SNP's trait associations on their LD scores (representing the sum of LD r^2 with all other SNPs). LDSC additionally estimates and corrects for any inflation of the test statistics that may arise through population stratification. SNPs were restricted to those within the high imputation quality HapMap2 reference panel (Frazer et al., 2007) and with minor allele frequency (MAF) >1%. LD scores were based upon the 1000G European reference cohort (Birney & Soranzo, 2015).

3.4 Results

3.4.1 BNST – amygdala subregion functional connectivity correlations

Pearson's correlation analysis between each of the BNST - amygdala subregion (see Figure 17) iFC variables revealed statistically significant positive correlations between all pairs ($p < 0.0001$) (Figure 19). The superficial and laterobasal amygdala subregion in general demonstrated the greatest correlations with the other amygdala regions (0.17 – 0.51), with the centromedial displaying much smaller correlations (0.07 – 0.27).

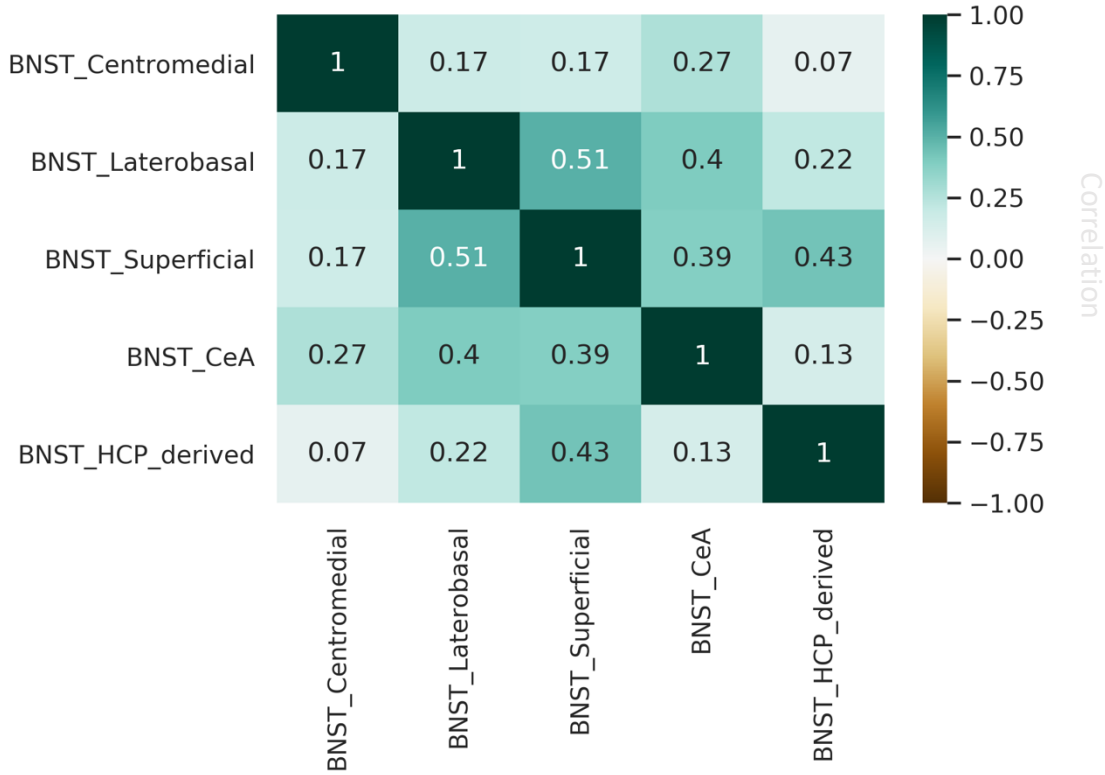

Figure 20: Correlations between the functional connectivity of each BNST-amygdala subregion pair

This figure demonstrates that all BNST-amygdala FC pairs were positively correlated and thus had some overlap with regards to the signal. The lowest correlation was between the centromedial amygdala and the HCP-derived subregion (0.07), and the highest correlation between the laterobasal and superficial amygdala regions (0.51). All correlations were statistically significant at p<0.0001.

3.4.2 BNST-amygdala functional connectivity regressions with anxiety and alcohol-use phenotypes.

Twenty regression analyses were run in total testing the association of each of the four anxiety / alcohol phenotypes on the five BNST-amygdala subregion functional connectivity pairs. None of the regression models were statistically significant after correction for false discovery rate. An exploratory analysis without the covariates included in the model did not have any meaningful effect on the outcomes. Results are presented in Table 8.

DEPENDENT VARIABLE	PREDICTOR	NROW	R2	R2_CORR	B	EBL	EBH	P	P (FDR-ADJ)	TVALUE	SE
BNST_CENTROMEDIAL	sr_alcohol	19808	0.00078	2.33E-04	0.45889	0.040687	0.877093	0.031506	0.210039	2.150778	0.21336
BNST_CENTROMEDIAL	sr_anxiety	19808	0.000707	1.60E-04	-0.06211	-0.13046	0.006231	0.074864	0.374322	-1.78139	0.034868
BNST_CENTROMEDIAL	hr_alcohol	19808	0.000555	8.41E-06	-0.03809	-0.22099	0.144801	0.683099	0.803645	-0.40824	0.093309
BNST_CENTROMEDIAL	hr_anxiety	19808	0.000791	2.45E-04	-0.16455	-0.31105	-0.01805	0.027704	0.210039	-2.20161	0.074742
BNST_LATEROBASAL	sr_alcohol	19808	0.00176	5.78E-05	0.228352	-0.18965	0.64635	0.284277	0.568554	1.07079	0.213255
BNST_LATEROBASAL	sr_anxiety	19808	0.001792	9.00E-05	-0.04655	-0.11485	0.02176	0.181671	0.488508	-1.33568	0.034849
BNST_LATEROBASAL	hr_alcohol	19808	0.001707	4.27E-06	-0.02714	-0.20993	0.155648	0.771027	0.811607	-0.29104	0.093255
BNST_LATEROBASAL	hr_anxiety	19808	0.001721	1.88E-05	-0.04556	-0.19199	0.10087	0.541954	0.746445	-0.60987	0.074707
BNST_SUPERFICIAL	sr_alcohol	19808	0.002486	1.29E-04	-0.34076	-0.75861	0.077087	0.109953	0.379892	-1.59848	0.213178
BNST_SUPERFICIAL	sr_anxiety	19808	0.002442	8.45E-05	-0.04511	-0.11339	0.023177	0.195403	0.488508	-1.2948	0.034838
BNST_SUPERFICIAL	hr_alcohol	19808	0.00239	3.19E-05	-0.07416	-0.25689	0.108564	0.426315	0.746445	-0.79553	0.093224
BNST_SUPERFICIAL	hr_anxiety	19808	0.002375	1.71E-05	0.043547	-0.10284	0.189931	0.559833	0.746445	0.583099	0.074682
BNST_CEA	sr_alcohol	19808	0.001826	3.21E-04	0.537989	0.120004	0.955973	0.011649	0.210039	2.522828	0.213248
BNST_CEA	sr_anxiety	19808	0.00157	6.52E-05	-0.03964	-0.10795	0.028678	0.255442	0.56765	-1.13726	0.034853
BNST_CEA	hr_alcohol	19808	0.001525	2.07E-05	-0.05972	-0.24252	0.123085	0.521965	0.7464446	-0.64033	0.093264
BNST_CEA	hr_anxiety	19808	0.001533	2.83E-05	-0.05593	-0.20238	0.090515	0.454108	0.746445	-0.7486	0.074714
BNST_HCP_DERIVED	sr_alcohol	19805	0.001437	6.20E-06	-0.07474	-0.49281	0.343322	0.726017	0.806686	-0.35043	0.21329
BNST_HCP_DERIVED	sr_anxiety	19805	0.001433	1.73E-06	0.006461	-0.06186	0.074781	0.852938	0.852939	0.185373	0.034856
BNST_HCP_DERIVED	hr_alcohol	19805	0.001557	1.26E-04	0.147418	-0.03538	0.330221	0.113967	0.379892	1.580679	0.093263
BNST_HCP_DERIVED	hr_anxiety	19805	0.001439	8.42E-06	0.030517	-0.11593	0.176969	0.682958	0.8036453	0.408436	0.074717

Table 8: Results from the regression analyses between BNST – amygdala subregion functional connectivity and the anxiety and alcohol use phenotypes.

None of the phenotypes were significantly predictive of any functional connectivity variable after false discovery rate (FDR) adjustment. sr = self-report, hr = healthcare record, HCP = human connectome project, CeA = central nucleus of the amygdala, NROW = number of non-NA values, R^2 = The r^r for the full model, R^2 COV = The r^2 of the total model – the r^2 of all of the covariates, B = the beta value, EBl = 95% confidence interval low, EBh = 95% confidence interval high, P = p-value, P (FDR-ADJ) = FDR adjusted p-values, T-value = the t statistic, SE = standard error.

3.4.3 SNP associations with BNST – amygdala functional connectivity

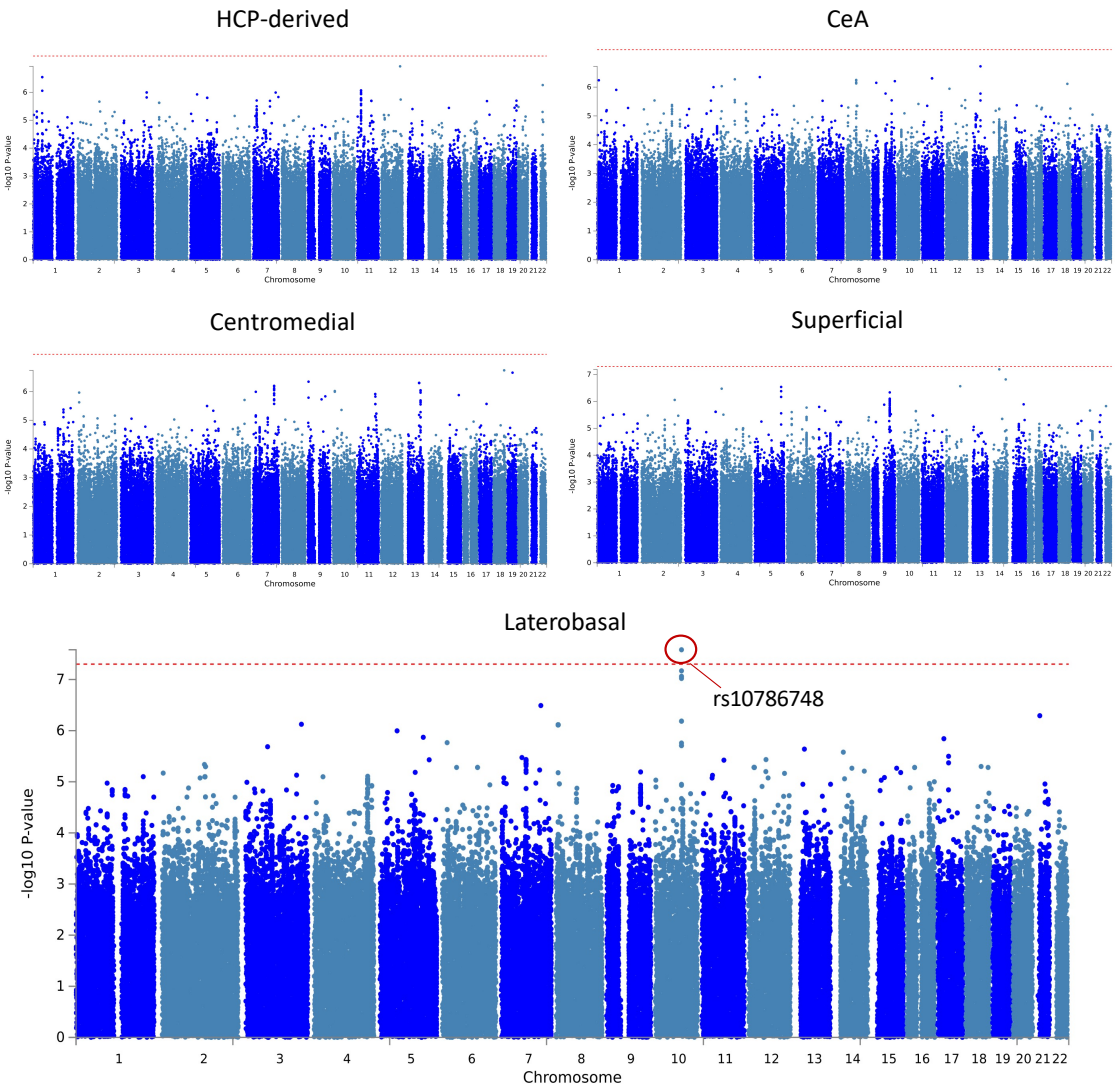

Figure 21: Manhatten plots depicting SNP associations with BNST-amygdala function connectivity

*Results from the BNST-amygdala functional connectivity GWAS analyses. Each dot represents a SNP, with the dotted red line indicating the level at which a SNP becomes significantly associated with the phenotype at p = 5 * 10^{-8}. The BNST-laterobasal functional connection had a genome-wide significant SNP, rs10786748, highlighted in red (bottom plot). CeA = Central nucleus of the amygdala.*

GWAS analyses revealed no genome-wide significant SNPs associations with BNST - HCP-derived, CeA, centromedial, or superficial amygdala functional connectivity (p > 5 * 10^{-8}) (Figure 20). GWAS of BNST-laterobasal amygdala functional connectivity demonstrated a single genome-wide significant SNP, rs10786748, located on

chromosome 10 (p = 2.616e-08) (Figure 20). Quantile-quantile (QQ) plots did not demonstrate evidence of population stratification effects (supplementary materials)

3.4.4 Functional annotation of BNST-laterobasal GWAS summary statistics

3.4.4.1 FUMA SNP linkage disequilibrium and gene association analyses

FUMA analysis of the GWAS summary statistics for the BNST-laterobasal functional connection identified 35 additional candidate SNPs in LD with lead SNP rs10786748, with 14 candidate GWAS tagged SNPs. SNP rs10786748 was identified as being intergenic, with the closest gene being Neuregulin 3 (NRG3) (Figure 21).

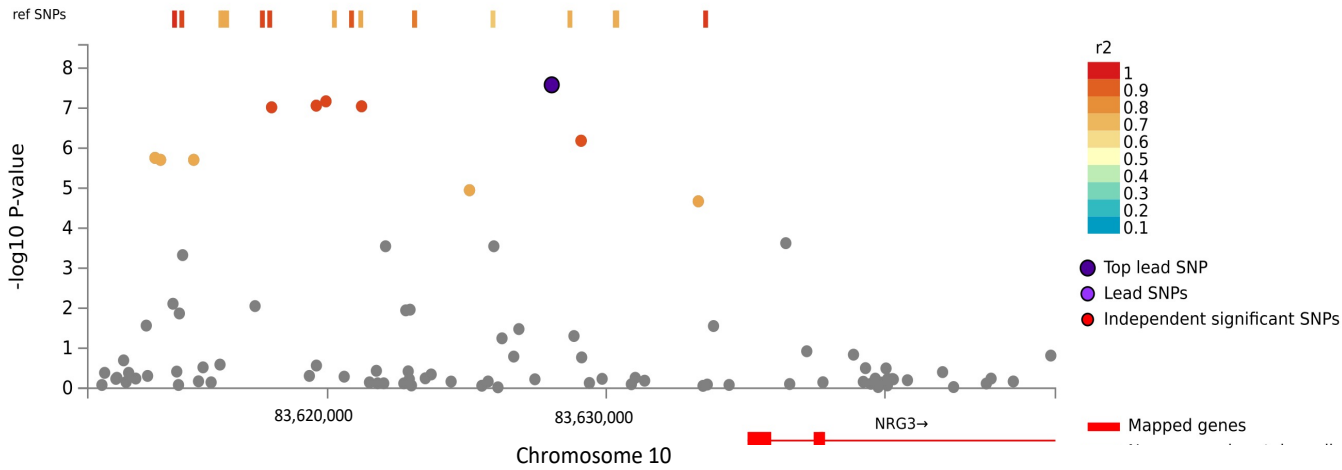

Figure 22: Regional plot of associated SNPs.

Plot displaying the lead SNP's location on chromosome 10 (purple) and the independently significant SNPs in LD with it (r^2 corelations colour coded). The SNPs are intergenic, with the closest gene (NRG3) visible on the bottom right. Figure generated via FUMA (Watanabe et al., 2017).

3.4.4.2 SNP e-QTL and gene expression analysis

Entering the lead SNP rs10786748 into the rSNPBase 3.1 database (Guo & Wang, 2018) demonstrated that this SNP was an eQTL (meaning that it contributes to variation in

the gene expression) of the gene NRG3. Investigation of the NRG3 gene via the HPA RNA expression database (Uhlén et al., 2015) revealed that the gene has enhanced expression throughout most of the brain. Of the fourteen brain regions studied, NRG3 is expressed most highly in the cerebral cortex, closely followed by the amygdala, and the hippocampal formation (Figure 22). The gene summary information provided by the NCBI database (Sayers et al., 2022) revealed that NRG3 is involved in cellular responses during development including proliferation, migration, differentiation, survival, and apoptosis.

3.4.4.3 SNP heritability analysis

SNP-based heritability analysis using LDSC (Bulik-Sullivan et al., 2015) revealed little to no SNP heritability for any of the BNST-amygdala FC pairs (Table 11).

FUNCTIONAL CONNECTIVITY PAIR	TOTAL OBSERVED HERITABILITY ESTIMATE
BNST - SUPERFICIAL AMYGDALA	h^2_{SNP}: -0.0018 (0.0264)
BNST - LATEROBASAL AMYGDALA	h^2_{SNP} : 0.0214 (0.0268)
BNST - HCP-DERIVED	h^2_{SNP} : 0.0313 (0.0263)
BNST - CENTROMEDIAL AMYGDALA	h^2_{SNP} : -0.0018 (0.0264)
BNST - CEA	h^2_{SNP} : 0.0288 (0.0276)

Table 9: SNP-based heritabilitiy estimates for each BNST-amygdala functional connectivity pair

LDSC heritibility analysis found little to no evidence for SNP-based heritability. Numbers in brackets represent the the standard error, which in all cases was greater than the $\boldsymbol{h^2_{SNP}}$
Negative heritability estimates can arise from low heritability plus measurement error.

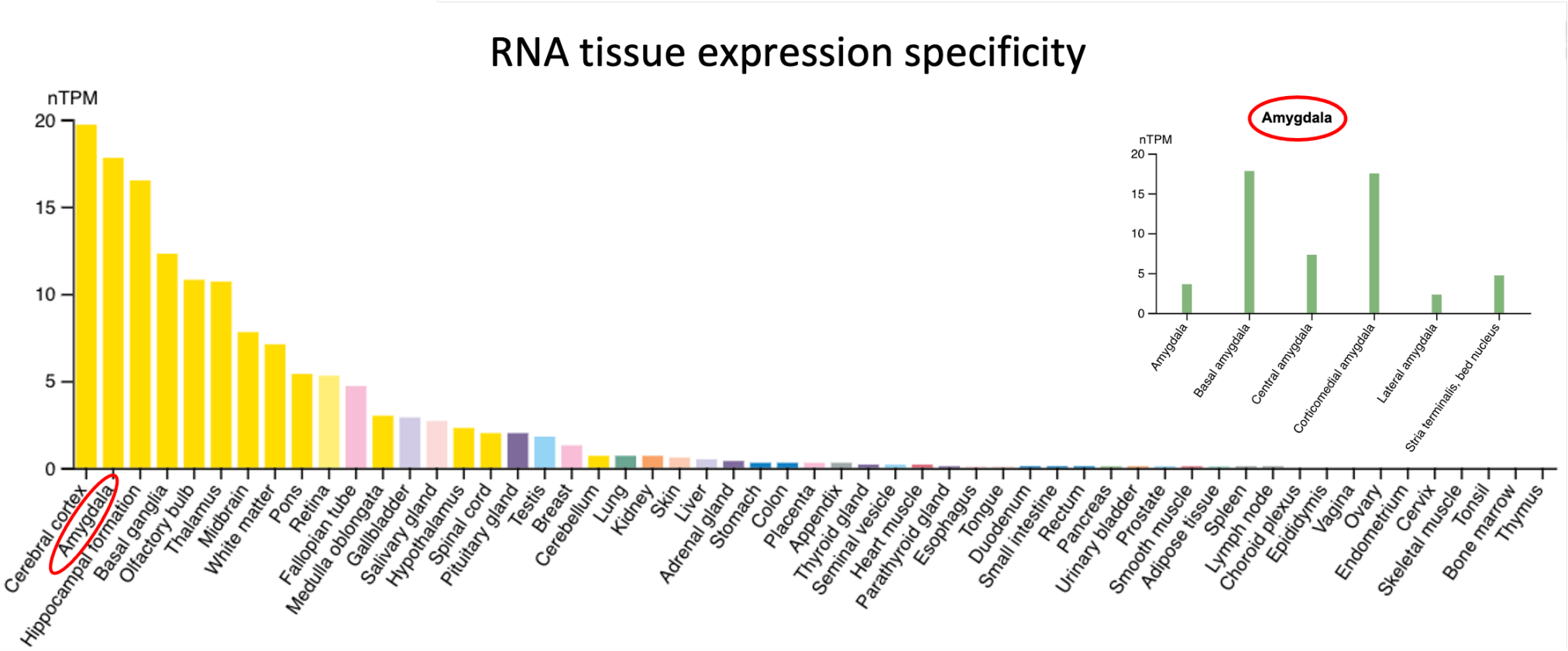
RNA tissue expression specificity
nTPM
20
15
10
5
0
Cerebral cortex
Amygdala
Hippocampal formation
Basal ganglia
Olfactory bulb
Thalamus
Midbrain
White matter
Pons
Retina
Fallopian tube
Medulla oblongata
Gallbladder
Salivary gland
Hypothalamus
Spinal cord
Pituitary gland
Testis
Breast
Cerebellum
Lung
Kidney
Skin
Liver
Adrenal gland
Stomach
Colon
Placenta
Appendix
Thyroid gland
Seminal vesicle
Heart muscle
Parathyroid gland
Esophagus
Tongue
Duodenum
Small intestine
Rectum
Pancreas
Urinary bladder
Prostate
Smooth muscle
Adipose tissue
Spleen
Lymph node
Choroid plexus
Epididymis
Vagina
Ovary
Endometrium
Cervix
Skeletal muscle
Tonsil
Bone marrow
Thymus
Amygdala
nTPM
20
15
10
5
0
Amygdala
Basal amygdala
Central amygdala
Corticomedial amygdala
Lateral amygdala
Stria terminalis, bed nucleus

3.5 Chapter Conclusions

3.5.1 Summary of findings

GWAS analyses of five BNST-amygdala FC pairs in the large UKBB sample revealed a single genome-wide significant SNP, rs10786748, associated with BNST – laterobasal amygdala FC. Genetic functional annotation tools demonstrated that this SNP is linked to the expression of the gene NRG3, which is expressed highly in many brain regions including the amygdala. Regression analysis of anxiety and alcohol-use measures on the five BNST-amygdala FC estimates provided no evidence for any associations. Additionally, SNP-based heritability analysis found little to no SNP-based heritability for any BNST-amygdala FC pair.

3.5.2 Missing heritability for BNST-amygdala functional connectivity pairs

Two previous studies used family-based samples to estimate genetic contributions to task-free FC between the BNST and different amygdala sub-regions in humans and macaques (Berry et al., 2020 [Chapter 2]; Fox et al., 2018). These studies reported a modest genetic contribution ($h^2 \sim 15$) to BNST FC with the centromedial and superficial amygdala subregions in humans (Berry et al., 2020), and a moderate ($h^2 \sim 45$) contribution to BNST FC with the CeA in macaques (Fox et al., 2018). Despite this, in our large human sample we did not find any evidence for SNP-based heritability above zero between the BNST and any amygdala subregion.

This could be due to several reasons. Firstly, as mentioned in section 2.5.3 of chapter 2, comparing the strength of heritability estimates across any given sample is challenging due to the effects of the particular environment on heritability estimates, something further confounded by comparisons across species (Turkheimer, 2016). Nonetheless, you may still expect that if a trait is heritable in one population-level

human sample (e.g. the HCP, n ~ 1200) then you should detect evidence for heritability in a similar population-level human sample (e.g. the UKBB n ~ 19,000). Part of this disparity is likely due to the different methods used to estimate heritability. It is frequently reported that twin-based analyses give higher heritability estimates than SNP-based methods (the 'missing heritability problem', Yang et al., 2010). This effect is often explained by several factors (discussed in General Introduction section 1.3), including overestimation of genetic effects in twin-samples due to confounding from shared environments, and the inability of SNP-based heritability methods to capture the effects of rare (MAF <0.01) variants (Yang et al., 2017).

No evidence for heritability in this sample may further be due to variations in imaging acquisition and pre-processing steps between the HCP and UKBB samples. Although, relative to many fMRI studies, these studies had similar acquisition parameters and pre-processing steps, important distinctions include the spatial resolution (2.4mm for the UKBB, 2mm for HCP) and a large discrepancy in the length of the scans (6.1 minutes for UKBB and four 15 min scans for the HCP). Scan length in particular has been shown to have a considerable effect on the reliability of tf-fMRI results, with the intraclass correlation coefficient increasing by around 20% when comparing 6 minute and 12 minute scans (Birn et al., 2013). Therefore, the short scan time in the UKBB sample may have increased the noise in the data making it hard to accurately detect, the typically smaller, underlying SNP-based heritability.

3.5.3 Anxiety and alcohol-use phenotypes are not associated with BNST-amygdala functional connectivity

The four alcohol and anxiety phenotypes (health-record alcohol, self-report alcohol, health-record anxiety, and self-report anxiety) were not associated with any of the BNST-amygdala tf-FC measures. Both the health-record and self-report data indicated whether a person had been diagnosed, or considered themselves as having an alcohol-use disorder (AUD) or anxiety disorder.

The BNST and amygdala have been frequently linked with alcohol and anxiety use disorders, with studies placing the two structures as key in networks underlying many associated traits and behaviours (Centanni et al., 2019; Lebow & Chen, 2016; Maita et al., 2021) (see also General Introduction section 1.2). In addition, some researchers have specifically implicated structural and functional connections between the amygdala and BNST in processes underlying both disorders (Figel et al., 2019; Hur et al., 2018; Maita et al., 2021). Below I suggest several reasons that could explain why in the current study I did not find and associations with the tf-FC measures.

Firstly, the UKBB sample is not entirely representative of the broader population. Studies have shown that volunteers are on average healthier and wealthier than the general population, and in particular with regards to alcohol are less likely to drink on a daily basis (Fry et al., 2017). This speaks to a broader point, which is that it is unlikely that people with serious alcohol use or anxiety disorders would be in a position to participate in the study, thus potentially reducing the power to detect an effect. For AUD, this is perhaps reflected in the discrepancy between the number in the health-record alcohol group (n=116) and the self-report alcohol group (n =22). Those in the health-record alcohol group includes those who have at any point in their lives been diagnosed with an alcohol related disorder, whereas the self-report group were answering whether they considered themselves to be alcohol dependent. The discrepancy likely means that many people with a history of alcohol dependency, but no current problem, did not consider themselves to be alcohol dependent. Therefore, although the health-record alcohol group was much larger, it may have contained many individuals who do not currently have an alcohol disorder, potentially diluting any tf-FC associations.

With regards to anxiety disorders, more people self-reported an anxiety disorder (n = 866) than had been medically diagnosed with one (181). Recent research indicates that self-report measures of anxiety have good agreement with clinical diagnoses (Davies et

al., 2022), thus suggesting either gaps within the medical records or that many people are reluctant to seek professional help (Kasper, 2006). That we did not have more clinically diagnosed anxiety patients may be a result of an ascertainment bias. Previous work has demonstrated that more anxious individuals are significantly less likely to undergo, or successfully complete, neuroimaging studies (Charpentier et al., 2020).

For both disorders, results may have been further impacted by the control group containing individuals who would typically meet the clinical criteria for a disorder, but for some reason have either never sought treatment or do not consider themselves to have a problem. This is particularly likely for alcohol disorders where, despite the UKBB sample drinking less than the average UK population, researchers have demonstrated that that 21% of UKBB participants meet the criterion for current hazardous/harmful alcohol use (Davis et al., 2020).

Lastly, although many studies have linked the amygdala and BNST to mechanisms underlying alcohol and anxiety disorders (e.g., Avery et al., 2016; Fox & Shackman, 2019; Lebow & Chen, 2016), there is much less evidence associating BNST-amygdala iFC alterations with these disorders. This is particularly true for AUD, with only one study to date showing FC alterations between the BNST and amygdala after healthy participants had consumed alcohol (Hur et al., 2018). Studies that have examined resting-state iFC associations with AUD have mostly demonstrated changes to large-scale ICN's rather than specific connections (e.g. Song et al., 2021; Zhu et al., 2017). Where the amygdala has specifically been studied, iFC alterations in AUD are seen with frontal and/or temporal regions rather than to basal forebrain areas such as the BNST (Dean et al., 2020). Therefore, although amygdala – BNST connectivity has been theorised to play a role in alcohol use disorders via mechanisms related to negative affect and withdrawal (Koob & Volkow, 2016; Roberto et al., 2020), there is currently little evidence to support the idea that the iFC of these regions is altered in people with AUD. For anxiety disorders, several studies have demonstrated alterations to FC between the BNST and amygdala, and in particular the CeA, under anxiety provoking

conditions. However, these same BNST- amygdala iFC perturbations have not been shown under task-free conditions, with one study demonstrating this precise discrepancy in the same group of clinical anxiety patients (Torrisi et al., 2019).

3.5.4 SNP association with BNST- laterobasal amygdala functional connectivity

The SNP rs107867448, significantly associated with BNST – laterobasal iFC, was shown by the rSNPBase 3.1 database to be linked to the expression of the *NRG3* gene. The protein atlas database, consisting of gene expression data from adult human subjects, showed that *NRG3* is expressed mostly in the brain, demonstrating a largely broad pattern of expression, with the highest subcortical expression in the amygdala (Figure 22). *NRG3* has been linked to neocortical development and in particular has been associated with the growth and differentiation of glial cells (Paterson et al., 2017). Its role post-development is less well understood, although expression in the brain continues to be widespread throughout the lifespan (Paterson et al., 2017). Differences in *NRG3* expression are linked to several psychiatric phenotypes, including schizophrenia, bipolar disorder, major depressive disorder, nicotine dependence, anxiety, and sociability levels (Kao et al., 2010; S. Meier et al., 2013; Paterson et al., 2017; Paterson & Law, 2014).

Although most researchers have focused on the CeA – BNST connection due to their well-established structural connections, there is also evidence for monosynaptic connections between the BNST and laterobasal amygdala, with some early evidence suggesting a link between these two regions and the initial encoding of fear memories (Russell et al., 2020). The relation of *NRG3* to this process though has not been investigated. In general, whilst the association of *NRG3* with BNST-laterobasal iFC is biologically plausible, given its links to amygdala expression and its associations with phenotypes also linked the BNST and amygdala (in particular those related to mood disorders), in absence of further replication and mechanistic follow-up studies this result should not be overinterpreted. The SNP association was only marginally above

the threshold of genome-wide significance and, especially given the very low heritability estimates, would only be explaining a small amount of iFC variance.

3.5.5 Limitations

This study has several limitations. Firstly, although having a large sample provides greater power to detect associations with genetic and trait variables, a trade-off is that manual delineation of brain regions becomes unrealistic. This is also the case for checking the accuracy of automated ROI registration. Although I followed standard protocols and used validated masks for our brain regions, I cannot rule out that individual variation introduced some noise into this process which made our functional connectivity estimates less precise. This may be evidenced by our only genetic association being with the largest ROI, the laterobasal amygdala, which could perhaps suggest that the smaller ROIs were less accurately registered across participants (X. Song et al., 2016). Second, although the sample was large for neuroimaging research, it is relatively small for modern GWAS analysis. Researchers have consistently demonstrated that more significantly associated SNP's are discovered linearly with increases in sample size (Hong & Park, 2012). UKBB is eventually aiming to release neuroimaging data on 100,000 people (Littlejohns et al., 2020), it is anticipated that reanalysis of a larger sample would reveal more robust genetic associations. Thirdly, the phenotypes were chosen in this study to reflect clinical disorders in a general population. Therefore I chose not to control for comorbidity or for the effects of medication taken. In addition, the phenotypic measures were suboptimal and analyses in future would benefit from more precise diagnostic screening, with consideration of disease onset and medication effects. Lastly, as discussed in Chapter 2 (section 2.5.5), the neuroimaging results may have been influenced by the particular choice of pre-processing parameters and the 'eyes-open' nature of the tf-fMRI acquisition.

3.5.6 Chapter conclusions and future directions

In conclusion, I used a large population-level sample to run a GWAS analysis on iFC between the BNST and five amygdala subregions. To my knowledge, this is the first GWAS analysis attempted using BNST phenotypes and thus represents a step forward from the heritability analyses used previously (Fox et al., 2018). In general, there was little evidence for a strong common genetic component underlying these connections, however there was an association between BNST-laterobasal iFC and a SNP involved in the expression of the gene *NRG3*, which in turn has been linked to the amygdala and various psychiatric phenotypes. Clinical diagnoses of anxiety and alcohol use disorders was not associated with any of the BNST-amygdala iFC pairs. Future considerations include increasing the scan times for tf-fMRI scans in large scale datasets, moving towards task-based methods (Finn, 2021) and refining the phenotypic measures used in the analysis (for a more detail see the General Discussion). As well, although this population-level sample contained clinically diagnosed individuals with both anxiety and alcohol use disorders, specific targeted recruitment of these groups would be preferable, with special attention paid to groups needs that are likely to go beyond those of the general population. Future studies could also make use of techniques which combine shared features of tf-FMRI and task-based fMRI, something shown to improve reliability and increase heritability estimates (M. L. Elliott et al., 2019). In general, larger samples with more precise phenotypic measures, both regarding the neuroimaging and psychiatric variables, would improve the accuracy of similar studies in future.

3.6 Supplementary Information

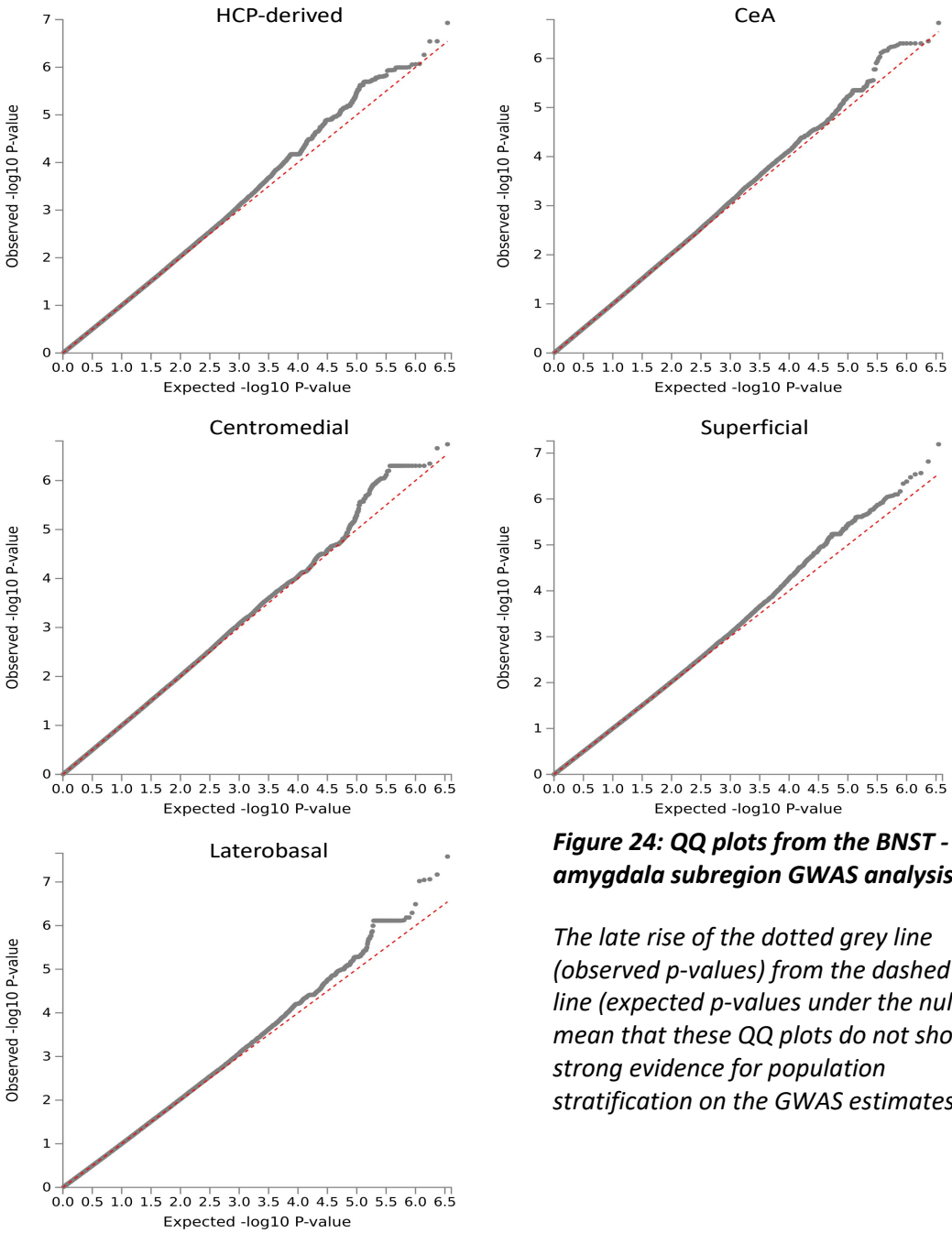

Figure 24: QQ plots from the BNST - amygdala subregion GWAS analysis.

The late rise of the dotted grey line (observed p-values) from the dashed red line (expected p-values under the null) mean that these QQ plots do not show strong evidence for population stratification on the GWAS estimates.

Group	*N*	*Age (mean/sd)*	*Sex (%f)*
Total	19808	62.54 (7.47)	52.9%
Sr_alcohol	22	60.27 (6.95)	31.8%
Sr_anxiety	866	61.06 (7.53)	65.4%
Hr_alcohol	116	62.2 (8.1)	23.3%
Hr_anxiety	181	62.1 (7.65)	65.7%

Table 10: Descriptive statistics of UK Biobank participants by phenotype group

Sr = self-report, Hr = health records, sd = standard deviation, %f = percentage of female participants.

Chapter 4: Subiculum – BNST Structural Connectivity in Humans and Macaques

4.1 Chapter Summary

Invasive tract-tracing studies in rodents implicate a direct connection between the subiculum and bed nucleus of the stria terminalis (BNST) as a key component of neural pathways mediating hippocampal regulation of the Hypothalamic-Pituitary-Adrenal (HPA) axis. A clear characterisation of the connections linking the subiculum and BNST in humans and non-human primates is lacking. To address this, in this chapter I describe work delineating the projections from the subiculum to the BNST using anterograde tracers injected into macaque monkeys, revealing evidence for a monosynaptic subiculum-BNST projection involving the fornix. Second, I use *in vivo* diffusion MRI tractography in macaques and humans to demonstrate substantial subiculum complex connectivity to the BNST in both species. This connection was primarily carried by the fornix, with additional connectivity via the amygdala, consistent with rodent anatomy. Third, utilising the twin-based nature of our human sample, I report that microstructural properties of these tracts were moderately heritable (h2 ~ 0.5). In a final analysis, I find no evidence of any significant association between subiculum complex-BNST tract microstructure and indices of perceived stress/dispositional negativity and alcohol use, derived from principal component analysis decomposition of self-report data. These findings address a key translational gap in our knowledge of the BNST-linked neurocircuitry regulating stress.

4.2 Introduction

Though widely studied for its role in episodic memory and spatial navigation, the hippocampal formation also plays an important role in fear, stress and anxiety (for review see Murray et al., 2017; Poppenk et al., 2013). In particular, structural connections between the main output region of the hippocampus, the subiculum (Aggleton & Christiansen, 2015; Böhm et al., 2018; Kishi et al., 2000), and the hypothalamic paraventricular nucleus (PVN) are implicated in control of the stress

response via modulation of the hypothalamic-pituitary -adrenal (HPA) axis (Herman et al., 2003, 2020). Altered hippocampal regulation of the stress axis has been linked to various forms of psychopathology (Belleau et al., 2019; Herman et al., 2020). Studies in the rat suggest that subiculum modulation of the HPA axis is routed principally via structural connections to a key intermediatory structure, the bed nucleus of the stria terminalis (BNST) (for reviews see Herman et al., 2020; Radley & Johnson, 2018).

Although numerous rat studies implicate the BNST as a crucial intermediary structure en route from the subiculum to the PVN, descriptions of subiculum-BNST structural connectivity in the monkey and human literature are conspicuous by their absence (Aggleton & Christiansen, 2015; Böhm et al., 2018; Fox & Shackman, 2019; Lebow & Chen, 2016; Roberts & Clarke, 2019). Therefore, the present study aims to bridge this translational gap by characterising, via ex-vivo anatomic tract-tracing and in-vivo diffusion MRI tractography, this overlooked yet potentially key stress-regulatory pathway in both humans and macaques.

4.2.1 Subiculum - BNST Connectivity in Rodents

Invasive tract-tracing has demonstrated that the subiculum-BNST connection in rats and mice emanates from the ventral subiculum and travels via the fornix, or through a route involving the amygdala, to the BNST (Bienkowski et al., 2018; Canteras & Swanson, 1992; Cullinan et al., 1993; Dong et al., 2001; Herman et al., 2020; Howell et al., 1991; Kishi et al., 2000; McDonald, 1998; Radley & Sawchenko, 2011; Shin et al., 2008; Swanson & Cowan, 1977).

In a key series of experiments, Cullinan, Herman, & Watson (1993) used the anterograde neuronal tracer Phaseolus vulgaris-leucoagglutinin (PHA-L) to reveal dense fornical and amygdala/ stria terminalis projections of ventral subiculum axons to the BNST in rats (Cullinan et al., 1993). They further used a mix of anterograde tracer PHA-L and retrograde tracer Flouro-gold to show that ventral subiculum neurons project to cells within the BNST that in turn project to the PVN (Cullinan et al., 1993).

The researchers demonstrated that this takes place via a polysynaptic glucocorticoid - GABAergic feedback inhibition system, with the subiculum stimulating the BNST, which then sends inhibitory signals to the PVN (Cullinan et al., 1993). Whilst it was previously known that the subiculum is involved in top-down regulation of the HPA-axis (e.g., Jacobson & Sapolsky, 1991), this study demonstrated that the ventral subiculum largely relies on the BNST as an intermediary structure to do so. These findings, and others since, have seen the BNST come to be understood as an important relay, or cortical processing hub (Radley & Johnson, 2018), integrating information from the hippocampus and other regions (Radley & Sawchenko, 2011) before regulating HPA axis activity (Cullinan et al., 1993; Herman et al., 2020; Lebow & Chen, 2016). Research in rats suggest a specific role of the ventral subiculum – BNST pathway in response to acute stressors involving exteroceptive triggers (e.g., stimuli connected with novel environments), but not interoceptive cues (e.g., hypoxia) (Herman et al., 1998, 2020; Mueller et al., 2004; Radley & Sawchenko, 2011). However, the precise intricacies of how this pathway is related to the stress response is likely to be complicated by the heterogenous and complex structure of the BNST, with researchers demonstrating sometimes opposing functions of different BNST sub-regions on the PVN (Choi, Evanson, et al., 2008; Choi, Furay, et al., 2008; Herman et al., 2020; Myers et al., 2012).

4.2.2 Subiculum – BNST Connectivity in Monkeys

Subiculum-BNST connectivity in monkeys has been far less extensively studied. Probably the first indications of a corresponding connection in monkeys were published in studies that used a mix of electrical stimulation and lesion-degeneration methods to investigate hippocampal outputs in squirrel monkeys (Poletti et al., 1973; Poletti & Creswell, 1977; Poletti & Sujatanond, 1980). This research uncovered evidence for a light subiculum connection to the BNST (Poletti et al., 1973; Poletti & Creswell, 1977; Poletti & Sujatanond, 1980). In agreement with subsequent work in the rat (e.g., Cullinan et al., 1993) Poletti and colleagues also reported that hippocampal-BNST connectivity was not completely reliant on the fornix, but rather that the BNST receives additional anterior hippocampal (corresponding to ventral hippocampus in rodents, Strange et al., 2014) influences; likely involving the stria

terminalis and/or the amygdalofugal pathway (Morrison & Poletti, 1980; Poletti et al., 1973; Poletti & Creswell, 1977; Poletti & Sujatanond, 1980). More recently, a ventral subiculum connection to the BNST has also been reported in the primate-like tree shrew (Ni et al., 2016).

4.2.3 Subiculum – BNST Connectivity in Humans

Diffusion MRI (dMRI) permits a non-invasive macro-scale estimate of white matter tracts in the brain by using the local restriction of water diffusion to infer the presence and orientation of white matter tracts (Jbabdi & Behrens, 2013). Researchers have demonstrated that pathways reconstructed in the human brain using dMRI often closely resemble those seen using monkey tract-tracing methods (Mars et al., 2018; Schmahmann et al., 2007), with an estimated 90% of 'ground truth' tracts being detectable (Maier-Hein et al., 2017). Owing to its small size and the relatively recent introduction of protocols for delineating the structure in the human brain, studies examining structural connections that include the BNST are rare. An exception (Avery et al., 2014) reported evidence of BNST structural connectivity to a variety of basal ganglia and limbic regions, including the hippocampus (Avery et al., 2014). Although only investigating the hippocampus as a single structure, an examination of the heat-map of connectivity strength within the hippocampus suggests that the subiculum is the principal driver of this connection (Avery et al., 2014).

As well as reconstructing tracts, dMRI estimates of water diffusion can be used to infer properties of white matter microstructure. For instance, fractional anisotropy (FA) can be used to estimate axonal myelination, axonal diameter, or fibre density (Basser, 1997; Dennis et al., 2021). Several human neuroimaging studies have reported associations, both phenotypic and genetic, between dMRI microstructure measures and human traits (e.g., Bauer et al., 2016; Cox et al., 2016; Gray et al., 2020; Rutten-Jacobs et al., 2018). Given rodent evidence implicating the subiculum– BNST connection in HPA-axis modulation (Herman et al., 2020), white matter microstructural

properties of this tract may be related to traits and behaviours associated with stress reactivity.

Stressor reactivity is hypothesised to play a key role in dispositional negativity (Hur et al., 2019; Shackman et al., 2016). This term refers to individual differences in the propensity to experience and express more frequent, intense, or enduring negative affect (Hur et al., 2019; Shackman et al., 2016). Dispositional negativity is relatively stable across the lifespan and is predictive of numerous negative life outcomes, including elevated risk for the development of stress-sensitive psychiatric diseases; such as anxiety or depressive disorders (for reviews see; Hur et al., 2019; Shackman et al., 2016, see also General Introduction section 1.2.2). Importantly, researchers have also connected the stress-response with potentially addictive behaviours, including alcohol use (Herman, 2012; Herman et al., 2020; Koob & Volkow, 2016). Evidence from both preclinical and human subjects have linked the hippocampus and the BNST to dispositional negativity and addictive behaviours (Hur et al., 2018; Lebow & Chen, 2016; Mira et al., 2020; Shackman et al., 2016). Alcohol consumption in particular has been shown to alter stress processing via drug-induced changes to PVN projecting limbic regions, including alterations to BNST and subiculum receptor signalling (Bach et al., 2021; Centanni et al., 2019; Haun et al., 2020; Mira et al., 2020). However, relationships between the microstructural properties of this putative subiculum-BNST pathway and dispositional negativity / alcohol use in humans are currently unknown.

4.2.4 Study Aims

This research will examine: 1) The evidence for a structural connection between the subiculum and the BNST in macaques and humans. 2) The spatial organisation of the structural connection between the subiculum and BNST in macaques and humans. 3) Whether individual differences in dMRI indices of white matter microstructure within subiculum - BNST tracts are phenotypically and/or genetically associated with self-reported stress-related traits. To do this, I first interpret results from a novel analysis obtained in collaboration with Prof John Aggleton from Cardiff University, who used a

series (n=7) of macaque monkeys with injections of tritiated amino acids in the hippocampal formation to examine evidence of direct projections to the BNST (Aggleton, 1986; Berry et al., 2022). Secondly, I use an open-source macaque monkey dMRI dataset (n=9) to conduct in-vivo dMRI tractography analysis (Shen, Bezgin, et al., 2019a). Next, I repeat the dMRI tractography analysis in a large human sample, the Young Adults Human Connectome Project (HCP) (n = 1206). As well as containing high quality neuroimaging data (Sotiropoulos et al., 2013; Van Essen et al., 2012), this sample has been richly phenotyped; allowing for the examination of relationships between dMRI white matter microstructure and stress-related traits (reflecting dispositional negativity and alcohol use, derived in a previous study (Berry et al., 2020)). Finally, I use the family structure of the HCP (Van Essen et al., 2012) to assess the heritability, and co-heritability, of our dMRI microstructure measures and derived stress-related traits.

4.3 Methods

4.3.1 Data Descriptions

4.3.1.1 Macaque Brain Tissue Data

Details of the macaque tissue data can be found the published manuscript associated with this chapter (Berry et al., 2022).

4.3.1.2 Macaque Diffusion-MRI Data

The dMRI monkey data were obtained from TheVirtualBrain Macaque MRI repository, made available through the OpenNEURO website (Shen, Bezgin, et al., 2019). The sample consists of nine macaque monkeys - eight male rhesus macaques (Macaca mulatta) and one male cynomolgus macaque (Macaca fasicularis). All surgical and

experimental procedures were approved by the Animal Use Subcommittee of the University of Western Ontario Council on Animal Care and were in accordance with the Canadian Council of Animal Care guidelines (Shen, Bezgin, et al., 2019).

4.3.1.3 Human Diffusion-MRI Data

Human participants were drawn from the April 2018 release of the Young Adults Human Connectome Project study (n=1206) (Van Essen et al., 2012). Participants were between the ages of 25-37 and primarily made up of family groups, with an average size of 3-4 members and most containing a MZ (273) or DZ (166) twin pair. Participants were excluded during initial recruitment for psychiatric, neurological, or other long-term illnesses, although participants who were overweight, smoked, or had a history of recreational drug use and/or heavy drinking were included (Van Essen et al., 2012). For the imaging analysis, our samples included participants who had a dMRI and T1-w structural MRI scan (n=1065). Of these, there were 575 females and 490 males. For detailed recruitment information and for a full list of procedures see: https://www.humanconnectome.org/study/hcp-young-adult. See the supplementary material for a further breakdown of participants' demographic information.

4.3.2 Hippocampal Injections

All of the histological work was performed by Prof. Aggleton at Cardiff University. A description of the methods can be found in the published manuscript associated with this work (Berry et al., 2022).

4.3.3 Diffusion-MRI Acquisition and Pre-processing

4.3.3.1 Macaque Sample Image Acquisition

Full imaging acquisition protocols have been described elsewhere (Shen, Bezgin, et al., 2019; Shen, Goulas, et al., 2019). Briefly, the monkeys were anaesthetised before

scanning and anaesthesia was maintained using 1-1.5% isoflurane during image acquisition. Images were acquired using a 7T Siemens MAGNETOM head scanner with an in-house designed and manufactured coil optimised for the Macaque head (Gilbert et al., 2016). Two diffusion-weighted scans were acquired for each animal, with each scan having opposite phase encoding in the superior-inferior direction at 1mm isotropic resolution. Six of the animals had data acquired with 2D echo planar imaging (EPI) diffusion and the remaining three had a multiband EPI diffusion sequence. Data were acquired for all animals with b=1000 s/mm2, 64 directions, 24 slices, and 2 b0 images (b-value = 0 s/mm2). A 3D T1w structural MRI scan was also collected for all animals (128 slices, 500 µm isotropic resolution) (Shen, Bezgin, et al., 2019a).

4.3.3.2 Human (HCP) Diffusion-MRI Acquisition

All images were acquired on a 3T Skyra Siemens system using a 32-channel head coil, a customised SC72 gradient insert (100 mT/m) and a customised body transmit coil. High resolution anatomical images were acquired using a 0.7 mm isotropic T1-weighted 3D magnetisation-prepared rapid gradient echo sequence (TR 2,400 ms, TE 2.14 ms, FOV 224 × 224 mm2, flip angle 8°). Diffusion-weighted images were acquired using a spin-echo EPI sequence (voxel resolution 1.25 x 1.25 x 1.25 mm3, 111 slices, TR 5520 ms, TE 89.5 ms, flip angle 78°, refocusing flip angle 160°, FOV 210x180, echo spacing 0.78ms, BW 1488 Hz/ Px, b-values 1000, 2000, 3000 s/mm3 with 90 directions each and 18 b0 images (b-value = 0 s/mm2). Full details regarding acquisition parameters can be found in the HCP 1200 subject reference manual https://humanconnectome.org/study/hcp-young-adult/document/1200-subjects-data-release (Glasser et al., 2013; Sotiropoulos et al., 2013; Van Essen et al., 2012).

4.3.3.3 Macaque Diffusion-MRI Pre-processing

The downloaded data had undergone pre-processing, including susceptibility-induced distortion correction using FSL's topup and eddy tools (Andersson & Sotiropoulos, 2016; Jenkinson et al., 2012; Shen, Goulas, et al., 2019). Skull stripping was performed

on the extracted B0 images using FSL BET (Jenkinson et al., 2012; Smith, 2002), BET parameters were optimised for each image. Binary masks of the extracted brains were multiplied with the respective 4D dMRI images to obtain skull-stripped diffusion weighted imaging (DWI) data (Jenkinson et al., 2012; Smith et al., 2004). All in-house scripts used for pre-processing with a step-by-step guide can be found online at https://github.com/El-Suri/Analyse-Monkey-Brain-Tracts.

4.3.3.4 Human (HCP) Diffusion-MRI Pre-processing

The HCP data were downloaded having already undergone the standard minimal pre-processing pipeline for the Human Connectome Project (Glasser et al., 2013). Similar to the macaque imaging data, the subjects' images were corrected for eddy currents and movement artifacts with the FSL eddy tool (Andersson & Sotiropoulos, 2016; Glasser et al., 2013). Images were skull-stripped using the FSL BET tool (Smith et al., 2001). The pipeline also included co-registration of subjects' diffusion-weighted and anatomical scans. Full pre-processing steps and the code to run the HCP pre-processing pipeline can be found at https://github.com/Washington-University/HCPpipelines.

4.3.4 Region of Interest Selection

For both the macaque and human dMRI data I extracted several regions of interest (ROIs) for our analyses. The seed region for all analyses was the subiculum ROI. The subiculum ROI here represents the subiculum complex, a term that incorporates the prosubiculum, subiculum, the presubiculum, and the parasubiculum (Ding, 2013; Lorente de No, 1934; O'Mara et al., 2001). The principal target region of interest was the BNST. There were had two positive comparison target regions, the anterior thalamic nuclei (ATN) and nucleus accumbens (NAc), both of which are located in close proximity to the BNST and show substantial structural connectivity with the subiculum, as revealed by tract-tracing (Aggleton & Christiansen, 2015; Christiansen et al., 2016; Friedman et al., 2002). For a negative comparison region I selected the external globus

pallidus (GPe), as this is also within close proximity of the BNST but does not appear to directly connect with the subiculum (Aggleton & Christiansen, 2015).

Some findings suggest that the primate fornix is not necessary for all subiculum to BNST connectivity, with evidence implicating a secondary path via the amygdala, involving the stria terminalis and/or the amygdalofugal pathway (Cullinan et al., 1993; Poletti et al., 1973, 1984; Poletti & Creswell, 1977; Poletti & Sujatanond, 1980). To assess this possibility, I ran an additional analysis using a fornix mask to exclude any connections passing through this region.

Although I expected some deviation in the definitions and boundaries of the ROIs between the macaque and human atlases, I tried to ensure that the structures analysed were closely comparable and that the relative sizes of the structures in the two species were as similar as possible. See Figure 25 & Figure 26 for a visual comparison of the ROIs, which are described further below.

4.3.4.1 Macaque Anatomical Regions of Interest

To create subject-specific brain ROIs I registered a standardised macaque brain atlas to individual subjects' native diffusion space. I used a high-resolution rhesus macaque MRI atlas containing 241 brain regions, created from the imaging of 10 post-mortem specimens (Calabrese et al., 2015). Although I had T1-w anatomical images for our macaque sample, the atlas included only T2-w anatomical images, and so to register the atlas to the individual macaque space I used the B0 images from both datasets. Registration was carried out using the FSL FLIRT tool (Jenkinson et al., 2012; Smith et al., 2004). To check the results of this registration, I registered the macaque T1-w scans to their respective B0 images and overlayed the T1-w image to the now subject-space atlas label images for visual inspection. An in-house script was then used to extract the specific brain ROIs from the subject-space atlases. All regions were identified from a published atlas (Calabrese et al., 2015). As previously mentioned, for the subiculum ROI I combined the prosubiculum, subiculum, presubiculum, and parasubiculum ROIs into a single mask (de Nó, 1934; Ding, 2013; O'Mara et al., 2001). For the NAc, the NAc

core and NAc shell ROIs were combined into a single mask. The ATN mask was a combination of the anteroventral and anteromedial thalamic ROIs. These two regions have been reported to have strong connectivity with the subiculum and together form a structure similar in size to the BNST (Aggleton & Christiansen, 2015). For the BNST, I used the central BNST ROI but manually removed the portion below the anterior commissure within FSL. This was done so that it matched our human BNST mask, which only contains the dorsal BNST (Theiss et al., 2017; Torrisi et al., 2015).

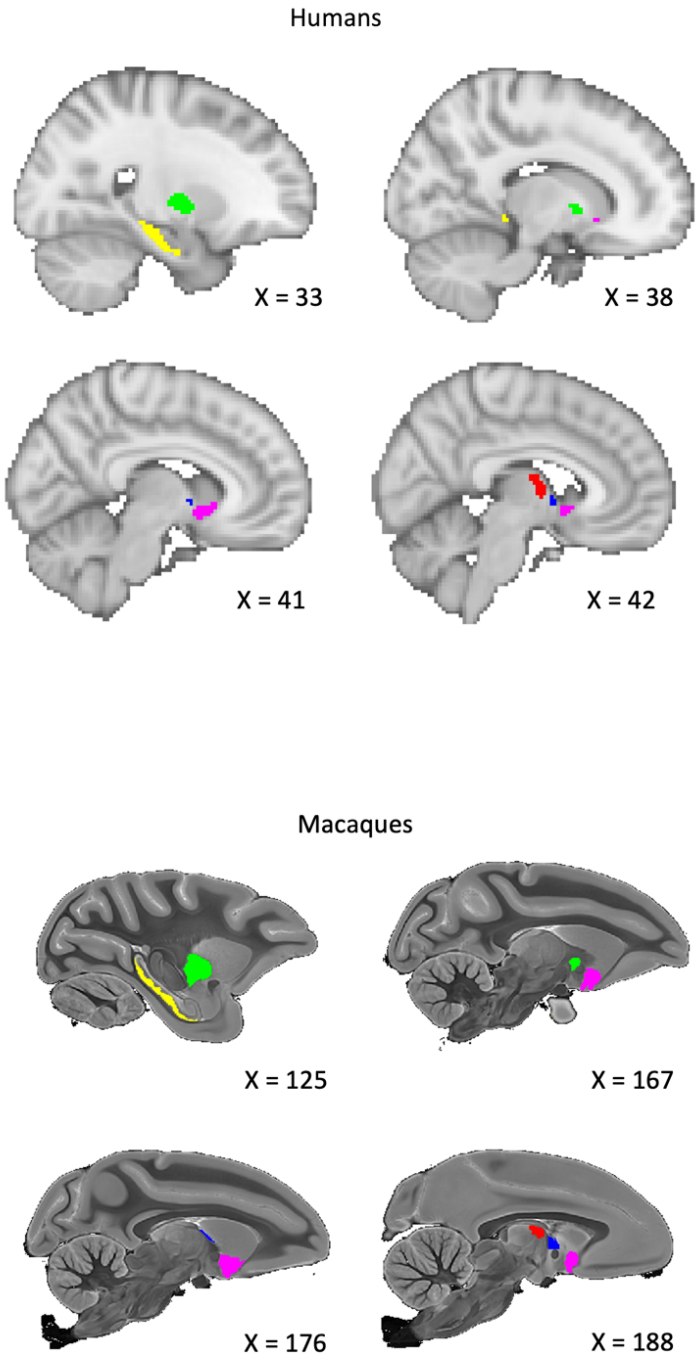

Figure 25: Probabilistic Tractography Regions of Interest for Humans and Macaques (Sagittal)

Sagittal view of the regions of interest for humans and macaques. Yellow = Subiculum, Green = External Globus Pallidus (GPe). Red = Anterior Thalamic Nuclei (ATN), Blue = BNST, Purple = Nucleus Accumbens (NAc). Coordinates for the macaque are taken from the atlas of Calabrese et al. (2015).

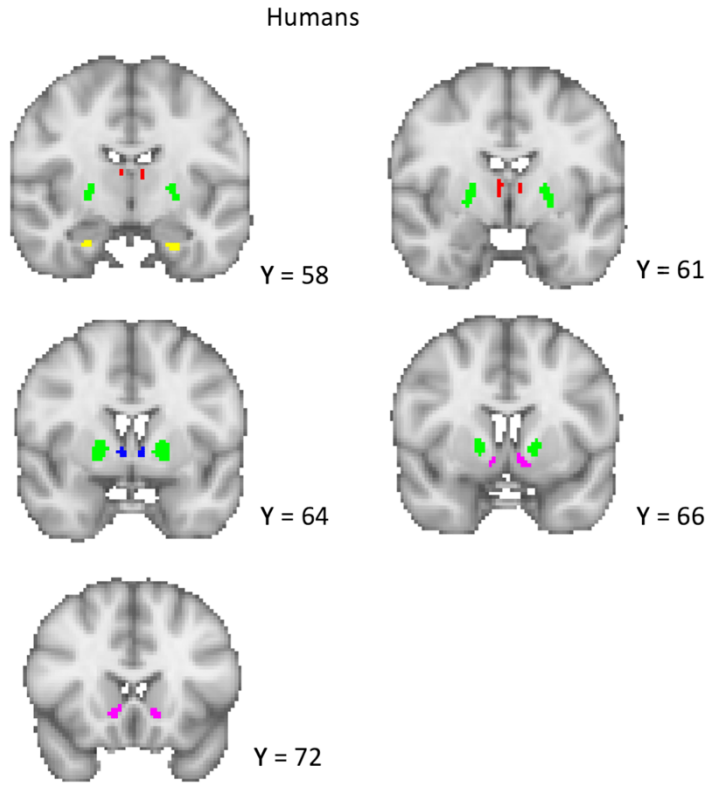

Figure 26: Probabilistic Tractography Regions of Interest for Humans and Macaques (coronal)

Coronal view of the regions of interest for humans and macaques. Yellow = Subiculum, Green = External Globus Pallidus (GPe). Red = Anterior Thalamic Nuclei (ATN), Blue = BNST, Purple = Nucleus Accumbens (NAc). Coordinates for the macaque are taken from the atlas of Calabrese et al. (2015).

4.3.4.2 Human Anatomical Regions of Interest

All HCP ROIs were defined in 2mm MNI space and then transformed to the subject diffusion space during the FSL PROBTRACKX2 analysis (see section 2.5.2) via the non-linear transformations provided by the HCP (Behrens et al., 2007). The subiculum and NAc ROIs were taken from the Harvard Oxford Subcortical atlas and, to better match the macaque ROIs, were thresholded to a minimum probability of 80% and 50% respectively (Jenkinson et al., 2012; Smith et al., 2004). The subiculum mask provided by the Harvard Oxford Subcortical atlas does not distinguish between the subicular sub-regions, and thus 'subiculum ROI' also refers to the larger subiculum complex (de Nó, 1934; Ding, 2013; O'Mara et al., 2001). The BNST mask was downloaded from the NeuroVault website (https://neurovault.org/collections/3245) , originally uploaded by Theiss et al (Mai et al., 2015; Theiss et al., 2017; Tillman et al., 2018). This mask was thresholded to a minimum probability of 25%, in accordance with previous studies (Berry et al., 2020; Theiss et al., 2017). The thalamic nuclei mask centred on the anteroventral ROI taken from the Automated Anatomical Labelling Atlas 3 (Rolls et al., 2020). This ROI includes the anteromedial area, thus matching the NHP sample (Iglesias et al., 2018; Rolls et al., 2020). The GPe ROI was downloaded from the NeuroVault website (https://identifiers.org/neurovault.collection:1380) and transformed to MNI 2mm space using FSL FLIRT (Jenkinson et al., 2012; Smittenaar et al., 2017). To better match the macaque ROI, this mask was thresholded at 50%. For our fornix mask, I used the fornix column and body mask from the ICBM-DTI-81 white-matter labels atlas in FSL (Hua et al., 2008; Jenkinson et al., 2012; Mori et al., 2008; Wakana et al., 2007). See Figure 25 & Figure 26 for a comparison of the macaque and human seed and target ROIs.

4.3.5 Probabilistic Diffusion Tractography

4.3.5.1 Tractography Analyses

White matter tractography was performed using FSLs (v 6.0.1) BEDPOSTX and PROBTRACKX2 (Behrens et al., 2007; Jenkinson et al., 2012). Briefly, BEDPOSTX uses Markov Chain Monte Carlo sampling to build up distributions on diffusion parameters. A 2-fibre model was applied to improve the modelling and resolution of crossing fibre populations (Behrens et al., 2007). PROBTRACKX2 then uses the outputs of BEDPOSTX to model the probabilities of white matter pathways in the brain. It does this by repeatedly initiating streamlines from a given seed region, iterating between drawing an orientation from the BEDPOSTX distributions, taking a step in this direction, and checking for any termination criteria (Behrens et al., 2007). The streamline distributions can be used to estimate the probability of structural connectivity between brain regions (see section 2.5.2) and image potential pathways (computational tract-tracing). For both our macaque and human samples I ran an ROI x ROI analysis. Although I were only interested in the subiculum ROI as the seed region, this analysis allowed us to run all subiculum-target ROI combinations at once. For the HCP sample only, to assess the contribution of the fornix to subiculum ROI - BNST connectivity, I ran two subiculum ROI - BNST analyses, one of which used a fornix mask as a NOT gate. This meant that any streamlines passing into the fornix would be eliminated from this analysis. Because our target ROIs varied in their distance from our seed, and because the distance between ROIs is a factor influencing successful reconstruction of a connection, I applied the distance correction setting within PROBTRACKX2 to account for this (Behrens et al., 2007). Probabilistic fibre tracking was initiated from every voxel within the ROI mask, with 5000 streamline samples being sent out from each voxel. I applied a step length of 0.2mm (NHP) or 0.5mm (HCP), and a curvature threshold of 0.2. For the full list of the parameters used during the PROBTRACKX2 analyses see the supplementary materials.

4.3.5.2 PROBTRACKX2 Data Transformation

The outputs of the PROBTRACKX2 analysis consist of an ROI by ROI connectivity matrix. Each number in the connectivity matrix refers to the total number of streamlines that were successfully reconstructed between each pair of ROIs. In this analysis, each ROI is treated as both a seed and a target, meaning that a reconstruction is run twice for

every ROI combination. The mean of each ROI to ROI combination was taken for a more robust estimate of the connectivity probability (Gschwind et al., 2012). As I was only interested in connectivity between the subiculum and the other ROIs, I did not use the data regarding other ROI to ROI streamlines (e.g., BNST to NAc). In order to express each subiculum to target ROI connectivity value as a proportion, relative to each subjects total number of subiculum streamlines, each mean subiculum - target ROI value was divided by the total number of streamlines successfully propagated from the subiculum for each participant (Gschwind et al., 2012). This gave us a proportion of connectivity for each seed-target combination between 0 and 1 (Gschwind et al., 2012). Therefore, I refer to this measure as a connection proportion.

4.3.5.3 Statistical Analysis of Connection Proportion Differences

To test whether the connection proportion between the seed and target regions were different, I ran two within-groups one-way ANOVA's, one for each species, with Target ROI as the IV and Connection Proportion as the DV. Outliers were removed if they were more than 1.5 * the inter-quartile range (IQR) above the third quartile or below the first quartile (e.g., Vinutha et al., 2018). Mauchly's test of sphericity and Levene's test of equality of error variances were run. Subsidiary pairwise t-tests were performed to assess the nature of the ROI differences. P-values for all subsidiary tests (6 per species) were corrected via the Bonferroni method.

4.3.5.4 Statistical Analysis of Between-Species Differences

To statistically test whether the subiculum ROI connectivity patterns of the NHP and human samples were different, I ran a post-hoc 2x4 mixed ANOVA, with Species as the between-groups variable and Target ROI as the within-groups variable.

4.3.5.5 Statistical Analysis of Fornix Exclusion Effects on Subiculum to BNST Connectivity.

Finally, I compared the number of streamlines that were successfully reconstructed between the subiculum ROI and BNST when a route via the fornix was, versus was not, available. For this comparison, I used the raw number of streamlines created between the two ROIs (i.e., not the connectivity proportion) when a) our fornix exclusion mask was not applied, and b) when our fornix exclusion mask was applied. These two sets of values were compared using a paired-samples t-test.

4.3.6 White Matter Microstructure and Stress-Related Traits and Behaviours.

4.3.6.1 Principal Component Analysis of Stress-related Traits and Behaviours

To assess the association between measures of white matter microstructure and stress-related traits and behaviours, I utilised the HCP self-report questionnaire data relating to these constructs (Weintraub et al., 2013). In Chapter 2 I used principal component analysis (PCA) to reduce nine questionnaire items and subscales relating to anxiety, depression, perceived stress, fear, and substance use to two principal components, one representing 'Dispositional negativity' and one 'Alcohol use' (section 2.3.3). These two principal components were thus used as our phenotypes of interest.

4.3.6.2 White Matter Microstructure

For our measures of white matter microstructure I utilised the tensor model, which assesses the properties of water diffusion along a tensor to infer the microstructural properties of white matter pathways (Basser, 1997). I extracted Fractional Anisotropy (FA), Mean Diffusivity (MD), Axial Diffusivity (AD), and Radial Diffusivity (RD) from the subiculum to BNST tracts. To do this I ran FSLs DTIFIT command on each subject's DWI data, providing FA and MD, and AD values across the brain. RD values were calculated by adding the L2 to the L3 image and dividing by two (Winklewski et al., 2018). A new PROBTRACKX2 analysis was then run with the subiculum ROI as the seed and the BNST as the only target. The resulting brain image, containing the probability distribution of connections between the two regions, was thresholded so that voxels with a less than

10% probability were excluded. This image was then binarized and transformed to subject space, where it was used to extract the mean FA, MD, AD, and RD values of the tracts.

4.3.6.3 Heritability and Association Analyses

I used the SOLARIUS package for R (Ziyatdinov et al., 2016) to assess the following: 1) the heritability of white-matter microstructure (FA, MD, AD, and RD) within the subiculum ROI - BNST tracts, 2) the co-heritability of these metrics with the dispositional negativity and alcohol use components, 3) the phenotypic, genetic, and environmental correlations between the subiculum-BNST white matter microstructure and component scores for dispositional negativity and alcohol use. SOLARIUS is the R version of the widely used SOLAR-eclipse software for genetic analysis (O'Donnell & Westin, 2011). SOLAR uses a kinship matrix to estimate the proportion of variance in a phenotype attributable to additive genetics, the environment, or to residual error. In this case, I was only permitted to calculate the additive genetic component, as partitioning environmental and error effects requires household information that is not provided by the HCP. In this model, monozygotic twins are given a score of 1 and dizygotic twins / siblings of 0.5 to indicate the estimated proportion of shared genetic variation. Half-siblings were excluded from the analysis (n = 191). The pedigree file was created using the HCP2Solar MATLAB function, a tool specifically designed for the HCP participants (https://brainder.org/2016/08/01/three-hcp-utilities) (Winkler et al., 2015). Because the model is sensitive to kurtosis, the phenotype values were inverse normally transformed. SOLARIUS allows analysis of co-heritability by computing bi-variate genetic correlations (Kochunov et al., 2019). During the analysis SOLARIUS computes an estimate of phenotypic, genetic, and environmental correlation between the variables, which I used to assess the relationships between white matter microstructure and the dispositional negativity and alcohol use components. The covariates for all analyses were sex, age, BMI, age2, sex * age, and sex * age2. The final number of participants in these analyses was n = 933. For discussion on using SOLAR for genetic neuroimaging see (Kochunov et al., 2019).

4.4 Results

4.4.1 Macaque Subiculum – BNST Neuroanatomical Tract-tracing

The Macaque neuroanatomical tract-tracing analysis was performed by Prof. Aggleton at Cardiff University and the full results are detailed in the published manuscript associated with this work (Berry et al., 2022). See also figures 27 and 28.

4.4.2 Subiculum Complex – BNST Probabilistic dMRI

4.4.2.1 Macaque Tractography Results

Macaque tractography analysis seeded from the subiculum ROI demonstrated the highest proportion of connectivity to the ATN, followed by the BNST, the NAc, and the GPe (Figure 29). ANOVA revealed a significant effect of ROI ($F(3,12) = 29.42$, $p < 0.0001$, Nagelkerke $r2 = 0.88$), with follow-up t-tests demonstrating a statistically significant difference between the ATN and the other regions (Table 11). No other subiculum-target ROI combinations were significantly different from each other (Table 11). Viewing the tractography output images, after thresholding by 10%, most reconstructed tracts appeared within the fornix, though some also passed through the amygdala via an area consistent with the amygdalofugal pathway (Figure 30). There was no evidence for connectivity beyond the anterior commissure at this threshold. An interactive combined output image, consisting of all 9 NHP tractography results, has been uploaded to NeuroVault at https://identifiers.org/neurovault.image:682610.

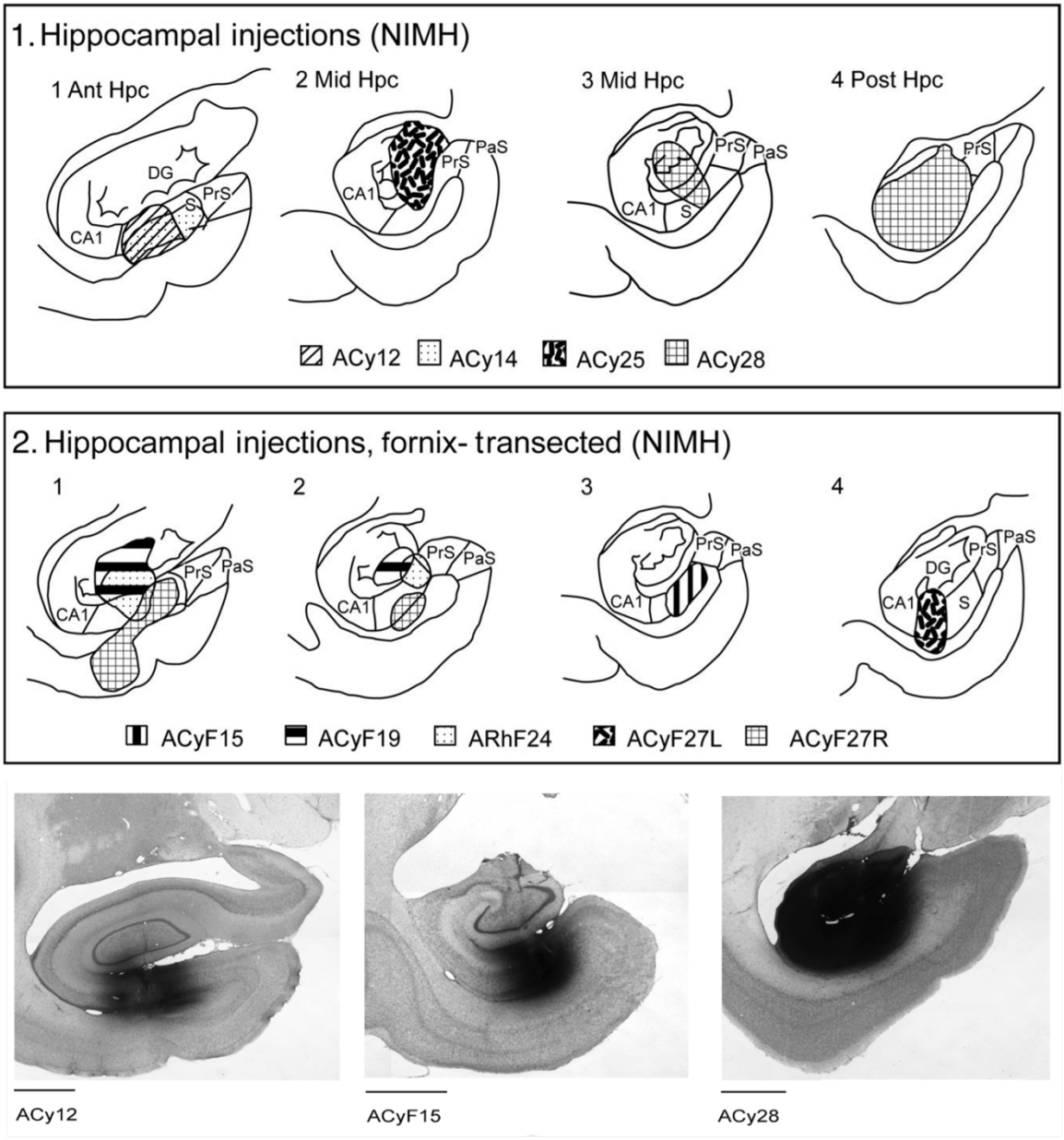

Figure 27: Hippocampal Injection Locations (image from Berry et al, 2022)

The upper two rows depict the core of each amino acid injection in the hippocampal formation drawn onto standard coronal sections at different anterior-posterior levels (all Macaca fascicularis cases). Row 1, intact cases. Row 2, cases with prior fornix transection. Row 3 contains coronal photomicrographs of the centre of the amino acid injection in three cases, at anterior (Ant), mid, and posterior (Post) levels, respectively. CA1, hippocampal field CA1; DG, dentate gyrus; Hpc, hippocampus; NIMH, National Institute of Mental Health; PaS, parasubiculum; PrS, presubiculum; S, subiculum. Scale bar = 2mm

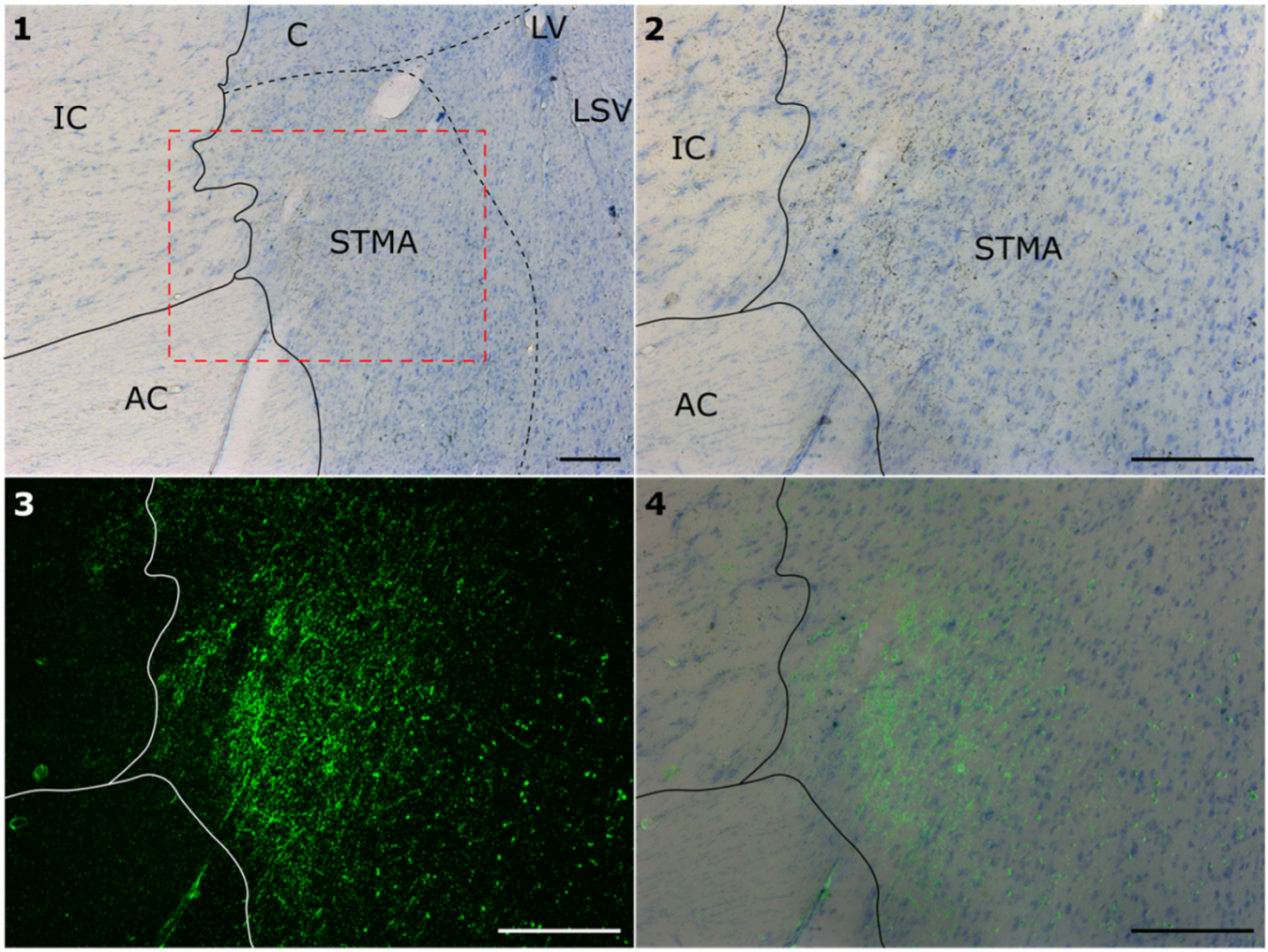

Figure 28: Hippocampal Labelling within the BNST (image from Berry et al, 2022)

Bright field (#1, #2), dark field (#3), and overlay (#4) showing anterogradely transported label (green) in the bed nucleus of the stria terminalis (BNST) following tracer injections in the posterior hippocampal formation of case ACy28. Image #2 is within that part of image #1 outlined with red dashes. Abbreviations: AC, anterior commissure; C, caudate nucleus; IC, internal capsule; LSV, lateral septum, ventral; LV, lateral ventricle; STMA, bed nucleus of the stria terminalis, antero-medial. All scale bars 250µm.

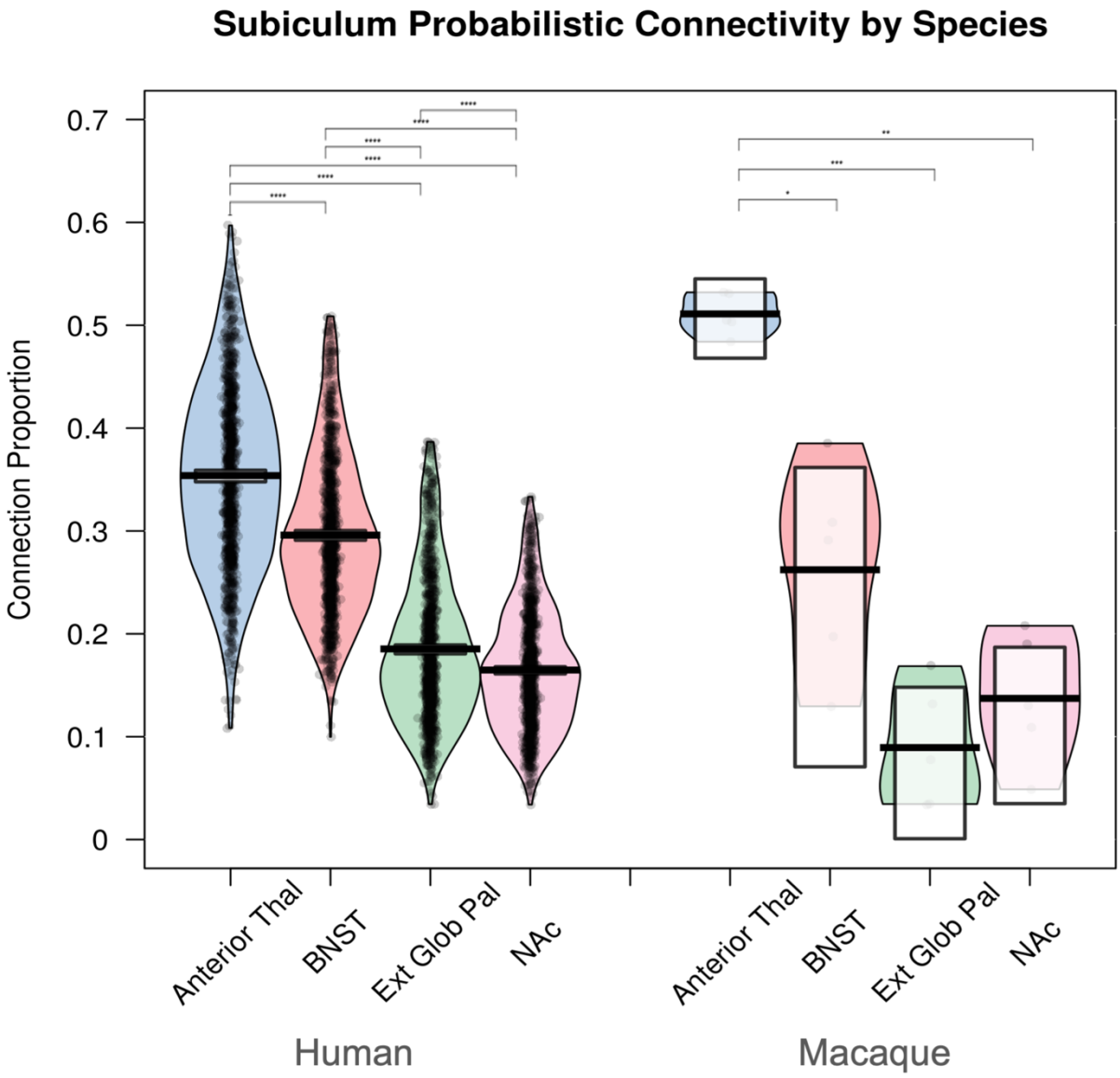

Figure 29: Proportional Structural Connectivity Results

The proportion of connectivity from the subiculum with each of the target regions for macaques and humans. Broadly the same pattern is seen across species, with the highest proportion of connectivity with the anterior thalamic nuclei (ATN), followed by the BNST, and then either the external globus pallidus (GPe) or nucleus accumbens (NAc). A mixed ANOVA revealed that there was a significant interaction of Species x ROI, but no main effect of Species. These ROI differences were highly significant after Bonferroni correction for every ROI in the HCP sample (n=985), but only for the anterior thalamic nuclei (ATN) in the NHP sample. (n=5).

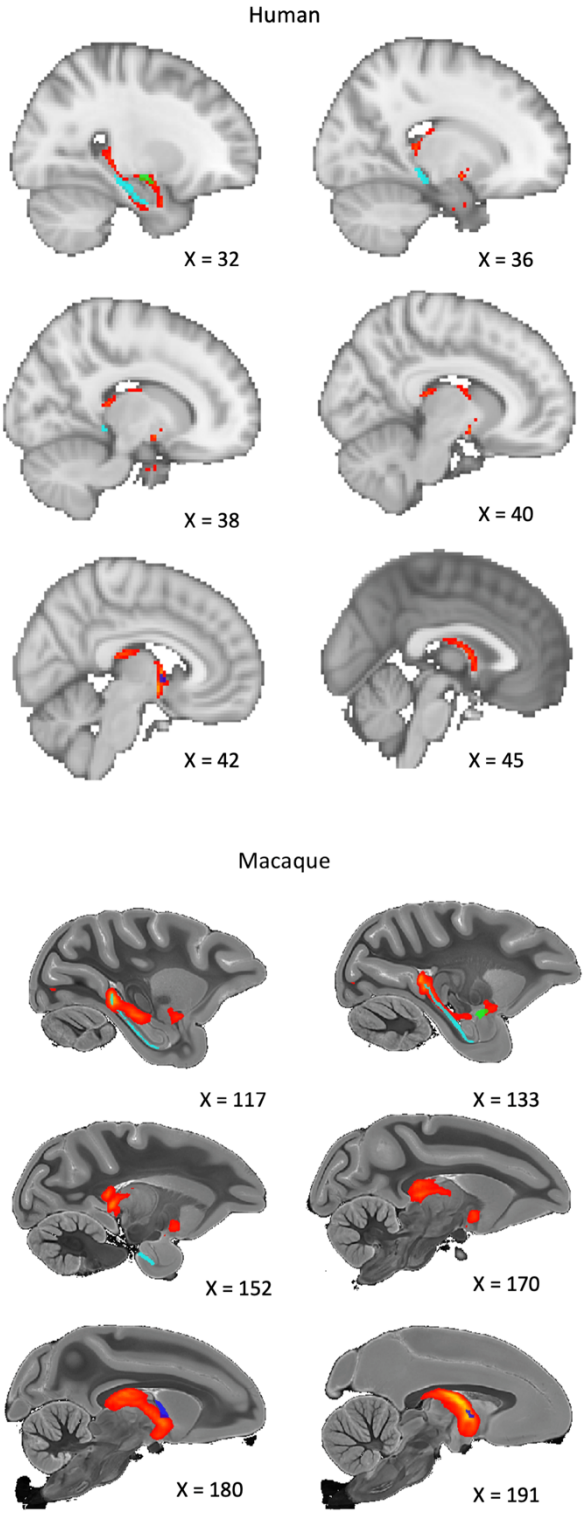

Figure 30: Probabilistic Tractography Results (Sagittal)

Human and macaque sagittal images from the probabilistic tractography analysis, seeded from the subiculum (light blue) with the BNST (dark blue) as the target. The connection is primarily via the fornix, however, significant connectivity is also observed through the amygdala (green). Images are thresholded at 10%.

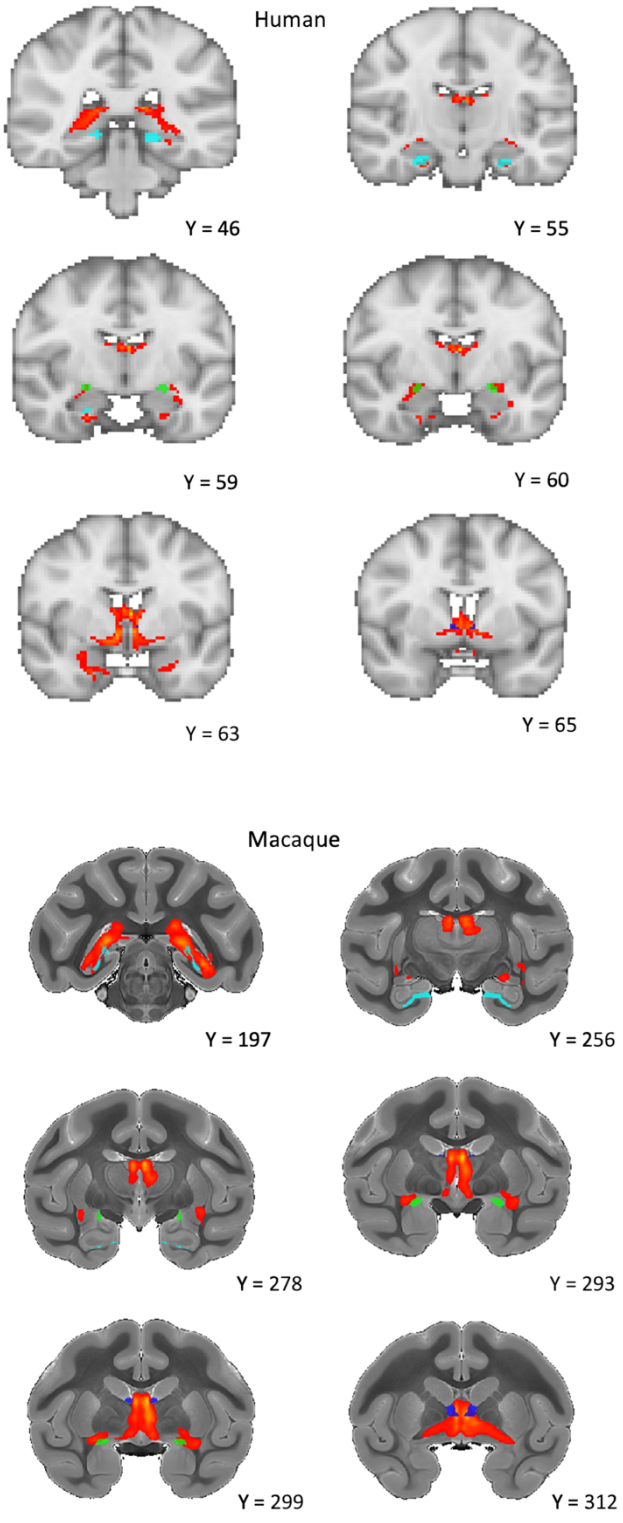

Figure 31: Probabilistic Tractograpgy Results (Coronal)

Human and macaque coronal images from the probabilistic tractography analysis, seeded from the subiculum (light blue) with the BNST (dark blue) as the target. The connection is primarily via the fornix, however, significant connectivity is also observed through the amygdala (green). Images are thresholded at 10%.

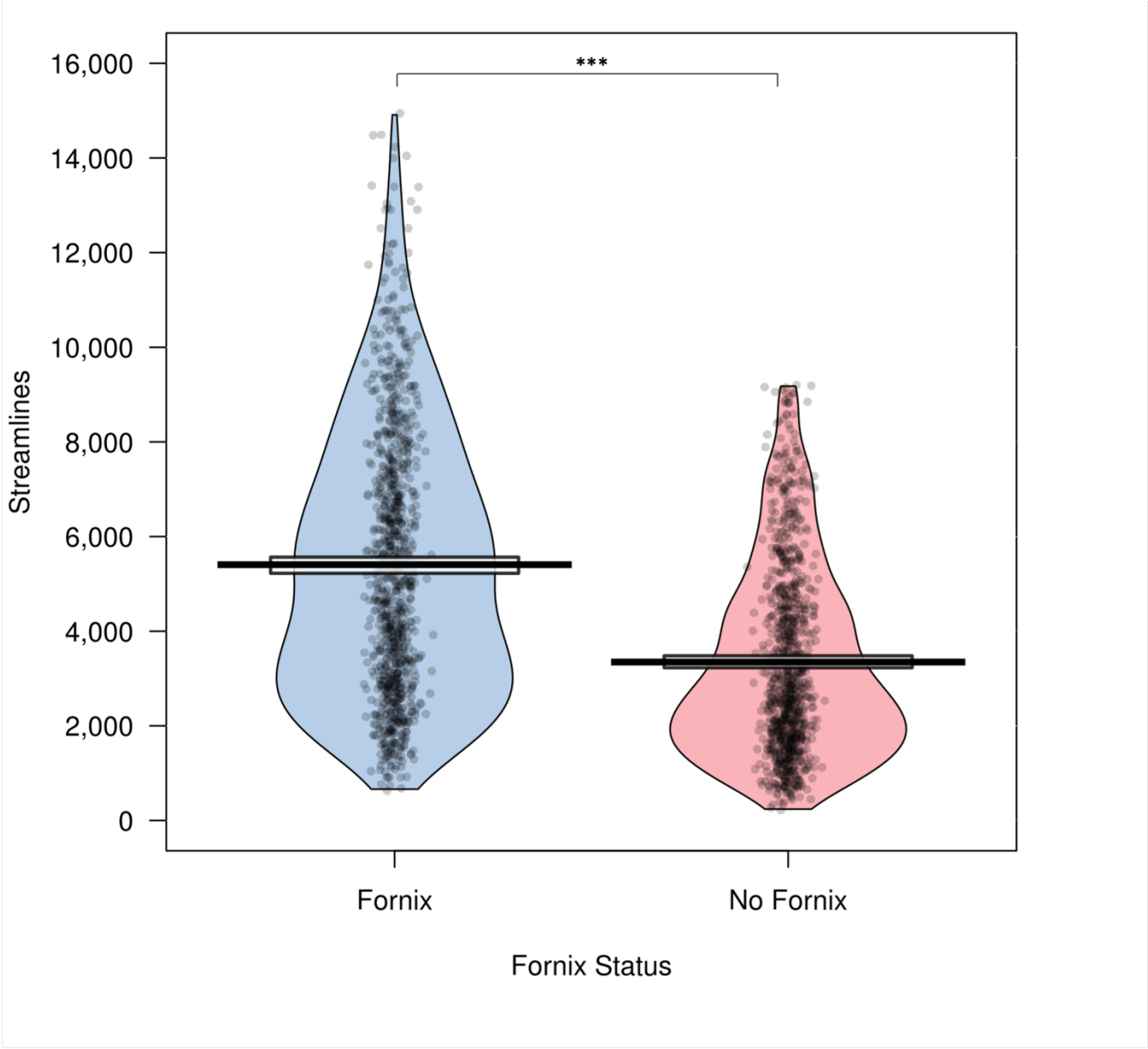

Figure 32: Effect of Fornix Exclusion on BNST Streamlines

Excluding the fornix from the tractography analysis between the subiculum and BNST in the HCP sample made a significant difference to the number of streamlines between the two regions. Notably, despite the removal of this major subiculum output pathway, there remains substantial connectivity with the BNST.

4.4.2.2 Human Tractography Results

Human dMRI tractography analysis seeded from the subiculum ROI demonstrated the highest proportion of connectivity to the ATN, followed by the BNST, the NAc, and the GPe (Figure 29). ANOVA revealed a significant effect of ROI ($F(2.65, 2612.46) = 1069.56$, $p < 0.0001$, Nagelkerke $r2 = 0.52$), with subsidiary pairwise comparisons demonstrating significant differences between all subiculum-target combinations (Table 11). Viewing the 10% thresholded tractography output image, the tractography findings were very similar to that of the macaques, with most of the tracts passing via the fornix but not extending in advance of the anterior commissure (Figure 31). An area of connectivity was also seen through the amygdala, via a route consistent with the amygdalofugal pathway. An interactive combined output image, consisting of the first 10 HCP tractography results, has been uploaded to NeuroVault at https://identifiers.org/neurovault.image:682612.

4.4.2.3 Statistical Comparison of Macaque and Human Subiculum Complex Tractography Results

The macaque and human dMRI tractography results showed largely the same pattern of connectivity, with the highest proportion of streamlines linking the subiculum ROI to the ATN, followed by the BNST, and then either the NAc or GPe (although statistically significantly more to the GPe in the HCP data) (Figure 29). Statistical analysis to formally assess these differences found a significant interaction of Species x ROI ($F(2.66, 2626) = 7.95$, $p < 0.0001$, $\eta p2 = 0.008$, Greenhouse-Geisser corrected), with a significant main effect of ROI ($F(2.66, 2626) = 50.3$, $p < 0.0001$, $\eta p2 = 0.048$, greenhouse-Geisser corrected) but no significant main effect of Species ($F(1, 988) < 0.001$, $p = 1$, $\eta p2 = 0$). This indicates that there is a difference between the species regarding which ROI x ROI combinations were significantly different. The direction of these effects is described in the previous sections (also see Figure 28).

4.4.2.4 Fornix Exclusion Results In Significantly Fewer Streamlines

Tractography of the subiculum ROI to the BNST that included the fornix contained significantly more streamlines (M = 5005, SD = 2827) than tractography without the fornix (M = 3348, SD = 2030) ($t = 38.4$, $df = 988$, $p < 0.0001$, Cohen's $d = 1.2$) (Figure 32).

4.4.3 Subiculum Complex - BNST Tract White Matter Microstructure Heritability and Phenotypic Associations

4.4.3.1 Univariate Heritability Analysis

SOLAR analysis revealed that tensor-derived microstructure indices (FA, MD, RD, and AD) extracted from the subiculum ROI - BNST tracts were all significantly heritable ($p<0.0001$ $h2 \sim .50$) (Table 12). This was also the case for the subiculum to BNST connections excluding the fornix ($P<0.0001$ $h2 \sim 0.5$) (Table 12).

4.4.3.2 Bivariate Heritability and Association Analysis

Bivariate heritability analysis for each microstructure measure with each of the two behavioural components (dispositional negativity and alcohol use) revealed no evidence for phenotypic, environmental, or genetic associations between any of the variables ($p > 0.05$, Table 13). This was also the case for the subiculum ROI - BNST connections excluding the fornix ($p > 0.05$, Table 13). However, the covariates BMI, age, and sex were highly significantly associated with the microstructural measures, within tracts both including and excluding the fornix (Table 13).

ROI 1	ROI 2	n	Mean Difference	95% Confidence Intervals for Difference (Bonferroni Corrected)	P-value (Bonferroni Corrected)
Anterior Thalamic Nuclei	BNST	5	0.249	0.024, 0.473	0.035 *
Anterior Thalamic Nuclei	External Globus Pallidus	5	0.422	0.289, 0.554	0.0006 ***
Anterior Thalamic Nuclei	Nucleus Accumbens	5	0.374	0.215, 0.533	0.002 **
BNST	External Globus Pallidus	5	0.173	-0.160, 0.505	0.39
BNST	Nucleus Accumbens	5	0.125	-0.211, 0.461	0.87
External Globus Pallidus	Nucleus Accumbens	5	0.048	-0.110, 0.206	1

ROI 1	ROI 2	n	Mean Difference	95% Confidence Intervals for Difference (Bonferroni Corrected)	P-value (Bonferroni Corrected)
Anterior Thalamic Nuclei	BNST	985	0.058	0.046 , 0.070	<0.0001***
Anterior Thalamic Nuclei	External Globus Pallidus	985	0.169	0.157, 0.180	<0.0001***
Anterior Thalamic Nuclei	Nucleus Accumbens	985	0.189	0.178, 0.200	<0.0001***
BNST	External Globus Pallidus	985	0.111	0.100, 0.121	<0.0001***
BNST	Nucleus Accumbens	985	0.131	0.122, 0.140	<0.0001***
External Globus Pallidus	Nucleus Accumbens	985	0.021	0.013, 0.028	<0.0001***

Table 11: T-test Results from Connectivity Proportion Comparisons

Macaque (top) and human (bottom) t-test demonstrating the differences between the connection proportion of each subiculum – region of interest (ROI) pair. BNST = Bed Nucleus of the Stria Terminalis.

Table 12 Table of Solarius Results

Correlation heatmap demonstrating the phenotypic (RhoP), environmental (RhoE), and genetic (RhoG) correlations following bivariate heritability analyses between each extracted DTI measure and each principal component (PC). The analysis revealed no significant correlations between any of the measures ($p > 0.05$). PC1 represented traits related to dispositional negativity, whereas PC2 reflected measures of alcohol use. See supplementary methods for p-values and standard errors.

Tract and Measure	Heritability	Significant Covariates
Subic - BNST with Fornix (Mean FA)	H^2r= 0.51, p < 0.0001	Sex (females < FA, p < 0.0001), All covars together accounted for 7% of the variance.
Subic - BNST excluding Fornix (Mean FA)	H^2r= 0.53 , p < 0.0001	Sex (females < FA, p < 0.0001). All covars together accounted for 8% of the variance.
Subic - BNST with Fornix (Mean MD)	H^2r= 0.66 , p < 0.0001	BMI (< MD, p<0.0001), Age (< MD, p=0.002), Sex (females < MD) p < 0.0001). All covars together accounted for 30% of the variance.
Subic - BNST excluding Fornix (Mean MD)	H^2r= 0.62 , p < 0.0001	BMI (< MD, p<0.0001), Age (< MD, p=0.005), Sex (females < MD, p < 0.0001). All covars together accounted for 26% of the variance.
Subic - BNST with Fornix (Mean AD)	H^2r= 0.86* , p < 0.0001	BMI (< AD, p<0.0001), Age (< AD, p = 0.005), Sex (females < AD p < 0.0001). All covars together accounted for 48% of the variance. *
Subic - BNST excluding Fornix (Mean AD)	H^2r= 0.81* , p < 0.0001	BMI (< AD, p<0.0001), Age(< AD, p=0.006), Sex (females < AD, p < 0.0001). All covars together accounted for 49% of the variance. *
Subic - BNST with Fornix (Mean RD)	H^2r= 0.54 , p < 0.0001	BMI (< RD, p<0.0001), Age(< RD, p=0.001), Sex (females < RD, p < 0.0005). All covars together accounted for 10% of the variance.
Subic - BNST excluding Fornix (Mean RD)	H^2r= 0.51 , p < 0.0001	BMI (< RD, p<0.0001), Age (< RD, p=0.02), Sex (females < RD, p < 0.001). All covars together accounted for 8% of the variance.

Table 13: Heritability of White Matter Microstructure Measures

*Univariate heritability analysis demonstrated that each DTI microstructure measure extracted from the subiculum to BNST connection was moderately heritable. BMI, Sex, and Age were frequently identified as being significant contributors to the variance of the measures. * The AD analysis resulted in warnings of high kurtosis, something known to affect heritability estimates. Despite transforming the variables using the inverse-log function, this could not be resolved. Therefore, the numbers given for the AD analyses should be interpreted with some caution. FA = Fractional Anisotropy, MD = Mean diffusivity, AD = Axial diffusivity, RD = Radial diffusivity.*

4.5 Chapter Conclusions

4.5.1 Summary of Results

I used MRI computational tract-tracing (tractography), supported by autoradiographic tract-tracing analysis results (Berry et al., 2022), to delineate structural connectivity between the subiculum complex and BNST in macaques and humans. Autoradiographic tracing revealed evidence for a direct monosynaptic projection from the hippocampal formation to the BNST, resulting in a discrete area of terminal label alongside labelled fibres (Berry et al., 2022). Follow-up analysis of a different macaque sample using probabilistic dMRI tractography revealed complementary in vivo evidence for a structural connection between the two regions. A similar pattern of results was found using probabilistic dMRI tractography in a large human sample from the HCP. Examination of the tract-tracing results show that this connection depends primarily on the fornix (Berry et al., 2022), with the diffusion tractography data suggesting an additional connection through a pathway involving the amygdala. In our human sample, I tested the heritability of white-matter microstructure indices (FA, MD, RD, AD), within the tracts and report that all measures were moderately heritable. Finally, in the HCP sample, I examined the putative functional correlates of the identified pathway, finding no evidence for a phenotypic, environmental, or genetic association between tract microstructure and components reflecting dispositional negativity and alcohol use. I did, however, find significant microstructure associations with the covariates BMI, age, and sex.

4.5.2 Autoradiographic Tract-Tracing of a Direct Hippocampal-BNST Projection in the Macaque

Results from the macaque autoradiographic tract-tracing indicate that there is a direct, fornical projection from the subiculum to the BNST (Berry et al., 2022). In contrast, no BNST label is seen when the subiculum is not involved in the tracer injection, nor in

those cases where the fornix was sectioned prior to tracer injection. In the case with the largest hippocampal injection (ACy28, posterior hippocampal injection) this projection was especially evident, principally terminating in the medial division of the anterior part of the BNST (STMA). Other cases showed evidence of termination in the same area, although it was much lighter, potentially reflecting the relative sizes of the injections. This evidence for a direct projection via the fornix accords with previous NHP studies using degeneration methods in squirrel monkeys (Morrison & Poletti, 1980; Poletti & Creswell, 1977). Aside from case ACy28, the projections observed in the study appeared modest, suggesting a potential difference from findings in rodent brains, which have emphasized significant ventral subicular connectivity with the BNST via the fornix (Berry et al., 2022; Canteras & Swanson, 1992; Cullinan et al., 1993) (Canteras & Swanson, 1992; Cullinan et al., 1993). It is, however, the case that the anterior hippocampal injections (cases ACy12, ACy14) (corresponding to rodent ventral hippocampus) were largely confined within restricted levels of the subiculum and presubiculum (Berry et al., 2022). In contrast, the extensive posterior hippocampal injection (ACy28) not only more completely filled the prosubiculum and subiculum, but also involved the CA fields and dentate gyrus. This same injection also extended over a greater AP distance. Consequently, while this posterior hippocampal projection in the primate brain to the BNST may reflect a species differences (Ding, 2013; Ding et al., 2020) it might stem from the far greater uptake of tracer in case ACy28.

It is also possible that more extensive projections would have been seen if the tracer injections had included the presubiculum, as in the rat this area also projects to the BNST (Howell et al., 1991). A further reason for the modest connectivity seen in the NHP autoradiographic sample may be that subiculum influences on the BNST are mediated via the amygdala to a larger extent than in rodents. Numerous authors have emphasised the importance of a non-fornical ventral/anterior subiculum – amygdala - BNST route in rodents and in NHPs (Cullinan et al., 1993; Ding et al., 2020; Herman et al., 2020; Morrison & Poletti, 1980; Poletti et al., 1984), with Poletti & Sujatanond (1980) arguing that the influence of the posterior hippocampus on the BNST is mediated exclusively via the fornix, while that of the anterior hippocampus is exerted primarily via a non-fornical route. If in primates this latter route is solely indirect, i.e.,

polysynaptic, then this connection would not be visible with the anterograde tracing method used in the present study.

Following an electrophysiological study of hippocampal - amygdala - basal-forebrain connectivity in rats, the authors suggested that unit activity response latency times were indicative of the amygdala serving as a relay between the subiculum and the basal forebrain (Morrison & Poletti, 1980; Poletti et al., 1984). Therefore, given these previous findings, and that the autoradiography only revealed fornical inputs with the monosynaptic tracer, it seems likely that in primates any substantial non-fornical influences will indeed prove to be polysynaptic. It is notable that rodents have more monosynaptic non-fornical hippocampal efferent routes to other subcortical targets (Dillingham et al., 2015; Meibach & Siegel, 1975, 1977) than those described in non-human primates, so the BNST may be a further case of this.

4.5.3 Macaque Tractography Evidence for Subiculum Complex – BNST Structural Connectivity

Results from the macaque diffusion tractography analysis revealed evidence for connectivity between the subiculum complex and the BNST. Comparing the proportion of connectivity to other ROIs, results suggest that the BNST is second in terms of connection proportion to the ATN, and above that of the GPe and NAc. The difference with the ATN, which numerous studies have shown to have dense connectivity with the subiculum (Aggleton, 1986; Aggleton & Christiansen, 2015), was statistically significant. However, the BNST's difference with either the negative comparison ROI (GPe), or the other positive comparison ROI (NAc) (see section 4.6) was not significant following Bonferroni correction. This likely reflects low sensitivity, given that the sample size was only five following outlier removal. Viewing the subiculum ROI – BNST tractography output image (Figures 30,31, also uploaded to Neurovault at https://identifiers.org/neurovault.image:682610) I see that the reconstructed tracts traversed dorsally via the fornix or ventrally via the amygdala, likely through the amygdalofugal pathway. This finding of a pathway involving the amygdala is consistent

with previous research in squirrel monkeys and rodents (Cullinan et al., 1993; Herman et al., 2020; Morrison & Poletti, 1980, 1980; Poletti et al., 1984). The limitations of tractography analysis mean that the results cannot differentiate between mono- and poly-synaptic pathways (Campbell & Pike, 2014), therefore, that I see an amygdala pathway with tractography but not autoradiography is consistent with the hypothesis that this connection is polysynaptic in nature (Morrison & Poletti, 1980).

4.5.4 HCP Probabilistic Tractography Findings

The HCP results suggest that the subiculum complex has substantial connectivity to the BNST in humans, with only the ATN receiving a higher proportion of streamlines of the tested ROIs. The reconstructed tracts appear to follow what would be expected given the rodent literature (Herman et al., 2020) and the macaque tractography results, with connectivity passing antero-dorsally through the fimbria/fornix and through another antero-ventral route via the amygdala, again supporting previous findings in the rat and squirrel monkey (Cullinan et al., 1993; Herman et al., 2020; Morrison & Poletti, 1980, 1980; Poletti et al., 1984). At least part of this amygdala route appeared consistent with the amygdalofugal pathway, as previously reported in rats (Poletti et al., 1984).

When testing whether excluding (via masking) the fornix had a significant effect on the number of streamlines between the subiculum ROI and the BNST, I found that this did indeed make a statistically significant difference. However, given that the fornix is the main output pathway of the hippocampus, the key insight garnered from this test was that more than half of the reconstructed streamlines remained. When viewing the fornix-excluded tractography output image (Figure 32, uploaded to Neurovault at https://identifiers.org/neurovault.image:682612), it is clear that some streamlines around the fornix structure remained. Part of this could be explained by imprecise registration of the NOT fornix mask to the subject space and individual differences in anatomy meaning that the NOT mask does not capture all the fornix pathway. Also likely, is that a substantial number of the remaining streamlines around the fornix NOT

mask are from the stria terminalis pathway, which runs just laterally to the columns of the fornix and is the primary input to the BNST from the amygdala (Alheid, 2009; Alheid et al., 1998; Oler et al., 2017).

4.5.5 Macaque and Human Diffusion Tractography Results are Strikingly Similar

The similarity of the macaque tractography results to those in the human sample suggests that macaque monkeys can be a useful model for further investigation of this connection in humans. Macaques are much closer to humans in evolutionary terms compared to rodents (Murray et al., 2017) and monkey experiments have already demonstrated their utility in other areas of BNST/ stress research (Fox et al., 2018; Mars et al., 2018; Oler et al., 2017). Thus, contingent on larger studies verifying the findings, the results demonstrate that key pathways from the subiculum complex to the BNST can be detected using tractography methods and that the results are very similar between macaques and humans.

4.5.6 Human Subiculum Complex – BNST Tract Microstructure Heritability and Potential Functional Attributes

Microstructure metrics extracted from the subiculum ROI to BNST tracts were all shown to be moderately to largely heritable, ranging from a h2 of .41 to .69. This is in line with other twin-based heritability studies, which have demonstrated that white matter microstructure is influenced to a large degree by genetic factors (Gustavson et al., 2019; Lee et al., 2017; Vuoksimaa et al., 2017). I did not find evidence for any of the microstructure indices being significantly associated, genetically or otherwise, with the two components representing dispositional negativity traits and alcohol use.

Many rodent studies implicate the subiculum – BNST - PVN connection as being key to stress-related processing, with aberrant stress-processing having been proposed as a key mechanism linked to dispositional negativity (Herman et al., 2020; Hur et al., 2019;

Radley & Johnson, 2018; Shackman et al., 2016). Structural and functional alterations of the hippocampus and/or BNST have previously been linked to stress-related traits and disorders (Avery et al., 2016; Hur et al., 2019). Although I could find no examples of studies investigating subiculum - BNST tract microstructure, a small number of studies have examined dMRI associations in the fornix with stress-related traits; with varying results (Barnea-Goraly et al., 2009; Benear et al., 2020; Modi et al., 2013; Yu et al., 2017).

One reason that I did not observe an association may be because the sample consists of a screened, relatively healthy population. Evidence for BNST involvement in dispositional negativity or stress-related traits generally comes from studies of clinical populations, or during experiments when states such as fear/anxiety have been induced (Brinkmann et al., 2018; Klumpers et al., 2017; Mobbs et al., 2010; Pedersen et al., 2020). In addition, some researchers have proposed that human self-report emotions should be considered as distinct from the sub-cortical and physiological processes often studied in animal models (LeDoux & Hofmann, 2018). If correct, this would render association between the self-report questionnaire data and the sub-cortical structural connection unlikely (see also Brandt & Mueller, 2022). Alternatively, a large-scale study (n=559) recently reported that stress-reactivity may be less important for traits related to dispositional negativity than previously thought (Mineka et al., 2020).

Both the hippocampus and the BNST have been associated with alcohol use, with the BNST being specifically implicated in alcohol-related alterations to stress-processing (Bach et al., 2021; Volkow et al., 2016). One recent small-scale study reported a greater number of streamlines between the hippocampus and the BNST in early abstinence women than in control women, a finding which was not seen in men (Flook et al., 2021). Although interesting, assessing streamlines in this way should generally be avoided in favour of microstructure measures, as individual differences in streamline variation are difficult to interpret (Jones et al., 2013). Whilst not specific to the BNST, white matter abnormalities of the fornix in adults with heavy drinking and

alcohol use disorder have been reported (Cardenas et al., 2013), although this was restricted to patients with AUD-linked thiamine deficiency and the diffusion MRI literature in general with regards to correlates of substance abuse is somewhat inconsistent (Benear et al., 2020). Similar to the dispositional negativity component, a reason I did not find such an association could be that the sample consisted of a screened, relatively healthy population (median drinks consumed per week being two), which likely reduced the chances of finding any association (Berry et al., 2020). Studies that have found associations between alcohol use and white matter metrics have generally been conducted either with clinical populations, or following experimental manipulations (Campbell et al., 2019; Cardenas et al., 2013; Flook et al., 2021).

I report an effect of the covariates BMI, age, and sex on nearly all the microstructure measures, on tracts both including and excluding the fornix (Table 13). These associations were expected given that all of these factors have been previously associated with global influences on white-matter microstructure (Dekkers et al., 2019; Lawrence et al., 2021; van Hemmen et al., 2017; Xiong & Mok, 2011; Yang et al., 2016). Due to these global effects, understanding microstructural relationships with these traits along specific tracts is a non-trivial problem that requires careful analysis. Specific investigation with regards to the associations of these factors with microstructural properties along the subiculum-BNST-PVN pathway would be informative, particularly as the BNST has been associated with feeding behaviours and is sexually dimorphic (Allen & Gorski, 1990; Lebow & Chen, 2016).

4.5.7 Limitations

An unexpected result was that the additional positive comparison region, the NAc, appeared to demonstrate little evidence of subiculum connectivity via probabilistic tractography in both macaques and humans. This connection was detected in the tract-tracing analysis and has been widely described elsewhere (Aggleton & Christiansen, 2015). This result is likely due to the limitations of tractography, which can struggle to resolve crossing and fanning fibre populations, even at relatively high image resolution (Schilling et al., 2017). The NAc is connected to the subiculum via the

fornix. The fornix bifurcates at the anterior commissure into the postcommissural and precommissural fornix, with part of the precommissural fornix travelling anteriorly and ventrally to terminate in the nucleus accumbens, with adjacent fibres reaching frontal areas (Aggleton & Christiansen, 2015; Brog et al., 1993; Friedman et al., 2002; Groenewegen et al., 1987). It may be that due to the nature of this bifurcating tract, the extent of the precommissural connection is underestimated by probabilistic tractography. Other researchers have noted that it is likely the specific properties of this connection that causes issues for tract reconstruction (Brown et al., 2017), we do not expect this to be an issue for other connections in the study which take a route often reproduced using DWI (Brown et al., 2017). A further limitation involves the use of self-report questionnaire data, which may only be indirectly (if at all) related to subcortical stress-processing mechanisms (LeDoux & Hofmann, 2018). This is covered in more detail within the General Discussion chapter. Finally, the BNST masks consisted only of the dorsal BNST, owing to difficulties delineating the ventral area using MRI (Torrisi et al., 2015). Previous research has demonstrated ventral BNST glutaminergic innervation from the subiculum in the rodent (Gungor & Paré, 2016). Thus, I may have detected an even greater proportion of connectivity had this region been included.

4.5.8 Conclusions and Future Directions

I used a multi-method, cross-species approach (Folloni et al., 2019) to demonstrate that a key anatomical connection identified in rodent stress research, between the subiculum complex and BNST, is present in macaques and humans. I show that this connection has a substantial fornical element, with the diffusion tractography results suggesting an additional route via the amygdala, which may be more polysynaptic in nature than the monosynaptic pathways described in rodent research (Cullinan et al., 1993; Poletti et al., 1984). As such, further research is needed to indicate to what extent the amygdala plays a role as an intermediary between the subiculum and BNST in primates. Further refinements should include using tractography to compare the BNST connectivity of subiculum sub-regions (e.g., the prosubiculum, subiculum, presubiculum, parasubiculum) as well as further addressing potential hippocampus long-axis variation, given that rodent research has implicated the ventral (anterior in

primates) subiculum, or prosubiculum, in connections to the BNST, with suggestions that connectivity differences are distributed along a ventral-dorsal gradient (Ding, 2013; Ding et al., 2020; Strange et al., 2014). Given that most of this research has taken place in rats, and given the potential species differences reported here (see also Poletti & Sujatanond, 1980), the nature of subicular subregion projections to the BNST should be further investigated in primates. Methods to achieve this include the application of advanced ultra-high field MRI techniques specifically developed to analyse hippocampal subfields (e.g., Hodgetts et al., 2017), or ultra- high resolution dMRI applied to post-mortem macaque brains (e.g. Sébille et al., 2019) alongside novel polysynaptic tracer experiments (Xu et al., 2020). Although I did not find any associations with the principal components relating to dispositional negativity or alcohol use, differences may yet be found when studying clinical populations (e.g., Cardenas et al., 2013), the impact of chronic early life stress (Petrican et al., 2021), or physiological and behavioural/cognitive biomarkers of stress-responding (e.g., Allen et al., 2017). In general, though I describe in humans and macaques the existence of a subiculum-BNST connection previously identified in rats, the appreciation of potential species differences demonstrated here has implications for the generalisability of rodent research to the understanding of human stress-related functional anatomy and its disorders.

4.6 Supplementary Material

Tract and Measure	PC1 - RhoP	PC1 RhoE	PC1 - RhoG	PC2 - RhoP	PC2 - RhoE	PC2 - RhoG
Subic - BNST with Fornix (Mean FA)	RhoP = 0.02 , p = 0.6	RhoE = 0.05(SE 0.08), p = 0.51	RhoG = -0.06 (SE 0.19), p = 0.75	RhoP = -0.05, p = 0.10	RhoE = -0.08 (SE 0.08), p = 0.32	RhoG = -0.003 (SE 0.18), p = 0.98
Subic - BNST excluding Fornix (Mean FA)	RhoP = 0.004, p = 0.89	RhoE = 0.05 (SE 0.09), p = 0.58	RhoG = -0.08 (SE 0.19), p = 0.66	RhoP = - 0.03, p = 0.39	RhoE = 0.02 (SE 0.08), p = 0.81	RhoG = -0.13 (SE 0.18), p = 0.47
Subic - BNST with Fornix (Mean MD)	RhoP = - 0.05, p = 0.12	RhoE = 0.004 (SE 0.9), p = 0.96	RhoG = -0.16 (SE 0.18), p = 0.34	RhoP = 0.01, p = 0.83	RhoE = 0.004 (SE 0.09), p = 0.96	RhoG = 0.01 (SE 0.17), p = 0.94
Subic - BNST excluding Fornix (Mean MD)	RhoP = - 0.03, p = 0.31	RhoE = -0.02 (SE 0.09), p = 0.81	RhoG = -0.06 (SE 0.19), p = 0.74	RhoP =-0.002 p = 0.94	RhoE = - 0.05 (SE 0.08), p = 0.52	RhoG = 0.10 (SE 0.18), p = 0.58
Subic - BNST with Fornix (Mean AD)	RhoP = - 0.05. p = 0.11	RhoE = 0.06 (SE 0.11), p = 0.55	RhoG = - 0.23 (SE 0.17), p = 0.17	RhoP = - 0.02, p = 0.52	RhoE = -0.06 (SE 0.10), p = 0.56	RhoG = 0.02 (SE 0.16), p = 0.89
Subic - BNST excluding Fornix (Mean AD)	RhoP = - 0.05, p = 0.09	RhoE = 0.01 (SE 0.10), p = 0.93	RhoG = -0.17 (SE 0.17), p = 0.32	RhoP = - 0.01, p = 0.85	RhoE = -0.02 (SE 0.09), p = 0.86	RhoG = 0.01 (SE 0.16), p = 0.96
Subic - BNST with Fornix (Mean RD)	RhoP = - 0.03, p = 0.33	RhoE = -0.01 (SE 0.08), p = 0.86	RhoG = -0.07 (SE 0.20), p = 0.71	RhoP = 0.01, p = 0.65	RhoE = 0.02 (SE 0.8), p = 0.82	RhoG = 0.007 (SE 0.19), p = 0.97
Subic - BNST excluding Fornix (Mean RD)	RhoP = - 0.01, p = 0.66	RhoE = -0.03 (SE 0.08), p = 0.70	RhoG = 0.03 (SE 0.21), p = 0.90	RhoP = - 0.01, p = 0.82	RhoE = -0.06 (SE 0.08), p = 0.47	RhoG = 0.11 (SE 0.19), p = 0.58

Table 14: Bivariate Heritability Analysis Results (Supplementary table)

Bivariate heritability analyses between each extracted DTI measure and each principal component revealed no phenotypic, environmental, or genetic associations. PC1 represented traits related to dispositional negativity, whereas PC2 reflected measures of alcohol use.

Chapter 5: General Discussion

5.1 Summary of Findings

This thesis examined the intrinsic functional and structural connectivity of the bed nucleus of the stria terminalis (BNST) - a critical node in stress response neurocircuitry (Lebow & Chen, 2016), additionally testing whether these connections were heritable and associated with phenotypes commonly linked to the BNST – namely negative emotionality and alcohol use. I used a variety of techniques, with a focus on leveraging "big data" (Van Horn & Toga, 2014) to explore phenotypic and genetic associations. As robust research requires many lines of evidence (Munafò & Davey Smith, 2018), in addition to big-data analysis in humans, I also employed a cross-species comparative approach (Mars et al., 2014) using samples of macaque monkeys.

In this chapter I will discuss how the findings from this thesis fit broadly within the literature, and make recommendations with regards to improving future research. Specifically, I will first discuss the results regarding BNST embedding within the wider neural network, focusing initially on whole-brain connectivity approaches and then analysis of specific structural and functional connections selected based upon *a priori* knowledge. Secondly, I will write about the lack of associations between psychological and imaging phenotypes reported throughout the chapters, discussing how these results fit with recent similar findings, and suggest better approaches to ascertain these relationships. Thirdly, I will discuss the implications of and future directions for the various genetic analyses reported here. Finally, I will discuss the utility of cross-species work and the usefulness of animal models of human psychological phenotypes. Before this, however, a brief summary of each chapter is outlined below.

5.1.1 Functional Connectivity Networks of the Extended Amygdala – A Population Study

In Chapter two I used data from the large family-based sample, the human connectome project (HCP) (Van Essen et al., 2012), to establish and compare the brain-wide intrinsic functional connectivity networks (ICN) (Buckner et al., 2013) of the BNST and its highly interconnected extended amygdala (ExtA) partner, the central nucleus of the amygdala (CeA) (Alheid, 2009). I found that the ICN of the BNST largely replicated the network of functional connections mapped in previous smaller-scale studies, additionally describing overlapping yet distinct ICN of the CeA. I did not find any evidence for an association between the ICNs of the BNST (or CeA) with two PCA-derived measures of self-reported dispositional negativity and alcohol use. Finally, twin-based heritability analysis revealed evidence for moderate heritability of intrinsic functional connectivity (iFC) between the BNST and centromedial amygdala, and the BNST and superficial amygdala. Contrary to a previous finding in non-human primates (NHP) (Fox et al., 2018) however, I found no evidence for a phenotypic association, or for co-heritability, between specific BNST-amygdala iFC and dispositional negativity.

5.1.2 A Genome-Wide Association Study of BNST-Amygdala Functional Connectivity in the UK Biobank.

Following the finding in Chapter Two that iFC between the BNST and amygdala is heritable, I used the UK biobank (UKBB) sample (n= ~19,000) (Alfaro-Almagro et al., 2018) to run a genome-wide association study (GWAS) of BNST iFC to five amygdala sub-regions (namely, the superficial, laterobasal, centromedial, CeA, and a cluster derived from the BNST ICN analysis in Chapter 2) (Jenkinson et al., 2012; Pauli et al., 2018). The analysis found evidence that a single common genetic variant (single nucleotide polymorphism, or SNP) was associated with BNST iFC to the laterobasal amygdala. This SNP (rs10786748) has been previously linked to expression of the gene *NRG3* (Neuregulin 3), which has been demonstrated to be highly specifically expressed within the brain, particularly in the amygdala (Uhlén et al., 2015). In addition, *NRG3* has been linked to a range of mood-disorder phenotypes, including anxiety (Kao et al., 2010; Meier et al., 2013; Paterson et al., 2017; Paterson & Law, 2014). Using both

linked medical record and self-report measures of anxiety and alcohol use disorders, I examined associations with BNST and amygdala subregion iFC, but similarly to chapter two, found no evidence for a phenotype relationship. Finally, SNP-based heritability analysis based upon the summary statistics from the GWAS found no evidence for SNP-based heritability, contrary to Chapter 2's finding of twin-based heritability, for any BNST-amygdala iFC.

5.1.3 Chapter Four Summary

In this chapter I focused on structural connectivity. More specifically, I examined whether a direct anatomical connection between the subiculum and BNST previously described in rodents, and implicated in psychological stress regulation (Herman et al., 2020), could be identified in humans and macaques. To do this I combined gold-standard ex-vivo anatomical tract tracing in macaques (n=7) and diffusion MRI (dMRI) tractography analysis in humans (HCP, n = ~1200) and macaques (n=9). Anatomical tract tracing revealed evidence for a monosynaptic connection between the subiculum and BNST via the fornix. dMRI probabilistic tractography analysis in macaques and humans showed a similar connection via the fornix and an additional pathway via the amygdala. Given the lack of evidence for a connection via the amygdala using the monosynaptic-specific tract-tracing analysis, I concluded that this amygdala route likely reflects a polysynaptic connection. This indicates a potential species' difference between primates and rodents, which may have important implications for rodent models of primate (including human) stress processing. In addition, I tested for associations between measures of DTI-derived white matter microstructure within the BNST – subiculum tracts and PCA - derived measures of self-report dispositional negativity and alcohol use, again finding no significant associations. Finally, heritability analysis in the HCP sample revealed evidence for moderate (~hr^2 = .5) twin-based heritability of all white-matter microstructure measures in the subiculum – BNST pathway.

5.2 The embedding of the BNST in wider neural networks

5.2.1 Whole-brain networks of the BNST

The BNST ICN pattern is discussed in detail in Chapter 2, but broadly this finding reiterated the BNST's position within a wide network that likely reflects its role as an integrator of signals from both top-down frontal and bottom-up limbic/ brainstem regions. The mapping of this network is important because, given the large and high-quality HCP sample, it gives significant weight to previous smaller-scale findings in healthy young adults (Avery et al., 2014; Gorka et al., 2018; Motzkin et al., 2015a; Oler et al., 2012; Tillman et al., 2018; Torrisi et al., 2015; Weis et al., 2019), suggesting this is a robust (i.e. replicable) network. Therefore, researchers could now move away from mapping the ICN of the BNST (at least in healthy young adults), and begin to examine both more complex models of the BNST network, and how differences in this network may be associated with clinically relevant phenotypes. Several suggestions are made below with regards to extending these initial findings.

To assess the BNST's ICN I used a static seed-based correlation analysis approach, which computes the Pearson's correlation between BNST and other regions' BOLD activation over an entire scanning period (Friston, 2011; S. Smith, Vidaurre, et al., 2013). Strengths of this method include its simplicity, both in implementation and explanation, its relative resistance to transient noise artifacts (e.g. deep breaths) (Hutchison et al., 2013), and its widespread use within the literature which has led to the identification of well characterised and replicable functional connectivity networks, for example the default mode network (Raichle, 2015; Yeo et al., 2011). A limitation, however, is that correlations across a long period fail to take into account how BOLD connectivity patterns vary over time. To address this, researchers typically employ dynamic functional connectivity (dFC) analysis (R. M. Hutchison et al., 2013). This is often performed via the use of sliding analysis windows, in which BOLD signal correlations are computed over a series of partially overlapping time frames (typically 30-60 seconds) (e.g. Menon & Krishnamurthy, 2019). This is generally followed by

clustering algorithms that reveal the spatial locations of these shorter-scale connectivity networks (for more details and other versions of dFC see Hutchison et al., 2013). dFC has been used to demonstrate whole brain connectivity variance differences across the lifespan and between clinical groups (e.g. schizophrenia patients) and controls (Escrichs et al., 2021; Weber et al., 2020). Therefore, dFC analysis may present a potentially interesting way to map variations in the BNST ICN, which may be uniquely tied to psychological phenotypes of interest (e.g. Chen et al., 2020).

Another increasingly common method for assessing ICNs is to use network analysis approaches. Graph-based network analysis describes meaningful properties regarding how parcellated brain regions are connected to each other (Farahani et al., 2019). It does this by treating each parcellation as a 'node' and each connection as an 'edge'. From this it constructs a graph that describes the connectivity of each and every node (Sporns, 2018). From this graph it is possible to extract properties, such as functional segregation, integration of information flow, small-worldness (Bullmore & Sporns, 2012), network resilience against failure, or node centrality. This could be particularly useful for analysis of the BNST as, for example, testing the node centrality of the BNST would allow to assess the commonly stated theory that the BNST is a key hub that integrates information from a broad network (Herman et al., 2020; Lebow & Chen, 2016; Maita et al., 2021). Graph theory has not been used with regards to the BNST network before. However, as well as providing insight into the properties of the BNST network, graph theory could be used in the future to reveal differences in network architecture relating to psychological phenotypes (Farahani et al., 2019).

Volumetric analysis provides an interesting tool for analysis of the BNST and its network. Previous evidence from preclinical models and a handful of post-mortem studies in humans have suggested that BNST size may be influenced by a number of variables, including levels of anxiety and sex (Chung et al., 2002; Flook et al., 2020; Hulsman et al., 2021; Lebow & Chen, 2016; Maita et al., 2021; Zhou et al., 1995). As well as assessing the size of individual brain regions, volumetric analysis can assess co-

variation across the brain, something suggested to indicate the presence of a network amongst co-varying structures (Colibazzi et al., 2007). Much of the BNST volumetric research in humans has been conducted in small samples and to my knowledge there does not exist a large-scale human neuroimaging study which attempts to measure BNST volume/ volumetric covariation associations with phenotypes (see also section 1.2.5). If systematic BNST volume differences do exist then this could have consequences for the validity of neuroimaging results obtained using standardised BNST masks, as they may poorly account for particular populations (Maita et al., 2021).

A further potentially interesting avenue for further exploration of the brain-wide BNST network would be to compare the functional network with results from probabilistic tractography analyses. Indeed this has been attempted before, with researchers demonstrating a moderate degree of overlap between structural and functional networks of the BNST (Avery et al., 2014). Nevertheless, important differences were present, for example between functional and structural connectivity estimates between the BNST and amygdala subregions (Avery et al., 2014). Recent advances in techniques that combine functional and structural imaging could push these findings further (Chu et al., 2018; Seguin et al., 2020; Suárez et al., 2020). For example, structural connectivity measures can be used to predict and penalise the estimation of functional connectivity, thus weighting the functional connections based upon the underlying anatomy (Bowman et al., 2012; Chu et al., 2018). Differences between functional and structural connectivity maps have also been used to evaluate whether divergence of these measures is related to psychological phenotypes (Andrews-Hanna et al., 2007). Finally, joint modelling approaches, that use techniques from graph theory, simultaneously use dMRI and fMRI data to generate a more complete description of the network. This has been used, for example, to extract specific functional networks (e.g. those involved in language processing) for both iFC and dMRI-based analyses (Chu et al., 2018; Venkataraman et al., 2012).

In sum, given the BNST ICN described here, and in agreement with several other studies (Avery et al., 2014; Gorka et al., 2018; Motzkin et al., 2015; Oler et al., 2012;

Tillman et al., 2018; Torrisi et al., 2015; Weis et al., 2019), researchers should move towards integrating different methodologies, such as dynamic network analyses, graph theoretical approaches, and structural imaging, in order to extract the maximum amount of information regarding the BNST network. Further, scientists could begin to test the variability of this network between people and examine changes across the lifespan. The use of longitudinal data to map network changes may be of particular importance across childhood and adolescence, as these are thought to be crucial periods for the development of many psychiatric disorders (Costello et al., 2003). For example, researchers recently used ICNs to predict pubertal status with better precision than chronological age, additionally finding connectivity correlates with cognitive variables (Gracia-Tabuenca et al., 2021). Researchers could undertake similar investigations of the BNST network with regards the development of stress-based phenotypes. These types of analyses are increasingly possible with the availability of largescale longitudinal human datasets from a wide variety of age groups (e.g. certain samples within the HCP (Van Essen et al., 2012), UKBB (Miller et al., 2016), and the ABCD (Karcher & Barch, 2021) datasets). Although interesting from a basic science standpoint, the functional utility of mapping the brain-wide BNST network is contingent upon changes in this network being meaningfully associated with functional processes, traits, or clinical diagnoses; a finding that so far has generally eluded researchers. This issue is discussed further in section 5.3.

5.2.2 Analysis of hypothesis-driven BNST connections and the difficulties of imaging small nuclei

Whilst mapping brain-wide networks can be an important step in understanding how brain regions are broadly imbedded within larger-scale systems, examining specific connections based upon prior knowledge remains important. For example, for assessing phenotypical associations in humans of specific connections implicated via animal research (Barré-Sinoussi & Montagutelli, 2015; Munafò & Davey Smith, 2018). In this section I discuss the results of this research using these more targeted methods, outline the challenges of using largescale MRI datasets for analysis of small brain

regions, and discuss ways this research could be further refined.

The results of the *a-priori* selected iFC analyses, performed in chapters 2 and 3, did not reveal the expected associations with psychological phenotypes. Nonetheless, I believe the selection of these areas was justified given the large amount of literature implicating the BNST and amygdala in dispositional negativity (DN) and related phenotypes (Avery et al., 2016; Lebow & Chen, 2016; Maita et al., 2021). Ways to improve these analyses include the use of the aforementioned dynamic functional connectivity approaches, which may reveal connectivity patterns on shorter time-frames that are related to these psychological variables. In addition, techniques such as effective connectivity analysis, which model the direction of functional connectivity between brain regions, could better capture phenotype –functional connectivity relationships. Indeed, researchers have reported this very finding in the HCP, reporting laterobasal amygdala effective connectivity with the BNST is related to anxiety scores (Hofmann & Straube, 2020). Additional reasons for the general lack of phenotypic associations reported throughout the thesis are discussed in the sections below.

In chapter 4, I used multiple methods to examine a specific subiculum-BNST anatomical connection across species. This added to the BNST literature by describing this connection the first time in humans and potentially highlighting a rodent-primate species difference. As noted by other researchers, in order to overcome the limitations of various methodologies, the use of diverse analyses techniques, preferably at different scales, represents a step forward in terms of improving the robustness of evidence. Thus, this technique could be further exploited to improve the analysis of other BNST connections, including those from the BNST – amygdala sub regions.

In both Chapters 2 and 3 I focused specifically on BNST iFC to the amygdala. The amygdala, though, is not a singular structure (Amunts et al., 2005), and so I partitioned the brain region into a number of smaller divisions, included the three amygdala sub-regions from the Juelich Histological Atlas, the centromedial, laterobasal, and superficial amygdala (Jenkinson et al., 2012). These parcellations are broad and do not

differentiate between many of the smaller nuclei present in the amygdala (e.g., Giardino & Pomrenze, 2021). To partly address this I also used a smaller CeA mask created from high resolution *in vivo* MRI data (Pauli et al., 2018), specifically selecting this region due to the large body of research linking the CeA and BNST (Ahrens et al., 2018; Alheid, 2009). However, despite the wealth of research describing BNST – CeA connectivity, the results from the Chapter 2 ICN analysis of the BNST revealed a connectivity cluster just outside of the CeA, mostly within small parts of the superficial and centromedial amygdala. This specific region was used for analysis of the UKBB in chapter 3, but along with the other subregions did not show any associations with specific phenotypes or common genetic variants. In future, researchers could aim to see whether the highest area of connectivity remains in this same region by replicating the seed-based correlation analysis of the BNST in the much larger UKBB sample. This was not possible in the current study due to the high computational cost involved analysis the large UKBB sample, however to avert this problem smaller-subset could be used, still representing an useful out of sample replication attempt.

These results likely reflect, at least in part, the difficulty of accurately delineating small regional subdivisions in large neuroimaging samples (Despotović et al., 2015). In general, this was a potential issue for the analyses in all chapters, which all made use of generic averaged ROI templates. In chapters 2 and 3, each subjects functional MRI data was warped to a common standard space before analysis. This approach is well validated and is useful for comparing results across subjects, however this method can struggle to accurately account for individual variations in smaller structures, such as the BNST (Hutchison et al., 2014). This is particularly the case for fMRI data, which typically contain more geometric distortions and signal loss (Hutchison et al., 2014). Therefore, the activity of the BNST may not have been accurately captured for all participants by the standard space BNST mask. It may also have been that the area of significant activity between the BNST and amygdala revealed in chapter 2 does actually represent the CeA, and that the standard space CeA mask was marginally misaligned for most participants (see Figure 12 for a visual comparison between the cluster and CeA mask). In Chapter 3, I detected an associated SNP with the laterobasal amygdala only, which may have been because this was the largest ROI and therefore was less

susceptible to registration error-induced noise (Song et al., 2016). These factors may have been further impacted by the well documented difficulties of accurately extracting information from the amygdala region, an effect caused by its proximity to areas of signal distortion and dropout (Boubela et al., 2015).

The gold standard method for delineating brain regions is still considered to be the manual prescription of ROIs, which involves researchers using high resolution (usually T1w) anatomical MRI images to draw around the brain areas for each participant; usually based upon a validated protocol (Alkemade et al., 2022). Whilst this method is more personalised, and manual delineation procedures do exist for the BNST (Theiss et al., 2017), it is resource intensive and thus is not usually practical in a large samples such as the HCP or UKBB. In addition, many of these small brain regions are difficult to distinguish when viewing at standard MRI resolution (Quattrini et al., 2020). Use of larger samples in these chapters was appropriate as I was aiming to make inferences regarding genetic and phenotypic associations, which requires large datasets (Van Horn & Toga, 2014). However given the small brain regions involved, using a smaller subset of participants with ultra-high field imaging and manual delineation of brain regions may have been a useful technique for confirming the accuracy of the masked brain regions (Gordon et al., 2017).

Alternatively, subject-specific automated brain parcellation techniques are available, the most common of which is implemented through the Freesurfer toolbox (Dale et al., 1999). This package uses individuals' structural images in subject space and consists of a pipeline that performs several pre-processing steps, before segmenting brain tissue into grey matter, white matter, and cerebral spinal fluid. In addition, Freesurfer projects the images onto a 2D surface in order to more accurately map brain regions according to an individual's unique cortical folds (see https://surfer.nmr.mgh.harvard.edu/fswiki/FreeSurferWiki). Recently, Freesurfer has included the demarcation of several amygdala and hippocampal subregions as well (Quattrini et al., 2020). This method has been shown to be accurate and reliable, and would likely represent an improvement on the methods used in my research

(McCarthy et al., 2015; Quattrini et al., 2020, though see Zhou et al., 2021). A downside of this approach, however, is that it is computationally expensive, and so would require considerable resources and/or time to perform on the larger UKBB sample. In addition, automated parcellation systems for the BNST still do not exist, meaning the principal structure of analysis in this case would still need to be masked by the generic standard-space template or manual delineation.

Although I have focused this section mostly on the BNST - amygdala iFC work, these points are equally relevant for the structural connectivity analyses in Chapter 4. Here I also relied upon standard-space masks to mark the regions for probabilistic tractography analysis. More precise delineation techniques could have reduced noise and permit more specific analysis of, for example, subiculum complex subregions (e.g., presubiculum, prosubiculum). Recent work suggests a connectivity gradient within the subiculum complex along both its anterior-posterior and medial-lateral axis (Dalton et al., 2019; Ding et al., 2020), meaning that analysing the structure as a whole likely obscures a more nuanced pattern of connectivity. This was observed when analysing the tract-tracing data, which differed according to the precise subiculum areas injected. Additionally, the human BNST standard space mask only included the region above the anterior commissure, which essentially occluded tractography analysis of this area, known to have significant connectivity to amygdala and hypothalamic areas (Maita et al., 2021).

Analysis of structural BNST tracts could also be improved by using more biologically informed measures of white matter microstructure. While tensor-derived indices, such as those used in Chapter 4, are only indirect measures inferred from water diffusion, and thus do not reflect more specific properties of white matter microstructure (Afzali et al., 2021), measures derived from biophysical models e.g. , CHARMED (Assaf & Basser, 2005), or NODDI (Zhang et al., 2012), may provide more informative tract information, that in turn may demonstrate evidence for specific microstructural features that are related to phenotypes of interest. Nonetheless, some researchers have shown that DTI can often be more sensitive to individual differences than more specific microstructure measures (De Santis et al., 2014).

Finally, once specific connections have been described within the brain, researchers can begin to use methods of causal inference to test the effects of manipulating these networks. This can achieved via simulation methods (e.g. through various graph theory approaches) or can be done directly, either by using animal models or through human brain stimulation (Etkin, 2018). Animal models represent an important tool with regards to inferring causality, as researchers are able to induce lesions, sometimes reversibly, into brain areas to assess subsequent changes in function (Buffalari & See, 2011). As well, researchers can test for molecular changes following the introduction of certain stimuli, or in disease models (Gururajan et al., 2019; Meier et al., 2019). Animal-based techniques have been used extensively when testing hypotheses regarding the BNST, particularly with regards to the effects of alcohol on BNST neurotransmitter and neuropeptide expression and the effects of selective BNST vs amygdala lesions on stress responding (Davis et al., 2010; de Guglielmo et al., 2019; Pleil et al., 2015) (see also General Introduction section 1.2). Although many subcortical brain regions are largely preserved across mammalian species (Murray et al., 2017), as the results in Chapter 4 highlighted researchers must be cautious when interpreting results from animal models as they do not necessarily always translate to humans. In particular with regards to DN-linked traits, as mentioned in the General Introduction section 1.2, much human neuroimaging research has implicated top-down mechanisms that may not even exist in rodent models (LeDoux & Hofmann, 2018).

Non-human primates represent a closer model than rodents, and use of combined primate neuroimaging and anatomical tract-tracing of primate tissue was useful in Chapter 4 for validating the human probabilistic tractography results. However, primate research is restricted in many countries for ethical reasons and thus new analyses, particularly in tissue, can be challenging. Recently, researchers have used non-invasive electrical brain stimulation of cortical areas to target connected subcortical regions, for example stimulating the hippocampus via an area of the pre-frontal cortex (Warren et al., 2019). Research in Chapter 2 revealed extensive BNST

cortical connectivity, which could potentially be exploited for non-invasive electrical BNST manipulation and subsequent testing of changed functionality.

In sum, hypothesis-driven analysis of specific BNST connections was particularly useful in this thesis when using probabilistic tractography analysis, which allowed for the novel human description of a potentially key BNST pathway. These methods could be improved, however, in particular by enabling more accurate delineations of individual brain regions through the use of more refined automated processing techniques and, where feasible, manual segmentation with ultra-high resolution images. As well, more complex functional connectivity models, such as the use of dynamic or effectivity connectivity analyses, and methods of causal inference, particularly by using animal models, may reveal more about the nature of these *a priori* selected connections.

5.3 On the lack of associations between BNST connectivity measures and dispositional negativity and alcohol use phenotypes.

The principal motivation for analysing the connections of the BNST was to understand how individual differences in this structural and functional connectivity may be related to dispositional negativity-linked (DN) traits, risk genes, and ultimately, disorders. In the General Introduction I outlined many examples, particularly from preclinical animal work, linking the BNST to these phenotypes. In all chapters of this thesis, however, I found no such associations. Methodological and sample-specific reasons for this lack of association are mentioned in the relevant chapters, however here I will write more broadly about how these findings fit within the literature and make some suggestions for future analyses.

5.3.1 Normal trait variation and clinical phenotypes

In Chapter 2, using the HCP dataset, I found no relationships between BNST iFC connectivity (across the whole network or specifically between the BNST and amygdala) and trait variation in DN or alcohol use. In the discussion of Chapter 2, I

mention similar findings from other BNST iFC research and suggest that one reason for this may be that network differences associated with normal trait variation may not be same as those implicated in clinical disorders (Porta-Casteràs et al., 2020). However, in Chapter 3, I tested people with self-reported or medically diagnosed anxiety or alcohol use disorders and found no associations. This finding does not negate the general hypothesis of different networks underlying trait variation and clinical disorders, however, because in the UKBB sample I only analysed iFC between the BNST and amygdala. This leaves open the possibility that clinical phenotypes may still be associated with BNST iFC to other regions (Porta-Casteràs et al., 2020). Results from recent studies suggest that this may indeed by the case. For example, BNST iFC in PTSD patients was reported to be altered to number of areas, such as striatum, anterior insula, and caudate nucleus, but there were no differences in connectivity with the amygdala (Rabellino et al., 2018). Regarding alcohol-use disorders however, differences across well-established ICNs, such as the default mode network, have been noted, but so far have not implicated the BNST (Song et al., 2021).

In addition, I found no trait associations with DTI-derived white matter microstructure metrics in the subiculum-BNST tracts. As described in Chapter 4, there is conflicting evidence with regards to white-matter associations with psychological phenotypes (e.g. Avinun et al., 2020). In agreement with the trend of the iFC results though, there is some evidence that differences are easier to detect when analysing psychiatric populations. For example, a recent large-scale study reported white matter abnormalities when studying OCD patients, but did not find differences related to symptom variation (Piras et al., 2021). Future research could consider analysing clinical phenotypes and white-matter associations in a range of BNST tracts, perhaps following up on those with hypothesised links to stress-based disorders which may demonstrate longer term white-matter changes (Johnson et al., 2017). In sum, although normal trait variation has proven difficult to associate with BNST iFC or white matter metrics, differences in clinical groups may yet be demonstrated.

5.3.2 Recent findings suggest brain - psychological phenotype associations are smaller than expected

I used large samples in my analyses due concerns regarding the replicability of findings from small imaging samples (Button et al., 2013) and because brain - psychological phenotype associations require large samples to be reliably detected, mostly due to psychological and neuroimaging phenotype measurement variability (Elliott et al., 2021; Thompson et al., 2014). Although anticipated, results from a recent landmark study suggest that expected correlations between common variation in imaging derived phenotypes (IDPs) (including iFC, white matter metrics) and variation in complex cognitive or mental health phenotypes may be even lower than previously thought (Marek et al., 2022). In a comprehensive analysis, consisting of over a billion statistical tests across three large datasets (including the HCP and UKBB, n > 50,000), researchers reported that the highest replicable univariate association between IDPs and cognitive and clinical phenotypes was r = 0.16, with the median being r = 0.01 and the top 1% being r > 0.06. Importantly, the authors showed that effects from these 'brain wide association studies' are only reliable when sample sizes are in the thousands (Marek et al., 2022). The authors used simulations on subsets of the data to demonstrate that many previously published effects of significant brain-behaviour relationships in MRI research were likely simply type-one errors caused by the high sampling variability seen with smaller samples; an effect probably augmented by systemic publication bias. Therefore, the fact that I found no associations between any of the imaging variables and behavioural phenotypes may be in line with this research (Marek et al., 2022). This is particularly the case in the analyses of the HCP data, which although larger than many neuroimaging studies, contained *only* 1000 participants, which may not be considered enough to explore these brain-wide associations. Indeed, a sensitivity power analysis modelling 1000 participants, with a two sided hypothesis, 0.05 alpha and 0.8 beta, only demonstrates the power to detect correlations of r>0.08 (Faul et al., 2009). It should be the case then, that further analyses using the larger UKBB releases (n=20,000 – 100,000) would provide an adequate sample size for a repeat of the brain-psychological phenotype tests attempted in this body of work. Furthermore, due to the variability between studies caused by differences in samples, acquisition, and pre-processing parameters, replicating findings of this nature out-of-

sample would be necessary to ensure the reliability and generalizability of any findings (Evans, 2017; Marek et al., 2022; Nosek & Errington, 2020). However, although increasing sample sizes may go some way to helping the field uncover brain-behavioural relationships, the utility of using ever bigger samples to find relationships that explain only small amount of variance is questionable (Smith & Little, 2018).

5.3.3 Psychological phenotypes and the brain – problems with broad phenotypes and moving from association to explanation

Aside from the well documented problems with the use of self-report questionnaires for measuring complex and often situationally dynamic psychological traits (Jayawickreme et al., 2021; Kormos & Gifford, 2014), another reason for the general absence of brain-psychological phenotype associations may have been due to the broad and static nature of the phenotype measures used.

In chapters 2 and 4 I correlated IDPs with principal component analysis (PCA)-derived measures of DN and alcohol-use. The use of PCA on these items was inspired by research that emphasises the overlap between traits associated with negative affect, such as depression and anxiety (Shackman, Tromp, et al., 2016). That the different negative-affect self-report questionnaire items each contributed highly to the same principal component (see Figure 15), provided evidence that this was generally a correct assumption. However, relying on highly abstracted traits, such as DN, can make it difficult to detect relationships with neuroimaging variables. This is because broad traits, like DN, describe a range of cognitive, behavioural, and affective mechanisms, which means that they are likely underpinned by a similarly diverse range of neural circuits (Allen et al., 2020, 2022). Therefore, any two people scoring the same on a measure of DN (or alcohol use) may be doing so for a variety of reasons that are not necessarily subserved by the same neural processes. Although, for example, high anxiety and depression may be psychometrically similar, this may not translate to a shared underlying neurobiology (Brandt & Mueller, 2022).

This may have also been the case for the clinical diagnostic measures used in the UKBB analysis in Chapter 3, in which simple binary variables represented whether someone had any type of anxiety or alcohol-related disorder. Thus, there are likely many separate neural processes contributing to these phenotypes, potentially diluting the power to detect a neural association. In contrast, some researchers maintain that broad psychological phenotypes are represented by similarly broad highly distributed systems (Allen et al., 2020; DeYoung, 2015). Therefore, given a large enough sample size, and perhaps use of more complex network analysis methods (Serin et al., 2021), reliable brain-wide associations with these meta-phenotypes could yet be detected (Hilger & Markett, 2021).

Further complicating matters, particular brain regions or connections can provide generalised processes for seemingly unrelated or opposing psychological factors (Allen et al., 2020). This was shown recently in a study which reported that all five of the five-factor personality measures (McCrae & Costa Jr., 2008) were related to volumetric indices of the dorsolateral prefrontal cortex (Avinun et al., 2020). Indeed, the BNST itself has been linked to opposing processes in terms of anxiolytic and anxiogenic processing (Maita et al., 2021). This means that even if successful in finding a neural correlate of a complex phenotype, simply knowing if a region is associated can have little explanatory value on its own.

Therefore, this approach of simply associating high-level complex phenotypes with neural processes may be 'jumping the gun'. This is because, as well as being difficult to detect, any associations are currently unlikely to have meaningful mechanistic explanations. For example, as mentioned in previous sections, there are still debates as to whether and under what conditions BNST-CeA connectivity is involved in the processing of threat stimuli (Fox & Shackman, 2019; Hulsman et al., 2021). Therefore, until we resolve this question, what would it mean for dispositional negativity to be correlated with greater BNST functional connectivity to the amygdala? Thus, creating a neural taxonomy of more basic biological and cognitive functions, is perhaps necessary before attempts to associate such broad phenotypes with particular brain regions or

connections can have any explanatory value. This could be achieved by systemically altering the parameters of experiments, building outwards in a methodical manner towards more ethologically relevant stimuli (e.g., from 2D image presentation to video or virtual reality-based stimuli (see also section 5.3.4). This would allow researchers to make theory-led predictions regarding particular aspects of meta-phenotypes, including dispositional negativity, that are based upon experimental evidence (Allen et al., 2020; DeYoung & Krueger, 2020; Haslbeck et al., 2021).

5.3.4 Task – based methods

Another suggestion, made in all chapters, is that task-based rather than task-free measures may better capture the underlying neural processes associated with psychological phenotypes (Finn, 2021). In the same way that a cardiac stress-test reveals symptoms not visible under conditions of rest, engaging the brain during a given task may better augment individual differences in neural signals (Greene et al., 2018; Sripada et al., 2020). Particularly in light of new evidence suggesting only tiny correlations between iFC and psychological phenotypes (see section 5.3.2), it seems reasonable to suggest that the use of task-based methods may be better placed to uncover the psychological relationships with the BNST that are suggested by preclinical work (Cole et al., 2021; Finn, 2021; Sripada et al., 2020).

In general, recent findings have supported this notion. For example, using multiple large samples researchers have described how task-induced brain-wide connectivity was better able to predict cognitive traits (fluid intelligence, reading comprehension) than resting state networks (Greene et al., 2018; Jiang et al., 2020; Sripada et al., 2020). Interestingly, these effects were seen irrespective of the type of task used, with one study demonstrating that tests of emotion identification, gambling, language, motor tasks, relational processing, social processing, and working memory all predicted higher variance in fluid intelligence than resting state networks (Greene et al., 2018). Other research has shown that combining both tf-fMRI and task-based fMRI can lead to more reliable results and higher heritability estimates than tf-fMRI alone

(Elliott et al., 2019). Whether these findings generalise to prediction of more emotion and personality-based variables, however, is an open question. The BNST has thus far been excluded from such studies due to its absence in the most commonly used anatomical parcellations. Given the evidence for the BNST's role in integration of bottom up and top-down processes relating to stress-processing (Herman et al., 2020; Radley & Sawchenko, 2011), researchers should strongly consider its inclusion in future task-induced functional connectome analyses, especially if predicting emotion or stress-associated phenotypes.

Specifically with regards to the BNST, task-based fMRI research has so far appeared to have had more success in comparison to task-free measures in predicting psychological variables (reviewed in Hulsman et al., 2021, also see General Introduction section 1.2). A clear example of this is seen in findings describing BNST-CeA functional connectivity differences in clinical anxiety patients that are only present when under sustained threat of shock (Torrisi et al., 2019). These differences were not seen in the same patients using task-free imaging, suggesting that differences relevant to clinical disorders may only become apparent under task-related conditions.

A challenge to many task-based imaging paradigms, including those used in most BNST research, comes from recent findings that question whether the brain regions implicated by many of the carefully controlled lab-based experiments are similarly activated during more ethologically relevant processing. For example, researchers tested the hypothesis that amygdala connectivity to frontal regions in response to faces changes depending upon anxiety levels (Robinson et al., 2011). Using a dynamic movie-viewing paradigm, instead of the typical 2d face presentation task, the experimenters did not find evidence to support this hypothesis (Kirk et al., 2022). Another study, which used independent raters continuous scoring of fear during a horror movie as a variable, described different brain networks that were associated with anticipatory anxiety and proximal fear (response to jump scares) (Hudson et al., 2020). However, in contrast to reports in less complex neuroimaging studies and many theories of fear and anxiety processing, none of these networks implicated the BNST (Hudson et al., 2020), in agreement with a similar earlier study (Nanni et al., 2018).

With regards to alcohol-use, a systematic review and meta-analysis of mostly experiential-based sampling research reported that, again contrary to many theories, the biggest predictor of alcohol use was positive, rather than negative affect (Tovmasyan et al., 2022). This finding may not be relevant to alcohol use disorders, however (Nguyen et al., 2020), thus again highlighting the caution required when extrapolating findings of normal trait variation to disorders. In general nonetheless, these (presumably) more ecologically valid experiments are important for validating research across contexts (Finn, 2021), and thus theories of BNST involvement in these processes must be able to account for such results.

Task-based imaging is not restricted to fMRI. As discussed in Chapter 4, tasks (or life events) have also been shown to induce changes in white matter microstructure, which may present an additional way to examine alterations across a longer time-span (e.g. Voelker et al., 2017). Examinations of task-induced (Huber et al., 2018), or life-event associated (Johnson et al., 2017), white-matter changes between the BNST and amygdala, or even subiculum – amygdala – BNST - hypothalamus, would be an interesting and novel analysis, especially because of the hypothesised long-term effects of stress on the brain during development (Meng et al., 2021). Novel techniques that use fMRI to model the BOLD response in white matter pathways may also prove useful for the study of BNST connections (Li et al., 2019).

5.4 BNST genetic analyses

Throughout this thesis I attempted to use the available genetic information to make novel inferences regarding BNST connectivity measures. This was principally successful in describing the twin-based heritability of functional and white matter microstructure metrics of BNST connections to amygdala sub-nuclei and the subiculum complex. As mentioned in the chapter-specific discussions, however, this finding is not in itself particularly informative, as we know that nearly all phenotypes are at least partly explained by genetic factors (Turkheimer, 1998). Therefore, I was more interested in detecting evidence for co-heritability with psychological phenotypes, which would

have suggested potentially shared genetic mechanisms. This was not the case in any of the twin-based heritability analyses. Similarly, SNP-based heritability analysis (using only the common SNPs present in the sample), revealed no evidence for heritability of iFC between the BNST and amygdala subregions in the UKBB. Genome-wide association analyses of these same connections found only a single significant SNP association, between the BNST and laterobasal amygdala. This variant has been linked to expression of a gene (*NRG3*) previously shown to be highly expressed within the amygdala; though not selectively so (Uhlén et al., 2015). However, this SNP explains only a tiny amount of the variance in BNST-laterobasal iFC, and so the implications of this are limited.

The genetic analyses in general could have been improved by employing many of the recommendations outlined in previous sections. Namely, the use of more precise imaging and psychological phenotypes, larger samples, and using more complex analyses methods (e.g. dynamic functional connectivity, network analyses) . An interesting alternative use of genetic neuroimaging was recently employed to study the *variability* of functional brain network organisation in the HCP (Anderson et al., 2021). This contrasts with most studies, which use pre-defined averaged templates of networks and test for differences in connectivity within them. The researchers reported that individual variation in ICN size and location was influenced by genetic factors, paving the way for future studies to examine whether this variability is co-heritable or otherwise associated with psychological phenotypes (Anderson et al., 2021). Genetic methods of generating connectomes are also available. For example, researchers have used gene-expression data from post-mortem human brain tissue to demonstrate differences along a gradient within the hippocampus (Vogel et al., 2020). This was followed up by comparing these differences with expression across the rest of brain, which along with previous functional connectivity data, was used to demonstrate distinct connectivity profiles of hippocampal regions (Vogel et al., 2020). Such analyses could be used for the BNST, especially for resolving connectivity questions regarding its internal organisation, the subsections of which are generally too small to resolve with MRI analyses (Hammack et al., 2021).

Other genetic analysis methods, such as mendelian randomisation (MR) analysis (Burgess et al., 2020; Davies et al., 2018), present opportunities to test causal relationships between BNST-linked imaging variables, psychological phenotypes, and genetic variants empirically. Put simply, MR assigns people into different groups based upon their genetic risk factors and compares outcomes in various life events (e.g., diagnosis of a disorder) in order to determine causality (see Davies et al., 2018 for a fuller explanation). This method is advantageous because, as genotypes are determined randomly during meiosis, they represent a form a natural randomised controlled trial (though see VanderWeele et al., 2014). This approach has so far been employed to, for example, demonstrate associations between white matter metrics and genetic risk for anorexia nervosa (Song et al., 2021).

The use of animal models may continue to be important for studying genetics associated with the BNST. For example, following a GWAS to identify genetic variants associated with anxiety disorders (Meier et al., 2018), researchers then used gene expression analysis within mice to show that an anxiety disorder implicated gene, (PDE4B) was raised in mice displaying anxiety-like behaviour (Meier et al., 2019). Interestingly, the two brain regions in which this was found were a part of the purported BNST-linked stress circuit, namely the hippocampus and (mouse) pre-frontal cortex (Meier et al., 2019; Radley & Sawchenko, 2011).

5.5 Conclusions

In this work I advanced knowledge of the BNST and its connections in the following ways. Firstly, I mapped the brain-wide intrinsic functional connectivity of the BNST in a large human sample, demonstrating significant agreement with studies in smaller populations. Secondly, I provided novel evidence of a structural connection between the subiculum complex and the BNST in humans and macaques. This was additionally supported by tract-tracing analysis (Berry et at., 2022), which along with the probabilistic tractography dMRI methods, suggested a potentially important species difference with rodents that may have implications for theories and treatments of

stress processing and the generalizability of work in rodents. Thirdly, I added to an increasing body of work demonstrating that (at least for iFC) detecting brain-wide associations with normal personality trait variation in psychological phenotypes is difficult, even in samples previously considered to be large. Fourthly, I did not repeat findings in humans from NHP work describing co-heritability between BNST-amygdala functional connectivity an DN-related trait (Fox et al., 2018). Fifth, I performed the first GWAS of a BNST related variable, using a large human neuroimaging dataset, the UKBB. The results from this analysis revealed little evidence for SNP-based heritability of iFC between the BNST and amygdala subnuclei, or clinical-phenotype and common genetic variant associations.

There is much to learn about the BNST and related neurocircuitry, and despite an increase in interest due to its purported links to DN and substance-misuse, the structure is often overlooked in MRI research (Lebow & Chen, 2016). In the general discussion, I suggested a variety of ways to improve BNST research. To summarise, I principally recommend increasing the precision of imaging small brain regions, using more complex and biologically informed neuroimaging analyses, moving away from resting state and towards naturalistic task-based imaging and interventional approaches, and focusing on first understanding more basic BNST-linked mechanisms before attempting to associate connections or activity with complex traits. I believe that genetic associations will likely follow improvements to the imaging and phenotype characterisation methods; though as is the case broadly across imaging genetics research, whether implicating common genetic associations of small effect prove informative is an open question. In general, I believe continuing to use a combination of techniques across different samples, as I have tried to do here, will lead to a greater understanding of this small, complex brain region.

References

Abler, B., Erk, S., Herwig, U., & Walter, H. (2007). Anticipation of aversive stimuli activates extended amygdala in unipolar depression. *Journal of Psychiatric Research*, *41*(6), 511–522. https://doi.org/10.1016/j.jpsychires.2006.07.020

Adhikari, B. M., Jahanshad, N., Shukla, D., Glahn, D. C., Blangero, J., Fox, P. T., Reynolds, R. C., Cox, R. W., Fieremans, E., Veraart, J., Novikov, D. S., Nichols, T. E., Hong, L. E., Thompson, P. M., & Kochunov, P. (2018). Comparison of heritability estimates on resting state fMRI connectivity phenotypes using the ENIGMA analysis pipeline. *Human Brain Mapping*, *39*(12), 4893–4902. https://doi.org/10.1002/hbm.24331

Aggleton, J. P. (1986). A description of the amygdalo-hippocampal interconnections in the macaque monkey. *Experimental Brain Research*, *64*(3), 515–526. https://doi.org/10.1007/BF00340489

Aggleton, J. P., & Christiansen, K. (2015). Chapter 4 - The subiculum: The heart of the extended hippocampal system. In S. O'Mara & M. Tsanov (Eds.), *Progress in Brain Research* (Vol. 219, pp. 65–82). Elsevier. https://doi.org/10.1016/bs.pbr.2015.03.003

Aggleton, J. P., Wright, N. F., Rosene, D. L., & Saunders, R. C. (2015). Complementary Patterns of Direct Amygdala and Hippocampal Projections to the Macaque Prefrontal Cortex. *Cerebral Cortex*, *25*(11), 4351–4373. https://doi.org/10.1093/cercor/bhv019

Ahrens, S., Wu, M. V., Furlan, A., Hwang, G.-R., Paik, R., Li, H., Penzo, M. A., Tollkuhn, J., & Li, B. (2018). A Central Extended Amygdala Circuit That Modulates Anxiety. *Journal of Neuroscience*, *38*(24), 5567–5583. https://doi.org/10.1523/JNEUROSCI.0705-18.2018

Alfaro-Almagro, F., Jenkinson, M., Bangerter, N. K., Andersson, J. L. R., Griffanti, L., Douaud, G., Sotiropoulos, S. N., Jbabdi, S., Hernandez-Fernandez, M., Vallee, E., Vidaurre, D., Webster, M., McCarthy, P., Rorden, C., Daducci, A., Alexander, D. C., Zhang, H., Dragonu, I., Matthews, P. M., … Smith, S. M. (2018). Image processing and Quality Control for the first 10,000 brain imaging datasets from UK Biobank. *NeuroImage*, *166*, 400–424. https://doi.org/10.1016/j.neuroimage.2017.10.034

Alheid, G. F. (2009). Extended Amygdala. In M. D. Binder, N. Hirokawa, & U. Windhorst (Eds.), *Encyclopedia of Neuroscience* (pp. 1501–1506). Springer Berlin Heidelberg. https://doi.org/10.1007/978-3-540-29678-2_3221

Alheid, G. F., Beltramino, C. A., De Olmos, J. S., Forbes, M. S., Swanson, D. J., & Heimer, L. (1998). The neuronal organization of the supracapsular part of the stria terminalis in the rat: The dorsal component of the extended amygdala. *Neuroscience*, *84*(4), 967–996.

Alheid, G. F., & Heimer, L. (1988). New perspectives in basal forebrain organization of special relevance for neuropsychiatric disorders: The striatopallidal, amygdaloid, and corticopetal components of substantia innominata. *Neuroscience*, *27*(1), 1–39.

Alkemade, A., Mulder, M. J., Trutti, A. C., & Forstmann, B. U. (2022). Manual delineation approaches for direct imaging of the subcortex. *Brain Structure and Function*, *227*(1), 219–297. https://doi.org/10.1007/s00429-021-02400-x

Allegrini, A. G., Cheesman, R., Rimfeld, K., Selzam, S., Pingault, J.-B., Eley, T. C., & Plomin, R. (2020). The p factor: Genetic analyses support a general dimension of psychopathology in childhood and adolescence. *Journal of Child Psychology and Psychiatry*, *61*(1), 30–39. https://doi.org/10.1111/jcpp.13113

Allen, A. P., Kennedy, P. J., Dockray, S., Cryan, J. F., Dinan, T. G., & Clarke, G. (2017). The Trier Social Stress Test: Principles and practice. *Neurobiology of Stress*, *6*, 113–126. https://doi.org/10.1016/j.ynstr.2016.11.001

Allen, L. S., & Gorski, R. A. (1990). Sex difference in the bed nucleus of the stria terminalis of the human brain. *Journal of Comparative Neurology*, *302*(4), 697–706. https://doi.org/10.1002/cne.903020402

Allen, T. A., Hall, N. T., Schreiber, A. M., & Hallquist, M. N. (2022). Explanatory personality science in the neuroimaging era: The map is not the territory. *Current Opinion in Behavioral Sciences*, *43*, 236–241. https://doi.org/10.1016/j.cobeha.2021.11.009

Allen, T. A., Schreiber, A. M., Hall, N. T., & Hallquist, M. N. (2020). From Description to Explanation: Integrating Across Multiple Levels of Analysis to Inform Neuroscientific Accounts of Dimensional Personality Pathology. *Journal of Personality Disorders*, *34*(5), 650–676. https://doi.org/10.1521/pedi.2020.34.5.650

Almasy, L., & Blangero, J. (2010). Variance Component Methods for Analysis of Complex Phenotypes. *Cold Spring Harbor Protocols*, *2010*(5), pdb.top77. https://doi.org/10.1101/pdb.top77

Alvarez, R. P., Chen, G., Bodurka, J., Kaplan, R., & Grillon, C. (2011). Phasic and sustained fear in humans elicits distinct patterns of brain activity. *NeuroImage*, *55*(1), 389–400. https://doi.org/10.1016/j.neuroimage.2010.11.057

Amunts, K., Kedo, O., Kindler, M., Pieperhoff, P., Mohlberg, H., Shah, N. J., Habel, U., Schneider, F., & Zilles, K. (2005). Cytoarchitectonic mapping of the human amygdala, hippocampal region and entorhinal cortex: Intersubject variability and probability maps. *Anatomy and Embryology*, *210*(5–6), 343–352. https://doi.org/10.1007/s00429-005-0025-5

Anderson, K. M., Ge, T., Kong, R., Patrick, L. M., Spreng, R. N., Sabuncu, M. R., Yeo, B. T. T., & Holmes, A. J. (2021). Heritability of individualized cortical network topography. *Proceedings of the National Academy of Sciences*, *118*(9), e2016271118. https://doi.org/10.1073/pnas.2016271118

Andersson, J. L. R., & Sotiropoulos, S. N. (2016). An integrated approach to correction for off-resonance effects and subject movement in diffusion MR imaging. *NeuroImage*, *125*, 1063–1078. https://doi.org/10.1016/j.neuroimage.2015.10.019

Andreatta, M., Glotzbach-Schoon, E., Mühlberger, A., Schulz, S. M., Wiemer, J., & Pauli, P. (2015). Initial and sustained brain responses to contextual conditioned anxiety in humans. *Cortex; a Journal Devoted to the Study of the Nervous System and Behavior*, *63*, 352–363. https://doi.org/10.1016/j.cortex.2014.09.014

Andrews-Hanna, J. R., Snyder, A. Z., Vincent, J. L., Lustig, C., Head, D., Raichle, M. E., & Buckner, R. L. (2007). Disruption of large-scale brain systems in advanced aging. *Neuron*, *56*(5), 924–935. https://doi.org/10.1016/j.neuron.2007.10.038

Ashworth, E., Brooks, S. J., & Schiöth, H. B. (2021). Neural activation of anxiety and depression in children and young people: A systematic meta-analysis of fMRI studies. *Psychiatry Research: Neuroimaging*, *311*, 111272. https://doi.org/10.1016/j.pscychresns.2021.111272

Avery, S. N., Clauss, J. A., & Blackford, J. U. (2016). The Human BNST: Functional Role in Anxiety and Addiction. *Neuropsychopharmacology: Official Publication of the American College of Neuropsychopharmacology*, *41*(1), 126–141. https://doi.org/10.1038/npp.2015.185

Avery, S. N., Clauss, J. A., Winder, D. G., Woodward, N., Heckers, S., & Blackford, J. U. (2014). BNST neurocircuitry in humans. *NeuroImage*, *91*, 311–323. https://doi.org/10.1016/j.neuroimage.2014.01.017

Avinun, R., Israel, S., Knodt, A. R., & Hariri, A. R. (2020). Little evidence for associations between the Big Five personality traits and variability in brain gray or white matter. *NeuroImage*, *220*, 117092. https://doi.org/10.1016/j.neuroimage.2020.117092

Bach, E. C., Ewin, S. E., Baldassaro, A. D., Carlson, H. N., & Weiner, J. L. (2021). Chronic intermittent ethanol promotes ventral subiculum hyperexcitability via increases in extrinsic basolateral amygdala input and local network activity. *Scientific Reports*, *11*(1), 8749. https://doi.org/10.1038/s41598-021-87899-0

Bangasser, D. A., & Wiersielis, K. R. (2018). Sex differences in stress responses: A critical role for corticotropin-releasing factor. *Hormones (Athens, Greece)*, *17*(1), 5–13. https://doi.org/10.1007/s42000-018-0002-z

Banks, S. J., Eddy, K. T., Angstadt, M., Nathan, P. J., & Phan, K. L. (2007). Amygdala–frontal connectivity during emotion regulation. *Social Cognitive and Affective Neuroscience*, *2*(4), 303–312. https://doi.org/10.1093/scan/nsm029

Barnea-Goraly, N., Chang, K. D., Karchemskiy, A., Howe, M. E., & Reiss, A. L. (2009). Limbic and corpus callosum aberrations in adolescents with bipolar disorder: A tract-based spatial statistics analysis. *Biological Psychiatry*, *66*(3), 238–244. https://doi.org/10.1016/j.biopsych.2009.02.025

Barré-Sinoussi, F., & Montagutelli, X. (2015). Animal models are essential to biological research: Issues and perspectives. *Future Science OA*, *1*(4), FSO63. https://doi.org/10.4155/fso.15.63

Baselmans, B. M. L., Willems, Y. E., van Beijsterveldt, C. E. M., Ligthart, L., Willemsen, G., Dolan, C. V., Boomsma, D. I., & Bartels, M. (2018). Unraveling the Genetic and Environmental Relationship Between Well-Being and Depressive Symptoms Throughout the Lifespan. *Frontiers in Psychiatry*, *9*, 261. https://doi.org/10.3389/fpsyt.2018.00261

Basser, P. J. (1997). New Histological and Physiological Stains Derived from Diffusion-Tensor MR Images. *Annals of the New York Academy of Sciences*, *820*(1), 123–138. https://doi.org/10.1111/j.1749-6632.1997.tb46192.x

Bates, D., Mächler, M., Bolker, B., & Walker, S. (2014). Fitting Linear Mixed-Effects Models using lme4. *ArXiv:1406.5823 [Stat]*. http://arxiv.org/abs/1406.5823

Battistella, G., Borghesani, V., Henry, M., Shwe, W., Lauricella, M., Miller, Z., Deleon, J., Miller, B. L., Dronkers, N., Brambati, S. M., Seeley, W. W., Mandelli, M. L., & Gorno-Tempini, M. L. (2020). Task-Free Functional Language Networks: Reproducibility and Clinical Application. *Journal of Neuroscience*, *40*(6), 1311–1320. https://doi.org/10.1523/JNEUROSCI.1485-19.2019

Bauer, I. E., Wu, M.-J., Meyer, T. D., Mwangi, B., Ouyang, A., Spiker, D., Zunta-Soares, G. B., Huang, H., & Soares, J. C. (2016). The role of white matter in personality traits and affective processing in bipolar disorder. *Journal of Psychiatric Research*, *80*, 64–72. https://doi.org/10.1016/j.jpsychires.2016.06.003

Beckmann, C. F., & Smith, S. M. (2004). Probabilistic independent component analysis for functional magnetic resonance imaging. *IEEE Transactions on Medical Imaging*, *23*(2), 137–152. https://doi.org/10.1109/TMI.2003.822821

Behrens, T. E. J., Berg, H. J., Jbabdi, S., Rushworth, M. F. S., & Woolrich, M. W. (2007). Probabilistic diffusion tractography with multiple fibre orientations: What can we gain? *NeuroImage*, *34*(1), 144–155. https://doi.org/10.1016/j.neuroimage.2006.09.018

Belleau, E. L., Treadway, M. T., & Pizzagalli, D. A. (2019). The Impact of Stress and Major Depressive Disorder on Hippocampal and Medial Prefrontal Cortex Morphology. *Biological Psychiatry*, *85*(6), 443–453. https://doi.org/10.1016/j.biopsych.2018.09.031

Benear, S. L., Ngo, C. T., & Olson, I. R. (2020). Dissecting the Fornix in Basic Memory Processes and Neuropsychiatric Disease: A Review. *Brain Connectivity*, *10*(7), 331–354. https://doi.org/10.1089/brain.2020.0749

Berry, S. C., Lawrence, A. D., Lancaster, T. M., Casella, C., Aggleton, J. P., & Postans, M. (2022). Subiculum—BNST Structural Connectivity in Humans and Macaques. *NeuroImage*, 119096. https://doi.org/10.1016/j.neuroimage.2022.119096

Berry, S. C., Wise, R. G., Lawrence, A. D., & Lancaster, T. M. (2020). Extended-amygdala intrinsic functional connectivity networks: A population study. *Human Brain Mapping*, *42*(6), 1594–1616. https://doi.org/10.1002/hbm.25314

Bienkowski, M. S., Bowman, I., Song, M. Y., Gou, L., Ard, T., Cotter, K., Zhu, M., Benavidez, N. L., Yamashita, S., Abu-Jaber, J., Azam, S., Lo, D., Foster, N. N., Hintiryan, H., & Dong, H.-W. (2018). Integration of gene expression and brain-wide connectivity reveals the multiscale organization of mouse hippocampal networks. *Nature Neuroscience*, *21*(11), 1628–1643. https://doi.org/10.1038/s41593-018-0241-y

Birn, R. M., Molloy, E. K., Patriat, R., Parker, T., Meier, T. B., Kirk, G. R., Nair, V. A., Meyerand, M. E., & Prabhakaran, V. (2013). The effect of scan length on the reliability of resting-state fMRI connectivity estimates. *NeuroImage*, *83*, 550–558. https://doi.org/10.1016/j.neuroimage.2013.05.099

Birn, R. M., Shackman, A. J., Oler, J. A., Williams, L. E., McFarlin, D. R., Rogers, G. M., Shelton, S. E., Alexander, A. L., Pine, D. S., Slattery, M. J., Davidson, R. J., Fox, A. S., & Kalin, N. H. (2014). Evolutionarily-conserved prefrontal-amygdalar dysfunction in early-life anxiety. *Molecular Psychiatry*, *19*(8), 915–922. https://doi.org/10.1038/mp.2014.46

Birney, E., & Soranzo, N. (2015). The end of the start for population sequencing. *Nature*, *526*(7571), Article 7571. https://doi.org/10.1038/526052a

Blomstedt, P., Naesström, M., & Bodlund, O. (2017). Deep brain stimulation in the bed nucleus of the stria terminalis and medial forebrain bundle in a patient with major depressive disorder and anorexia nervosa. *Clinical Case Reports*, *5*(5), 679–684. https://doi.org/10.1002/ccr3.856

Böhm, C., Peng, Y., Geiger, J. R. P., & Schmitz, D. (2018). Routes to, from and within the subiculum. *Cell and Tissue Research*, *373*(3), 557–563. https://doi.org/10.1007/s00441-018-2848-4

Bota, M., Sporns, O., & Swanson, L. W. (2012). Neuroinformatics analysis of molecular expression patterns and neuron populations in gray matter regions: The rat BST as a rich exemplar. *Brain Research*, *1450*, 174–193. https://doi.org/10.1016/j.brainres.2012.02.034

Bouarab, C., Thompson, B., & Polter, A. M. (2019). VTA GABA Neurons at the Interface of Stress and Reward. *Frontiers in Neural Circuits*, *13*. https://www.frontiersin.org/article/10.3389/fncir.2019.00078

Boubela, R. N., Kalcher, K., Huf, W., Seidel, E.-M., Derntl, B., Pezawas, L., Našel, C., & Moser, E. (2015). FMRI measurements of amygdala activation are confounded by stimulus correlated signal fluctuation in nearby veins draining distant brain regions. *Scientific Reports*, *5*(1), Article 1. https://doi.org/10.1038/srep10499

Bourbon-Teles, J., Bells, S., Jones, D. K., Coulthard, E., Rosser, A., & Metzler-Baddeley, C. (2019). Myelin Breakdown in Human Huntington's Disease: Multi-Modal Evidence from Diffusion MRI and Quantitative Magnetization Transfer. *Neuroscience*, *403*, 79–92. https://doi.org/10.1016/j.neuroscience.2017.05.042

Bowman, F. D., Zhang, L., Derado, G., & Chen, S. (2012). Determining functional connectivity using fMRI data with diffusion-based anatomical weighting. *NeuroImage*, *62*(3), 1769–1779. https://doi.org/10.1016/j.neuroimage.2012.05.032

Boyle, E. A., Li, Y. I., & Pritchard, J. K. (2017). An Expanded View of Complex Traits: From Polygenic to Omnigenic. *Cell*, *169*(7), 1177–1186. https://doi.org/10.1016/j.cell.2017.05.038

BOZZOLI, C., DEATON, A., & QUINTANA-DOMEQUE, C. (2009). Adult Height and Childhood Disease. *Demography*, *46*(4), 647–669.

Brandt, A., & Mueller, E. M. (2022). Negative affect related traits and the chasm between self-report and neuroscience. *Current Opinion in Behavioral Sciences*, *43*, 216–223. https://doi.org/10.1016/j.cobeha.2021.11.002

Brinkmann, L., Buff, C., Feldker, K., Neumeister, P., Heitmann, C. Y., Hofmann, D., Bruchmann, M., Herrmann, M. J., & Straube, T. (2018a). Inter-individual differences in trait anxiety shape the functional connectivity between the bed nucleus of the stria terminalis and the amygdala during brief threat processing. *NeuroImage*, *166*, 110–116. https://doi.org/10.1016/j.neuroimage.2017.10.054

Brinkmann, L., Buff, C., Feldker, K., Neumeister, P., Heitmann, C. Y., Hofmann, D., Bruchmann, M., Herrmann, M. J., & Straube, T. (2018b). Inter-individual differences in trait anxiety shape the functional connectivity between the bed nucleus of the stria terminalis and the amygdala during brief threat processing. *NeuroImage*, *166*, 110–116. https://doi.org/10.1016/j.neuroimage.2017.10.054

Brinkmann, L., Buff, C., Feldker, K., Tupak, S. V., Becker, M. P. I., Herrmann, M. J., & Straube, T. (2017). Distinct phasic and sustained brain responses and connectivity of amygdala and bed nucleus of the stria terminalis during threat anticipation in panic disorder. *Psychological Medicine*, *47*(15), 2675–2688. https://doi.org/10.1017/S0033291717001192

Brinkmann, L., Buff, C., Neumeister, P., Tupak, S. V., Becker, M. P. I., Herrmann, M. J., & Straube, T. (2017). Dissociation between amygdala and bed nucleus of the stria terminalis during threat anticipation in female post-traumatic stress disorder patients. *Human Brain Mapping*, *38*(4), 2190–2205. https://doi.org/10.1002/hbm.23513

Brog, J. S., Salyapongse, A., Deutch, A. Y., & Zahm, D. S. (1993). The patterns of afferent innervation of the core and shell in the 'accumbens' part of the rat ventral striatum: Immunohistochemical detection of retrogradely transported fluoro-gold. *The Journal of Comparative Neurology*, *338*(2), 255–278. https://doi.org/10.1002/cne.903380209

Brown, C. A., Johnson, N. F., Anderson-Mooney, A. J., Jicha, G. A., Shaw, L. M., Trojanowski, J. Q., Van Eldik, L. J., Schmitt, F. A., Smith, C. D., & Gold, B. T. (2017). Development, validation and application of a new fornix template for studies of aging and preclinical Alzheimer's disease. *NeuroImage: Clinical*, *13*, 106–115. https://doi.org/10.1016/j.nicl.2016.11.024

Brown, Z. J., Tribe, E., D'souza, N. A., & Erb, S. (2009). Interaction between noradrenaline and corticotrophin-releasing factor in the reinstatement of cocaine seeking in the rat. *Psychopharmacology*, *203*(1), 121–130. https://doi.org/10.1007/s00213-008-1376-4

Buckner, R. L., Krienen, F. M., & Yeo, B. T. T. (2013). Opportunities and limitations of intrinsic functional connectivity MRI. *Nature Neuroscience*, *16*(7), Article 7. https://doi.org/10.1038/nn.3423

Buff, C., Brinkmann, L., Bruchmann, M., Becker, M. P. I., Tupak, S., Herrmann, M. J., & Straube, T. (2017). Activity alterations in the bed nucleus of the stria terminalis and amygdala during threat anticipation in generalized anxiety disorder. *Social Cognitive and Affective Neuroscience*, *12*(11), 1766–1774. https://doi.org/10.1093/scan/nsx103

Buffalari, D. M., & See, R. E. (2011). Inactivation of the bed nucleus of the stria terminalis in an animal model of relapse: Effects on conditioned cue-induced reinstatement and its enhancement by yohimbine. *Psychopharmacology*, *213*(1), 19–27. https://doi.org/10.1007/s00213-010-2008-3

Bulik-Sullivan, B. K., Loh, P.-R., Finucane, H. K., Ripke, S., Yang, J., Schizophrenia Working Group of the Psychiatric Genomics Consortium, Patterson, N., Daly, M. J., Price, A. L., & Neale, B. M. (2015). LD Score regression distinguishes confounding from polygenicity in genome-wide association studies. *Nature Genetics*, *47*(3), 291–295. https://doi.org/10.1038/ng.3211

Bullmore, E., & Sporns, O. (2012). The economy of brain network organization. *Nature Reviews Neuroscience*, *13*(5), Article 5. https://doi.org/10.1038/nrn3214

Burgess, S., Foley, C. N., Allara, E., Staley, J. R., & Howson, J. M. M. (2020). A robust and efficient method for Mendelian randomization with hundreds of genetic variants. *Nature Communications*, *11*(1), Article 1. https://doi.org/10.1038/s41467-019-14156-4

Button, K. S., Ioannidis, J. P. A., Mokrysz, C., Nosek, B. A., Flint, J., Robinson, E. S. J., & Munafò, M. R. (2013). Power failure: Why small sample size undermines the reliability of neuroscience. *Nature Reviews Neuroscience*, *14*(5), Article 5. https://doi.org/10.1038/nrn3475

Bycroft, C., Freeman, C., Petkova, D., Band, G., Elliott, L. T., Sharp, K., Motyer, A., Vukcevic, D., Delaneau, O., O'Connell, J., Cortes, A., Welsh, S., Young, A., Effingham, M., McVean, G., Leslie, S., Allen, N., Donnelly, P., & Marchini, J. (2018). The UK Biobank resource with deep phenotyping and genomic data. *Nature*, *562*(7726), 203–209. https://doi.org/10.1038/s41586-018-0579-z

Cabeza, R., Stanley, M. L., & Moscovitch, M. (2018). Process-specific alliances (PSAs) in cognitive neuroscience. *Trends in Cognitive Sciences*, *22*(11), 996–1010. https://doi.org/10.1016/j.tics.2018.08.005

Calabrese, E., Badea, A., Coe, C. L., Lubach, G. R., Shi, Y., Styner, M. A., & Johnson, G. A. (2015). A diffusion tensor MRI atlas of the postmortem rhesus macaque brain. *NeuroImage*, *117*, 408–416. https://doi.org/10.1016/j.neuroimage.2015.05.072

Campbell, J. S. W., & Pike, G. B. (2014). Potential and limitations of diffusion MRI tractography for the study of language. *Brain and Language*, *131*, 65–73. https://doi.org/10.1016/j.bandl.2013.06.007

Campbell, R. R., Domingo, R. D., Williams, A. R., Wroten, M. G., McGregor, H. A., Waltermire, R. S., Greentree, D. I., Goulding, S. P., Thompson, A. B., Lee, K. M., Quadir, S. G., Jimenez Chavez, C. L., Coelho, M. A., Gould, A. T., von Jonquieres, G., Klugmann, M., Worley, P. F., Kippin, T. E., & Szumlinski, K. K. (2019). Increased alcohol-drinking induced by manipulations of mGlu5 phosphorylation within the bed nucleus of the stria terminalis. *The Journal of Neuroscience: The Official Journal of the Society for Neuroscience*. https://doi.org/10.1523/JNEUROSCI.1909-18.2018

Cano-Gamez, E., & Trynka, G. (2020). From GWAS to Function: Using Functional Genomics to Identify the Mechanisms Underlying Complex Diseases. *Frontiers in Genetics*, *11*. https://www.frontiersin.org/article/10.3389/fgene.2020.00424

Canteras, N. S., & Swanson, L. W. (1992). Projections of the ventral subiculum to the amygdala, septum, and hypothalamus: A PHAL anterograde tract-tracing study in the rat. *Journal of Comparative Neurology*, *324*(2), 180–194. https://doi.org/10.1002/cne.903240204

Carboni, E., Silvagni, A., Rolando, M. T., & Di Chiara, G. (2000). Stimulation of in vivo dopamine transmission in the bed nucleus of stria terminalis by reinforcing drugs. *The Journal of Neuroscience: The Official Journal of the Society for Neuroscience*, *20*(20), RC102.

Cardenas, V. A., Greenstein, D., Fouche, J.-P., Ferrett, H., Cuzen, N., Stein, D. J., & Fein, G. (2013). Not lesser but Greater fractional anisotropy in adolescents with alcohol use disorders. *NeuroImage. Clinical*, *2*, 804–809. https://doi.org/10.1016/j.nicl.2013.06.002

Cassell, M. D., Freedman, L. J., & Shi, C. (1999). The intrinsic organization of the central extended amygdala. *Annals of the New York Academy of Sciences*, *877*, 217–241.

Castanheira, L., Silva, C., Cheniaux, E., & Telles-Correia, D. (2019). Neuroimaging Correlates of Depression—Implications to Clinical Practice. *Frontiers in Psychiatry*, *10*, 703. https://doi.org/10.3389/fpsyt.2019.00703

Centanni, S. W., Bedse, G., Patel, S., & Winder, D. G. (2019). Driving the Downward Spiral: Alcohol-Induced Dysregulation of Extended Amygdala Circuits and Negative Affect. *Alcoholism, Clinical and Experimental Research*. https://doi.org/10.1111/acer.14178

Chambers, T., Escott-Price, V., Legge, S., Baker, E., Singh, K. D., Walters, J. T. R., Caseras, X., & Anney, R. J. L. (2022). Genetic common variants associated with cerebellar volume and their overlap with mental disorders: A study on 33,265 individuals from the UK-Biobank. *Molecular Psychiatry*, 1–9. https://doi.org/10.1038/s41380-022-01443-8

Chang, C. C., Chow, C. C., Tellier, L. C., Vattikuti, S., Purcell, S. M., & Lee, J. J. (2015). Second-generation PLINK: Rising to the challenge of larger and richer datasets. *GigaScience*, *4*(1), s13742-015-0047–0048. https://doi.org/10.1186/s13742-015-0047-8

Charpentier, C. J., Faulkner, P., pool, eva, Ly, V., Tollenaar, M. S., Kluen, L. M., Fransen, A., Yamamori, Y., Lally, N., Mkrtchian, A., Valton, V., Huys, Q. J., Sarigiannidis, I., Morrow, K., Krenz, V., Kalbe, F., Cremer, A., Zerbes, G., Kausche, F. M., … O'Doherty, J. (2020). *How representative are neuroimaging samples? Large-scale evidence for trait anxiety differences between MRI and behaviour-only research participants.* [Preprint]. PsyArXiv. https://doi.org/10.31234/osf.io/cqdne

Chen, Y., Cui, Q., Xie, A., Pang, Y., Sheng, W., Tang, Q., Li, D., Huang, J., He, Z., Wang, Y., & Chen, H. (2020). Abnormal dynamic functional connectivity density in patients with generalized anxiety disorder. *Journal of Affective Disorders*, *261*, 49–57. https://doi.org/10.1016/j.jad.2019.09.084

Chiba, T., Kayahara, T., & Nakano, K. (2001). Efferent projections of infralimbic and prelimbic areas of the medial prefrontal cortex in the Japanese monkey, Macaca fuscata. *Brain Research*, *888*(1), 83–101. https://doi.org/10.1016/S0006-8993(00)03013-4

Ch'ng, S., Fu, J., Brown, R. M., McDougall, S. J., & Lawrence, A. J. (2018). The intersection of stress and reward: BNST modulation of aversive and appetitive states. *Progress in Neuro-Psychopharmacology and Biological Psychiatry*, *87*, 108–125. https://doi.org/10.1016/j.pnpbp.2018.01.005

Choi, D. C., Evanson, N. K., Furay, A. R., Ulrich-Lai, Y. M., Ostrander, M. M., & Herman, J. P. (2008). The anteroventral bed nucleus of the stria terminalis differentially regulates hypothalamic-pituitary-adrenocortical axis responses to acute and chronic stress. *Endocrinology*, *149*(2), 818–826. https://doi.org/10.1210/en.2007-0883

Choi, D. C., Furay, A. R., Evanson, N. K., Ulrich-Lai, Y. M., Nguyen, M. M. N., Ostrander, M. M., & Herman, J. P. (2008). The role of the posterior medial bed nucleus of the stria terminalis in modulating hypothalamic-pituitary-adrenocortical axis responsiveness to acute and chronic stress. *Psychoneuroendocrinology*, *33*(5), 659–669. https://doi.org/10.1016/j.psyneuen.2008.02.006

Choi, J. M., Padmala, S., & Pessoa, L. (2012). Impact of state anxiety on the interaction between threat monitoring and cognition. *NeuroImage*, *59*(2), 1912–1923. https://doi.org/10.1016/j.neuroimage.2011.08.102

Choi, S. W., Mak, T. S.-H., & O'Reilly, P. F. (2020). Tutorial: A guide to performing polygenic risk score analyses. *Nature Protocols*, *15*(9), Article 9. https://doi.org/10.1038/s41596-020-0353-1

Christiansen, K., Dillingham, C. M., Wright, N. F., Saunders, R. C., Vann, S. D., & Aggleton, J. P. (2016). Complementary subicular pathways to the anterior thalamic nuclei and mammillary bodies in the rat and macaque monkey brain. *European Journal of Neuroscience*, *43*(8), 1044–1061. https://doi.org/10.1111/ejn.13208

Chu, S.-H., Parhi, K. K., & Lenglet, C. (2018). Function-specific and Enhanced Brain Structural Connectivity Mapping via Joint Modeling of Diffusion and Functional MRI. *Scientific Reports*, *8*(1), Article 1. https://doi.org/10.1038/s41598-018-23051-9

Chung, W. C. J., Vries, G. J. D., & Swaab, D. F. (2002). Sexual Differentiation of the Bed Nucleus of the Stria Terminalis in Humans May Extend into Adulthood. *Journal of Neuroscience*, *22*(3), 1027–1033. https://doi.org/10.1523/JNEUROSCI.22-03-01027.2002

Claro, F., Segovia, S., Guilamón, A., & Del Abril', A. (1995). Lesions in the medial posterior region of the BST impair sexual behavior in sexually experienced and inexperienced male rats. *Brain Research Bulletin*, *36*(1), 1–10. https://doi.org/10.1016/0361-9230(94)00118-K

Clauss, J. (2019). Extending the neurocircuitry of behavioural inhibition: A role for the bed nucleus of the stria terminalis in risk for anxiety disorders. *General Psychiatry*, *32*(6), e100137. https://doi.org/10.1136/gpsych-2019-100137

Clauss, J. A., Avery, S. N., Benningfield, M. M., & Blackford, J. U. (2019). Social anxiety is associated with BNST response to unpredictability. *Depression and Anxiety*, *36*(8), 666–675. https://doi.org/10.1002/da.22891

Colclough, G. L., Smith, S. M., Nichols, T. E., Winkler, A. M., Sotiropoulos, S. N., Glasser, M. F., Essen, D. C. V., & Woolrich, M. W. (2017, July 26). *The heritability of multi-modal connectivity in human brain activity*. ELife. https://doi.org/10.7554/eLife.20178

Cole, M. W., Ito, T., Cocuzza, C., & Sanchez-Romero, R. (2021). The Functional Relevance of Task-State Functional Connectivity. *Journal of Neuroscience*, *41*(12), 2684–2702. https://doi.org/10.1523/JNEUROSCI.1713-20.2021

Colibazzi, T., Zhu, H., Bansal, R., Schultz, R. T., Wang, Z., & Peterson, B. S. (2007). Latent volumetric structure of the human brain: Exploratory factor analysis and structural equation modeling of gray matter volumes in healthy children and adults. *Human Brain Mapping*, *29*(11), 1302–1312. https://doi.org/10.1002/hbm.20466

Conley, D., Rauscher, E., Dawes, C., Magnusson, P. K. E., & Siegal, M. L. (2013). Heritability and the equal environments assumption: Evidence from multiple samples of misclassified twins. *Behavior Genetics*, *43*(5), 415–426. https://doi.org/10.1007/s10519-013-9602-1

Costello, E. J., Mustillo, S., Erkanli, A., Keeler, G., & Angold, A. (2003). Prevalence and development of psychiatric disorders in childhood and adolescence. *Archives of General Psychiatry*, *60*(8), 837–844. https://doi.org/10.1001/archpsyc.60.8.837

Costumero, V., Bueichekú, E., Adrián-Ventura, J., & Ávila, C. (2020). Opening or closing eyes at rest modulates the functional connectivity of V1 with default and salience networks. *Scientific Reports*, *10*(1), Article 1. https://doi.org/10.1038/s41598-020-66100-y

Cox, S. R., Ritchie, S. J., Tucker-Drob, E. M., Liewald, D. C., Hagenaars, S. P., Davies, G., Wardlaw, J. M., Gale, C. R., Bastin, M. E., & Deary, I. J. (2016). Ageing and brain white matter structure in 3,513 UK Biobank participants. *Nature Communications*, *7*(1), 13629. https://doi.org/10.1038/ncomms13629

Crawford, B., Muhlert, N., MacDonald, G., & Lawrence, A. D. (2020). Brain structure correlates of expected social threat and reward. *Scientific Reports*, *10*(1), Article 1. https://doi.org/10.1038/s41598-020-74334-z

Cremers, H. R., Demenescu, L. R., Aleman, A., Renken, R., van Tol, M.-J., van der Wee, N. J. A., Veltman, D. J., & Roelofs, K. (2010). Neuroticism modulates amygdala-prefrontal connectivity in response to negative emotional facial expressions. *NeuroImage*, *49*(1), 963–970. https://doi.org/10.1016/j.neuroimage.2009.08.023

Crestani, C. C., Alves, F. H. F., Correa, F. M. A., Guimarães, F. S., & Joca, S. R. L. (2010). Acute reversible inactivation of the bed nucleus of stria terminalis induces antidepressant-like effect in the rat forced swimming test. *Behavioral and Brain Functions: BBF*, *6*, 30. https://doi.org/10.1186/1744-9081-6-30

Crestani, C. C., Alves, F. H., Gomes, F. V., Resstel, L. B., Correa, F. M., & Herman, J. P. (2013). Mechanisms in the Bed Nucleus of the Stria Terminalis Involved in Control of Autonomic and Neuroendocrine Functions: A Review. *Current Neuropharmacology*, *11*(2), 141–159. https://doi.org/10.2174/1570159X11311020002

Cullinan, W. E., Herman, J. P., & Watson, S. J. (1993). Ventral subicular interaction with the hypothalamic paraventricular nucleus: Evidence for a relay in the bed nucleus of the stria terminalis. *The Journal of Comparative Neurology*, *332*(1), 1–20. https://doi.org/10.1002/cne.903320102

Dagher, A., Tannenbaum, B., Hayashi, T., Pruessner, J. C., & McBride, D. (2009). An acute psychosocial stress enhances the neural response to smoking cues. *Brain Research*, *1293*, 40–48. https://doi.org/10.1016/j.brainres.2009.07.048

Dale, A. M., Fischl, B., & Sereno, M. I. (1999). Cortical Surface-Based Analysis: I. Segmentation and Surface Reconstruction. *NeuroImage*, *9*(2), 179–194. https://doi.org/10.1006/nimg.1998.0395

Dalton, M. A., McCormick, C., & Maguire, E. A. (2019). Differences in functional connectivity along the anterior-posterior axis of human hippocampal subfields. *NeuroImage*, *192*, 38–51. https://doi.org/10.1016/j.neuroimage.2019.02.066

Davies, M. R., Buckman, J. E. J., Adey, B. N., Armour, C., Bradley, J. R., Curzons, S. C. B., Davies, H. L., Davis, K. A. S., Goldsmith, K. A., Hirsch, C. R., Hotopf, M., Hübel, C., Jones, I. R., Kalsi, G., Krebs, G., Lin, Y., Marsh, I., McAtarsney-Kovacs, M., McIntosh, A. M., … Eley, T. C. (2022). Comparison of symptom-based versus self-reported diagnostic measures of anxiety and depression disorders in the GLAD and COPING cohorts. *Journal of Anxiety Disorders*, *85*, 102491. https://doi.org/10.1016/j.janxdis.2021.102491

Davies, N. M., Holmes, M. V., & Smith, G. D. (2018). Reading Mendelian randomisation studies: A guide, glossary, and checklist for clinicians. *BMJ*, *362*, k601. https://doi.org/10.1136/bmj.k601

Davis, K. A. S., Coleman, J. R. I., Adams, M., Allen, N., Breen, G., Cullen, B., Dickens, C., Fox, E., Graham, N., Holliday, J., Howard, L. M., John, A., Lee, W., McCabe, R., McIntosh, A., Pearsall, R., Smith, D. J., Sudlow, C., Ward, J., … Hotopf, M. (2020). Mental health in UK Biobank – development, implementation and results from an online questionnaire completed by 157 366 participants: A reanalysis. *BJPsych Open*, *6*(2), e18. https://doi.org/10.1192/bjo.2019.100

Davis, M., Walker, D. L., Miles, L., & Grillon, C. (2010). Phasic vs sustained fear in rats and humans: Role of the extended amygdala in fear vs anxiety. *Neuropsychopharmacology: Official Publication of the American College of Neuropsychopharmacology*, *35*(1), 105–135. https://doi.org/10.1038/npp.2009.109

de Guglielmo, G., Kallupi, M., Pomrenze, M. B., Crawford, E., Simpson, S., Schweitzer, P., Koob, G. F., Messing, R. O., & George, O. (2019). Inactivation of a CRF-dependent amygdalofugal pathway reverses addiction-like behaviors in alcohol-dependent rats. *Nature Communications*, *10*(1), 1238. https://doi.org/10.1038/s41467-019-09183-0

De Olmos, J. S., & Ingram, W. R. (1972). The projection field of the stria terminalis in the rat brain. An experimental study. *The Journal of Comparative Neurology*, *146*(3), 303–334. https://doi.org/10.1002/cne.901460303

de Voogd, L. D., Klumpers, F., Fernández, G., & Hermans, E. J. (2017). Intrinsic functional connectivity between amygdala and hippocampus during rest predicts enhanced memory under stress. *Psychoneuroendocrinology*, *75*, 192–202. https://doi.org/10.1016/j.psyneuen.2016.11.002

de Vries, L. P., van Beijsterveldt, T. C. E. M., Maes, H., Colodro-Conde, L., & Bartels, M. (2021). Genetic Influences on the Covariance and Genetic Correlations in a Bivariate Twin Model: An Application to Well-Being. *Behavior Genetics*, *51*(3), 191–203. https://doi.org/10.1007/s10519-021-10046-y

Dean, S. F., Fede, S. J., Diazgranados, N., & Momenan, R. (2020). Addiction neurocircuitry and negative affect: A role for neuroticism in understanding amygdala connectivity and alcohol use disorder. *Neuroscience Letters*, *722*, 134773. https://doi.org/10.1016/j.neulet.2020.134773

Dekkers, I. A., Jansen, P. R., & Lamb, H. J. (2019). Obesity, Brain Volume, and White Matter Microstructure at MRI: A Cross-sectional UK Biobank Study. *Radiology*, *291*(3), 763–771. https://doi.org/10.1148/radiol.2019181012

Dennis, E. L., Disner, S. G., Fani, N., Salminen, L. E., Logue, M., Clarke, E. K., Haswell, C. C., Averill, C. L., Baugh, L. A., Bomyea, J., Bruce, S. E., Cha, J., Choi, K., Davenport, N. D., Densmore, M., du Plessis, S., Forster, G. L., Frijling, J. L., Gonenc, A., … Morey, R. A. (2021). Altered white matter microstructural organization in posttraumatic stress disorder across 3047 adults: Results from the PGC-ENIGMA PTSD consortium. *Molecular Psychiatry*, *26*(8), 4315–4330. https://doi.org/10.1038/s41380-019-0631-x

Despotović, I., Goossens, B., & Philips, W. (2015). MRI Segmentation of the Human Brain: Challenges, Methods, and Applications. *Computational and Mathematical Methods in Medicine*, *2015*, e450341. https://doi.org/10.1155/2015/450341

DeYoung, C. G. (2015). Cybernetic Big Five Theory. *Journal of Research in Personality*, *56*, 33–58. https://doi.org/10.1016/j.jrp.2014.07.004

DeYoung, C. G., & Krueger, R. F. (2020). To Wish Impossible Things: On the Ontological Status of Latent Variables and the Prospects for Theory in Psychology. *Psychological Inquiry*, *31*(4), 289–296. https://doi.org/10.1080/1047840X.2020.1853462

Dickie, E. W., Anticevic, A., Smith, D. E., Coalson, T. S., Manogaran, M., Calarco, N., Viviano, J. D., Glasser, M. F., Essen, D. C. V., & Voineskos, A. N. (2019). ciftify: A framework for surface-based analysis of legacy MR acquisitions. *BioRxiv*, 484428. https://doi.org/10.1101/484428

Dillingham, C. M., Erichsen, J. T., O'Mara, S. M., Aggleton, J. P., & Vann, S. D. (2015). Fornical and nonfornical projections from the rat hippocampal formation to the anterior thalamic nuclei. *Hippocampus*, *25*(9), 977–992. https://doi.org/10.1002/hipo.22421

Ding, S.-L. (2013). Comparative anatomy of the prosubiculum, subiculum, presubiculum, postsubiculum, and parasubiculum in human, monkey, and rodent. *The Journal of Comparative Neurology*, *521*(18), 4145–4162. https://doi.org/10.1002/cne.23416

Ding, S.-L., Yao, Z., Hirokawa, K. E., Nguyen, T. N., Graybuck, L. T., Fong, O., Bohn, P., Ngo, K., Smith, K. A., Koch, C., Phillips, J. W., Lein, E. S., Harris, J. A., Tasic, B., & Zeng, H. (2020). Distinct Transcriptomic Cell Types and Neural Circuits of the Subiculum and Prosubiculum along the Dorsal-Ventral Axis. *Cell Reports*, *31*(7), 107648. https://doi.org/10.1016/j.celrep.2020.107648

Dong, H.-W., Petrovich, G. D., & Swanson, L. W. (2000). Organization of projections from the juxtacapsular nucleus of the BST: A PHAL study in the rat. *Brain Research*, *859*(1), 1–14. https://doi.org/10.1016/S0006-8993(99)02246-5

Dong, H.-W., Petrovich, G. D., & Swanson, L. W. (2001). Topography of projections from amygdala to bed nuclei of the stria terminalis. *Brain Research Reviews*, *38*(1), 192–246. https://doi.org/10.1016/S0165-0173(01)00079-0

Dong, H.-W., & Swanson, L. W. (2003). Projections from the rhomboid nucleus of the bed nuclei of the stria terminalis: Implications for cerebral hemisphere regulation of ingestive behaviors. *Journal of Comparative Neurology*, *463*(4), 434–472. https://doi.org/10.1002/cne.10758

Dong, H.-W., & Swanson, L. W. (2004). Organization of axonal projections from the anterolateral area of the bed nuclei of the stria terminalis. *Journal of Comparative Neurology*, *468*(2), 277–298. https://doi.org/10.1002/cne.10949

Dong, H.-W., & Swanson, L. W. (2006). Projections from bed nuclei of the stria terminalis, dorsomedial nucleus: Implications for cerebral hemisphere integration of neuroendocrine, autonomic, and drinking responses. *The Journal of Comparative Neurology*, *494*(1), 75–107. https://doi.org/10.1002/cne.20790

Eickhoff, S. B., Stephan, K. E., Mohlberg, H., Grefkes, C., Fink, G. R., Amunts, K., & Zilles, K. (2005). A new SPM toolbox for combining probabilistic cytoarchitectonic maps and functional imaging data. *NeuroImage*, *25*(4), 1325–1335. https://doi.org/10.1016/j.neuroimage.2004.12.034

Eliot, L., Ahmed, A., Khan, H., & Patel, J. (2021). Dump the "dimorphism": Comprehensive synthesis of human brain studies reveals few male-female differences beyond size. *Neuroscience & Biobehavioral Reviews*, *125*, 667–697. https://doi.org/10.1016/j.neubiorev.2021.02.026

Elliott, L. T., Sharp, K., Alfaro-Almagro, F., Shi, S., Miller, K. L., Douaud, G., Marchini, J., & Smith, S. M. (2018). Genome-wide association studies of brain imaging phenotypes in UK Biobank. *Nature*, *562*(7726), 210–216. https://doi.org/10.1038/s41586-018-0571-7

Elliott, M. L., Knodt, A. R., Cooke, M., Kim, M. J., Melzer, T. R., Keenan, R., Ireland, D., Ramrakha, S., Poulton, R., Caspi, A., Moffitt, T. E., & Hariri, A. R. (2019). General functional connectivity: Shared features of resting-state and task fMRI drive reliable and heritable individual differences in functional brain networks. *NeuroImage*, *189*, 516–532. https://doi.org/10.1016/j.neuroimage.2019.01.068

Elliott, M. L., Knodt, A. R., & Hariri, A. R. (2021). Striving toward translation: Strategies for reliable fMRI measurement. *Trends in Cognitive Sciences*, *25*(9), 776–787. https://doi.org/10.1016/j.tics.2021.05.008

Elliott, M. L., Knodt, A. R., Ireland, D., Morris, M. L., Poulton, R., Ramrakha, S., Sison, M. L., Moffitt, T. E., Caspi, A., & Hariri, A. R. (2020). What Is the Test-Retest Reliability of Common Task-Functional MRI Measures? New Empirical Evidence and a Meta-Analysis: *Psychological Science*. https://doi.org/10.1177/0956797620916786

Enoch, M.-A., Rosser, A. A., Zhou, Z., Mash, D. C., Yuan, Q., & Goldman, D. (2014). Expression of glutamatergic genes in healthy humans across 16 brain regions; altered expression in the hippocampus after chronic exposure to alcohol or cocaine. *Genes, Brain and Behavior*, *13*(8), 758–768. https://doi.org/10.1111/gbb.12179

Erb, S., & Stewart, J. (1999). A Role for the Bed Nucleus of the Stria Terminalis, But Not the Amygdala, in the Effects of Corticotropin-Releasing Factor on Stress-Induced Reinstatement of Cocaine Seeking. *Journal of Neuroscience*, *19*(20), RC35–RC35. https://doi.org/10.1523/JNEUROSCI.19-20-j0006.1999

Erikson, C. M., Wei, G., & Walker, B. M. (2018). Maladaptive behavioral regulation in alcohol dependence: Role of kappa-opioid receptors in the bed nucleus of the stria terminalis. *Neuropharmacology*, *140*, 162–173. https://doi.org/10.1016/j.neuropharm.2018.07.034

Escrichs, A., Biarnes, C., Garre-Olmo, J., Fernández-Real, J. M., Ramos, R., Pamplona, R., Brugada, R., Serena, J., Ramió-Torrentà, L., Coll-De-Tuero, G., Gallart, L., Barretina, J., Vilanova, J. C., Mayneris-Perxachs, J., Essig, M., Figley, C. R., Pedraza, S., Puig, J., & Deco, G. (2021). Whole-Brain Dynamics in Aging: Disruptions in Functional Connectivity and the Role of the Rich Club. *Cerebral Cortex*, *31*(5), 2466–2481. https://doi.org/10.1093/cercor/bhaa367

Etkin, A. (2018). Addressing the Causality Gap in Human Psychiatric Neuroscience. *JAMA Psychiatry*, *75*(1), 3–4. https://doi.org/10.1001/jamapsychiatry.2017.3610

Evans, S. (2017). What Has Replication Ever Done for Us? Insights from Neuroimaging of Speech Perception. *Frontiers in Human Neuroscience*, *11*, 41. https://doi.org/10.3389/fnhum.2017.00041

Fanselow, M. S. (1994). Neural organization of the defensive behavior system responsible for fear. *Psychonomic Bulletin & Review*, *1*(4), 429–438. https://doi.org/10.3758/BF03210947

Farahani, F. V., Karwowski, W., & Lighthall, N. R. (2019). Application of Graph Theory for Identifying Connectivity Patterns in Human Brain Networks: A Systematic Review. *Frontiers in Neuroscience*, *13*. https://www.frontiersin.org/article/10.3389/fnins.2019.00585

Faul, F., Erdfelder, E., Buchner, A., & Lang, A.-G. (2009). Statistical power analyses using G*Power 3.1: Tests for correlation and regression analyses. *Behavior Research Methods*, *41*(4), 1149–1160. https://doi.org/10.3758/BRM.41.4.1149

Feltenstein, M. W., & See, R. E. (2008). The neurocircuitry of addiction: An overview. *British Journal of Pharmacology*, *154*(2), 261–274. https://doi.org/10.1038/bjp.2008.51

Feola, B., Melancon, S. N. T., Clauss, J. A., Noall, M. P., Mgboh, A., Flook, E. A., Benningfield, M. M., & Blackford, J. U. (2021). Bed nucleus of the stria terminalis and amygdala responses to unpredictable threat in children. *Developmental Psychobiology*, *63*(8), e22206. https://doi.org/10.1002/dev.22206

Figel, B., Brinkmann, L., Buff, C., Heitmann, C. Y., Hofmann, D., Bruchmann, M., Becker, M. P. I., Herrmann, M. J., & Straube, T. (2019). Phasic amygdala and BNST activation during the anticipation of temporally unpredictable social observation in social anxiety disorder patients. *NeuroImage. Clinical*, *22*, 101735. https://doi.org/10.1016/j.nicl.2019.101735

Finn, E. S. (2021). Is it time to put rest to rest? *Trends in Cognitive Sciences*, *25*(12), 1021–1032. https://doi.org/10.1016/j.tics.2021.09.005

Finn, E. S., Scheinost, D., Finn, D. M., Shen, X., Papademetris, X., & Constable, R. T. (2017). Can brain state be manipulated to emphasize individual differences in functional connectivity? *NeuroImage*, *160*, 140–151. https://doi.org/10.1016/j.neuroimage.2017.03.064

Fisher, R. A. (1915). Frequency Distribution of the Values of the Correlation Coefficient in Samples from an Indefinitely Large Population. *Biometrika*, *10*(4), 507–521. JSTOR. https://doi.org/10.2307/2331838

Fitzgerald, P. B., Segrave, R., Richardson, K. E., Knox, L. A., Herring, S., Daskalakis, Z. J., & Bittar, R. G. (2018). A pilot study of bed nucleus of the stria terminalis deep brain stimulation in treatment-resistant depression. *Brain Stimulation*, *11*(4), 921–928. https://doi.org/10.1016/j.brs.2018.04.013

Flook, E. A., Feola, B., Avery, S. N., Winder, D. G., Woodward, N. D., Heckers, S., & Blackford, J. U. (2020). BNST-insula structural connectivity in humans. *NeuroImage*, *210*, 116555. https://doi.org/10.1016/j.neuroimage.2020.116555

Flook, E. A., Feola, B., Benningfield, M. M., Silveri, M. M., Winder, D. G., & Blackford, J. U. (2021). Alterations in connectivity of the bed nucleus of the stria terminalis during early abstinence in individuals with alcohol use disorder. *Alcoholism: Clinical and Experimental Research*, *45*(5), 1028–1038. https://doi.org/10.1111/acer.14596

Folloni, D., Sallet, J., Khrapitchev, A. A., Sibson, N., Verhagen, L., & Mars, R. B. (2019). Dichotomous organization of amygdala/temporal-prefrontal bundles in both humans and monkeys. *ELife*, *8*, e47175. https://doi.org/10.7554/eLife.47175

Fox, A. S., & Kalin, N. H. (2014). A Translational Neuroscience Approach to Understanding the Development of Social Anxiety Disorder and its Pathophysiology. *The American Journal of Psychiatry*, *171*(11), 1162–1173. https://doi.org/10.1176/appi.ajp.2014.14040449

Fox, A. S., Oler, J. A., Birn, R. M., Shackman, A. J., Alexander, A. L., & Kalin, N. H. (2018). Functional connectivity within the primate extended amygdala is heritable and associated with early-life anxious temperament. *Journal of Neuroscience*, 0102–0118. https://doi.org/10.1523/JNEUROSCI.0102-18.2018

Fox, A. S., Oler, J. A., Shackman, A. J., Shelton, S. E., Raveendran, M., McKay, D. R., Converse, A. K., Alexander, A., Davidson, R. J., Blangero, J., Rogers, J., & Kalin, N. H. (2015). Intergenerational neural mediators of early-life anxious temperament. *Proceedings of the National Academy of Sciences*, *112*(29), 9118–9122. https://doi.org/10.1073/pnas.1508593112

Fox, A. S., Oler, J. A., Tromp, D. P. M., Fudge, J. L., & Kalin, N. H. (2015). Extending the amygdala in theories of threat processing. *Trends in Neurosciences*, *38*(5), 319–329. https://doi.org/10.1016/j.tins.2015.03.002

Fox, A. S., & Shackman, A. J. (2019). The central extended amygdala in fear and anxiety: Closing the gap between mechanistic and neuroimaging research. *Neuroscience Letters*, *693*, 58–67. https://doi.org/10.1016/j.neulet.2017.11.056

Fox, A. S., Shelton, S. E., Oakes, T. R., Converse, A. K., Davidson, R. J., & Kalin, N. H. (2010). Orbitofrontal Cortex Lesions Alter Anxiety-Related Activity in the Primate Bed Nucleus of Stria Terminalis. *Journal of Neuroscience*, *30*(20), 7023–7027. https://doi.org/10.1523/JNEUROSCI.5952-09.2010

Fox, A. S., Shelton, S. E., Oakes, T. R., Davidson, R. J., & Kalin, N. H. (2008). Trait-like brain activity during adolescence predicts anxious temperament in primates. *PloS One*, *3*(7), e2570. https://doi.org/10.1371/journal.pone.0002570

Fox, H. C., Seo, D., Tuit, K., Hansen, J., Kimmerling, A., Morgan, P. T., & Sinha, R. (2012). Guanfacine effects on stress, drug craving and prefrontal activation in cocaine dependent individuals: Preliminary findings. *Journal of Psychopharmacology*, *26*(7), 958–972. https://doi.org/10.1177/0269881111430746

Frazer, K. A., Ballinger, D. G., Cox, D. R., Hinds, D. A., Stuve, L. L., Gibbs, R. A., Belmont, J. W., Boudreau, A., Hardenbol, P., Leal, S. M., Pasternak, S., Wheeler, D. A., Willis, T. D., Yu, F., Yang, H., Zeng, C., Gao, Y., Hu, H., Hu, W., … The SNP Consortium. (2007). A second generation human haplotype map of over 3.1 million SNPs. *Nature*, *449*(7164), Article 7164. https://doi.org/10.1038/nature06258

Friedman, D. P., Aggleton, J. P., & Saunders, R. C. (2002). Comparison of hippocampal, amygdala, and perirhinal projections to the nucleus accumbens: Combined anterograde and retrograde tracing study in the Macaque brain. *The Journal of Comparative Neurology*, *450*(4), 345–365. https://doi.org/10.1002/cne.10336

Friston, K. J. (2011). Functional and Effective Connectivity: A Review. *Brain Connectivity*, *1*(1), 13–36. https://doi.org/10.1089/brain.2011.0008

Frontiers | A comparison of FreeSurfer-generated data with and without manual intervention | Neuroscience. (n.d.). Retrieved 22 March 2022, from https://www.frontiersin.org/articles/10.3389/fnins.2015.00379/full

Fry, A., Littlejohns, T. J., Sudlow, C., Doherty, N., Adamska, L., Sprosen, T., Collins, R., & Allen, N. E. (2017). Comparison of Sociodemographic and Health-Related Characteristics of UK Biobank Participants With Those of the General Population. *American Journal of Epidemiology*, *186*(9), 1026–1034. https://doi.org/10.1093/aje/kwx246

Fudge, J. L., Kelly, E. A., Pal, R., Bedont, J. L., Park, L., & Ho, B. (2017). Beyond the Classic VTA: Extended Amygdala Projections to DA-Striatal Paths in the Primate. *Neuropsychopharmacology*, *42*(8), 1563–1576. https://doi.org/10.1038/npp.2017.38

Gaspar, P., Berger, B., Alvarez, C., Vigny, A., & Henry, J. P. (1985). Catecholaminergic innervation of the septal area in man: Immunocytochemical study using TH and DBH antibodies. *The Journal of Comparative Neurology*, *241*(1), 12–33. https://doi.org/10.1002/cne.902410103

Gaspar, P., Berger, B., Lesur, A., Borsotti, J. P., & Febvret, A. (1987). Somatostatin 28 and neuropeptide Y innervation in the septal area and related cortical and subcortical structures of the human brain. Distribution, relationships and evidence for differential coexistence. *Neuroscience*, *22*(1), 49–73. https://doi.org/10.1016/0306-4522(87)90197-7

Giardino, W. J., Eban-Rothschild, A., Christoffel, D. J., Li, S.-B., Malenka, R. C., & Lecea, L. de. (2018). Parallel circuits from the bed nuclei of stria terminalis to the lateral hypothalamus drive opposing emotional states. *Nature Neuroscience*, *21*(8), 1084. https://doi.org/10.1038/s41593-018-0198-x

Giardino, W. J., & Pomrenze, M. B. (2021). Extended Amygdala Neuropeptide Circuitry of Emotional Arousal: Waking Up on the Wrong Side of the Bed Nuclei of Stria Terminalis. *Frontiers in Behavioral Neuroscience*, *15*, 6. https://doi.org/10.3389/fnbeh.2021.613025

Gilbert, K. M., Gati, J. S., Barker, K., Everling, S., & Menon, R. S. (2016). Optimized parallel transmit and receive radiofrequency coil for ultrahigh-field MRI of monkeys. *NeuroImage*, *125*, 153–161. https://doi.org/10.1016/j.neuroimage.2015.10.048

Gilpin, N. W., Herman, M. A., & Roberto, M. (2015). The central amygdala as an integrative hub for anxiety and alcohol use disorders. *Biological Psychiatry*, *77*(10), 859–869. https://doi.org/10.1016/j.biopsych.2014.09.008

Glangetas, C., & Georges, F. (2016). Pharmacology of the Bed Nucleus of the Stria Terminalis. *Current Pharmacology Reports*, *2*(6), 262–270. https://doi.org/10.1007/s40495-016-0077-7

Glasser, M. F., Smith, S. M., Marcus, D. S., Andersson, J. L. R., Auerbach, E. J., Behrens, T. E. J., Coalson, T. S., Harms, M. P., Jenkinson, M., Moeller, S., Robinson, E. C., Sotiropoulos, S. N., Xu, J., Yacoub, E., Ugurbil, K., & Van Essen, D. C. (2016). The Human Connectome Project's neuroimaging approach. *Nature Neuroscience*, *19*(9), Article 9. https://doi.org/10.1038/nn.4361

Glasser, M. F., Sotiropoulos, S. N., Wilson, J. A., Coalson, T. S., Fischl, B., Andersson, J. L., Xu, J., Jbabdi, S., Webster, M., Polimeni, J. R., Van Essen, D. C., & Jenkinson, M. (2013). The minimal preprocessing pipelines for the Human Connectome Project. *NeuroImage*, *80*, 105–124. https://doi.org/10.1016/j.neuroimage.2013.04.127

Goode, T. D., Acca, G. M., & Maren, S. (2020). Threat imminence dictates the role of the bed nucleus of the stria terminalis in contextual fear. *Neurobiology of Learning and Memory*, *167*, 107116. https://doi.org/10.1016/j.nlm.2019.107116

Goode, T. D., & Maren, S. (2017). Role of the bed nucleus of the stria terminalis in aversive learning and memory. *Learning & Memory*, *24*(9), 480–491. https://doi.org/10.1101/lm.044206.116

Goode, T. D., Ressler, R. L., Acca, G. M., Miles, O. W., & Maren, S. (2019). Bed nucleus of the stria terminalis regulates fear to unpredictable threat signals. *ELife*, *8*. https://doi.org/10.7554/eLife.46525

Goossen, B., van der Starre, J., & van der Heiden, C. (2019). A review of neuroimaging studies in generalized anxiety disorder: "So where do we stand?" *Journal of Neural Transmission*, *126*(9), 1203–1216. https://doi.org/10.1007/s00702-019-02024-w

Gordon, E. M., Laumann, T. O., Gilmore, A. W., Newbold, D. J., Greene, D. J., Berg, J. J., Ortega, M., Hoyt-Drazen, C., Gratton, C., Sun, H., Hampton, J. M., Coalson, R. S., Nguyen, A. L., McDermott, K. B., Shimony, J. S., Snyder, A. Z., Schlaggar, B. L., Petersen, S. E., Nelson, S. M., & Dosenbach, N. U. F. (2017). Precision Functional Mapping of Individual Human Brains. *Neuron*, *95*(4), 791-807.e7. https://doi.org/10.1016/j.neuron.2017.07.011

Gorka, A. X., Torrisi, S., Shackman, A. J., Grillon, C., & Ernst, M. (2018). Intrinsic Functional Connectivity of the Central Nucleus of the Amygdala and Bed Nucleus of the Stria Terminalis. *NeuroImage*, *168*, 392–402. https://doi.org/10.1016/j.neuroimage.2017.03.007

Gracia-Tabuenca, Z., Moreno, M. B., Barrios, F. A., & Alcauter, S. (2021). Development of the brain functional connectome follows puberty-dependent nonlinear trajectories. *NeuroImage*, *229*, 117769. https://doi.org/10.1016/j.neuroimage.2021.117769

Gray, J. C., Thompson, M., Bachman, C., Owens, M. M., Murphy, M., & Palmer, R. (2020). Associations of cigarette smoking with gray and white matter in the UK Biobank. *Neuropsychopharmacology*, *45*(7), 1215–1222. https://doi.org/10.1038/s41386-020-0630-2

Greene, A. S., Gao, S., Scheinost, D., & Constable, R. T. (2018). Task-induced brain state manipulation improves prediction of individual traits. *Nature Communications*, *9*, 2807. https://doi.org/10.1038/s41467-018-04920-3

Griffanti, L., Salimi-Khorshidi, G., Beckmann, C. F., Auerbach, E. J., Douaud, G., Sexton, C. E., Zsoldos, E., Ebmeier, K. P., Filippini, N., Mackay, C. E., Moeller, S., Xu, J., Yacoub, E., Baselli, G., Ugurbil, K., Miller, K. L., & Smith, S. M. (2014). ICA-based artefact removal and accelerated fMRI acquisition for improved resting state network imaging. *NeuroImage*, *95*, 232–247. https://doi.org/10.1016/j.neuroimage.2014.03.034

Grillon, C., Ameli, R., Foot, M., & Davis, M. (1993). Fear-potentiated startle: Relationship to the level of state/trait anxiety in healthy subjects. *Biological Psychiatry*, *33*(8), 566–574. https://doi.org/10.1016/0006-3223(93)90094-T

Groenewegen, H. J., Vermeulen-Van der Zee, E., te Kortschot, A., & Witter, M. P. (1987). Organization of the projections from the subiculum to the ventral striatum in the rat. A study using anterograde transport of Phaseolus vulgaris leucoagglutinin. *Neuroscience*, *23*(1), 103–120. https://doi.org/10.1016/0306-4522(87)90275-2

Grupe, D. W., Oathes, D. J., & Nitschke, J. B. (2013). Dissecting the anticipation of aversion reveals dissociable neural networks. *Cerebral Cortex (New York, N.Y.: 1991)*, *23*(8), 1874–1883. https://doi.org/10.1093/cercor/bhs175

Gschwind, M., Pourtois, G., Schwartz, S., Van De Ville, D., & Vuilleumier, P. (2012). White-Matter Connectivity between Face-Responsive Regions in the Human Brain. *Cerebral Cortex*, *22*(7), 1564–1576. https://doi.org/10.1093/cercor/bhr226

Gungor, N. Z., & Paré, D. (2016). Functional Heterogeneity in the Bed Nucleus of the Stria Terminalis. *The Journal of Neuroscience*, *36*(31), 8038–8049. https://doi.org/10.1523/JNEUROSCI.0856-16.2016

Guo, L., & Wang, J. (2018). rSNPBase 3.0: An updated database of SNP-related regulatory elements, element-gene pairs and SNP-based gene regulatory networks. *Nucleic Acids Research*, *46*(D1), D1111–D1116. https://doi.org/10.1093/nar/gkx1101

Gururajan, A., Reif, A., Cryan, J. F., & Slattery, D. A. (2019). The future of rodent models in depression research. *Nature Reviews Neuroscience*, *20*(11), Article 11. https://doi.org/10.1038/s41583-019-0221-6

Gustavson, D. E., Hatton, S. N., Elman, J. A., Panizzon, M. S., Franz, C. E., Hagler, D. J., Fennema-Notestine, C., Eyler, L. T., McEvoy, L. K., Neale, M. C., Gillespie, N., Dale, A. M., Lyons, M. J., & Kremen, W. S. (2019). Predominantly Global Genetic Influences on Individual White Matter Tract Microstructure. *NeuroImage*, *184*, 871–880. https://doi.org/10.1016/j.neuroimage.2018.10.016

Hall, C. N., Howarth, C., Kurth-Nelson, Z., & Mishra, A. (2016). Interpreting BOLD: Towards a dialogue between cognitive and cellular neuroscience. *Philosophical Transactions of the Royal Society B: Biological Sciences*, *371*(1705), 20150348. https://doi.org/10.1098/rstb.2015.0348

Hammack, S. E., Braas, K. M., & May, V. (2021). Chapter 26 - Chemoarchitecture of the bed nucleus of the stria terminalis: Neurophenotypic diversity and function. In D. F. Swaab, F. Kreier, P. J. Lucassen, A. Salehi, & R. M. Buijs (Eds.), *Handbook of Clinical Neurology* (Vol. 179, pp. 385–402). Elsevier. https://doi.org/10.1016/B978-0-12-819975-6.00025-X

Hammack, S. E., Todd, T. P., Kocho-Schellenberg, M., & Bouton, M. E. (2015). Role of the bed nucleus of the stria terminalis in the acquisition of contextual fear at long or short context-shock intervals. *Behavioral Neuroscience*, *129*(5), 673–678. https://doi.org/10.1037/bne0000088

Han, Y., & Adolphs, R. (2020). Estimating the heritability of psychological measures in the Human Connectome Project dataset. *PLOS ONE*, *15*(7), e0235860. https://doi.org/10.1371/journal.pone.0235860

Harrewijn, A., Cardinale, E. M., Groenewold, N. A., Bas-Hoogendam, J. M., Aghajani, M., Hilbert, K., Cardoner, N., Porta-Casteràs, D., Gosnell, S., Salas, R., Jackowski, A. P., Pan, P. M., Salum, G. A., Blair, K. S., Blair, J. R., Hammoud, M. Z., Milad, M. R., Burkhouse, K. L., Phan, K. L., … Pine, D. S. (2021). Cortical and subcortical brain structure in generalized anxiety disorder: Findings from 28 research sites in the ENIGMA-Anxiety Working Group. *Translational Psychiatry*, *11*, 502. https://doi.org/10.1038/s41398-021-01622-1

Harris, N. A., & Winder, D. G. (2018). Synaptic Plasticity in the Bed Nucleus of the Stria Terminalis: Underlying Mechanisms and Potential Ramifications for Reinstatement of Drug- and Alcohol-Seeking Behaviors. *ACS Chemical Neuroscience*, *9*(9), 2173–2187. https://doi.org/10.1021/acschemneuro.8b00169

Haslbeck, J. M. B., Ryan, O., Robinaugh, D. J., Waldorp, L. J., & Borsboom, D. (2021). Modeling psychopathology: From data models to formal theories. *Psychological Methods*. https://doi.org/10.1037/met0000303

Haun, H. L., Griffin, W. C., Lopez, M. F., & Becker, H. C. (2020). Kappa opioid receptors in the bed nucleus of the stria terminalis regulate binge-like alcohol consumption in male and female mice. *Neuropharmacology*, *167*, 107984. https://doi.org/10.1016/j.neuropharm.2020.107984

Hengartner, M. P., Ajdacic-Gross, V., Wyss, C., Angst, J., & Rössler, W. (2016). Relationship between personality and psychopathology in a longitudinal community study: A test of the predisposition model. *Psychological Medicine*, *46*(8), 1693–1705. https://doi.org/10.1017/S0033291716000210

Herman, J. P. (2012). Neural Pathways of Stress Integration. *Alcohol Research : Current Reviews*, *34*(4), 441–447.

Herman, J. P., Figueiredo, H., Mueller, N. K., Ulrich-Lai, Y., Ostrander, M. M., Choi, D. C., & Cullinan, W. E. (2003). Central mechanisms of stress integration: Hierarchical circuitry controlling hypothalamo–pituitary–adrenocortical responsiveness. *Frontiers in Neuroendocrinology*, *24*(3), 151–180. https://doi.org/10.1016/j.yfrne.2003.07.001

Herman, J. P., Nawreen, N., Smail, M. A., & Cotella, E. M. (2020). Brain mechanisms of HPA axis regulation: Neurocircuitry and feedback in context Richard Kvetnansky lecture. *Stress*, *23*(6), 617–632. https://doi.org/10.1080/10253890.2020.1859475

Herrmann, M. J., Boehme, S., Becker, M. P. I., Tupak, S. V., Guhn, A., Schmidt, B., Brinkmann, L., & Straube, T. (2016). Phasic and sustained brain responses in the amygdala and the bed nucleus of the stria terminalis during threat anticipation. *Human Brain Mapping*, *37*(3), 1091–1102. https://doi.org/10.1002/hbm.23088

Hidalgo-Lopez, E., Mueller, K., Harris, T., Aichhorn, M., Sacher, J., & Pletzer, B. (2020). Human menstrual cycle variation in subcortical functional brain connectivity: A multimodal analysis approach. *Brain Structure & Function*, *225*(2), 591–605. https://doi.org/10.1007/s00429-019-02019-z

Hilger, K., & Markett, S. (2021). Personality network neuroscience: Promises and challenges on the way toward a unifying framework of individual variability. *Network Neuroscience*, *5*(3), 631–645. https://doi.org/10.1162/netn_a_00198

Hofmann, D., & Straube, T. (2019). Resting-state fMRI effective connectivity between the bed nucleus of the stria terminalis and amygdala nuclei. *Human Brain Mapping*, *40*(9), 2723–2735. https://doi.org/10.1002/hbm.24555

Hofmann, D., & Straube, T. (2020). Effective connectivity between bed nucleus of the stria terminalis and amygdala: Reproducibility and relation to anxiety. *Human Brain Mapping*, *42*(3), 824–836. https://doi.org/10.1002/hbm.25265

Hong, E. P., & Park, J. W. (2012). Sample Size and Statistical Power Calculation in Genetic Association Studies. *Genomics & Informatics*, *10*(2), 117–122. https://doi.org/10.5808/GI.2012.10.2.117

Howell, G. A., Perez-Clausell, J., & Frederickson, C. J. (1991). Zinc containing projections to the bed nucleus of the stria terminalis. *Brain Research*, *562*(2), 181–189. https://doi.org/10.1016/0006-8993(91)90620-B

Hua, K., Zhang, J., Wakana, S., Jiang, H., Li, X., Reich, D. S., Calabresi, P. A., Pekar, J. J., van Zijl, P. C. M., & Mori, S. (2008). Tract Probability Maps in Stereotaxic Spaces: Analyses of White Matter Anatomy and Tract-Specific Quantification. *NeuroImage*, *39*(1), 336–347. https://doi.org/10.1016/j.neuroimage.2007.07.053

Huber, E., Donnelly, P. M., Rokem, A., & Yeatman, J. D. (2018). Rapid and widespread white matter plasticity during an intensive reading intervention. *Nature Communications*, *9*(1), Article 1. https://doi.org/10.1038/s41467-018-04627-5

Hudson, M., Seppälä, K., Putkinen, V., Sun, L., Glerean, E., Karjalainen, T., Karlsson, H. K., Hirvonen, J., & Nummenmaa, L. (2020). Dissociable neural systems for unconditioned acute and sustained fear. *NeuroImage*, *216*, 116522. https://doi.org/10.1016/j.neuroimage.2020.116522

Hulsman, A. M., Terburg, D., Roelofs, K., & Klumpers, F. (2021). Chapter 28—Roles of the bed nucleus of the stria terminalis and amygdala in fear reactions. In D. F. Swaab, F. Kreier, P. J. Lucassen, A. Salehi, & R. M. Buijs (Eds.), *Handbook of Clinical Neurology* (Vol. 179, pp. 419–432). Elsevier. https://doi.org/10.1016/B978-0-12-819975-6.00027-3

Hur, J., Kaplan, C. M., Smith, J. F., Bradford, D. E., Fox, A. S., Curtin, J. J., & Shackman, A. J. (2018). Acute alcohol administration dampens central extended amygdala reactivity. *Scientific Reports*, *8*. https://doi.org/10.1038/s41598-018-34987-3

Hur, J., Smith, J. F., DeYoung, K. A., Anderson, A. S., Kuang, J., Kim, H. C., Tillman, R. M., Kuhn, M., Fox, A. S., & Shackman, A. J. (2020). Anxiety and the neurobiology of uncertain threat anticipation. *BioRxiv*, 2020.02.25.964734. https://doi.org/10.1101/2020.02.25.964734

Hur, J., Stockbridge, M. D., Fox, A. S., & Shackman, A. J. (2019). Dispositional negativity, cognition, and anxiety disorders: An integrative translational neuroscience framework. *Progress in Brain Research*, *247*, 375–436. https://doi.org/10.1016/bs.pbr.2019.03.012

Hutchison, J. L., Hubbard, N. A., Brigante, R. M., Turner, M., Sandoval, T. I., Hillis, G. A. J., Weaver, T., & Rypma, B. (2014). The efficiency of fMRI region of interest analysis methods for detecting group differences. *Journal of Neuroscience Methods*, *226*, 57–65. https://doi.org/10.1016/j.jneumeth.2014.01.012

Hutchison, R. M., Womelsdorf, T., Allen, E. A., Bandettini, P. A., Calhoun, V. D., Corbetta, M., Della Penna, S., Duyn, J. H., Glover, G. H., Gonzalez-Castillo, J., Handwerker, D. A., Keilholz, S., Kiviniemi, V., Leopold, D. A., de Pasquale, F., Sporns, O., Walter, M., & Chang, C. (2013). Dynamic functional connectivity: Promise, issues, and interpretations. *NeuroImage*, *80*, 360–378. https://doi.org/10.1016/j.neuroimage.2013.05.079

Hyman, S. E. (2018). The daunting polygenicity of mental illness: Making a new map. *Philosophical Transactions of the Royal Society of London. Series B, Biological Sciences*, *373*(1742). https://doi.org/10.1098/rstb.2017.0031

Jacobson, L., & Sapolsky, R. (1991). The Role of the Hippocampus in Feedback Regulation of the Hypothalamic-Pituitary-Adrenocortical Axis*. *Endocrine Reviews*, *12*(2), 118–134. https://doi.org/10.1210/edrv-12-2-118

Jadzic, D., Bassareo, V., Carta, A. R., & Carboni, E. (2021). Nicotine, cocaine, amphetamine, morphine, and ethanol increase norepinephrine output in the bed nucleus of stria terminalis of freely moving rats. *Addiction Biology*, *26*(1), e12864. https://doi.org/10.1111/adb.12864

Janak, P. H., & Tye, K. M. (2015). From circuits to behaviour in the amygdala. *Nature*, *517*(7534), 284–292. https://doi.org/10.1038/nature14188

Jansen, A. G., Mous, S. E., White, T., Posthuma, D., & Polderman, T. J. C. (2015). What Twin Studies Tell Us About the Heritability of Brain Development, Morphology, and Function: A Review. *Neuropsychology Review*, *25*(1), 27–46. https://doi.org/10.1007/s11065-015-9278-9

Jayawickreme, E., Fleeson, W., Beck, E. D., Baumert, A., & Adler, J. M. (2021). Personality Dynamics. *Personality Science*, *2*, 1–18. https://doi.org/10.5964/ps.6179

Jbabdi, S., & Behrens, T. E. (2013). Long-range connectomics. *Annals of the New York Academy of Sciences*, *1305*(1), 83–93. https://doi.org/10.1111/nyas.12271

Jelenkovic, A., Sund, R., Hur, Y.-M., Yokoyama, Y., Hjelmborg, J. v B., Möller, S., Honda, C., Magnusson, P. K. E., Pedersen, N. L., Ooki, S., Aaltonen, S., Stazi, M. A., Fagnani, C., D'Ippolito, C., Freitas, D. L., Maia, J. A., Ji, F., Ning, F., Pang, Z., … Silventoinen, K. (2016). Genetic and environmental influences on height from infancy to early adulthood: An individual-based pooled analysis of 45 twin cohorts. *Scientific Reports*, *6*(1), 28496. https://doi.org/10.1038/srep28496

Jenkinson, M., Bannister, P., Brady, M., & Smith, S. (2002). Improved optimization for the robust and accurate linear registration and motion correction of brain images. *NeuroImage*, *17*(2), 825–841.

Jenkinson, M., Beckmann, C. F., Behrens, T. E. J., Woolrich, M. W., & Smith, S. M. (2012). FSL. *NeuroImage*, *62*(2), 782–790. https://doi.org/10.1016/j.neuroimage.2011.09.015

Jiang, R., Zuo, N., Ford, J. M., Qi, S., Zhi, D., Zhuo, C., Xu, Y., Fu, Z., Bustillo, J., Turner, J. A., Calhoun, V. D., & Sui, J. (2020). Task-induced brain connectivity promotes the detection of individual differences in brain-behavior relationships. *NeuroImage*, *207*, 116370. https://doi.org/10.1016/j.neuroimage.2019.116370

Jobes, M. L., Ghitza, U. E., Epstein, D. H., Phillips, K. A., Heishman, S. J., & Preston, K. L. (2011). Clonidine blocks stress-induced craving in cocaine users. *Psychopharmacology*, *218*(1), 83–88. https://doi.org/10.1007/s00213-011-2230-7

Johnson, A. D., McQuoid, D. R., Steffens, D. C., Payne, M. E., Beyer, J. L., & Taylor, W. D. (2017). Effects of stressful life events on cerebral white matter hyperintensity progression. *International Journal of Geriatric Psychiatry*, *32*(12), e10–e17. https://doi.org/10.1002/gps.4644

Johnston, J. B. (1923). Further contributions to the study of the evolution of the forebrain. *Journal of Comparative Neurology*, *35*(5), 337–481. https://doi.org/10.1002/cne.900350502

Jolliffe, I. T., & Cadima, J. (2016). Principal component analysis: A review and recent developments. *Philosophical Transactions of the Royal Society A: Mathematical, Physical and Engineering Sciences*, *374*(2065), 20150202. https://doi.org/10.1098/rsta.2015.0202

Jones, D. K., Knösche, T. R., & Turner, R. (2013). White matter integrity, fiber count, and other fallacies: The do's and don'ts of diffusion MRI. *NeuroImage*, *73*, 239–254. https://doi.org/10.1016/j.neuroimage.2012.06.081

Kalin, N. H., Shelton, S. E., Fox, A. S., Oakes, T. R., & Davidson, R. J. (2005). Brain Regions Associated with the Expression and Contextual Regulation of Anxiety in Primates. *Biological Psychiatry*, *58*(10), 796–804. https://doi.org/10.1016/j.biopsych.2005.05.021

Kamali, A., Sair, H. I., Blitz, A. M., Riascos, R. F., Mirbagheri, S., Keser, Z., & Hasan, K. M. (2016). Revealing the ventral amygdalofugal pathway of the human limbic system using high spatial resolution diffusion tensor tractography. *Brain Structure & Function*, *221*(7), 3561–3569. https://doi.org/10.1007/s00429-015-1119-3

Kao, W.-T., Wang, Y., Kleinman, J. E., Lipska, B. K., Hyde, T. M., Weinberger, D. R., & Law, A. J. (2010). Common genetic variation in Neuregulin 3 (NRG3) influences risk for schizophrenia and impacts NRG3 expression in human brain. *Proceedings of the National Academy of Sciences of the United States of America*, *107*(35), 15619–15624. https://doi.org/10.1073/pnas.1005410107

Karcher, N. R., & Barch, D. M. (2021). The ABCD study: Understanding the development of risk for mental and physical health outcomes. *Neuropsychopharmacology*, *46*(1), Article 1. https://doi.org/10.1038/s41386-020-0736-6

Kash, T. L. (2012). The role of biogenic amine signaling in the bed nucleus of the stria terminals in alcohol abuse. *Alcohol*, *46*(4), 303–308. https://doi.org/10.1016/j.alcohol.2011.12.004

Kash, T. L., Pleil, K. E., Marcinkiewcz, C. A., Lowery-Gionta, E. G., Crowley, N., Mazzone, C., Sugam, J., Hardaway, J. A., & McElligott, Z. A. (2015). Neuropeptide Regulation of Signaling and Behavior in the BNST. *Molecules and Cells*, *38*(1), 1–13. https://doi.org/10.14348/molcells.2015.2261

Kasper, S. (2006). Anxiety disorders: Under-diagnosed and insufficiently treated. *International Journal of Psychiatry in Clinical Practice*, *10*(sup1), 3–9. https://doi.org/10.1080/13651500600552297

Kedo, O., Zilles, K., Palomero-Gallagher, N., Schleicher, A., Mohlberg, H., Bludau, S., & Amunts, K. (2018). Receptor-driven, multimodal mapping of the human amygdala. *Brain Structure and Function*, *223*(4), 1637–1666. https://doi.org/10.1007/s00429-017-1577-x

Kim, M. J., Loucks, R. A., Palmer, A. L., Brown, A. C., Solomon, K. M., Marchante, A. N., & Whalen, P. J. (2011). The structural and functional connectivity of the amygdala: From normal emotion to pathological anxiety. *Behavioural Brain Research*, *223*(2), 403–410. https://doi.org/10.1016/j.bbr.2011.04.025

Kim, S.-Y., Adhikari, A., Lee, S. Y., Marshel, J. H., Kim, C. K., Mallory, C. S., Lo, M., Pak, S., Mattis, J., Lim, B. K., Malenka, R. C., Warden, M. R., Neve, R., Tye, K. M., & Deisseroth, K. (2013). Diverging neural pathways assemble a behavioural state from separable features in anxiety. *Nature*, *496*(7444), 219–223. https://doi.org/10.1038/nature12018

Kirk, P. A., Robinson, O. J., & Skipper, J. I. (2022). Anxiety and amygdala connectivity during movie-watching. *Neuropsychologia*, *169*, 108194. https://doi.org/10.1016/j.neuropsychologia.2022.108194

Kishi, T., Tsumori, T., Ono, K., Yokota, S., Ishino, H., & Yasui, Y. (2000). Topographical organization of projections from the subiculum to the hypothalamus in the rat. *Journal of Comparative Neurology*, *419*(2), 205–222. https://doi.org/10.1002/(SICI)1096-9861(20000403)419:2<205::AID-CNE5>3.0.CO;2-0

Klein, R. J., Zeiss, C., Chew, E. Y., Tsai, J.-Y., Sackler, R. S., Haynes, C., Henning, A. K., SanGiovanni, J. P., Mane, S. M., Mayne, S. T., Bracken, M. B., Ferris, F. L., Ott, J., Barnstable, C., & Hoh, J. (2005). Complement Factor H Polymorphism in Age-Related Macular Degeneration. *Science*. https://doi.org/10.1126/science.1109557

Klingler, J., & Gloor, P. (1960). The connections of the amygdala and of the anterior temporal cortex in the human brain. *The Journal of Comparative Neurology*, *115*, 333–369. https://doi.org/10.1002/cne.901150305

Klumpers, F., Kroes, M. C., Heitland, I., Everaerd, D., Akkermans, S. E. A., Oosting, R. S., van Wingen, G., Franke, B., Kenemans, J. L., Fernández, G., & Baas, J. M. P. (2015). Dorsomedial Prefrontal Cortex Mediates the Impact of Serotonin Transporter Linked Polymorphic Region Genotype on Anticipatory Threat Reactions. *Biological Psychiatry*, *78*(8), 582–589. https://doi.org/10.1016/j.biopsych.2014.07.034

Klumpers, F., Kroes, M. C. W., Baas, J. M. P., & Fernández, G. (2017). How Human Amygdala and Bed Nucleus of the Stria Terminalis May Drive Distinct Defensive Responses. *Journal of Neuroscience*, *37*(40), 9645–9656. https://doi.org/10.1523/JNEUROSCI.3830-16.2017

Kochunov, P., Patel, B., Ganjgahi, H., Donohue, B., Ryan, M., Hong, E. L., Chen, X., Adhikari, B., Jahanshad, N., Thompson, P. M., Van't Ent, D., den Braber, A., de Geus, E. J. C., Brouwer, R. M., Boomsma, D. I., Hulshoff Pol, H. E., de Zubicaray, G. I., McMahon, K. L., Martin, N. G., … Nichols, T. E. (2019). Homogenizing Estimates of Heritability Among SOLAR-Eclipse, OpenMx, APACE, and FPHI Software Packages in Neuroimaging Data. *Frontiers in Neuroinformatics*, *13*. https://doi.org/10.3389/fninf.2019.00016

Koller, K., Hatton, C. M., Rogers, R. D., & Rafal, R. D. (2019). Stria terminalis microstructure in humans predicts variability in orienting towards threat. *The European Journal of Neuroscience*. https://doi.org/10.1111/ejn.14504

Koob, G. F., & Volkow, N. D. (2016). Neurobiology of addiction: A neurocircuitry analysis. *The Lancet Psychiatry*, *3*(8), 760–773. https://doi.org/10.1016/S2215-0366(16)00104-8

Kormos, C., & Gifford, R. (2014). The validity of self-report measures of proenvironmental behavior: A meta-analytic review. *Journal of Environmental Psychology*, *40*, 359–371. https://doi.org/10.1016/j.jenvp.2014.09.003

Kranzler, H. R., Zhou, H., Kember, R. L., Vickers Smith, R., Justice, A. C., Damrauer, S., Tsao, P. S., Klarin, D., Baras, A., Reid, J., Overton, J., Rader, D. J., Cheng, Z., Tate, J. P., Becker, W. C., Concato, J., Xu, K., Polimanti, R., Zhao, H., & Gelernter, J. (2019). Genome-wide association study of alcohol consumption and use disorder in 274,424 individuals from multiple populations. *Nature Communications*, *10*. https://doi.org/10.1038/s41467-019-09480-8

Krawczyk, M., Sharma, R., Mason, X., DeBacker, J., Jones, A. A., & Dumont, É. C. (2011). A Switch in the Neuromodulatory Effects of Dopamine in the Oval Bed Nucleus of the Stria Terminalis Associated with Cocaine Self-Administration in Rats. *Journal of Neuroscience*, *31*(24), 8928–8935. https://doi.org/10.1523/JNEUROSCI.0377-11.2011

Krueger, R. F., Kotov, R., Watson, D., Forbes, M. K., Eaton, N. R., Ruggero, C. J., Simms, L. J., Widiger, T. A., Achenbach, T. M., Bach, B., Bagby, R. M., Bornovalova, M. A., Carpenter, W. T., Chmielewski, M., Cicero, D. C., Clark, L. A., Conway, C., DeClercq, B., DeYoung, C. G., … Zimmermann, J. (2018). Progress in achieving quantitative classification of psychopathology. *World Psychiatry*, *17*(3), 282–293. https://doi.org/10.1002/wps.20566

Krüger, O., Shiozawa, T., Kreifelts, B., Scheffler, K., & Ethofer, T. (2015). Three distinct fiber pathways of the bed nucleus of the stria terminalis to the amygdala and prefrontal cortex. *Cortex*, *66*, 60–68. https://doi.org/10.1016/j.cortex.2015.02.007

Laird, A. R., Fox, P. M., Eickhoff, S. B., Turner, J. A., Ray, K. L., McKay, D. R., Glahn, D. C., Beckmann, C. F., Smith, S. M., & Fox, P. T. (2011). Behavioral Interpretations of Intrinsic Connectivity Networks. *Journal of Cognitive Neuroscience*, *23*(12), 4022–4037. https://doi.org/10.1162/jocn_a_00077

Lawrence, K. E., Abaryan, Z., Laltoo, E., Hernandez, L. M., Gandal, M., McCracken, J. T., & Thompson, P. M. (2021). *White matter microstructure shows sex differences in late childhood: Evidence from 6,797 children* (p. 2021.08.19.456728). https://doi.org/10.1101/2021.08.19.456728

Le Bihan, D., & Breton, E. (1985). Imagerie de diffusion in vivo par résonance magnétique nucléaire. *Imagerie de Diffusion in Vivo Par Résonance Magnétique Nucléaire*, *301*(15), 1109–1112.

Le Bihan, D., Breton, E., Lallemand, D., Grenier, P., Cabanis, E., & Laval-Jeantet, M. (1986). MR imaging of intravoxel incoherent motions: Application to diffusion and perfusion in neurologic disorders. *Radiology*, *161*(2), 401–407. https://doi.org/10.1148/radiology.161.2.3763909

Lebel, C., & Deoni, S. (2018). The development of brain white matter microstructure. *NeuroImage*, *182*, 207–218. https://doi.org/10.1016/j.neuroimage.2017.12.097

Lebow, M. A., & Chen, A. (2016). Overshadowed by the amygdala: The bed nucleus of the stria terminalis emerges as key to psychiatric disorders. *Molecular Psychiatry*, *21*(4), 450–463. https://doi.org/10.1038/mp.2016.1

LeDoux, J. E., & Hofmann, S. G. (2018). The subjective experience of emotion: A fearful view. *Current Opinion in Behavioral Sciences*, *19*, 67–72. https://doi.org/10.1016/j.cobeha.2017.09.011

Lee, S. J., Steiner, R. J., Yu, Y., Short, S. J., Neale, M. C., Styner, M. A., Zhu, H., & Gilmore, J. H. (2017). Common and heritable components of white matter microstructure predict cognitive function at 1 and 2 y. *Proceedings of the National Academy of Sciences*, *114*(1), 148–153. https://doi.org/10.1073/pnas.1604658114

Lesur, A., Gaspar, P., Alvarez, C., & Berger, B. (1989). Chemoanatomic compartments in the human bed nucleus of the stria terminalis. *Neuroscience*, *32*(1), 181–194. https://doi.org/10.1016/0306-4522(89)90117-6

Lezak, K. R., Missig, G., & Carlezon Jr, W. A. (2017). Behavioral methods to study anxiety in rodents. *Dialogues in Clinical Neuroscience*, *19*(2), 181–191.

Li, M., Newton, A. T., Anderson, A. W., Ding, Z., & Gore, J. C. (2019). Characterization of the hemodynamic response function in white matter tracts for event-related fMRI. *Nature Communications*, *10*(1), Article 1. https://doi.org/10.1038/s41467-019-09076-2

Li, T., Hu, J., Wang, S., & Zhang, H. (2020). Super-variants identification for brain connectivity. *Human Brain Mapping*, *42*(5), 1304–1312. https://doi.org/10.1002/hbm.25294

Lieberman, L., Gorka, S. M., Shankman, S. A., & Phan, K. L. (2017). Impact of Panic on Psychophysiological and Neural Reactivity to Unpredictable Threat in Depression and Anxiety. *Clinical Psychological Science : A Journal of the Association for Psychological Science*, *5*(1), 52–63. https://doi.org/10.1177/2167702616666507

Littlejohns, T. J., Holliday, J., Gibson, L. M., Garratt, S., Oesingmann, N., Alfaro-Almagro, F., Bell, J. D., Boultwood, C., Collins, R., Conroy, M. C., Crabtree, N., Doherty, N., Frangi, A. F., Harvey, N. C., Leeson, P., Miller, K. L., Neubauer, S., Petersen, S. E., Sellors, J., … Allen, N. E. (2020). The UK Biobank imaging enhancement of 100,000 participants: Rationale, data collection, management and future directions. *Nature Communications*, *11*, 2624. https://doi.org/10.1038/s41467-020-15948-9

Liu, X., Lai, H., Li, J., Becker, B., Zhao, Y., Cheng, B., & Wang, S. (2021). Gray matter structures associated with neuroticism: A meta-analysis of whole-brain voxel-based morphometry studies. *Human Brain Mapping*, *42*(9), 2706–2721. https://doi.org/10.1002/hbm.25395

Lorente de No, R. (1934). Studies on the structure of the cerebral cortex. Continuation of the study on the ammonic system. *J Psychol Neurol*, *46*, 113–117.

Luna, B., Padmanabhan, A., & O'Hearn, K. (2010). What has fMRI told us about the development of cognitive control through adolescence? *Brain and Cognition*, *72*(1), 101–113. https://doi.org/10.1016/j.bandc.2009.08.005

Maejima, S., Ohishi, N., Yamaguchi, S., & Tsukahara, S. (2015). A neural connection between the central part of the medial preoptic nucleus and the bed nucleus of the stria terminalis to regulate sexual behavior in male rats. *Neuroscience Letters*, *606*, 66–71. https://doi.org/10.1016/j.neulet.2015.08.047

Mai, J. K., Majtanik, M., & Paxinos, G. (2015). *Atlas of the Human Brain*. Academic Press.

Maier-Hein, K. H., Neher, P. F., Houde, J.-C., Côté, M.-A., Garyfallidis, E., Zhong, J., Chamberland, M., Yeh, F.-C., Lin, Y.-C., Ji, Q., Reddick, W. E., Glass, J. O., Chen, D. Q., Feng, Y., Gao, C., Wu, Y., Ma, J., He, R., Li, Q., … Descoteaux, M. (2017). The challenge of mapping the human connectome based on diffusion tractography. *Nature Communications*, *8*(1), 1349. https://doi.org/10.1038/s41467-017-01285-x

Maita, I., Bazer, A., Blackford, J. U., & Samuels, B. A. (2021). Chapter 27 - Functional anatomy of the bed nucleus of the stria terminalis–hypothalamus neural circuitry: Implications for valence surveillance, addiction, feeding, and social behaviors. In D. F. Swaab, F. Kreier, P. J. Lucassen, A. Salehi, & R. M. Buijs (Eds.), *Handbook of Clinical Neurology* (Vol. 179, pp. 403–418). Elsevier. https://doi.org/10.1016/B978-0-12-819975-6.00026-1

Marees, A. T., de Kluiver, H., Stringer, S., Vorspan, F., Curis, E., Marie-Claire, C., & Derks, E. M. (2018). A tutorial on conducting genome-wide association studies: Quality control and statistical analysis. *International Journal of Methods in Psychiatric Research*, *27*(2), e1608. https://doi.org/10.1002/mpr.1608

Marek, S., Tervo-Clemmens, B., Calabro, F. J., Montez, D. F., Kay, B. P., Hatoum, A. S., Donohue, M. R., Foran, W., Miller, R. L., Hendrickson, T. J., Malone, S. M., Kandala, S., Feczko, E., Miranda-Dominguez, O., Graham, A. M., Earl, E. A., Perrone, A. J., Cordova, M., Doyle, O., … Dosenbach, N. U. F. (2022). Reproducible brain-wide association studies require thousands of individuals. *Nature*. https://doi.org/10.1038/s41586-022-04492-9

Mars, R. B., Neubert, F.-X., Verhagen, L., Sallet, J., Miller, K. L., Dunbar, R. I. M., & Barton, R. A. (2014). Primate comparative neuroscience using magnetic resonance imaging: Promises and challenges. *Frontiers in Neuroscience*, *8*. https://www.frontiersin.org/article/10.3389/fnins.2014.00298

Mars, R. B., Sotiropoulos, S. N., Passingham, R. E., Sallet, J., Verhagen, L., Khrapitchev, A. A., Sibson, N., & Jbabdi, S. (2018). Whole brain comparative anatomy using connectivity blueprints. *ELife*, *7*, e35237. https://doi.org/10.7554/eLife.35237

Martin, L. J., Powers, R. E., Dellovade, T. L., & Price, D. L. (1991). The bed nucleus-amygdala continuum in human and monkey. *The Journal of Comparative Neurology*, *309*(4), 445–485. https://doi.org/10.1002/cne.903090404

McCarthy, C. S., Ramprashad, A., Thompson, C., Botti, J.-A., Coman, I. L., & Kates, W. R. (2015). A comparison of FreeSurfer-generated data with and without manual intervention. *Frontiers in Neuroscience*, *9*, 379. https://doi.org/10.3389/fnins.2015.00379

McCarthy, S., Das, S., Kretzschmar, W., Delaneau, O., Wood, A. R., Teumer, A., Kang, H. M., Fuchsberger, C., Danecek, P., Sharp, K., Luo, Y., Sidore, C., Kwong, A., Timpson, N., Koskinen, S., Vrieze, S., Scott, L. J., Zhang, H., Mahajan, A., … the Haplotype Reference Consortium. (2016). A reference panel of 64,976 haplotypes for genotype imputation. *Nature Genetics*, *48*(10), Article 10. https://doi.org/10.1038/ng.3643

McCrae, R. R., & Costa Jr., P. T. (2008). The five-factor theory of personality. In *Handbook of personality: Theory and research, 3rd ed* (pp. 159–181). The Guilford Press.

McDonald, A. J. (1998). Cortical pathways to the mammalian amygdala. *Progress in Neurobiology*, *55*(3), 257–332. https://doi.org/10.1016/S0301-0082(98)00003-3

McFarland, K., Davidge, S. B., Lapish, C. C., & Kalivas, P. W. (2004). Limbic and Motor Circuitry Underlying Footshock-Induced Reinstatement of Cocaine-Seeking Behavior. *Journal of Neuroscience*, *24*(7), 1551–1560. https://doi.org/10.1523/JNEUROSCI.4177-03.2004

McMenamin, B. W., Langeslag, S. J. E., Sirbu, M., Padmala, S., & Pessoa, L. (2014). Network organization unfolds over time during periods of anxious anticipation. *The Journal of Neuroscience: The Official Journal of the Society for Neuroscience*, *34*(34), 11261–11273. https://doi.org/10.1523/JNEUROSCI.1579-14.2014

Meibach, R. C., & Siegel, A. (1975). The origin of fornix fibers which project to the mammillary bodies in the rat: A horseradish peroxidase study. *Brain Research*, *88*(3), 508–512. https://doi.org/10.1016/0006-8993(75)90662-9

Meibach, R. C., & Siegel, A. (1977). Efferent connections of the hippocampal formation in the rat. *Brain Research*, *124*(2), 197–224. https://doi.org/10.1016/0006-8993(77)90880-0

Meier, S. M., Trontti, K., Purves, K. L., Als, T. D., Grove, J., Laine, M., Pedersen, M. G., Bybjerg-Grauholm, J., Bækved-Hansen, M., Sokolowska, E., Mortensen, P. B., Hougaard, D. M., Werge, T., Nordentoft, M., Breen, G., Børglum, A. D., Eley, T. C., Hovatta, I., Mattheisen, M., & Mors, O. (2019). Genetic Variants Associated With Anxiety and Stress-Related Disorders. *JAMA Psychiatry*, *76*(9), 924–932. https://doi.org/10.1001/jamapsychiatry.2019.1119

Meier, S., Strohmaier, J., Breuer, R., Mattheisen, M., Degenhardt, F., Mühleisen, T. W., Schulze, T. G., Nöthen, M. M., Cichon, S., Rietschel, M., & Wüst, S. (2013). Neuregulin 3 is associated with attention deficits in schizophrenia and bipolar disorder. *The International Journal of Neuropsychopharmacology*, *16*(3), 549–556. https://doi.org/10.1017/S1461145712000697

Meier, S., Trontti, K., Als, T. D., Laine, M., Pedersen, M. G., Bybjerg-Grauholm, J., Hansen, M. B., Sokolowska, E., Mortensen, P. B., Hougaard, D. M., Werge, T., Nordentoft, M., Borglum, A., Hovatta, I., Mattheisen, M., & Mors, O. (2018). Genome-wide Association Study of Anxiety and Stress-related Disorders in the iPSYCH Cohort. *BioRxiv*, 263855. https://doi.org/10.1101/263855

Mekki, Y., Guillemot, V., Lemaître, H., Carrión-Castillo, A., Forkel, S., Frouin, V., & Philippe, C. (2021). The genetic architecture of language functional connectivity. *NeuroImage*, *249*, 118795. https://doi.org/10.1016/j.neuroimage.2021.118795

Meng, L., Shan, T., Li, K., & Gong, Q. (2021). Long-term tract-specific white matter microstructural changes after acute stress. *Brain Imaging and Behavior*, *15*(4), 1868–1875. https://doi.org/10.1007/s11682-020-00380-w

Menon, S. S., & Krishnamurthy, K. (2019). A Comparison of Static and Dynamic Functional Connectivities for Identifying Subjects and Biological Sex Using Intrinsic Individual Brain Connectivity. *Scientific Reports*, *9*(1), Article 1. https://doi.org/10.1038/s41598-019-42090-4

Miles, O. W., & Maren, S. (2019). Role of the Bed Nucleus of the Stria Terminalis in PTSD: Insights From Preclinical Models. *Frontiers in Behavioral Neuroscience*, *13*. https://doi.org/10.3389/fnbeh.2019.00068

Miller, K. L., Alfaro-Almagro, F., Bangerter, N. K., Thomas, D. L., Yacoub, E., Xu, J., Bartsch, A. J., Jbabdi, S., Sotiropoulos, S. N., Andersson, J. L., Griffanti, L., Douaud, G., Okell, T. W., Weale, P., Dragonu, I., Garratt, S., Hudson, S., Collins, R., Jenkinson, M., … Smith, S. M. (2016). Multimodal population brain imaging in the UK Biobank prospective epidemiological study. *Nature Neuroscience*, *19*(11), 1523–1536. https://doi.org/10.1038/nn.4393

Mineka, S., Williams, A. L., Wolitzky-Taylor, K., Vrshek-Schallhorn, S., Craske, M. G., Hammen, C., & Zinbarg, R. E. (2020). Five-year prospective neuroticism–stress effects on major depressive episodes: Primarily additive effects of the general neuroticism factor and stress. *Journal of Abnormal Psychology*, *129*(6), 646–657. https://doi.org/10.1037/abn0000530

Mira, R. G., Lira, M., Tapia-Rojas, C., Rebolledo, D. L., Quintanilla, R. A., & Cerpa, W. (2020). Effect of Alcohol on Hippocampal-Dependent Plasticity and Behavior: Role of Glutamatergic Synaptic Transmission. *Frontiers in Behavioral Neuroscience*, *13*, 288. https://doi.org/10.3389/fnbeh.2019.00288

Mobbs, D., Yu, R., Rowe, J. B., Eich, H., FeldmanHall, O., & Dalgleish, T. (2010). Neural activity associated with monitoring the oscillating threat value of a tarantula. *Proceedings of the National Academy of Sciences of the United States of America*, *107*(47), 20582–20586. https://doi.org/10.1073/pnas.1009076107

Modi, S., Trivedi, R., Singh, K., Kumar, P., Rathore, R. K. S., Tripathi, R. P., & Khushu, S. (2013). Individual differences in trait anxiety are associated with white matter tract integrity in fornix and uncinate fasciculus: Preliminary evidence from a DTI based tractography study. *Behavioural Brain Research*, *238*, 188–192. https://doi.org/10.1016/j.bbr.2012.10.007

Mori, S., Oishi, K., Jiang, H., Jiang, L., Li, X., Akhter, K., Hua, K., Faria, A. V., Mahmood, A., Woods, R., Toga, A., Pike, B., Neto, P. R., Evans, A., Zhang, J., Huang, H., Miller, M. I., Zijl, P. van, & Mazziotta, J. (2008). Stereotaxic White Matter Atlas Based on Diffusion Tensor Imaging in an ICBM Template. *NeuroImage*, *40*(2), 570–582. https://doi.org/10.1016/j.neuroimage.2007.12.035

Morrison, F., & Poletti, C. E. (1980). Hippocampal influence on amygdala unit activity in awake squirrel monkeys. *Brain Research*, *192*(2), 353–369. https://doi.org/10.1016/0006-8993(80)90889-6

Motzkin, J. C., Philippi, C. L., Oler, J. A., Kalin, N. H., Baskaya, M. K., & Koenigs, M. (2015a). Ventromedial prefrontal cortex damage alters resting blood flow to the bed nucleus of stria terminalis. *Cortex; a Journal Devoted to the Study of the Nervous System and Behavior*, *64*, 281–288. https://doi.org/10.1016/j.cortex.2014.11.013

Motzkin, J. C., Philippi, C. L., Oler, J. A., Kalin, N. H., Baskaya, M. K., & Koenigs, M. (2015b). Ventromedial prefrontal cortex damage alters resting blood flow to the bed nucleus of stria terminalis. *Cortex*, *64*, 281–288. https://doi.org/10.1016/j.cortex.2014.11.013

Müller, M. J., Geisler, C., Blundell, J., Dulloo, A., Schutz, Y., Krawczak, M., Bosy-Westphal, A., Enderle, J., & Heymsfield, S. B. (2018). The case of GWAS of obesity: Does body weight control play by the rules? *International Journal of Obesity (2005)*, *42*(8), 1395–1405. https://doi.org/10.1038/s41366-018-0081-6

Müller, M. J., Krawczak, M., Heymsfield, S., Schutz, Y., Dulloo, A., Blundell, J., Geisler, C., & Bosy-Westphal, A. (2019). Thanks for opening an overdue discussion on GWAS of BMI: A reply to Prof. Speakman et al. *International Journal of Obesity*, *43*(1), 217–218. https://doi.org/10.1038/s41366-018-0264-1

Munafò, M. R., & Davey Smith, G. (2018). Robust research needs many lines of evidence. *Nature*, *553*(7689), 399–401. https://doi.org/10.1038/d41586-018-01023-3

Münsterkötter, A. L., Notzon, S., Redlich, R., Grotegerd, D., Dohm, K., Arolt, V., Kugel, H., Zwanzger, P., & Dannlowski, U. (2015). SPIDER OR NO SPIDER? NEURAL CORRELATES OF SUSTAINED AND PHASIC FEAR IN SPIDER PHOBIA. *Depression and Anxiety*, *32*(9), 656–663. https://doi.org/10.1002/da.22382

Murphy, K., & Fox, M. D. (2017). Towards a consensus regarding global signal regression for resting state functional connectivity MRI. *Neuroimage*, *154*, 169–173. https://doi.org/10.1016/j.neuroimage.2016.11.052

Murray, E. A., Wise, S. P., & Graham, K. S. (2017). *The Evolution of Memory Systems: Ancestors, Anatomy, and Adaptations*. Oxford University Press.

Myers, B., McKlveen, J. M., & Herman, J. P. (2012). Neural regulation of the stress response: The many faces of feedback. *Cellular and Molecular Neurobiology*, 10.1007/s10571-012-9801-y. https://doi.org/10.1007/s10571-012-9801-y

Naaz, F., Knight, L. K., & Depue, B. E. (2019). Explicit and Ambiguous Threat Processing: Functionally Dissociable Roles of the Amygdala and Bed Nucleus of the Stria Terminalis. *Journal of Cognitive Neuroscience*, 1–17. https://doi.org/10.1162/jocn_a_01369

Najafi, M., Kinnison, J., & Pessoa, L. (2017). Dynamics of Intersubject Brain Networks during Anxious Anticipation. *Frontiers in Human Neuroscience*, *11*. https://doi.org/10.3389/fnhum.2017.00552

Nanni, M., Martínez-Soto, J., Gonzalez-Santos, L., & Barrios, F. A. (2018). Neural correlates of the natural observation of an emotionally loaded video. *PLoS ONE*, *13*(6), e0198731. https://doi.org/10.1371/journal.pone.0198731

Nguyen, L.-C., Durazzo, T. C., Dwyer, C. L., Rauch, A. A., Humphreys, K., Williams, L. M., & Padula, C. B. (2020). Predicting relapse after alcohol use disorder treatment in a high-risk cohort: The roles of anhedonia and smoking. *Journal of Psychiatric Research*, *126*, 1–7. https://doi.org/10.1016/j.jpsychires.2020.04.003

Ni, R.-J., Luo, P.-H., Shu, Y.-M., Chen, J.-T., & Zhou, J.-N. (2016). Whole-brain mapping of afferent projections to the bed nucleus of the stria terminalis in tree shrews. *Neuroscience*, *333*, 162–180. https://doi.org/10.1016/j.neuroscience.2016.07.017

Nichols, T., Brett, M., Andersson, J., Wager, T., & Poline, J.-B. (2005). Valid conjunction inference with the minimum statistic. *NeuroImage*, *25*(3), 653–660. https://doi.org/10.1016/j.neuroimage.2004.12.005

Northcote, J., & Livingston, M. (2011). Accuracy of Self-Reported Drinking: Observational Verification of 'Last Occasion' Drink Estimates of Young Adults. *Alcohol and Alcoholism*, *46*(6), 709–713. https://doi.org/10.1093/alcalc/agr138

Nosek, B. A., & Errington, T. M. (2020). What is replication? *PLOS Biology*, *18*(3), e3000691. https://doi.org/10.1371/journal.pbio.3000691

O'Daly, O. G., Trick, L., Scaife, J., Marshall, J., Ball, D., Phillips, M. L., Williams, S. S. C., Stephens, D. N., & Duka, T. (2012). Withdrawal-associated increases and decreases in functional neural connectivity associated with altered emotional regulation in alcoholism. *Neuropsychopharmacology: Official Publication of the American College of Neuropsychopharmacology*, *37*(10), 2267–2276. https://doi.org/10.1038/npp.2012.77

Oler, J. A., Birn, R. M., Patriat, R., Fox, A. S., Shelton, S. E., Burghy, C. A., Stodola, D. E., Essex, M. J., Davidson, R. J., & Kalin, N. H. (2012). Evidence for coordinated functional activity within the extended amygdala of non-human and human primates. *Neuroimage*, *61*(4), 1059–1066. https://doi.org/10.1016/j.neuroimage.2012.03.045

Oler, J. A., Tromp, D. P. M., Fox, A. S., Kovner, R., Davidson, R. J., Alexander, A. L., McFarlin, D. R., Birn, R. M., Berg, B., deCampo, D. M., Kalin, N. H., & Fudge, J. L. (2017a). Connectivity between the central nucleus of the amygdala and the bed nucleus of the stria terminalis in the non-human primate: Neuronal tract tracing and developmental neuroimaging studies. *Brain Structure & Function*, *222*(1), 21–39. https://doi.org/10.1007/s00429-016-1198-9

Oler, J. A., Tromp, D. P. M., Fox, A. S., Kovner, R., Davidson, R. J., Alexander, A. L., McFarlin, D. R., Birn, R. M., Berg, B., deCampo, D. M., Kalin, N. H., & Fudge, J. L. (2017b). Connectivity between the central nucleus of the amygdala and the bed nucleus of the stria terminalis in the non-human primate: Neuronal tract tracing and developmental neuroimaging studies. *Brain Structure & Function*, *222*(1), 21–39. https://doi.org/10.1007/s00429-016-1198-9

O'Mara, S. M., Commins, S., Anderson, M., & Gigg, J. (2001). The subiculum: A review of form, physiology and function. *Progress in Neurobiology*, *64*(2), 129–155. https://doi.org/10.1016/S0301-0082(00)00054-X

Ortiz-Juza, M. M., Alghorazi, R. A., & Rodriguez-Romaguera, J. (2021). Cell-type diversity in the bed nucleus of the stria terminalis to regulate motivated behaviors. *Behavioural Brain Research*, *411*, 113401. https://doi.org/10.1016/j.bbr.2021.113401

Pardo-Bellver, C., Cadiz-Moretti, B., Novejarque, A., Martinez-Garcia, F., & Lanuza, E. (2012). Differential efferent projections of the anterior, posteroventral, and posterodorsal subdivisions of the medial amygdala in mice. *Frontiers in Neuroanatomy*, *6*. https://www.frontiersin.org/article/10.3389/fnana.2012.00033

Park, Y.-H., Shin, S. A., Kim, S., & Lee, J.-M. (2021). Key Intrinsic Connectivity Networks for Individual Identification With Siamese Long Short-Term Memory. *Frontiers in Neuroscience*, *15*. https://www.frontiersin.org/article/10.3389/fnins.2021.660187

Paterson, C., & Law, A. J. (2014). Transient Overexposure of Neuregulin 3 during Early Postnatal Development Impacts Selective Behaviors in Adulthood. *PLoS ONE*, *9*(8), e104172. https://doi.org/10.1371/journal.pone.0104172

Paterson, C., Wang, Y., Hyde, T. M., Weinberger, D. R., Kleinman, J. E., & Law, A. J. (2017). Temporal, Diagnostic, and Tissue-Specific Regulation of NRG3 Isoform Expression in Human Brain Development and Affective Disorders. *The American Journal of Psychiatry*, *174*(3), 256–265. https://doi.org/10.1176/appi.ajp.2016.16060721

Pauli, W. M., Nili, A. N., & Tyszka, J. M. (2018). A high-resolution probabilistic in vivo atlas of human subcortical brain nuclei. *Scientific Data*, *5*, 180063. https://doi.org/10.1038/sdata.2018.63

Pedersen, W. S. (2017). *Investigating the Functional Connectivity of the Bed Nucleus of the Stria Terminalis During Conditions of Threat and Safety Using High Resolution 7 Tesla FMRI*.

Pedersen, W. S., Schaefer, S. M., Gresham, L. K., Lee, S. D., Kelly, M. P., Mumford, J. A., Oler, J. A., & Davidson, R. J. (2020). Higher Resting-state BNST-CeA Connectivity is Associated with Greater Corrugator Supercilii Reactivity to Negatively Valenced Images. *NeuroImage*, *207*, 116428. https://doi.org/10.1016/j.neuroimage.2019.116428

Perusini, J. N., & Fanselow, M. S. (2015). Neurobehavioral perspectives on the distinction between fear and anxiety. *Learning & Memory*, *22*(9), 417–425. https://doi.org/10.1101/lm.039180.115

Petrican, R., Miles, S., Rudd, L., Wasiewska, W., Graham, K. S., & Lawrence, A. D. (2021). Pubertal Timing and Functional Neurodevelopmental Alterations Independently Mediate the Effect of Family Conflict on Adolescent Psychopathology. *Developmental Cognitive Neuroscience*, 101032. https://doi.org/10.1016/j.dcn.2021.101032

Pezuk, P., Aydin, E., Aksoy, A., & Canbeyli, R. (2008). Effects of BNST lesions in female rats on forced swimming and navigational learning. *Brain Research*, *1228*, 199–207. https://doi.org/10.1016/j.brainres.2008.06.071

Picó-Pérez, M., Radua, J., Steward, T., Menchón, J. M., & Soriano-Mas, C. (2017). Emotion regulation in mood and anxiety disorders: A meta-analysis of fMRI cognitive reappraisal studies. *Progress in Neuro-Psychopharmacology and Biological Psychiatry*, *79*, 96–104. https://doi.org/10.1016/j.pnpbp.2017.06.001

Pilkonis, P. A., Choi, S. W., Salsman, J., Butt, Z., Moore, T. L., Lawrence, S. M., Zill, N., Cyranowski, J. M., Kelly, M. A. R., Knox, S. S., & Cella, D. (2013). Assessment of self-reported negative affect in the NIH Toolbox. *Psychiatry Research*, *206*(1), 88–97. https://doi.org/10.1016/j.psychres.2012.09.034

Piras, F., Piras, F., Abe, Y., Agarwal, S. M., Anticevic, A., Ameis, S., Arnold, P., Banaj, N., Bargalló, N., Batistuzzo, M. C., Benedetti, F., Beucke, J.-C., Boedhoe, P. S. W., Bollettini, I., Brem, S., Calvo, A., Cho, K. I. K., Ciullo, V., Dallaspezia, S., … Spalletta, G. (2021). White matter microstructure and its relation to clinical features of obsessive-compulsive disorder: Findings from the ENIGMA OCD Working Group. *Translational Psychiatry*, *11*(1), 173. https://doi.org/10.1038/s41398-021-01276-z

Plana-Ripoll, O., Pedersen, C. B., Holtz, Y., Benros, M. E., Dalsgaard, S., Jonge, P. de, Fan, C. C., Degenhardt, L., Ganna, A., Greve, A. N., Gunn, J., Iburg, K. M., Kessing, L. V., Lee, B. K., Lim, C. C. W., Mors, O., Nordentoft, M., Prior, A., Roest, A. M., … McGrath, J. J. (2019). Exploring Comorbidity Within Mental Disorders Among a Danish National Population. *JAMA Psychiatry*, *76*(3), 259–270. https://doi.org/10.1001/jamapsychiatry.2018.3658

Pleil, K. E., Helms, C. M., Sobus, J. R., Daunais, J. B., Grant, K. A., & Kash, T. L. (2016). Effects of chronic alcohol consumption on neuronal function in the non-human primate BNST. *Addiction Biology*, *21*(6), 1151–1167. https://doi.org/10.1111/adb.12289

Pleil, K. E., Rinker, J. A., Lowery-Gionta, E. G., Mazzone, C. M., McCall, N. M., Kendra, A. M., Olson, D. P., Lowell, B. B., Grant, K. A., Thiele, T. E., & Kash, T. L. (2015). NPY signaling inhibits extended amygdala CRF neurons to suppress binge alcohol drinking. *Nature Neuroscience*, *18*(4), 545–552. https://doi.org/10.1038/nn.3972

Polderman, T. J. C., Benyamin, B., de Leeuw, C. A., Sullivan, P. F., van Bochoven, A., Visscher, P. M., & Posthuma, D. (2015). Meta-analysis of the heritability of human traits based on fifty years of twin studies. *Nature Genetics*, *47*(7), 702–709. https://doi.org/10.1038/ng.3285

Poletti, C. E., & Creswell, G. (1977). Fornix system efferent projections in the squirrel monkey: An experimental degeneration study. *The Journal of Comparative Neurology*, *175*(1), 101–128. https://doi.org/10.1002/cne.901750107

Poletti, C. E., Kinnard, M. A., & MacLean, P. D. (1973). Hippocampal influence on unit activity of hypothalamus, preoptic region, and basal forebrain in awake, stting squirrel monkeys. *Journal of Neurophysiology*. https://doi.org/10.1152/jn.1973.36.2.308

Poletti, C. E., & Sujatanond, M. (1980). Evidence for a second hippocampal efferent pathway to hypothalamus and basal forebrain comparable to fornix system: A unit study in the awake monkey. *Journal of Neurophysiology*, *44*(3), 514–531. https://doi.org/10.1152/jn.1980.44.3.514

Poli, E., & Angrilli, A. (2015). Greater general startle reflex is associated with greater anxiety levels: A correlational study on 111 young women. *Frontiers in Behavioral Neuroscience*, *9*, 10. https://doi.org/10.3389/fnbeh.2015.00010

Poppenk, J., Evensmoen, H. R., Moscovitch, M., & Nadel, L. (2013). Long-axis specialization of the human hippocampus. *Trends in Cognitive Sciences*, *17*(5), 230–240. https://doi.org/10.1016/j.tics.2013.03.005

Porta-Casteràs, D., Fullana, M. A., Tinoco, D., Martínez-Zalacaín, I., Pujol, J., Palao, D. J., Soriano-Mas, C., Harrison, B. J., Via, E., & Cardoner, N. (2020). Prefrontal-amygdala connectivity in trait anxiety and generalized anxiety disorder: Testing the boundaries between healthy and pathological worries. *Journal of Affective Disorders*, *267*, 211–219. https://doi.org/10.1016/j.jad.2020.02.029

Power, J. D., Barnes, K. A., Snyder, A. Z., Schlaggar, B. L., & Petersen, S. E. (2012). Spurious but systematic correlations in functional connectivity MRI networks arise from subject motion. *Neuroimage*, *59*(3), 2142–2154. https://doi.org/10.1016/j.neuroimage.2011.10.018

Quattrini, G., Pievani, M., Jovicich, J., Aiello, M., Bargalló, N., Barkhof, F., Bartres-Faz, D., Beltramello, A., Pizzini, F. B., Blin, O., Bordet, R., Caulo, M., Constantinides, M., Didic, M., Drevelegas, A., Ferretti, A., Fiedler, U., Floridi, P., Gros-Dagnac, H., … Marizzoni, M. (2020). Amygdalar nuclei and hippocampal subfields on MRI: Test-retest reliability of automated volumetry across different MRI sites and vendors. *NeuroImage*, *218*, 116932. https://doi.org/10.1016/j.neuroimage.2020.116932

Rabellino, D., Densmore, M., Harricharan, S., Jean, T., McKinnon, M. C., & Lanius, R. A. (2018). Resting-state functional connectivity of the bed nucleus of the stria terminalis in post-traumatic stress disorder and its dissociative subtype. *Human Brain Mapping*, *39*(3), 1367–1379. https://doi.org/10.1002/hbm.23925

Radley, J. J., & Johnson, S. B. (2018). Anteroventral bed nuclei of the stria terminalis neurocircuitry: Towards an integration of HPA axis modulation with coping behaviors - Curt Richter Award Paper 2017. *Psychoneuroendocrinology*, *89*, 239–249. https://doi.org/10.1016/j.psyneuen.2017.12.005

Radley, J. J., & Sawchenko, P. E. (2011). A Common Substrate for Prefrontal and Hippocampal Inhibition of the Neuroendocrine Stress Response. *The Journal of Neuroscience*, *31*(26), 9683–9695. https://doi.org/10.1523/JNEUROSCI.6040-10.2011

Raichle, M. E. (2015). The brain's default mode network. *Annual Review of Neuroscience*, *38*, 433–447. https://doi.org/10.1146/annurev-neuro-071013-014030

Ramakrishnan, A. P. (2013). Linkage Disequilibrium. In S. Maloy & K. Hughes (Eds.), *Brenner's Encyclopedia of Genetics (Second Edition)* (pp. 252–253). Academic Press. https://doi.org/10.1016/B978-0-12-374984-0.00870-6

Regev, L., Neufeld-Cohen, A., Tsoory, M., Kuperman, Y., Getselter, D., Gil, S., & Chen, A. (2011). Prolonged and site-specific over-expression of corticotropin-releasing factor reveals differential roles for extended amygdala nuclei in emotional regulation. *Molecular Psychiatry*, *16*(7), 714–728. https://doi.org/10.1038/mp.2010.64

Ritchie, S. J., Cox, S. R., Shen, X., Lombardo, M. V., Reus, L. M., Alloza, C., Harris, M. A., Alderson, H., Hunter, S., Neilson, E., Liewald, D. C., Auyeung, B., Whalley, H. C., Lawrie, S. M., Gale, C. R., Bastin, M. E., McIntosh, A. M., & Deary, I. J. (2018). *Sex Differences In The Adult Human Brain: Evidence From 5,216 UK Biobank Participants*. https://doi.org/10.1101/123729

Roberto, M., Kirson, D., & Khom, S. (2020). The Role of the Central Amygdala in Alcohol Dependence. *Cold Spring Harbor Perspectives in Medicine*. https://doi.org/10.1101/cshperspect.a039339

Roberts, A. C., & Clarke, H. F. (2019). Why we need nonhuman primates to study the role of ventromedial prefrontal cortex in the regulation of threat- and reward-elicited responses. *Proceedings of the National Academy of Sciences*, *116*(52), 26297–26304. https://doi.org/10.1073/pnas.1902288116

Robinson, O. J., Letkiewicz, A. M., Overstreet, C., Ernst, M., & Grillon, C. (2011). The effect of induced anxiety on cognition: Threat of shock enhances aversive processing in healthy individuals. *Cognitive, Affective, & Behavioral Neuroscience*, *11*(2), 217. https://doi.org/10.3758/s13415-011-0030-5

Rogers, B. P., Morgan, V. L., Newton, A. T., & Gore, J. C. (2007). Assessing Functional Connectivity in the Human Brain by FMRI. *Magnetic Resonance Imaging*, *25*(10), 1347–1357. https://doi.org/10.1016/j.mri.2007.03.007

Rosenman, R., Tennekoon, V., & Hill, L. G. (2011). Measuring bias in self-reported data. *International Journal of Behavioural & Healthcare Research*, *2*(4), 320–332. https://doi.org/10.1504/IJBHR.2011.043414

Roshchupkin, G. V., Gutman, B. A., Vernooij, M. W., Jahanshad, N., Martin, N. G., Hofman, A., McMahon, K. L., van der Lee, S. J., van Duijn, C. M., de Zubicaray, G. I., Uitterlinden, A. G., Wright, M. J., Niessen, W. J., Thompson, P. M., Ikram, M. A., & Adams, H. H. H. (2016). Heritability of the shape of subcortical brain structures in the general population. *Nature Communications*, *7*, 13738. https://doi.org/10.1038/ncomms13738

Russell, J. S., Trouche, S., & Reijmers, L. G. (2020). Functional characterization of the basal amygdala—Dorsal BNST pathway during contextual fear conditioning. *ENeuro*. https://doi.org/10.1523/ENEURO.0163-20.2020

Rutten-Jacobs, L. C. A., Tozer, D. J., Duering, M., Malik, R., Dichgans, M., Markus, H. S., & Traylor, M. (2018). Genetic Study of White Matter Integrity in UK Biobank (N=8448) and the Overlap With Stroke, Depression, and Dementia. *Stroke*, *49*(6), 1340–1347. https://doi.org/10.1161/STROKEAHA.118.020811

Saleeba, C., Dempsey, B., Le, S., Goodchild, A., & McMullan, S. (2019). A Student's Guide to Neural Circuit Tracing. *Frontiers in Neuroscience*, *0*. https://doi.org/10.3389/fnins.2019.00897

Salimi-Khorshidi, G., Douaud, G., Beckmann, C. F., Glasser, M. F., Griffanti, L., & Smith, S. M. (2014). Automatic denoising of functional MRI data: Combining independent component analysis and hierarchical fusion of classifiers. *NeuroImage*, *90*, 449–468. https://doi.org/10.1016/j.neuroimage.2013.11.046

Saviola, F., Pappaianni, E., Monti, A., Grecucci, A., Jovicich, J., & De Pisapia, N. (2020). Trait and state anxiety are mapped differently in the human brain. *Scientific Reports*, *10*(1), 11112. https://doi.org/10.1038/s41598-020-68008-z

Sayers, E. W., Bolton, E. E., Brister, J. R., Canese, K., Chan, J., Comeau, D. C., Connor, R., Funk, K., Kelly, C., Kim, S., Madej, T., Marchler-Bauer, A., Lanczycki, C., Lathrop, S., Lu, Z., Thibaud-Nissen, F., Murphy, T., Phan, L., Skripchenko, Y., … Sherry, S. T. (2022). Database resources of the national center for biotechnology information. *Nucleic Acids Research*, *50*(D1), D20–D26. https://doi.org/10.1093/nar/gkab1112

Schilling, K., Gao, Y., Janve, V., Stepniewska, I., Landman, B. A., & Anderson, A. W. (2017). Can increased spatial resolution solve the crossing fiber problem for diffusion MRI? *NMR in Biomedicine*, *30*(12), 10.1002/nbm.3787. https://doi.org/10.1002/nbm.3787

Schmahmann, J. D., Pandya, D. N., Wang, R., Dai, G., D'Arceuil, H. E., de Crespigny, A. J., & Wedeen, V. J. (2007). Association fibre pathways of the brain: Parallel observations from diffusion spectrum imaging and autoradiography. *Brain: A Journal of Neurology*, *130*(Pt 3), 630–653. https://doi.org/10.1093/brain/awl359

Schmitt, M., & Blum, G. S. (2020). State/Trait Interactions. In V. Zeigler-Hill & T. K. Shackelford (Eds.), *Encyclopedia of Personality and Individual Differences* (pp. 5206–5209). Springer International Publishing. https://doi.org/10.1007/978-3-319-24612-3_1922

Schwabe, I., Janss, L., & van den Berg, S. M. (2017). Can We Validate the Results of Twin Studies? A Census-Based Study on the Heritability of Educational Achievement. *Frontiers in Genetics*, *8*. https://www.frontiersin.org/article/10.3389/fgene.2017.00160

Schwaferts, P. M. (2017). *Effects of Signal Dropout inResting-State fMRI Data of the HumanConnectome Project on FunctionalConnectivity*. https://doi.org/10.5282/ubm/epub.41007

Sébille, S. B., Rolland, A.-S., Welter, M.-L., Bardinet, E., & Santin, M. D. (2019). Post mortem high resolution diffusion MRI for large specimen imaging at 11.7 T with 3D segmented echo-planar imaging. *Journal of Neuroscience Methods*, *311*, 222–234. https://doi.org/10.1016/j.jneumeth.2018.10.010

Seeley, W. W., Menon, V., Schatzberg, A. F., Keller, J., Glover, G. H., Kenna, H., Reiss, A. L., & Greicius, M. D. (2007). Dissociable Intrinsic Connectivity Networks for Salience Processing and Executive Control. *Journal of Neuroscience*, *27*(9), 2349–2356. https://doi.org/10.1523/JNEUROSCI.5587-06.2007

Seguin, C., Tian, Y., & Zalesky, A. (2020). Network communication models improve the behavioral and functional predictive utility of the human structural connectome. *Network Neuroscience*, *4*(4), 980–1006. https://doi.org/10.1162/netn_a_00161

Serin, E., Zalesky, A., Matory, A., Walter, H., & Kruschwitz, J. D. (2021). NBS-Predict: A prediction-based extension of the network-based statistic. *NeuroImage*, *244*, 118625. https://doi.org/10.1016/j.neuroimage.2021.118625

Shackman, A. J., & Fox, A. S. (2021). Two Decades of Anxiety Neuroimaging Research: New Insights and a Look to the Future. *American Journal of Psychiatry*, *178*(2), 106–109. https://doi.org/10.1176/appi.ajp.2020.20121733

Shackman, A. J., Stockbridge, M. D., Tillman, R. M., Kaplan, C. M., Tromp, D. P. M., Fox, A. S., & Gamer, M. (2016). The neurobiology of dispositional negativity and attentional biases to threat: Implications for understanding anxiety disorders in adults and youth. *Journal of Experimental Psychopathology*, *7*(3), 311–342. https://doi.org/10.5127/jep.054015

Shackman, A. J., Tromp, D. P. M., Stockbridge, M. D., Kaplan, C. M., Tillman, R. M., & Fox, A. S. (2016). Dispositional negativity: An integrative psychological and neurobiological perspective. *Psychological Bulletin*, *142*(12), 1275–1314. https://doi.org/10.1037/bul0000073

Shackman, A. J., Weinstein, J. S., Hudja, S. N., Bloomer, C. D., Barstead, M. G., Fox, A. S., & Lemay, E. P. (2018). Dispositional negativity in the wild: Social environment governs momentary emotional experience. *Emotion (Washington, D.C.)*, *18*(5), 707–724. https://doi.org/10.1037/emo0000339

Shen, K., Bezgin, G., Schirner, M., Ritter, P., Everling, S., & McIntosh, A. R. (2019). A macaque connectome for large-scale network simulations in TheVirtualBrain. *Scientific Data*, *6*(1), 123. https://doi.org/10.1038/s41597-019-0129-z

Shen, K., Goulas, A., Grayson, D. S., Eusebio, J., Gati, J. S., Menon, R. S., McIntosh, A. R., & Everling, S. (2019). Exploring the limits of network topology estimation using diffusion-based tractography and tracer studies in the macaque cortex. *NeuroImage*, *191*, 81–92. https://doi.org/10.1016/j.neuroimage.2019.02.018

Shi, H., Kichaev, G., & Pasaniuc, B. (2016). Contrasting the Genetic Architecture of 30 Complex Traits from Summary Association Data. *The American Journal of Human Genetics*, *99*(1), 139–153. https://doi.org/10.1016/j.ajhg.2016.05.013

Shiba, Y., Oikonomidis, L., Sawiak, S., Fryer, T. D., Hong, Y. T., Cockcroft, G., Santangelo, A. M., & Roberts, A. C. (2017). Converging Prefronto-Insula-Amygdala Pathways in Negative Emotion Regulation in Marmoset Monkeys. *Biological Psychiatry*, *82*(12), 895–903. https://doi.org/10.1016/j.biopsych.2017.06.016

Shin, J.-W., Geerling, J. C., & Loewy, A. D. (2008). Inputs to the ventrolateral bed nucleus of the stria terminalis. *The Journal of Comparative Neurology*, *511*(5), 628–657. https://doi.org/10.1002/cne.21870

Silberman, Y., Matthews, R. T., & Winder, D. G. (2013). A Corticotropin Releasing Factor Pathway for Ethanol Regulation of the Ventral Tegmental Area in the Bed Nucleus of the Stria Terminalis. *Journal of Neuroscience*, *33*(3), 950–960. https://doi.org/10.1523/JNEUROSCI.2949-12.2013

Silverman, M. H., Wilson, S., Ramsay, I. S., Hunt, R. H., Thomas, K. M., Krueger, R. F., & Iacono, W. G. (2019). Trait Neuroticism and Emotion Neurocircuitry: FMRI Evidence for a Failure in Emotion Regulation. *Development and Psychopathology*, *31*(3), 1085–1099. https://doi.org/10.1017/S0954579419000610

Smith, P. L., & Little, D. R. (2018). Small is beautiful: In defense of the small-N design. *Psychonomic Bulletin & Review*, *25*(6), 2083–2101. https://doi.org/10.3758/s13423-018-1451-8

Smith, S. M. (2002). Fast robust automated brain extraction. *Human Brain Mapping*, *17*(3), 143–155. https://doi.org/10.1002/hbm.10062

Smith, S. M., Andersson, J., Auerbach, E. J., Beckmann, C. F., Bijsterbosch, J., Douaud, G., Duff, E., Feinberg, D. A., Griffanti, L., Harms, M. P., Kelly, M., Laumann, T., Miller, K. L., Moeller, S., Petersen, S., Power, J., Salimi-Khorshidi, G., Snyder, A. Z., Vu, A., … Glasser, M. F. (2013). Resting-state fMRI in the Human Connectome Project. *NeuroImage*, *80*, 144–168. https://doi.org/10.1016/j.neuroimage.2013.05.039

Smith, S. M., Douaud, G., Chen, W., Hanayik, T., Alfaro-Almagro, F., Sharp, K., & Elliott, L. T. (2021). An expanded set of genome-wide association studies of brain imaging phenotypes in UK Biobank. *Nature Neuroscience*, *24*(5), Article 5. https://doi.org/10.1038/s41593-021-00826-4

Smith, S. M., & Nichols, T. E. (2009). Threshold-free cluster enhancement: Addressing problems of smoothing, threshold dependence and localisation in cluster inference. *NeuroImage*, *44*(1), 83–98. https://doi.org/10.1016/j.neuroimage.2008.03.061

Smith, S. M., Vidaurre, D., Beckmann, C. F., Glasser, M. F., Jenkinson, M., Miller, K. L., Nichols, T. E., Robinson, E. C., Salimi-Khorshidi, G., Woolrich, M. W., Barch, D. M., Uğurbil, K., & Essen, D. C. V. (2013). Functional connectomics from resting-state fMRI. *Trends in Cognitive Sciences*, *17*(12), 666–682. https://doi.org/10.1016/j.tics.2013.09.016

Smoller, J. W., Finn, C. T., & Gardner-Schuster, E. E. (2008). CHAPTER 63—Genetics and Psychiatry. In T. A. Stern, J. F. Rosenbaum, M. Fava, J. Biederman, & S. L. Rauch (Eds.), *Massachusetts General Hospital Comprehensive Clinical Psychiatry* (pp. 853–883). Mosby. https://doi.org/10.1016/B978-0-323-04743-2.50065-2

Soares, J. M., Magalhães, R., Moreira, P. S., Sousa, A., Ganz, E., Sampaio, A., Alves, V., Marques, P., & Sousa, N. (2016). A Hitchhiker's Guide to Functional Magnetic Resonance Imaging. *Frontiers in Neuroscience*, *10*. https://www.frontiersin.org/article/10.3389/fnins.2016.00515

Soares, J. M., Marques, P., Alves, V., & Sousa, N. (2013). A hitchhiker's guide to diffusion tensor imaging. *Frontiers in Neuroscience*, *7*, 31. https://doi.org/10.3389/fnins.2013.00031

Somerville, L. H., Wagner, D. D., Wig, G. S., Moran, J. M., Whalen, P. J., & Kelley, W. M. (2013). Interactions between transient and sustained neural signals support the generation and regulation of anxious emotion. *Cerebral Cortex (New York, N.Y.: 1991)*, *23*(1), 49–60. https://doi.org/10.1093/cercor/bhr373

Song, W., Qian, W., Wang, W., Yu, S., & Lin, G. N. (2021). Mendelian randomization studies of brain MRI yield insights into the pathogenesis of neuropsychiatric disorders. *BMC Genomics*, *22*(Suppl 3), 342. https://doi.org/10.1186/s12864-021-07661-8

Song, X., Panych, L. P., & Chen, N.-K. (2016). Data-Driven and Predefined ROI-Based Quantification of Long-Term Resting-State fMRI Reproducibility. *Brain Connectivity*, *6*(2), 136–151. https://doi.org/10.1089/brain.2015.0349

Song, Z., Chen, J., Wen, Z., & Zhang, L. (2021). Abnormal functional connectivity and effective connectivity between the default mode network and attention networks in patients with alcohol-use disorder. *Acta Radiologica*, *62*(2), 251–259. https://doi.org/10.1177/0284185120923270

Speakman, J. R., Loos, R. J. F., O'Rahilly, S., Hirschhorn, J. N., & Allison, D. B. (2018). GWAS for BMI: A treasure trove of fundamental insights into the genetic basis of obesity. *International Journal of Obesity*, *42*(8), 1524–1531. https://doi.org/10.1038/s41366-018-0147-5

Sporns, O. (2018). Graph theory methods: Applications in brain networks. *Dialogues in Clinical Neuroscience*, *20*(2), 111–121.

Sripada, C., Angstadt, M., Rutherford, S., Taxali, A., & Shedden, K. (2020). Toward a "treadmill test" for cognition: Improved prediction of general cognitive ability from the task activated brain. *Human Brain Mapping*, *41*(12), 3186–3197. https://doi.org/10.1002/hbm.25007

Stamatakis, A. M., Sparta, D. R., Jennings, J. H., McElligott, Z. A., Decot, H., & Stuber, G. D. (2014). Amygdala and Bed Nucleus of the Stria Terminalis Circuitry: Implications for addiction-related behaviors. *Neuropharmacology*, *76*(0 0). https://doi.org/10.1016/j.neuropharm.2013.05.046

Stefanacci, L., & Amaral, D. G. (2002). Some observations on cortical inputs to the macaque monkey amygdala: An anterograde tracing study. *Journal of Comparative Neurology*, *451*(4), 301–323. https://doi.org/10.1002/cne.10339

Steimer, T. (2002). The biology of fear- and anxiety-related behaviors. *Dialogues in Clinical Neuroscience*, *4*(3), 231–249.

Stewart, J. L., Coan, J. A., Towers, D. N., & Allen, J. J. B. (2014). Resting and task-elicited prefrontal EEG alpha asymmetry in depression: Support for the capability model. *Psychophysiology*, *51*(5), 446–455. https://doi.org/10.1111/psyp.12191

Strange, B. A., Witter, M. P., Lein, E. S., & Moser, E. I. (2014). Functional organization of the hippocampal longitudinal axis. *Nature Reviews. Neuroscience*, *15*(10), 655–669. https://doi.org/10.1038/nrn3785

Straube, T., Mentzel, H.-J., & Miltner, W. H. R. (2007). Waiting for spiders: Brain activation during anticipatory anxiety in spider phobics. *NeuroImage*, *37*(4), 1427–1436. https://doi.org/10.1016/j.neuroimage.2007.06.023

Suárez, L. E., Markello, R. D., Betzel, R. F., & Misic, B. (2020). Linking Structure and Function in Macroscale Brain Networks. *Trends in Cognitive Sciences*, *24*(4), 302–315. https://doi.org/10.1016/j.tics.2020.01.008

Sudlow, C., Gallacher, J., Allen, N., Beral, V., Burton, P., Danesh, J., Downey, P., Elliott, P., Green, J., Landray, M., Liu, B., Matthews, P., Ong, G., Pell, J., Silman, A., Young, A., Sprosen, T., Peakman, T., & Collins, R. (2015). UK Biobank: An Open Access Resource for Identifying the Causes of a Wide Range of Complex Diseases of Middle and Old Age. *PLOS Medicine*, *12*(3), e1001779. https://doi.org/10.1371/journal.pmed.1001779

Swan, G. E., Carmelli, D., Rosenman, R. H., Fabsitz, R. R., & Christian, J. C. (1990). Smoking and alcohol consumption in adult male twins: Genetic heritability and shared environmental influences. *Journal of Substance Abuse*, *2*(1), 39–50. https://doi.org/10.1016/S0899-3289(05)80044-6

Swanson, L. W., & Cowan, W. M. (1977). An autoradiographic study of the organization of the efferent connections of the hippocampal formation in the rat. *The Journal of Comparative Neurology*, *172*(1), 49–84. https://doi.org/10.1002/cne.901720104

Sylvester, C. M., Yu, Q., Srivastava, A. B., Marek, S., Zheng, A., Alexopoulos, D., Smyser, C. D., Shimony, J. S., Ortega, M., Dierker, D. L., Patel, G. H., Nelson, S. M., Gilmore, A. W., McDermott, K. B., Berg, J. J., Drysdale, A. T., Perino, M. T., Snyder, A. Z., Raut, R. V., … Dosenbach, N. U. F. (2020). Individual-specific functional connectivity of the amygdala: A substrate for precision psychiatry. *Proceedings of the National Academy of Sciences*. https://doi.org/10.1073/pnas.1910842117

Takagi, Y., Sakai, Y., Abe, Y., Nishida, S., Harrison, B. J., Martínez-Zalacaín, I., Soriano-Mas, C., Narumoto, J., & Tanaka, S. C. (2018). A common brain network among state, trait, and pathological anxiety from whole-brain functional connectivity. *NeuroImage*, *172*, 506–516. https://doi.org/10.1016/j.neuroimage.2018.01.080

Tam, V., Patel, N., Turcotte, M., Bossé, Y., Paré, G., & Meyre, D. (2019). Benefits and limitations of genome-wide association studies. *Nature Reviews Genetics*, *20*(8), 467–484. https://doi.org/10.1038/s41576-019-0127-1

Teeuw, J., Brouwer, R. M., Guimarães, J. P. O. F. T., Brandner, P., Koenis, M. M. G., Swagerman, S. C., Verwoert, M., Boomsma, D. I., & Hulshoff Pol, H. E. (2019). Genetic and environmental influences on functional connectivity within and between canonical cortical resting-state networks throughout adolescent development in boys and girls. *NeuroImage*, *202*, 116073. https://doi.org/10.1016/j.neuroimage.2019.116073

Theiss, J. D., Ridgewell, C., McHugo, M., Heckers, S., & Blackford, J. U. (2017). Manual segmentation of the human bed nucleus of the stria terminalis using 3T MRI. *NeuroImage*, *146*, 288–292. https://doi.org/10.1016/j.neuroimage.2016.11.047

Thomas Yeo, B. T., Krienen, F. M., Sepulcre, J., Sabuncu, M. R., Lashkari, D., Hollinshead, M., Roffman, J. L., Smoller, J. W., Zöllei, L., Polimeni, J. R., Fischl, B., Liu, H., & Buckner, R. L. (2011). The organization of the human cerebral cortex estimated by intrinsic functional connectivity. *Journal of Neurophysiology*, *106*(3), 1125–1165. https://doi.org/10.1152/jn.00338.2011

Thompson, P. M., Jahanshad, N., Ching, C. R. K., Salminen, L. E., Thomopoulos, S. I., Bright, J., Baune, B. T., Bertolín, S., Bralten, J., Bruin, W. B., Bülow, R., Chen, J., Chye, Y., Dannlowski, U., de Kovel, C. G. F., Donohoe, G., Eyler, L. T., Faraone, S. V., Favre, P., … Zelman, V. (2020). ENIGMA and global neuroscience: A decade of large-scale studies of the brain in health and disease across more than 40 countries. *Translational Psychiatry*, *10*(1), Article 1. https://doi.org/10.1038/s41398-020-0705-1

Thompson, P. M., Stein, J. L., Medland, S. E., Hibar, D. P., Vasquez, A. A., Renteria, M. E., Toro, R., Jahanshad, N., Schumann, G., Franke, B., Wright, M. J., Martin, N. G., Agartz, I., Alda, M., Alhusaini, S., Almasy, L., Almeida, J., Alpert, K., Andreasen, N. C., … Drevets, W. (2014). The ENIGMA Consortium: Large-scale collaborative analyses of neuroimaging and genetic data. *Brain Imaging and Behavior*, *8*(2), 153–182. https://doi.org/10.1007/s11682-013-9269-5

Tillman, R. M., Stockbridge, M. D., Nacewicz, B. M., Torrisi, S., Fox, A. S., Smith, J. F., & Shackman, A. J. (2018). Intrinsic functional connectivity of the central extended amygdala. *Human Brain Mapping*, *39*(3), 1291–1312. https://doi.org/10.1002/hbm.23917

Torrisi, S., Alvarez, G. M., Gorka, A. X., Fuchs, B., Geraci, M., Grillon, C., & Ernst, M. (2019). Resting-state connectivity of the bed nucleus of the stria terminalis and the central nucleus of the amygdala in clinical anxiety. *Journal of Psychiatry & Neuroscience : JPN*, *44*(5), 313–323. https://doi.org/10.1503/jpn.180150

Torrisi, S., O'Connell, K., Davis, A., Reynolds, R., Balderston, N., Fudge, J. L., Grillon, C., & Ernst, M. (2015). Resting state connectivity of the bed nucleus of the stria terminalis at ultra-high field. *Human Brain Mapping*, *36*(10), 4076–4088. https://doi.org/10.1002/hbm.22899

Tovmasyan, A., Monk, R. L., & Heim, D. (2022). Towards an affect intensity regulation hypothesis: Systematic review and meta-analyses of the relationship between affective states and alcohol consumption. *PLOS ONE*, *17*(1), e0262670. https://doi.org/10.1371/journal.pone.0262670

Turkheimer, E. (1998). Heritability and biological explanation. *Psychological Review*, *105*(4), 782–791. https://doi.org/10.1037/0033-295X.105.4.782-791

Turkheimer, E. (2016). Weak Genetic Explanation 20 Years Later: Reply to Plomin et al. (2016). *Perspectives on Psychological Science: A Journal of the Association for Psychological Science*, *11*(1), 24–28. https://doi.org/10.1177/1745691615617442

Tyszka, J. M., & Pauli, W. M. (2016). In vivo delineation of subdivisions of the human amygdaloid complex in a high-resolution group template. *Human Brain Mapping*, *37*(11), 3979–3998. https://doi.org/10.1002/hbm.23289

Uffelmann, E., Huang, Q. Q., Munung, N. S., de Vries, J., Okada, Y., Martin, A. R., Martin, H. C., Lappalainen, T., & Posthuma, D. (2021). Genome-wide association studies. *Nature Reviews Methods Primers*, *1*(1), Article 1. https://doi.org/10.1038/s43586-021-00056-9

Uhlén, M., Fagerberg, L., Hallström, B. M., Lindskog, C., Oksvold, P., Mardinoglu, A., Sivertsson, Å., Kampf, C., Sjöstedt, E., Asplund, A., Olsson, I., Edlund, K., Lundberg, E., Navani, S., Szigyarto, C. A.-K., Odeberg, J., Djureinovic, D., Takanen, J. O., Hober, S., … Pontén, F. (2015). Proteomics. Tissue-based map of the human proteome. *Science (New York, N.Y.)*, *347*(6220), 1260419. https://doi.org/10.1126/science.1260419

van der Merwe, C., Jahanshad, N., Cheung, J. W., Mufford, M., Groenewold, N. A., Koen, N., Ramesar, R., Dalvie, S., ENIGMA Consortium PGC-PTSD, Knowles, J. A., Hibar, D. P., Nievergelt, C. M., Koenen, K. C., Liberzon, I., Ressler, K. J., Medland, S. E., Morey, R. A., Thompson, P. M., & Stein, D. J. (2019). Concordance of genetic variation that increases risk for anxiety disorders and posttraumatic stress disorders and that influences their underlying neurocircuitry. *Journal of Affective Disorders*, *245*, 885–896. https://doi.org/10.1016/j.jad.2018.11.082

Van Essen, D. C., Ugurbil, K., Auerbach, E., Barch, D., Behrens, T. E. J., Bucholz, R., Chang, A., Chen, L., Corbetta, M., Curtiss, S. W., Della Penna, S., Feinberg, D., Glasser, M. F., Harel, N., Heath, A. C., Larson-Prior, L., Marcus, D., Michalareas, G., Moeller, S., … WU-Minn HCP Consortium. (2012). The Human Connectome Project: A data acquisition perspective. *NeuroImage*, *62*(4), 2222–2231. https://doi.org/10.1016/j.neuroimage.2012.02.018

van Hemmen, J., Saris, I. M. J., Cohen-Kettenis, P. T., Veltman, D. J., Pouwels, P. J. W., & Bakker, J. (2017). Sex Differences in White Matter Microstructure in the Human Brain Predominantly Reflect Differences in Sex Hormone Exposure. *Cerebral Cortex (New York, N.Y.: 1991)*, *27*(5), 2994–3001. https://doi.org/10.1093/cercor/bhw156

Van Horn, J. D., & Toga, A. W. (2014). Human neuroimaging as a "Big Data" science. *Brain Imaging and Behavior*, *8*(2), 323–331. https://doi.org/10.1007/s11682-013-9255-y

VanderWeele, T. J., Tchetgen Tchetgen, E. J., Cornelis, M., & Kraft, P. (2014). Methodological challenges in Mendelian randomization. *Epidemiology (Cambridge, Mass.)*, *25*(3), 427–435. https://doi.org/10.1097/EDE.0000000000000081

Venkataraman, A., Rathi, Y., Kubicki, M., Westin, C.-F., & Golland, P. (2012). Joint modeling of anatomical and functional connectivity for population studies. *IEEE Transactions on Medical Imaging*, *31*(2), 164–182. https://doi.org/10.1109/TMI.2011.2166083

Vinutha, H. P., Poornima, B., & Sagar, B. M. (2018). Detection of Outliers Using Interquartile Range Technique from Intrusion Dataset. In S. C. Satapathy, J. M. R. S. Tavares, V. Bhateja, & J. R. Mohanty (Eds.), *Information and Decision Sciences* (pp. 511–518). Springer. https://doi.org/10.1007/978-981-10-7563-6_53

Visscher, P. M., Wray, N. R., Zhang, Q., Sklar, P., McCarthy, M. I., Brown, M. A., & Yang, J. (2017). 10 Years of GWAS Discovery: Biology, Function, and Translation. *American Journal of Human Genetics*, *101*(1), 5–22. https://doi.org/10.1016/j.ajhg.2017.06.005

Voelker, P., Piscopo, D., Weible, A., Lynch, G., Rothbart, M. K., Posner, M. I., & Niell, C. M. (2017). How Changes in White Matter Might Underlie Improved Reaction Time Due to Practice. *Cognitive Neuroscience*, *8*(2), 112–118. https://doi.org/10.1080/17588928.2016.1173664

Vogel, J. W., La Joie, R., Grothe, M. J., Diaz-Papkovich, A., Doyle, A., Vachon-Presseau, E., Lepage, C., Vos de Wael, R., Thomas, R. A., Iturria-Medina, Y., Bernhardt, B., Rabinovici, G. D., & Evans, A. C. (2020). A molecular gradient along the longitudinal axis of the human hippocampus informs large-scale behavioral systems. *Nature Communications*, *11*(1), Article 1. https://doi.org/10.1038/s41467-020-14518-3

Volkow, N. D., Koob, G. F., & McLellan, A. T. (2016). Neurobiologic Advances from the Brain Disease Model of Addiction. *New England Journal of Medicine*, *374*(4), 363–371. https://doi.org/10.1056/NEJMra1511480

Vranjkovic, O., Gasser, P. J., Gerndt, C. H., Baker, D. A., & Mantsch, J. R. (2014). Stress-Induced Cocaine Seeking Requires a Beta-2 Adrenergic Receptor-Regulated Pathway from the Ventral Bed Nucleus of the Stria Terminalis That Regulates CRF Actions in the Ventral Tegmental Area. *Journal of Neuroscience*, *34*(37), 12504–12514. https://doi.org/10.1523/JNEUROSCI.0680-14.2014

Vranjkovic, O., Pina, M., Kash, T. L., & Winder, D. G. (2017). The bed nucleus of the stria terminalis in drug-associated behavior and affect: A circuit-based perspective. *Neuropharmacology*, *122*, 100–106. https://doi.org/10.1016/j.neuropharm.2017.03.028

Vuoksimaa, E., Panizzon, M. S., Hagler, D. J., Hatton, S. N., Fennema-Notestine, C., Rinker, D., Eyler, L. T., Franz, C. E., Lyons, M. J., Neale, M. C., Tsuang, M. T., Dale, A. M., & Kremen, W. S. (2017). Heritability of white matter microstructure in late middle age: A twin study of tract-based fractional anisotropy and absolute diffusivity indices. *Human Brain Mapping*, *38*(4), 2026–2036. https://doi.org/10.1002/hbm.23502

Wakana, S., Caprihan, A., Panzenboeck, M. M., Fallon, J. H., Perry, M., Gollub, R. L., Hua, K., Zhang, J., Jiang, H., Dubey, P., Blitz, A., van Zijl, P., & Mori, S. (2007). Reproducibility of Quantitative Tractography Methods Applied to Cerebral White Matter. *NeuroImage*, *36*(3), 630–644. https://doi.org/10.1016/j.neuroimage.2007.02.049

Walker, D. L., Miles, L. A., & Davis, M. (2009). Selective participation of the bed nucleus of the stria terminalis and CRF in sustained anxiety-like versus phasic fear-like responses. *Progress in Neuro-Psychopharmacology and Biological Psychiatry*, *33*(8), 1291–1308. https://doi.org/10.1016/j.pnpbp.2009.06.022

Walter, A., Mai, J. K., Lanta, L., & Görcs, T. (1991). Differential distribution of immunohistochemical markers in the bed nucleus of the stria terminalis in the human brain. *Journal of Chemical Neuroanatomy*, *4*(4), 281–298. https://doi.org/10.1016/0891-0618(91)90019-9

Wang, M., Cao, L., Li, H., Xiao, H., Ma, Y., Liu, S., Zhu, H., Yuan, M., Qiu, C., & Huang, X. (2021). Dysfunction of Resting-State Functional Connectivity of Amygdala Subregions in Drug-Naïve Patients With Generalized Anxiety Disorder. *Frontiers in Psychiatry*, *12*, 1677. https://doi.org/10.3389/fpsyt.2021.758978

Warren, K. N., Hermiller, M. S., Nilakantan, A. S., & Voss, J. L. (2019). Stimulating the hippocampal posterior-medial network enhances task-dependent connectivity and memory. *ELife*, *8*, e49458. https://doi.org/10.7554/eLife.49458

Waszczuk, M. A., Eaton, N. R., Krueger, R. F., Shackman, A. J., Waldman, I. D., Zald, D. H., Lahey, B. B., Patrick, C. J., Conway, C. C., Ormel, J., Hyman, S. E., Fried, E. I., Forbes, M. K., Docherty, A. R., Althoff, R. R., Bach, B., Chmielewski, M., DeYoung, C. G., Forbush, K. T., … Kotov, R. (2020). Redefining Phenotypes to Advance Psychiatric Genetics: Implications from Hierarchical Taxonomy of Psychopathology. *Journal of Abnormal Psychology*, *129*(2), 143–161. https://doi.org/10.1037/abn0000486

Watanabe, K., Taskesen, E., Bochoven, A. van, & Posthuma, D. (2017). Functional mapping and annotation of genetic associations with FUMA. *Nature Communications*, *8*(1), 1–11. https://doi.org/10.1038/s41467-017-01261-5

Weber, S., Johnsen, E., Kroken, R. A., Løberg, E.-M., Kandilarova, S., Stoyanov, D., Kompus, K., & Hugdahl, K. (2020). Dynamic Functional Connectivity Patterns in Schizophrenia and the Relationship With Hallucinations. *Frontiers in Psychiatry*, *11*, 227. https://doi.org/10.3389/fpsyt.2020.00227

Wegener, G. (2016, March 30). *Thomas A. Ban: The RDoC in historical perspective*. http://inhn.org/perspectives/thomas-a-ban-the-rdoc-in-historical-perspective.html

Weintraub, S., Dikmen, S. S., Heaton, R. K., Tulsky, D. S., Zelazo, P. D., Bauer, P. J., Carlozzi, N. E., Slotkin, J., Blitz, D., Wallner-Allen, K., Fox, N. A., Beaumont, J. L., Mungas, D., Nowinski, C. J., Richler, J., Deocampo, J. A., Anderson, J. E., Manly, J. J., Borosh, B., … Gershon, R. C. (2013). Cognition assessment using the NIH Toolbox. *Neurology*, *80*(11 Suppl 3), S54–S64. https://doi.org/10.1212/WNL.0b013e3182872ded

Weis, C., Huggins, A. A., Bennett, K. P., Parisi, E. A., & Larson, C. L. (2019). High resolution resting state functional connectivity of the extended amygdala. *Brain Connectivity*. https://doi.org/10.1089/brain.2019.0688

Welch, J. D., Kozareva, V., Ferreira, A., Vanderburg, C., Martin, C., & Macosko, E. Z. (2019). Single-Cell Multi-omic Integration Compares and Contrasts Features of Brain Cell Identity. *Cell*, *177*(7), 1873-1887.e17. https://doi.org/10.1016/j.cell.2019.05.006

White, A., Castle, I.-J. P., Chen, C. M., Shirley, M., Roach, D., & Hingson, R. (2015). Converging Patterns of Alcohol Use and Related Outcomes Among Females and Males in the United States, 2002 to 2012. *Alcoholism, Clinical and Experimental Research*, *39*(9), 1712–1726. https://doi.org/10.1111/acer.12815

Wicherts, J. M., Veldkamp, C. L. S., Augusteijn, H. E. M., Bakker, M., van Aert, R. C. M., & van Assen, M. A. L. M. (2016). Degrees of Freedom in Planning, Running, Analyzing, and Reporting Psychological Studies: A Checklist to Avoid p-Hacking. *Frontiers in Psychology*, *7*, 1832. https://doi.org/10.3389/fpsyg.2016.01832

Wiersch, L., & Weis, S. (2021). Sex differences in the brain: More than just male or female. *Cognitive Neuroscience*, *12*(3–4), 187–188. https://doi.org/10.1080/17588928.2020.1867084

Williams, L. E., Oler, J. A., Fox, A. S., McFarlin, D. R., Rogers, G. M., Jesson, M. A. L., Davidson, R. J., Pine, D. S., & Kalin, N. H. (2015). Fear of the unknown: Uncertain anticipation reveals amygdala alterations in childhood anxiety disorders. *Neuropsychopharmacology: Official Publication of the American College of Neuropsychopharmacology*, *40*(6), 1428–1435. https://doi.org/10.1038/npp.2014.328

Winkler, A. M., Webster, M. A., Brooks, J. C., Tracey, I., Smith, S. M., & Nichols, T. E. (2016). Non-parametric combination and related permutation tests for neuroimaging. *Human Brain Mapping*, *37*(4), 1486–1511. https://doi.org/10.1002/hbm.23115

Winkler, A. M., Webster, M. A., Vidaurre, D., Nichols, T. E., & Smith, S. M. (2015). Multi-level block permutation. *NeuroImage*, *123*, 253–268. https://doi.org/10.1016/j.neuroimage.2015.05.092

Winklewski, P. J., Sabisz, A., Naumczyk, P., Jodzio, K., Szurowska, E., & Szarmach, A. (2018). Understanding the Physiopathology Behind Axial and Radial Diffusivity Changes—What Do We Know? *Frontiers in Neurology*, *9*, 92. https://doi.org/10.3389/fneur.2018.00092

Xiong, Y. Y., & Mok, V. (2011). Age-Related White Matter Changes. *Journal of Aging Research*, *2011*, 617927. https://doi.org/10.4061/2011/617927

Xu, C., Krabbe, S., Gründemann, J., Botta, P., Fadok, J. P., Osakada, F., Saur, D., Grewe, B. F., Schnitzer, M. J., Callaway, E. M., & Lüthi, A. (2016). Distinct Hippocampal Pathways Mediate Dissociable Roles of Context in Memory Retrieval. *Cell*, *167*(4), 961-972.e16. https://doi.org/10.1016/j.cell.2016.09.051

Xu, J., & Potenza, M. N. (2012). White matter integrity and five-factor personality measures in healthy adults. *NeuroImage*, *59*(1), 800–807. https://doi.org/10.1016/j.neuroimage.2011.07.040

Xu, J., Van Dam, N. T., Feng, C., Luo, Y., Ai, H., Gu, R., & Xu, P. (2019). Anxious brain networks: A coordinate-based activation likelihood estimation meta-analysis of resting-state functional connectivity studies in anxiety. *Neuroscience & Biobehavioral Reviews*, *96*, 21–30. https://doi.org/10.1016/j.neubiorev.2018.11.005

Xu, J., Yin, X., Ge, H., Han, Y., Pang, Z., Liu, B., Liu, S., & Friston, K. (2017). Heritability of the Effective Connectivity in the Resting-State Default Mode Network. *Cerebral Cortex (New York, N.Y.: 1991)*, *27*(12), 5626–5634. https://doi.org/10.1093/cercor/bhw332

Xu, X., Holmes, T. C., Luo, M.-H., Beier, K. T., Horwitz, G. D., Zhao, F., Zeng, W., Hui, M., Semler, B. L., & Sandri-Goldin, R. M. (2020). Viral Vectors for Neural Circuit Mapping and Recent Advances in Trans-synaptic Anterograde Tracers. *Neuron*, *107*(6), 1029–1047. https://doi.org/10.1016/j.neuron.2020.07.010

Yang, A. C., Tsai, S.-J., Liu, M.-E., Huang, C.-C., & Lin, C.-P. (2016). The Association of Aging with White Matter Integrity and Functional Connectivity Hubs. *Frontiers in Aging Neuroscience*, *8*, 143. https://doi.org/10.3389/fnagi.2016.00143

Yang, J., Benyamin, B., McEvoy, B. P., Gordon, S., Henders, A. K., Nyholt, D. R., Madden, P. A., Heath, A. C., Martin, N. G., Montgomery, G. W., Goddard, M. E., & Visscher, P. M. (2010). Common SNPs explain a large proportion of the heritability for human height. *Nature Genetics*, *42*(7), 565–569. https://doi.org/10.1038/ng.608

Yang, J., Mao, Y., Niu, Y., Wei, D., Wang, X., & Qiu, J. (2020). Individual differences in neuroticism personality trait in emotion regulation. *Journal of Affective Disorders*, *265*, 468–474. https://doi.org/10.1016/j.jad.2020.01.086

Yang, J., Zeng, J., Goddard, M. E., Wray, N. R., & Visscher, P. M. (2017). Concepts, estimation and interpretation of SNP-based heritability. *Nature Genetics*, *49*(9), Article 9. https://doi.org/10.1038/ng.3941

Yang, Z., Zuo, X.-N., McMahon, K. L., Craddock, R. C., Kelly, C., de Zubicaray, G. I., Hickie, I., Bandettini, P. A., Castellanos, F. X., Milham, M. P., & Wright, M. J. (2016). Genetic and Environmental Contributions to Functional Connectivity Architecture of the Human Brain. *Cerebral Cortex (New York, NY)*, *26*(5), 2341–2352. https://doi.org/10.1093/cercor/bhw027

Yassa, M. A., Hazlett, R. L., Stark, C. E. L., & Hoehn-Saric, R. (2012). Functional MRI of the amygdala and bed nucleus of the stria terminalis during conditions of uncertainty in generalized anxiety disorder. *Journal of Psychiatric Research*, *46*(8), 1045–1052. https://doi.org/10.1016/j.jpsychires.2012.04.013

Young, A. I. (2019). Solving the missing heritability problem. *PLOS Genetics*, *15*(6), e1008222. https://doi.org/10.1371/journal.pgen.1008222

Yu, S.-T., Lee, K.-S., & Lee, S.-H. (2017). Fornix microalterations associated with early trauma in panic disorder. *Journal of Affective Disorders*, *220*, 139–146. https://doi.org/10.1016/j.jad.2017.05.043

Zhang, Y., Brady, M., & Smith, S. (2001). Segmentation of brain MR images through a hidden Markov random field model and the expectation-maximization algorithm. *IEEE Transactions on Medical Imaging*, *20*(1), 45–57. https://doi.org/10.1109/42.906424

Zheng, Y., Plomin, R., & Stumm, S. von. (2016). Heritability of Intraindividual Mean and Variability of Positive and Negative Affect: Genetic Analysis of Daily Affect Ratings Over a Month. *Psychological Science*. https://doi.org/10.1177/0956797616669994

Zhou, J.-N., Hofman, M. A., Gooren, L. J. G., & Swaab, D. F. (1995). A sex difference in the human brain and its relation to transsexuality. *Nature*, *378*(6552), 68–70. https://doi.org/10.1038/378068a0

Zhu, X., Cortes, C. R., Mathur, K., Tomasi, D., & Momenan, R. (2017). Model-free functional connectivity and impulsivity correlates of alcohol dependence: A resting-state study. *Addiction Biology*, *22*(1), 206–217. https://doi.org/10.1111/adb.12272

Ziyatdinov, A., Brunel, H., Martinez-Perez, A., Buil, A., Perera, A., & Soria, J. M. (2016). solarius: An R interface to SOLAR for variance component analysis in pedigrees. *Bioinformatics*, *32*(12), 1901–1902. https://doi.org/10.1093/bioinformatics/btw080